X-733-68-354

PREPRINT

NASA TM X-63338

A TDM SYNCHRONIZATION SYSTEM FOR MULTIPLE ACCESS SATELLITE COMMUNICATION

SEPTEMBER 1968

GSFC

GODDARD SPACE FLIGHT CENTER

GREENBELT, MARYLAND

A TDM SYNCHRONIZATION SYSTEM

FOR

MULTIPLE ACCESS SATELLITE COMMUNICATION

Edited by

Walter K. Allen
James L. Singleton

CONTENTS

ILLUSTRATIONS

PREFACE

This document reports on contract NAS5-10123 with ITT Federal Laboratories. Under this contract Time Division Multiple Access (TDMA) hardware was designed and built, and feasibility was established through an experiment performed using equipment at Nutley, N.J. and the Relay II satellite.

This document is a consolidation of the two principal reports delivered under this contract. The phase I report covered the theory and construction design of the TDMA equipment. The phase II report included the final experimental system description and results of the actual experiment. This document has been edited in the interest of brevity and clarity. Readers desirous of more detailed information on the construction and conduct of the experiment are referred to Mr. Walter Allen, Code 733, Goddard Space Flight Center, Greenbelt, Md. This constitutes the final document concerning this effort.

1. INTRODUCTION

Time Division Multiple Access (TDMA) is a system by which several ground stations can simultaneously share a satellite repeater. The station designated as the master transmits a repetitive sync burst to the other stations via the satellite. This provides the time reference for a time division multiplex format in which the frame period is divided into a number of time intervals. Each station can transmit data bursts during an assigned time interval without causing interference to other stations.

The central problem associated with a TDMA system is that of providing system time synchronization. Each station must adjust the timing of its transmitted data bursts to insure that they arrive at the satellite during their assigned time interval. This problem is particularly difficult for a system using a medium altitude satellite because the range and therefore propagation delay from any station to the satellite is rapidly changing.

This report contains descriptions of a TDMA synchronization technique and an experiment which successfully established the feasibility of this technique for synchronizing system users. The technique will enable a system including small ground stations to access a medium altitude communications satellite in the desired time interval. The stations are completely independent with no need for a central control other than the timing burst originated by a master station. This enables the use of time division in such a system with its advantages of higher communications efficiency by the minimization of intermodulation noise, interference between stations, and the need for individual power control.

The terminal was designed as nonoperational experimental equipment and contains flexibility which would not be provided in operational equipment. A large number of the design parameters, such as the phase locked loop bandwidths, were made selectable. Both manual and automatic acquisition modes were provided. In addition, the electrical and mechanical design provides for easy circuit modividations without regard to size or weight. The scope of the terminal design did not include the data modulation part of the system. However, any type of pulse modulation such as PAM-FM or PCM could be used.

Two TDMA terminals were designed, constructed and installed in the ITT Nutley ground station. One terminal is shown in Figure 1-1. The installation was arranged so that the two terminals shared the station transmitter and receiver but otherwise functioned independently. The normal station performance was degraded to correspond to that of a small station (i.e., 300°K and a 10 foot antenna.) The Relay II medium altitude satellite was used for all experiments. The tests were conducted from 15 January, 1967 to 1 June, 1967, during which time experiments were performed on 55 passes. The test period was sufficient to permit experiments with maximum and minimum range, doppler and doppler rate orbits.

This system employs a doppler compensation technique in which the master station tracks the doppler actively and the other stations track it passively. The implementation of this technique at the master and slave stations is described. The system calculations are primarily based on the use of the Nutley ground station and the Relay satellite. However, the performance of a smaller station is also estimated.

The doppler compensation technique removes the first order doppler shift on the sync signal at the satellite. A theoretical analysis of the residual frequency error on the satellite timing due to the second order doppler effects and other sources of timing

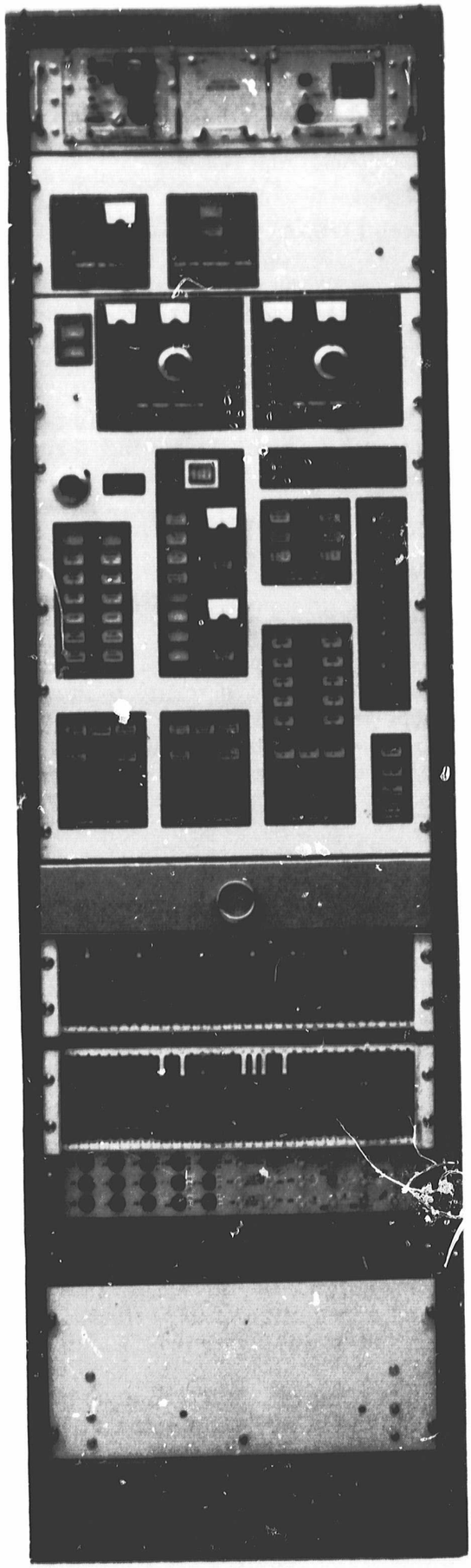

Figure 1-1. TDMA Terminal
Front View

error are considered and a determination of these effects are included in this report. Analytical and experimental results necessary to the design of various portions of the terminal are also included as are an analysis of the effect of propagation delay on signal suppression characteristics of the Relay transponder.

The experiment uses a time division format which provides for up to ten stations accessing the satellite simultaneously. Again, in the interest of economy, the format specified was not chosen to optimize efficiency but was chosen to correspond to available bandwidth and also to previous circuit designs. Thus, 1.25 microsecond guard times were used between 10 microsecond information bursts although test results demonstrated that timing could be maintained to such a degree as to permit reduction of this guard time by a factor of ten.

In order to adequately simulate an actual communications system, each terminal was provided with the capability of inserting unmodulated carrier bursts at any point in the format. This provided a means for simulating any desired amount of system loading.

Feasibility and performance were demonstrated by conducting experiments to measure timing error, acquisition time and range prediction accuracy. The typical timing error was measured to be 25 nanoseconds, and the timing error was always less than 75 nanoseconds. The acquisition time for a terminal averaged 25 seconds and was always less than one minute. This represents a small fraction of the total duration of a pass. Techniques for automating this procedure and minimizing acquisition time should be investigated.

It was concluded that the fundamental concepts in systems tested were highly satisfactory. The successful results of this experiment suggest the desirability of a follow-on effort to further develop the technique. Experiments should be conducted to optimize system parameters and determine the maximum number of users possible within a given satellite bandwidth. These experiments could lead to the evolution of a complete communications system consisting of several small ground stations working through a hard-limiting medium altitude satellite.

2. DESCRIPTION OF TDMA SYSTEM

2.1 TIME DIVISION MULTIPLE ACCESS SYSTEM

Various systems which permit several ground stations to simultaneously share a satellite repeater have been discussed in the literature (Ref. 2-1). Frequency division multiple access and time division multiple access are two such systems. FDMA is the subdivision of the available bandwidth in the transponder, where each ground station transmits in an assigned portion of the bandwidth spectrum. TDMA divides time so that each ground station transmits in an assigned time interval.

The time division multiple access system is potentially capable of high efficiency because none of the transponder output power is wasted in inter-modulation noise. In addition, it does not require transmitter power control in the ground stations as other techniques do. However, it does require network synchronization to realize these advantages.

The general configuration of a TDMA system is shown in Figure 2.1-1. One station designated the master transmits a repetitive sync burst to the other stations via the satellite. This provides the time reference for a time division multiplex format in which the frame period is divided into a number of time intervals. Each station can transmit data bursts during an assigned time interval without causing interference to other stations.

A central problem associated with a TDMA system is that of providing system time synchronization. Each station must adjust the timing of its transmitted data bursts to insure that they arrive at the satellite during their assigned time interval. This is illustrated in Figure 2.1-2 which shows the timing of the signals transmitted from the master and a slave station which have different ranges to the satellite. The synchronization problem is particularly difficult for a system using a medium altitude satellite because the range and therefore propagation delay from any station to the satellite is rapidly changing.

The TDMA format chosen for the experimental system is also shown in Figure 2.1-2. All timing is obtained by dividing down from a basic 800 kHz clock frequency. This particular frequency and several other aspects of the format were chosen to make use of conveniently available equipment. The format consists of a frame which contains one sync burst and ten data bursts of 10 μs duration and a guard time of one 1.25 μs clock period between bursts. The sync burst is modulated by the 800 kHz clock which is accurate to within one part/10^8 as transmitted from the satellite. Table 2-1 summarizes the system parameters.

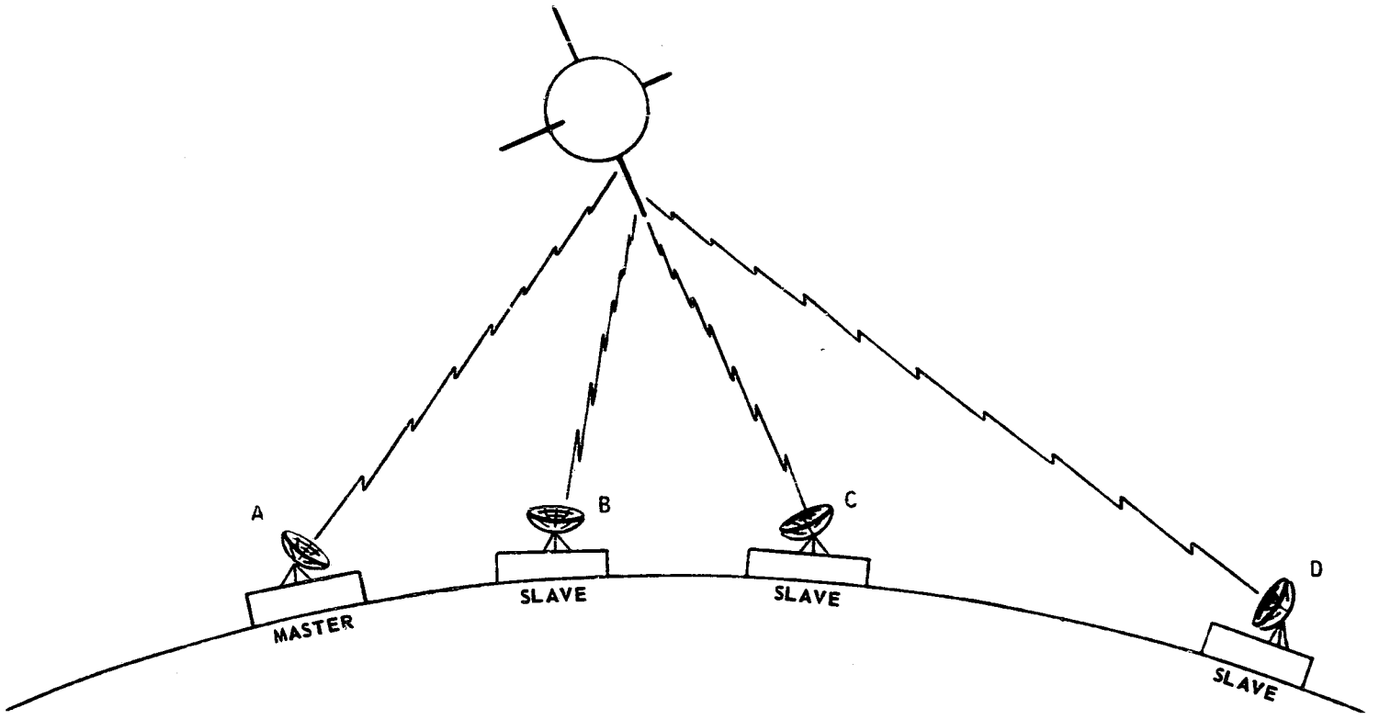

Figure 2.1-1. Time Division Multiple Access System

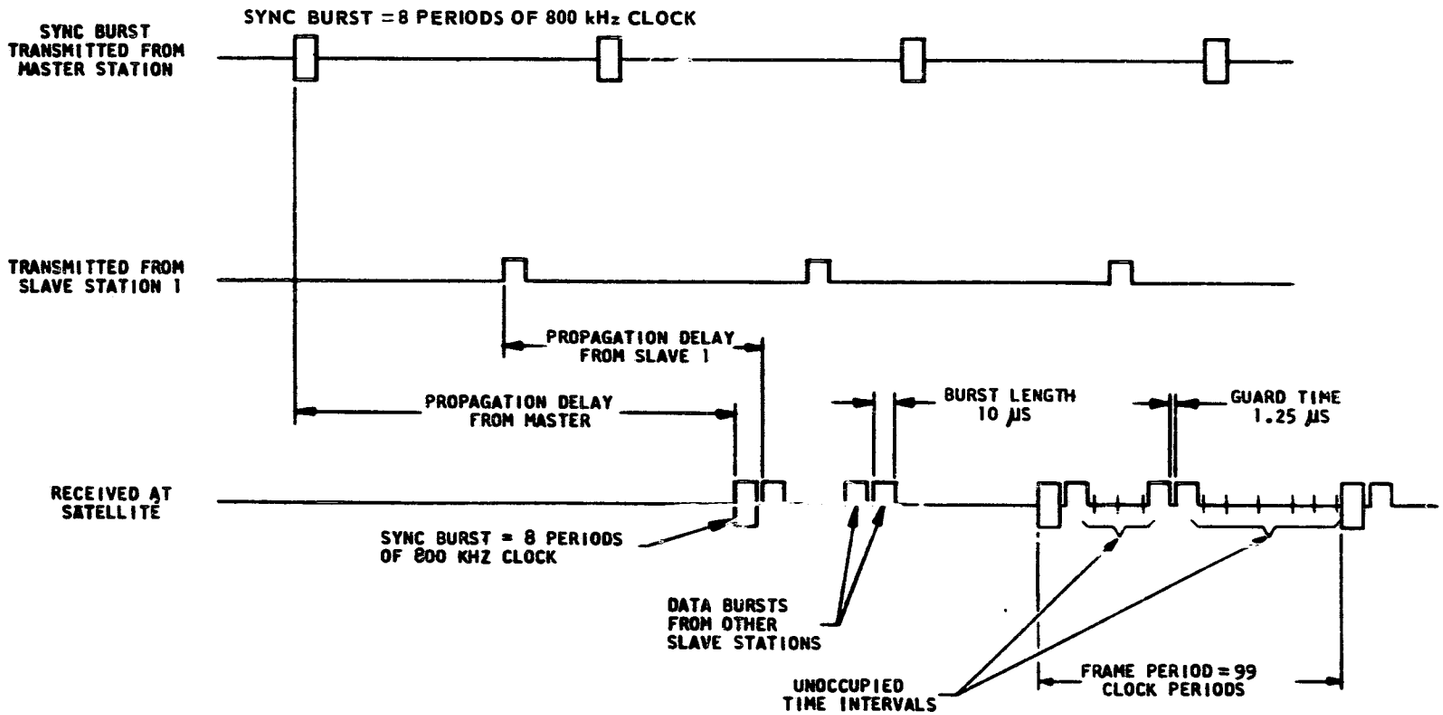

Figure 2.1-2. TDMA System Timing

TABLE 2-1. TDMA SYSTEM PARAMETERS

Maximum number of channels	10 (5 Full Duplex)
Frame period	123.75 μs
Format (number of bursts per frame)	
Channel	10
Sync	1
Total	11
Burst width	10 μs
Guard time (between bursts)	1.25 μs
Type of sync modulation	Phase
Modulation index	$\pi/4$ (approx.)
Carrier frequencies	
Uplink	1725 MHz
Downlink	4169.720 MHz
Clock rate	800 kHz
Sync burst	8 cycles of 800 kHz square wave

2.2 DOPPLER COMPENSATION TECHNIQUE

The accuracy of the clock frequency is maintained at the satellite by the doppler compensation technique illustrated in Figure 2.2-1. This technique off-sets the transmit clock frequency based on the observed doppler shift of the received clock frequency. This is done in such a manner as to maintain a clock frequency at the satellite essentially uneffected by doppler.

Letting ω_R and ω_T denote the receive and transmit frequencies, respectively, this may be written as

$$\omega_R + \omega_T = 1\ \omega_o \tag{2.2-1}$$

Assuming that ω_T is decreased by a doppler ω_d in transmission, the satellite frequency will be

$$\omega_s = \omega_T - \omega_d \tag{2.2-2}$$

Ignoring second order effects, the receive frequency will be equal to the satellite frequency reduced by

$$\omega_R = \omega_s - \omega_d \tag{2.2-3}$$

Substituting the last two equations into the first equation shows that the satellite frequency is ω_o.

ω_R – Ground station received frequency

ω_T – Ground station transmitted frequency

$2\omega_0$ – Frequency standard

ω_D – Doppler differential frequency

ω_S – Frequency at satellite

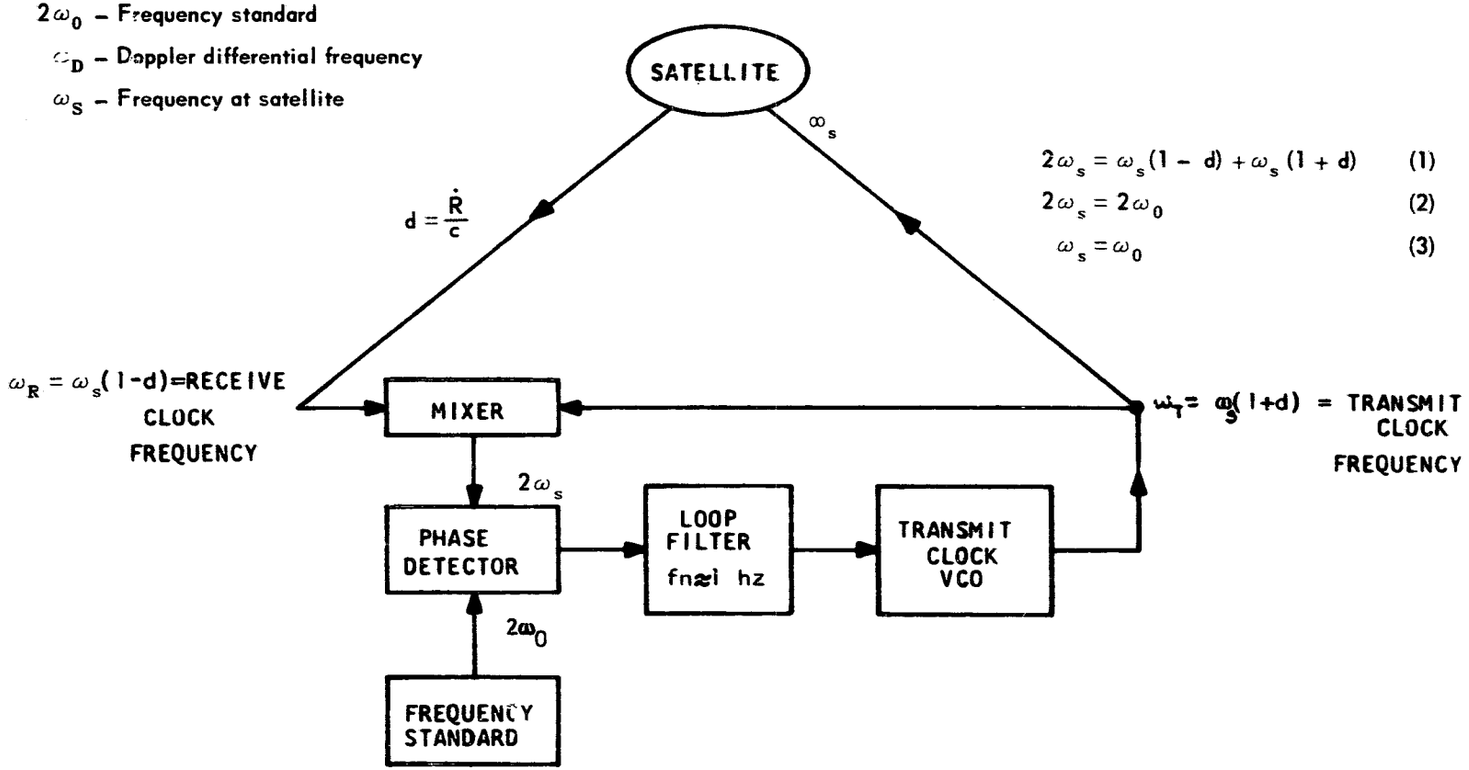

$$2\omega_s = \omega_s(1 - d) + \omega_s(1 + d) \quad (1)$$

$$2\omega_s = 2\omega_0 \quad (2)$$

$$\omega_s = \omega_0 \quad (3)$$

Figure 2.2-1. Doppler Compensation System

The master station transmits the sync burst consisting of 800 kHz minus its own doppler and receives it as 800 kHz plus its own doppler. The transmitted frequency is adjusted so that the sum of the transmitted and received frequencies is a constant. This method of doppler tracking assures that the sync signal at the satellite is a true 800 kHz.

A slave station receives the pulsed signal from the master station via the satellite. Since the signal was a true 800 kHz at the satellite, it will be received with the true doppler of the slave station. The slave station uses this to preset its transmitted frame rate by a technique identical to that used by the master station for doppler tracking. The slave station uses a pseudo noise code ranging technique to determine the correct initial phase for its transmitted format.

An exact analysis of the performance of this method of doppler compensation is given in Section 3.

2.3 TDMA TERMINALS

Figure 2.3-1 shows a simplified block diagram of the master station. The master sync burst is generated by gating the output of a carrier phase modulator. The carrier burst is phase modulated by the 800 kHz transmit clock frequency. The gate control signal is generated in the transmit timer by dividing down from the transmit clock.

The received i-f signal is demodulated by the carrier tracking phase locked loop. The resulting 800 kHz sync burst is used to lock the receive clock tracking phase locked loop, generating a continuous 800 kHz clock which drives the receive timer. This, in turn, generates the gating pulse for the carrier tracking and receive clock tracking phase locked loops. Initially neither of these loops are locked. To aid acquisition, the output of the carrier tracking phase locked loop drives the sync burst detector. This circuit contains an 800 kHz filter, envelope detector, and threshold detector. It will detect the time of occurrence of the sync burst even before the carrier tracking phase locked loop acquires. The occurrence of the sync burst resets the phase of the receive timer to within a fraction of a burst. This is sufficient for the carrier tracking and receive clock phase locked loops to lock.

The receive clock phase locked loop may lock in such a manner that the receive timer is an integral number of clock cycles out of correct phase. The receive clock loop contains an error detector to measure relative timing between received burst and local gating pulse. If an error exists, the receive timer is stepped in the proper direction until it is operating in correct phase.

The transmit clock generator contains the doppler compensation circuit which adjusts the transmitted clock frequency to maintain the satellite clock frequency at exactly 800 kHz, independent of first order doppler effects. This is implemented by passing the receive and transmit clock frequencies through a mixer which extracts their sum frequency, comparing the sum frequency with a 1600 kHz standard, and adjusting the phase of the transmit frequency to keep the sum exactly 1600 kHz.

A simplified block diagram of the slave terminal is shown in Figure 2.3-2. The slave terminal has the same circuits used in the master for receiving the master sync burst and generating the receive clock and doppler compensated transmit clock. In the case of the slave terminal, however, this doppler compensation is an open loop operation. It cannot correct the differences between the 1600 kHz standards at the master and slave terminals or for second order frequency errors in the satellite clock frequency. In addition, the initial phase of the transmit timer must be adjusted according to the range of the satellite from the slave station.

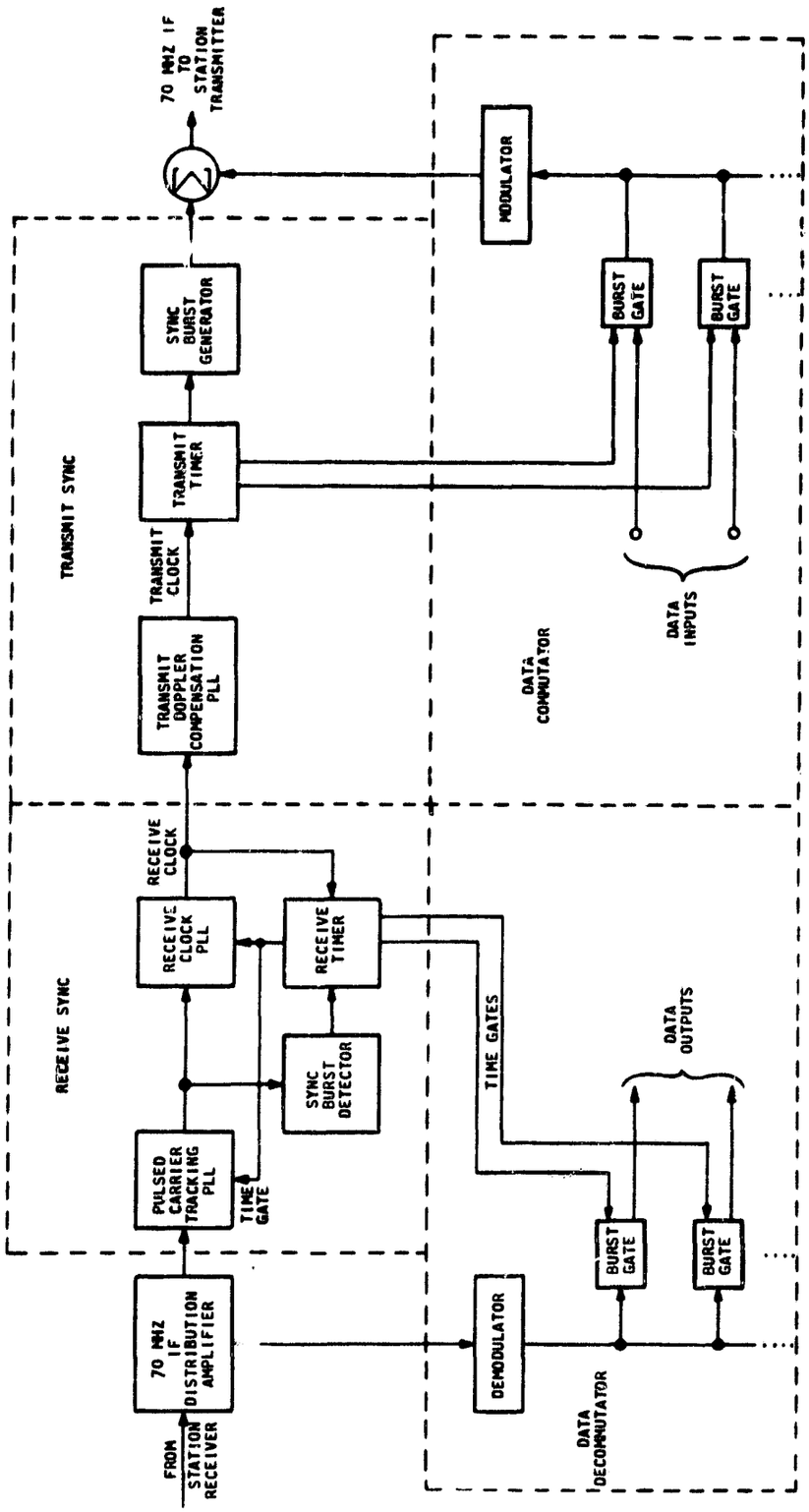

Figure 2.3-1. Master Terminal Block Diagram

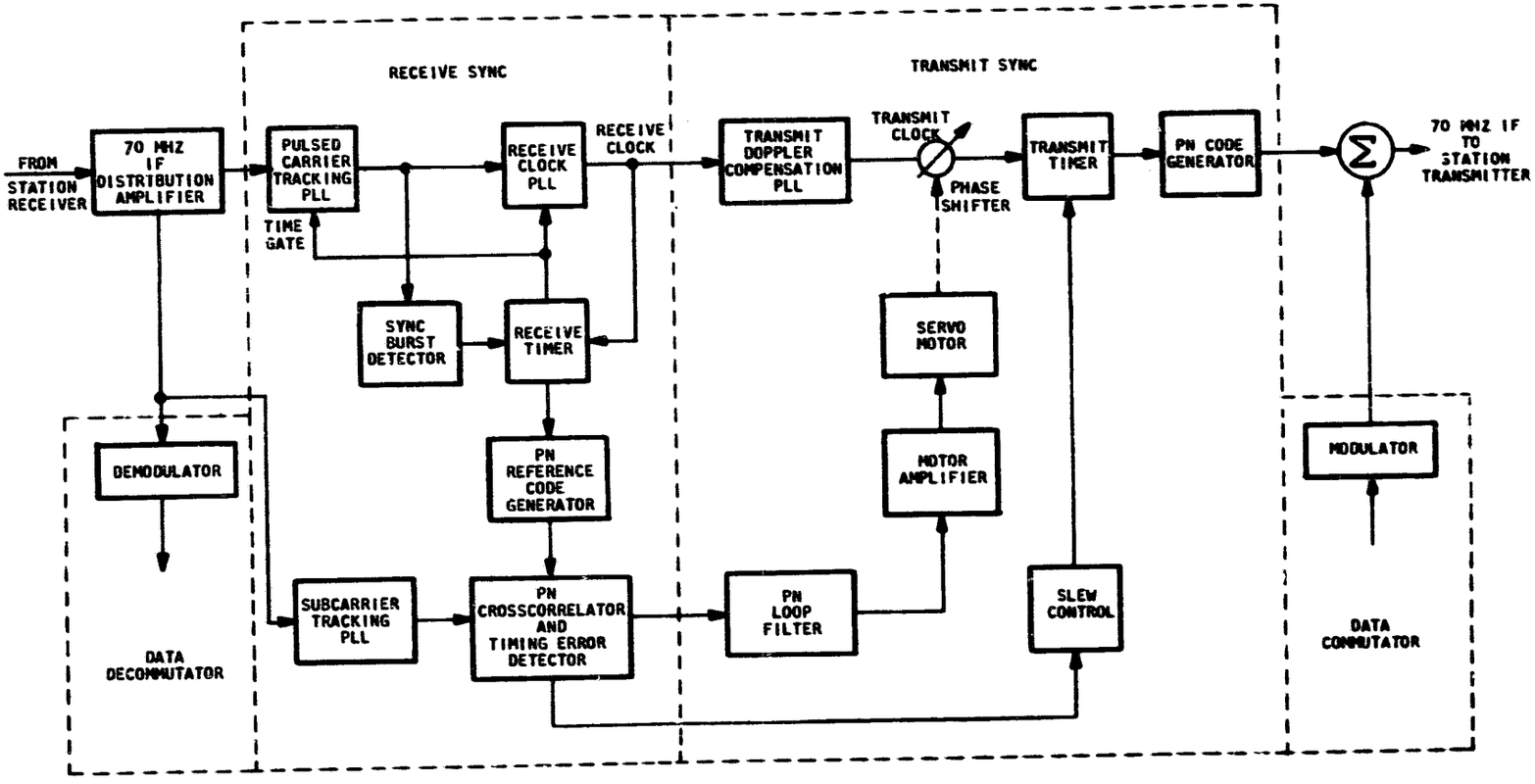

Figure 2.3-2. Slave Terminal Block Diagram

The open loop doppler compensation of the transmit clock is supplemented during acquisition by the pseudo noise ranging phase locked loop. The slave transmits a cw subcarrier signal which is phase modulated by a code. The subcarrier frequency is 2 mhz from the master carrier and at a level low enough to cause no interference to the sync burst or to any data bursts.

The subcarrier tracking phase locked loop is used to demodulate the received pseudo noise ranging signal. The demodulated signal is compared with the demodulated sync burst as follows: The receive timer, which is locked to the demodulated sync burst, generates a reference sequence. This is compared with the demodulated signal in the cross correlator. The phase of the transmit timer is stepped until a lock to within a fraction of a burst is obtained.

Once this approximate lock has been obtained, the timing error between the received and reference sequences is measured. The timing error signal is used to correct the phase of the transmit clock first digitally and then by a motor driven phase shifter. Once this phase locked loop has slewed in, it tracks the residual frequency error of the doppler compensation system described above.

2.4 ELECTRICAL DESCRIPTION OF TDMA TERMINAL

A block diagram of the TDMA terminal is given in Figure 2.4-1.

The TDMA terminal includes all equipment functions to make it operate as master or slave terminal. In the master station, the transmission of master sync is enabled and pseudo noise ranging is disabled. In slave station, the transmission of master sync is disabled and the pseudo noise ranging is enabled.

The functions in the terminal are related to one another and operate in the following manner.

The received i-f enters the terminal at the 70 MHz distribution amplifier, which consists of a set of buffers arranged to provide the following buffered outputs.

- Modulator i-f
- Carrier i-f
- Subcarrier i-f

The modulator i-f provides an output to the modulator unit where communication data is demultiplexed and processed.

Carrier i-f is the input to the carrier tracking phase locked loop where the master sync signal is extracted.

Subcarrier i-f is the input to the subcarrier tracking phase locked loop where the pseudo noise code is extracted.

The carrier tracking phase locked loop shown in Figure 2.4-2 is used as a phase demodulator.

The demodulated signal is then used to lock a 6.4 MHz voltage controlled crystal oscillator in the receive clock tracking phase locked loop. Since the 800 khz in the received sync burst contains the satellite to ground doppler, a clock is obtained which is proportional to the receive frame interval. The phase locked loop also serves as narrow band filter for the incoming 800 kHz sync signal. Included in the receive clock tracking phase locked loop is a set of correlators which measure the phase integrity of local receive frame referenced with the incoming sync and the local frame clock.

FOLDOUT FRAME 1

PRECEDING PAGE BLANK NOT FILMED.

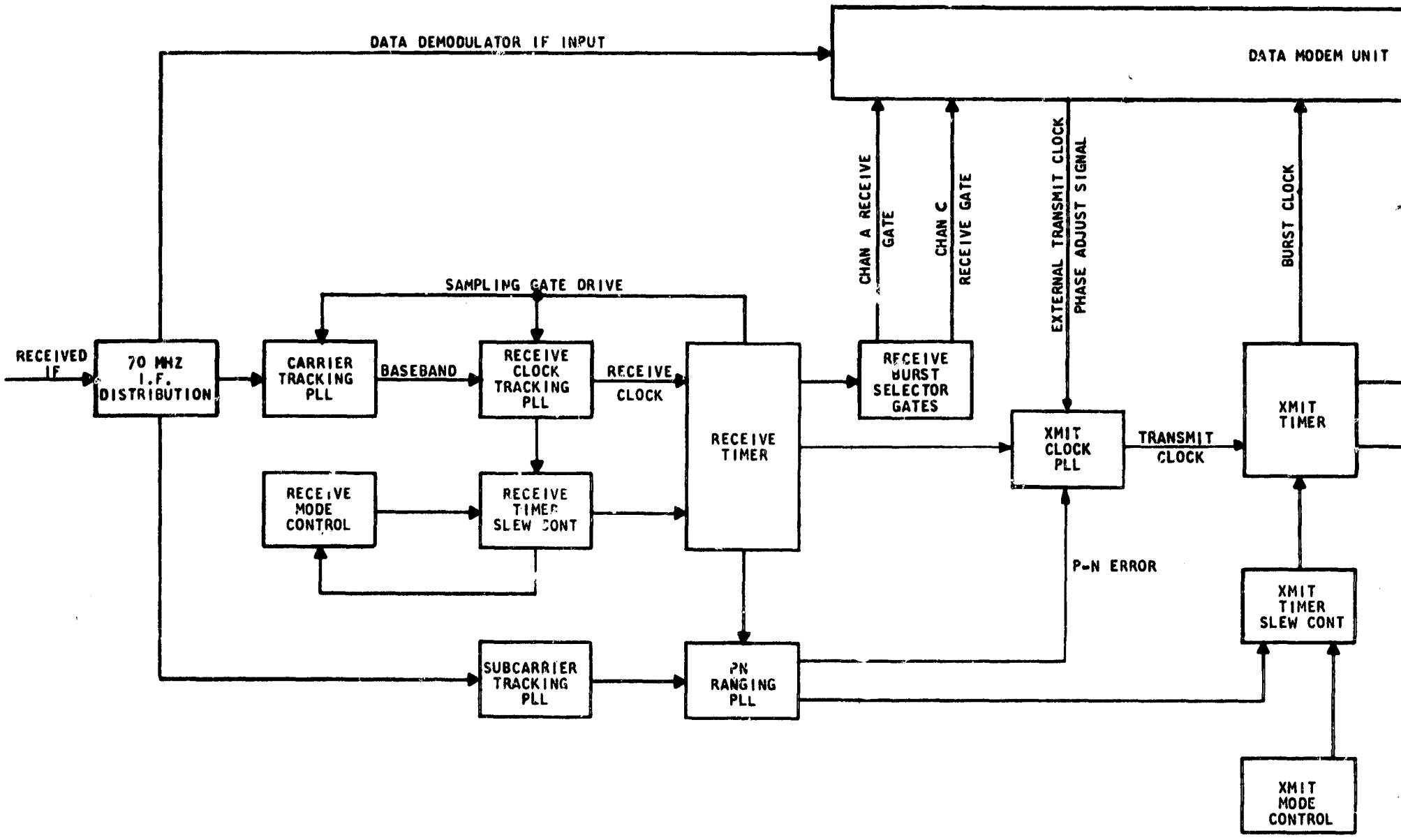

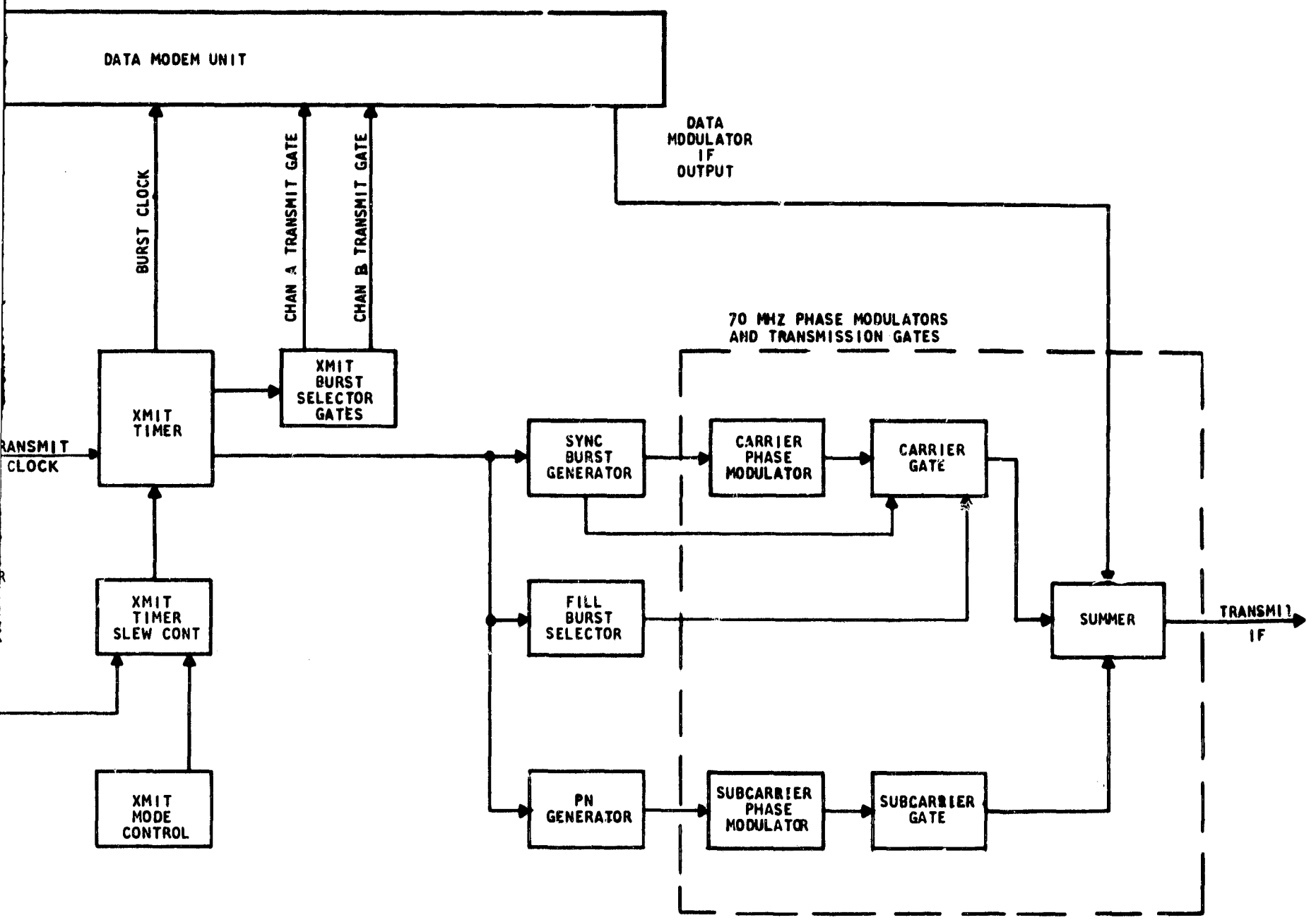

Figure 2.4-1. TDMA Terminal Block Diagram

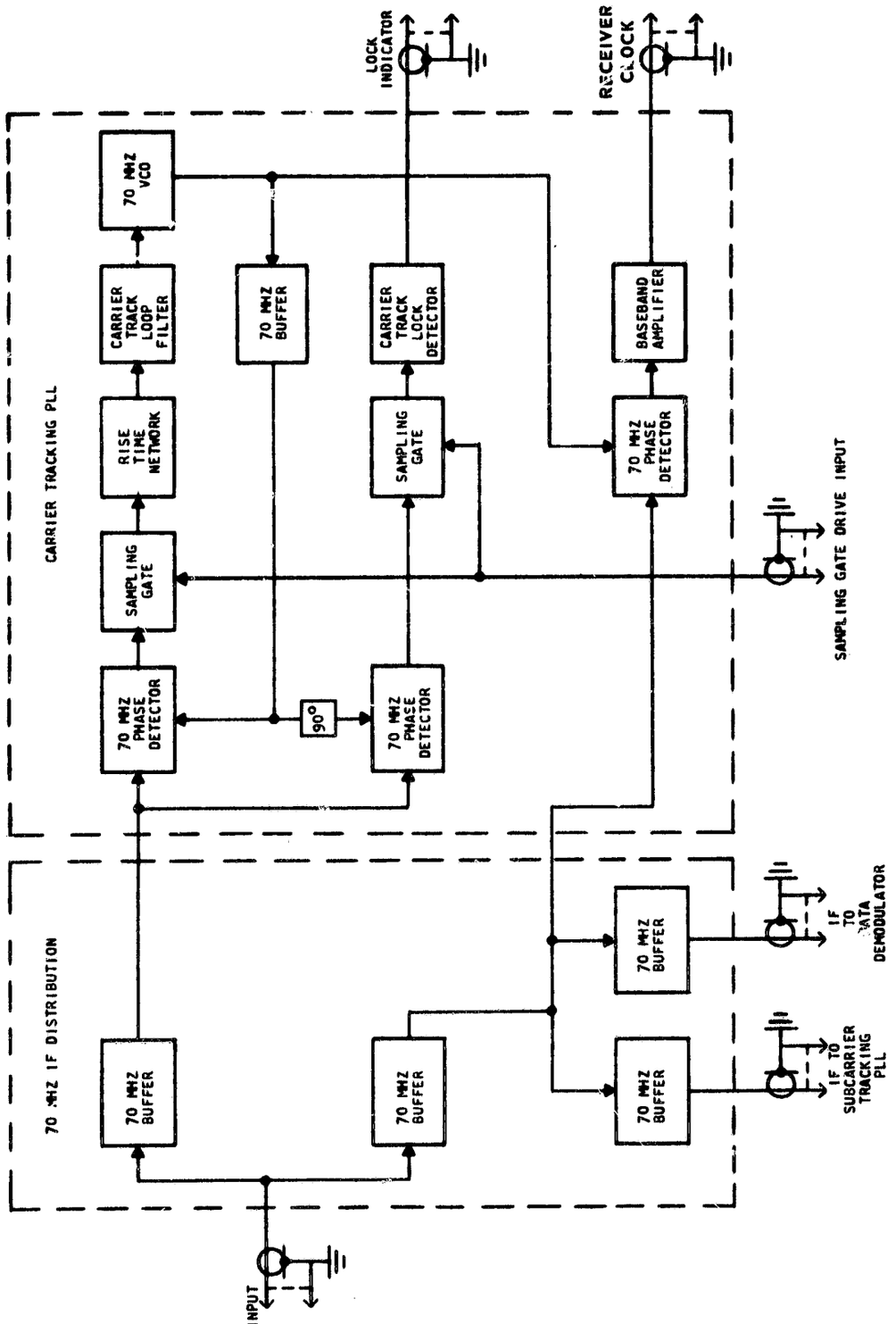

Figure 2.4-2. Carrier Tracking PLL Block Diagram

The local receive frame interval is generated by the receive timer. The receive timer consists of a set of cyclic counters clocked from the 6.4 mhz in the receive tracking clock phase locked loop which are arranged to generate the TDMA frame interval. Since the clock driving these counters is receive doppler compensated, the receive frame is correct in frequency. The receive frame is phase corrected by receive slew control and receive mode control based on correlator outputs from receive clock tracking phase locked loop.

All time references for the receive frame interval are provided by the receive timer. These include:

- Signal to gate the carrier tracking phase locked loop
- Signal to gate the receive clock tracking phase locked loop
- Sync reference signals to drive the sync early-late correlator
- Pseudo-noise reference signals to drive the pseudo-noise ranging phase locked loop correlator
- Burst reference signals to the receive channel gate. The channel gate generates the gate signal used by the modulator unit to demultiplex data channels.
- 800 kHz receive signal to the transmit clock phase locked loop.

In the transmit clock phase locked loop the receiver 800 kHz is added to locally generated 800 kHz signals. The resultant is then compared to a 1600 kHz standard. The resulting error in turn drives a 6.4 MHz voltage controlled crystal oscillator from which the local 800 kHz was derived by dividing the 6.4 MHz by eight. This arrangement forms a phase locked loop, which in conjunction with the receive clock tracking phase locked loop, forms the method of doppler compensation. A detailed discussion of the doppler compensation was given in Section 2.2.

To compensate for secondary effect of doppler and to correct for the other factors such as error in standards, the transmit clock phase locked loop includes a mechanical phase shifter driven by servo motor. This is enabled in a slave terminal. The output of the voltage controlled crystal oscillator passes through the phase shifter and is then used to clock the transmit timer. For a detailed discussion of transmit phase locked loop see Section 3.2.

The transmit timer is structually identical to the receive timer. It consists of a set of three cyclic counters arranged to count out the transmit frame interval. All time references of the transmit frame interval are derived from the transmit timer. When the receive and transmit phase locked loops are locked and the proper drive is provided to the servo motor, the transmit frame is correct in frequency.

The transmit frame is phase corrected through the logic in transmit slew control and transmit mode control based on correlator outputs from the pseudo noise ranging phase locked loop. The servo and phase correction logic for the transmit timer are only used at a slave terminal. The transmit timer in a master terminal is considered the reference. Therefore, under normal conditions the servo motor and the slew control are made inoperative in a master terminal.

All timing signals for transmit frame interval are derived from the transmit timer. These include:

- Gate signal to generate the master sync burst.
- Signal to modulate the master sync burst.
- Burst signals to drive the fill burst selector switches.
- Burst signals to drive the pseudo noise generator.
- Burst clock to modulator for data processing.
- Burst reference signals to drive the transmit channel gate. The transmit channel gate generates the gate signal used by the modulator unit to time multiplex data channels.

The above signals constitute the transmit control for the TDMA terminal. A brief description of their operation follows.

The master sync signal is used to phase modulate the output of a 68 MHz oscillator. The modulated 68 MHz is then gated by the sync burst generator into the summer through the carrier gate, thus transmitting the master sync burst. The unmodulated 68 MHz carrier is also gated into the summer to select the fill bursts. The function of the fill bursts was included to simulate a varied TDMA channel load. The master sync transmission is only operative when the terminal is a master.

For a slave unit the subcarrier is enabled. The output of the pseudo noise generator phase modulates, the output of a 70 MHz crystal oscillator, and the modulated 70 MHz is then gated into the summer by the subcarrier gate. The summer mixes the carrier, sub-carrier, and output of modulator unit and presents the signals to the station for transmission.

The processing of the carrier signal was described previously. However, it should be noted that a transmitted i-f of 68 MHz is received at 76 MHz. The relay transponder contains a tripler and the exciter in the station causes a sideband inversion. However, the subcarrier is transmitted as 70 MHz returns as 70 MHz to the TDMA terminal.

At this point the pseudo noise ranging circuitry will be discussed. The subcarrier i-f goes through a 70 MHz bandpass filter and limiter. The limiter output drives the subcarrier tracking phase locked loop which acts as a phase demodulator. The received pseudo noise code at the baseband output of the subcarrier phase locked loop is correlated with the reference pseudo noise code derived from the receive timer in the pseudo noise ranging correlators.

The output of the correlators provides the basis for adjusting the transmit timer phase.

A summary of the pseudo noise ranging phase locked loop parameters is given in Table 2-2.

TABLE 2-2. PSEUDO NOISE RANGING PHASE LOCKED LOOP SUMMARY

Loop Filter Switch Position	f_n - Loop Bandwidth = hertz				
Gate Selector position:	1	2	3	4	5
Gate Width: us	1.25	3.75	6.25	8.75	11.25
0	0.509	0.170	0.102	0.0726	0.0566
1	0.994	0.332	0.198	0.142	0.110
2	1.58	0.528	0.315	0.225	0.176
3	2.08	0.698	0.417	0.298	0.232
4	3.06	1.02	0.610	0.436	0.340
5	4.59	1.53	0.918	0.654	0.510
6	6.11	2.04	1.22	0.871	0.679
7	9.16	3.06	1.83	1.31	1.02
8	14.3	4.77	2.87	2.04	1.59
9	17.3	5.78	3.56	2.47	1.92

2.5 RELAY II PARAMETERS

The design of the TDMA equipment was based on the orbit parameters for Relay II shown in Table 2.5-1. The maximum delay, doppler, and doppler rate are used in later sections for the phase locked loop design. The maximum range is used in the system calculations in Section 2.6.

The carrier tracking phase locked loops were designed for a maximum carrier frequency offset of approximately 400 kHz. This requirement is based on the specified stabilities for the local oscillators in the Nutley station and the Relay transponder and on the maximum expected doppler shift. The calculation is summarized by Figure 2.5-1. A block diagram of the Relay transponder is shown in Figure 3.9-3 (see Reference 2-2).

TABLE 2.5-1. RELAY II ORBIT PARAMETERS

Launch Date	January 21, 1964
Apogee Altitude	7434 Km
Perigee Altitude	2068 Km
Inclination	46.3 Deg.
Period	194.7 Min.
Maximum Range (See Note)	11,600 Km
Maximum One Way Delay	38.6 Ms
Minimum One Way Delay	6.9 Ms
Maximum Doppler	19 Parts/10^6
Maximum Doppler Rate	6.5 Parts/10^8/sec.

NOTE: Minimum Elevation = 5 Deg.

MODEL - RELAY II AND ITTFL NUTLEY GROUND STATION
MAX. DOPPLER SHIFT 17 Hz/MHz

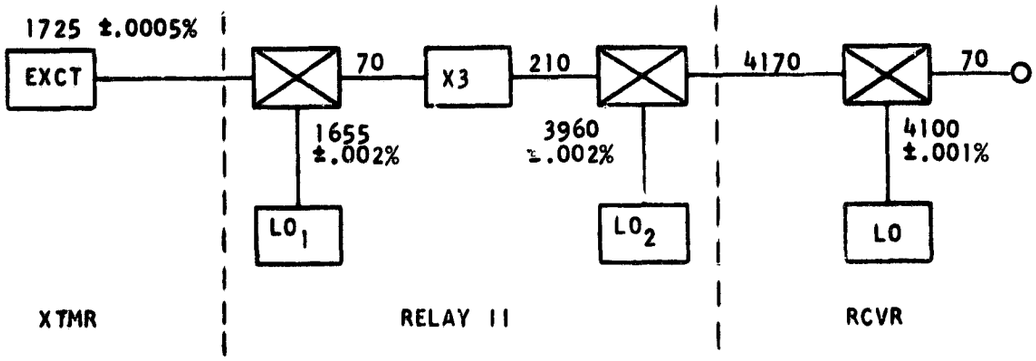

TRANSMITTER FREQ ACCURACY	± 8.65 kHz
UPLINK DOPPLER SHIFT	29.3
LO_1 FREQ ACCURACY	33.1
TOTAL UPLINK ACCURACY	± 71.1 kHz
UPLINK ACCURACY AFTER TRIPLER	± 213.3 kHz
LO_2 FREQ ACCURACY	79.0
DOWN LINK DOPPLER SHIFT	71.0
RCVR LO ACCURACY	41.0
TOTAL DEVIATION	± 404.3 kHz

Figure 2.5-1. Carrier Frequency Accuracy

2.6 DEMODULATOR PERFORMANCE

This section describes how phase locked loops are used as phase demodulators in the system.

The master sync burst is a carrier pulse phase modulated by a 800 kHz square wave. The pseudo noise ranging signal is a subcarrier, phase modulated by a code m(t) which only takes the binary amplitudes of ±1. The return from the satellite for either of these phase modulated signals may be written as

$$s(t) = \sqrt{2P_r}\ \sin\left[\omega_c t + \theta_1(t) + pm(t)\right], \qquad (2.6\text{-}1)$$

where P_r = received signal power

$\theta_1(t)$ = doppler on return carrier

p = peak phase deviation.

These phase modulated signals are demodulated by carrier tracking phase locked loops such as the one shown in Figure 2.6-1. The noise n(t) at the loop input is assumed to have a bandwidth much greater than the signal bandwidth and to have a constant power density of N_o watts/Hz. The voltage controlled oscillator output is a sinusoid of power P_x,

$$x(t) = \sqrt{2P_x}\ \cos\left[\omega_c t + \theta_2(t)\right], \qquad (2.6\text{-}2)$$

where $\theta_2(t)$ is the loop's estimate of carrier doppler.

The phase detector is a multiplier whose output e(t) is equal to the product of the voltage controlled oscillator output and the phase locked loop input.

$$e(t) = \left[s(t) + n(t)\right]\ x(t). \qquad (2.6\text{-}3)$$

Substituting 2.6-1 and 2.6-2 into 2.6-3 and expanding the trigonometric functions gives

$$e(t) = \sqrt{P_r P_x}\ \cos p \sin\varphi + \sqrt{P_s P_x}\ (\cos\varphi)\, m(t) + \sqrt{P_r P_x}\ \sin\left[2\omega_c t + \theta_1(t) + p\, m(t) + \theta_2(t)\right] + n'(t), \qquad (2.6\text{-}4)$$

where

$\varphi = \theta_1 - \theta_2$ = doppler tracking error

$P_s = P_r \sin^2 p$ = received sideband power

$n'(t) = \sqrt{2P_x}\ n(t) \cos(\omega_c t + \theta_2)$ = noise at phase detector output.

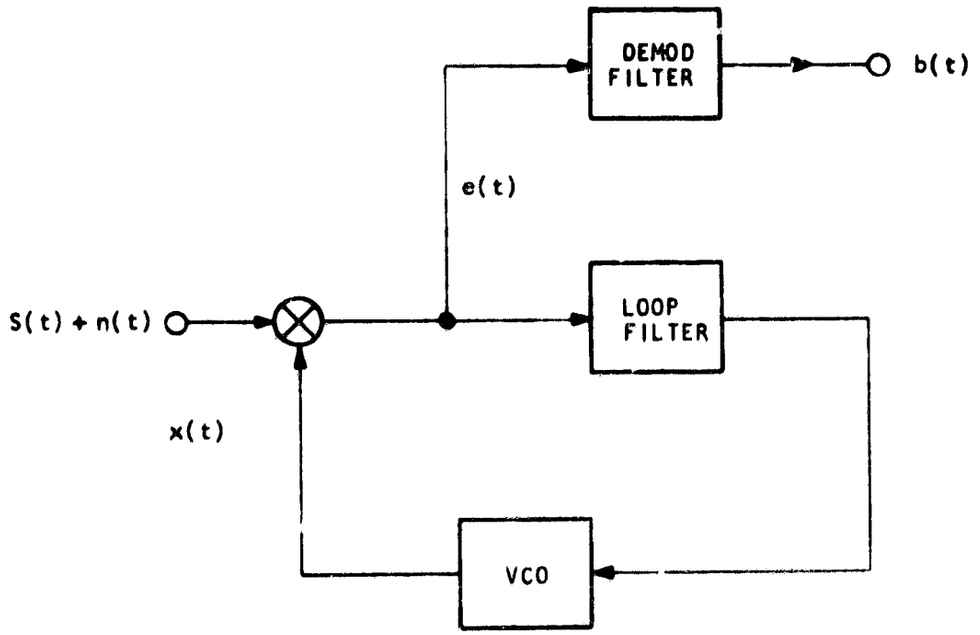

Figure 2.6-1. Carrier Tracking Phase Locked Loop as Phase Demodulator

The first term on the right hand side of 2.6-4 is the loop error signal which is passed by the loop filter. For this loop the phase detector gain (see Section 3.5) is

$$K_E = \cos p \sqrt{P_r P_x}. \qquad (2.6\text{-}5)$$

The second term on the right hand side of 2.6-4 is the demodulated signal passed by the circuits which follow the phase locked loop as indicated by the demodulator filter. The third term is at the second harmonic of the carrier and is filtered out by the phase detector circuit. The last term n'(t) corresponds to the input noise n(t) translated down to baseband. It also has a constant power density of

$$N_o' = P_x N_o, \text{ watts/Hz}. \qquad (2.6\text{-}6)$$

The demodulator output b(t) may be written as

$$b(t) = \sqrt{P_d}\, m(t) + n'(t), \qquad (2.6\text{-}7)$$

where

$$P_d = P_s P_x \cos^2 \varphi \qquad (2.6\text{-}8)$$

denotes the demodulated signal power. The demodulated signal power to noise density ratio is thus

$$\frac{P_d}{N_o'} = \frac{P_s}{N_o} \cos^2 \varphi . \qquad (2.6\text{-}9)$$

Except for the factor $\cos^2\varphi$ which corresponds to loss of signal due to tracking error, the demodulated signal power to noise density ratio at the phase locked loop output is the same as the total sideband power to noise density ratio at the phase locked loop input.

2.7 SYSTEM CALCULATIONS

Calculations for two TDMA system applications are summarized in this section. The first was the experimental system to be tested with the Relay satellite using the Nutley ground station. The second was a TDMA system using a small ground station which was defined as a station with a 10 foot antenna and a 300 K noise temperature. The characteristics of the Nutley station and the Relay satellite were taken from published data (see Reference 2-2). Characteristics such as satellite transponder and orbit parameters are assumed the same for both cases.

The system calculations for the Nutley station, Table 2.7-1A, show that the minimum P_r/N_0 ratio is 70.9 db. The uplink calculations are based on 10 kw transmitter power and actual antenna gain for the Nutley station. It can be seen that the received signal power at the satellite is -72.5 dbm at maximum range. This is not sufficient to obtain the full transponder output power of 10 watts. A transponder output power loss of 2 db (below the output power of 40 dbm) corresponding to the -72.5 dbm input power is used for the downlink calculation (see Reference 2-3). The system temperature for the Nutley station was taken as 360°K.

The system calculations for the small station are shown in Table 2.7-1B. This calculation is idealized to the extent that no losses are assumed and that the satellite antenna gain is taken as 0 db. It is seen that the resulting P_r/N_0 is 66.6 db. This is the value of P_r/N_0 used in the following TDMA timing accuracy calculations since it is smaller than the value obtained for the Nutley ground station.

The timing accuracy calculations for the small station are shown in Tables 2.7-2 and 3. The calculations for master sync burst reception are shown in Table 2.7-2 and assume that the received signal power to noise density ratio is 66.6 db. These calculations apply to either a master or slave station.

The calculations for the carrier tracking phase locked loop show that the rms phase jitter is small enough to be ignored in further calculations. For example, Equation 2.6-9 shows that a 10 degree phase error corresponds to a loss of demodulated signal power of 0.15 db. The jitter on receive clock is calculated by using Equation 3.6-10 and is seen to vary between 10 and 30 nanoseconds rms depending on receive clock loop bandwidth. The transmit clock is obtained by folding over the receive clock (800 kHz -d to 800 kHz +d) and passing it through the transmit phase locked loop. The transmit phase locked loop has a much smaller bandwidth and removes timing jitter by the ratio of their bandwidths. As expected, the transmit clock jitter is independent of receive clock phase locked loop bandwidth. The jitter is only on the order of 1 or 2 nanoseconds rms and is small compared to the error (40 ns max., see Figure 3.5-3) due to doppler.

The calculations for the pseudo noise ranging timing jitter, Table 2.6-3, apply only to a slave station and are based on the assumption that the ranging signal is received 20 db below the peak power of the master sync signal. This was considered as a level low enough to prevent interference to the sync signal or to occupied time intervals. The phase error on the sub-carrier tracking phase locked loop, 6 to 20 degrees rms, was considered small enough to neglect in calculating the

timing jitter in the ranging phase locked loop. The calculation of the latter timing jitter was based on Equation 3.6-11 and varies from 15 to 80 nanoseconds rms depending on loop bandwidth and gate width (see Section 4.10).

TABLE 2.7-1A. CALCULATIONS FOR NUTLEY GROUND STATION

	Ground To Spacecraft	Spacecraft To Ground
Frequency, MHz	1725	4169.720
Transmitter, dbm	70	38
Losses, db	2	2
Transmitter antenna gain, db	39	-1
Path loss (6300 nm), db	178.5	186.2
Receiver antenna gain, db	-1	50
Received signal power, dbm	-72.5	-101.2
Receiver noise density, dbm/Hz	-160	-173.1
Uplink noise contribution, db	-	1.0
Receiver noise bandwidth, MHz	30	-
Total receiver noise power, dbm	-85.2	-
Signal to noise ratio, db	12.7	-
P_r/N_o, db	-	70.9

TABLE 2.7-1B. CALCULATIONS FOR SMALL GROUND STATION (Spacecraft To Ground Only)

Frequency, MHz	4169.720
Transmitter, dbm	40
Path loss, db	186.2
Receiver antenna gain, db (see Note)	39
P_r - Received signal power, dbm	-107.2
N_o - Receiver noise density (300 K), dbm/Hz	-173.8
P_r/N_o, db	66.6

Note: Gain for 54 per cent efficient 10 foot parabolic antenna

TABLE 2.7-2. SYSTEM CALCULATIONS - SMALL STATION - RECEIVE AND TRANSMIT CLOCKS

CARRIER TRACKING PHASE LOCKED LOOP

P_r/N_o - Received signal power to noise density		66.6		db, assumed
P_c/N_o - Received carrier power to noise density		63.6		db, modulation index p = $\pi/4$
f_n - Loop natural frequency	100	300	1000	hertz
B_L - Loop noise bandwidth	25.2	30	35.2	db, Figure 3.5-3
P_c/N_oB_L - Carrier-to-noise ratio in loop bandwidth	38.4	33.6	28.4	db
σ - RMS phase jitter	2.4	4.2	7.7	deg, Equation 3.6-9

RECEIVE CLOCK TRACKING PHASE LOCKED LOOP

P_r/N_o - Received signal power to noise density		66.6		db, assumed
P_s/N_o - Sideband power to noise density		63.6		db, modulation index p = $\pi/4$
f_n - Loop natural frequency	100	300	1000	hertz
B_L - Loop noise bandwidth	25.0	29.2	32.5	db, Figure 3.5-3
P_s/N_oB_L - Signal-to-noise ratio in loop bandwidth	38.6	34.4	31.1	db
σ_φ - RMS phase jitter on receive clock	3.9	6.0	8.8	deg, Equation 3.6-10
σ_τ - RMS timing jitter on receive clock	13.3	20.7	30.5	ns

TABLE 2.7-2. SYSTEM CALCULATIONS - SMALL STATION - RECEIVE AND TRANSMIT CLOCKS (Cont)

TRANSMIT PHASE LOCKED LOOP

Transmit PLL Natural Frequency					
	Receive Clock phase locked loop - f_n B_L (Receive)	100 25.0	300 29.2	1000 32.5	db
0.5 hz	B_L (Transmit)		2.2		db, Figure 3.5-3
	B_L (Receive)/B_L (Transmit)	22.8	27.0	30.3	db
	RMS timing jitter on transmit clock	0.96	0.93	0.93	ns
1.0 hz	B_L (Transmit)		5.2		db, Figure 3.5-3
	B_L (Receive)/B_L (Transmit)	19.8	24.0	27.3	db
	RMS timing jitter on transmit clock	1.4	1.3	1.3	ns
2.0 hz	B_L (Transmit)		8.2		db, Figure 3.5-3
	B_L (Receive)/B_L (Transmit)	16.8	21.0	24.3	db
	RMS timing jitter on transmit clock	1.9	1.8	1.9	ns

TABLE 2.7-3. SYSTEM CALCULATIONS - SMALL STATION - PN RANGING

SUBCARRIER TRACKING PHASE LOCKED LOOP

P_r/N_o - Received signal power to noise density		46.6		db, assumed
P_c/N_o - Received carrier power to noise density		43.6		db, modulation index p = $\pi/4$
f_n - Loop natural frequency	100	300	1000	hertz
B_L - Loop noise bandwidth	25.2	30	35.2	db, Figure 3.5-3
P_c/N_oB_L - Carrier-to-noise ratio in loop bandwidth	8.4	13.6	8.4	db
σ - RMS phase jitter	6.9	12.0	21.8	deg, Equation 3.6-9

PSEUDO NOISE RANGING PHASE LOCKED LOOP

P_r/N_o - Received signal power to noise density		46.6		db, assumed
P_s/N_o - Sideband power to noise density		43.6		db, modulation index p = $\pi/4$
f_n - Loop natural frequency	0.5	1	2	hertz
B_L - Loop noise bandwidth	-1.1	2.0	5.0	db, Equation 3.6-7
P_s/N_oB_L - Signal-to-noise ratio in loop bandwidth	44.7	41.6	38.6	db
σ - RMS timing jitter	14.9	21.0	29.8	ns, tg = 1.25μs Equation 3.6-11
σ - RMS timing jitter	40.0	56.0	80.5	ns, tg = 11.25μs Equation 3.6-11

2.8 REFERENCES

2-1 J.W. Schwartz, et al., "Modulation Techniques For Multiple Access To A Hard-Limiting Satellite Repeater", Proc. IEEE, Volume 54, pp. 763-777, May, 1966.

2-2 Final Report On The Relay I Program, NASA SP-76, 1965, Chapters 5 and 11.

2-3 Project Relay Third Interim Engineering Report, COMNUT Narrow Band Experiments, January - May 1964, Prepared by ITT Federal Laboratories on Contract NAS 5-2056, June 1964, Figure 5-3.

3. THEORY OF OPERATION

This chapter contains analyses of several aspects of the TDMA system. A detailed analysis of the theoretical performance of the doppler compensation system is contained in Section 3.1 through 3.4. A different but parallel analysis of the doppler compensation can be found in Reference 3-1. Section 3.5 is a summary of the design procedure used for the various phase locked loops in the system. Section 3.6 contains formulas for expressing the tracking errors in these phase locked loops due to noise and satellite motion.

The next two sections are concerned with the effect of propagation delay on the stability of the phase locked loops. Section 3.7 describes a computer simulation which was performed to determine the effect of propagation delay on the nonlinear pseudo noise ranging phase locked loop. Section 3.8 describes the effect of propagation delay on the stability and the noise bandwidth of linear phase locked loops.

Finally, Section 3.9 describes an experiment which was performed to determine the nonlinear signal suppression characteristic of the Relay transponder which contains an i-f tripler.

3.1 SUMMARY OF DOPPLER COMPENSATION ANALYSIS

3.1.1 Introduction

The purpose of this section is to provide an over-all view of the theoretical performance of the TDMA doppler compensation system.

Figure 3.1-1 illustrates the main features of the system. It has a master station, one or more slave stations, and a satellite.

The master station has a transmitter at A, a receiver at C, and a frequency standard. The transmitted frequency at the master station is determined by the local standard and the locally received frequency.

The slave station has a transmitter at E, a frequency standard, a receiver at D which measures the locally received version of the master frequency, and a receiver at F which measures the phase error between the master frequency and the slave frequency. The transmitted slave frequency is formed in two steps. First the slave standard frequency and the master received frequency are combined to form an approximate slave transmitted frequency. Then the approximate slave transmitted frequency is phase shifted to form the slave transmitted frequency. The phase shifter is driven by a motor which is controlled by the phase error between the master frequency and the slave frequency.

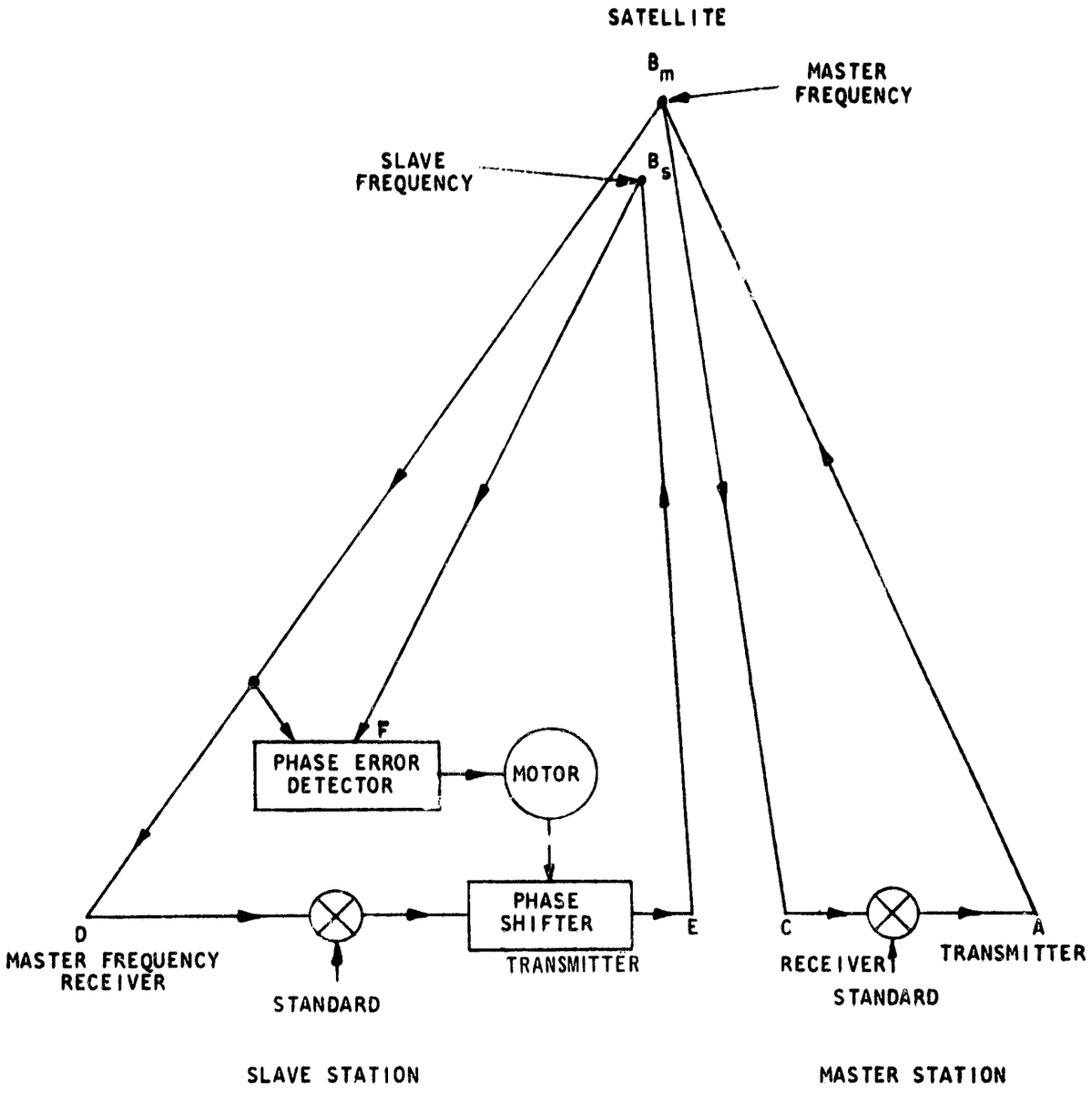

Figure 3.1-1. TDMA Doppler Compensation System

The satellite receives and retransmits both the master frequency and the slave frequency. On the diagram, the point B_m represents the master frequency at the satellite and the point B_s represents the slave frequency at the satellite. The master frequency is transmitted from A and received at C, D and F. The slave frequency is transmitted from E and received at F.

The analysis of this system is divided into three parts.

1. The triangle A B_m C, the master frequency closed loop, is a servomechanism which adjusts the frequency at A so that the frequency at the satellite at B_m is equal to the standard frequency: $\omega = 2\pi$ x 800 kHz.
2. The triangle B_m D E B_s, the slave frequency open loop, with the phase shifter fixed at a reference angle, is an open loop by which the slave station compensates for doppler so that the slave frequency received at the satellite at B_s exactly equals the master frequency received at the satellite at B_m.
3. The triangle B_s F E is the slave phase locked loop by which the slave station adjusts its transmitted phase at E so that the slave frequency received received at the satellite at B_s has the desired phase relation to the master frequency received at the satellite at B_m.

Numerical values for the actual system are as follows: The master frequency is represented by master sync bursts. The leading edges of adjacent master sync bursts are separated at the satellite by 123.75 microseconds. The slave channel bursts are to be spaced within a fraction of a microsecond from their nominal position. The maximum round trip path delay and doppler are on the order of 0.1 second and 10^{-5}, respectively, for Relay.

The following describes the sources of errors in the various loops.

3.1.2 Master Frequency Closed Loop

The master frequency loop is drawn in Figure 3.1-2, which illustrates its implementation. The satellite receives and retransmits the correct frequency w. (Here ω is 2π x 800 kHz.) Because the distance r between the satellite and the master frequency is changing with time, the frequency received at the master receiver will be to first order terms ω (1-d) where d is the doppler coefficient $\frac{1}{c}\frac{dr}{dt}$. Next the received frequency is subtracted from the master

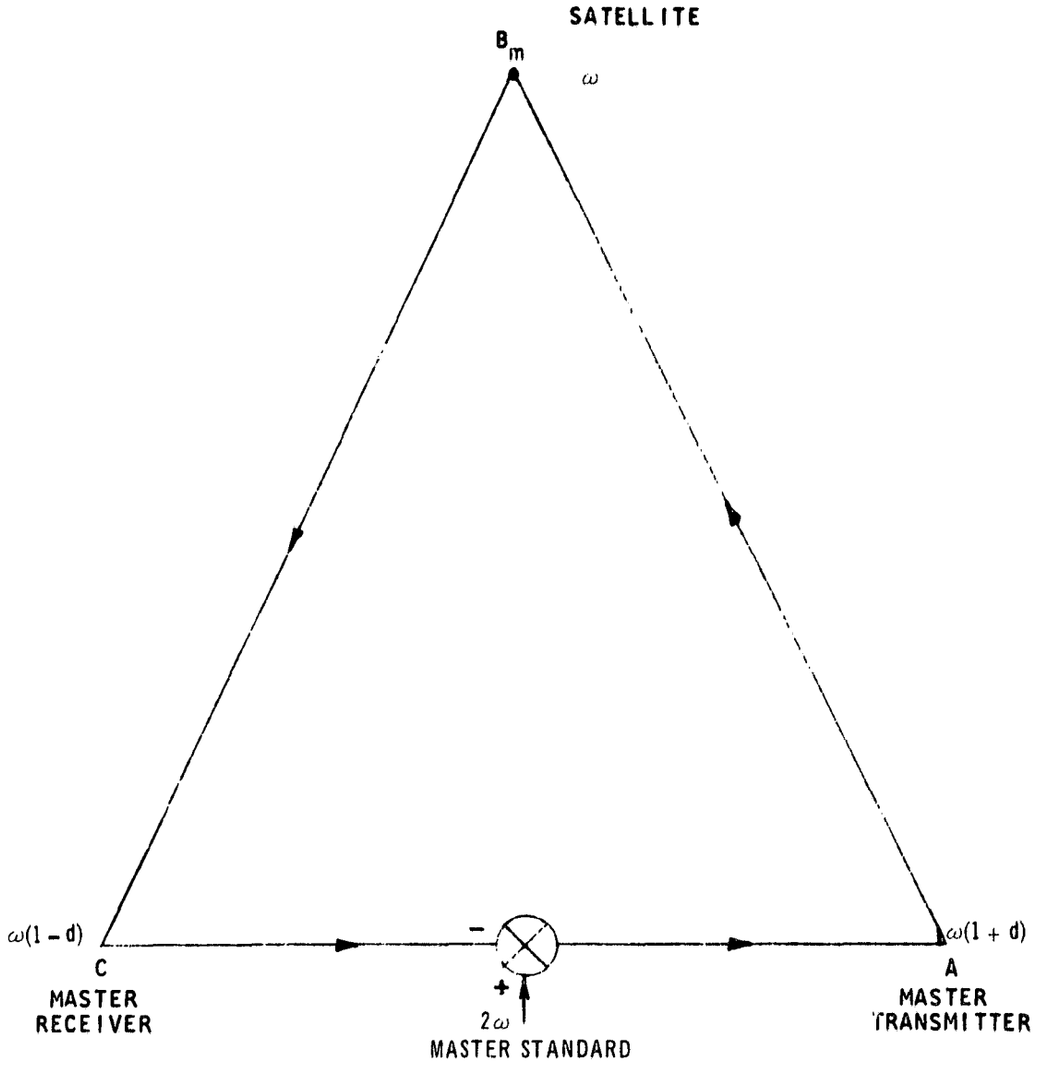

Figure 3.1-2. Nominal Master Frequency Loop

standard 2w which produces a transmitted frequency w (1 + d). Because of the doppler, the frequency transmitted from the master station is received at the satellite with the correct frequency w.

The master frequency loop is supposed to place the reference frequency w in the satellite. However, the satellite frequency will, in practice, differ from the reference frequency because of the following series of errors which will be analyzed in the following sections.

1. Frequency error in master standard.
2. Satellite motion. Although first order doppler terms are cancelled by this loop, higher order error terms remain.
3. Servomechanism error in this loop. The loop should make the sum of received frequency and transmitted frequency at the master station exactly equal to the master standard 2w. However, the loop as shown in unstable and the filtering, inherent in the transmit phase locked loop, needed to make it stable produces a servomechanism error.
4. Phase shifts and delays at the satellite and at the master station.

The diagram in Figure 3.1-2 leaves out various details of this loop which are covered in equipment diagrams and more detailed analysis. These details include how the frequency is modulated on the carrier, shifts of the carrier frequency, amplification of the signal, filtering of the signals, detection of the signal, and the phase lock loop needed to make the over-all loop stable.

The effect of satellite motion on the master frequency closed loop is found in Section 3.2. In that section the idealized loop shown in Figure 3.1-2 is used. The term idealized refers to the assumption that the other sources of error, 1, 3, and 4 above, are ignored.

The main result of Section 3.2 is that the fractional frequency error at the satellite is approximately (Equation 3.2-38).

$$\frac{\omega_m - \omega}{\omega} = - \frac{\dot{r}_m^2 + r_m \ddot{r}_m}{c^2} \qquad (3.1\text{-}1)$$

where

$\omega \quad \omega$ = standard frequency

$\omega_m - \omega$ = master sync frequency error at satellite

r_m = satellite range from master

c = velocity of propagation

Section 3.3 is concerned with the calculation of the magnitude of this frequency error from the parameters of the satellite orbit. It is shown that the maximum error occurs when the ground station is in the plane of the orbit, the satellite is at perigee, and the satellite is at the station's zenith. (These are the same conditions for maximum doppler rate.) The value of the maximum error is (Equation 3.3-29).

$$\left(\frac{\omega_m - \omega}{\omega}\right)_{max} = \frac{4\pi^2 a^2}{c^2 \tau^2 (1-e)} = \left[e + \frac{R}{a(1-e)}\right] , \qquad (3.1\text{-}2)$$

where

a = semi-major axis of orbit ellipse

e = eccentricity

τ = orbit period

R = radius of earth.

For the Relay II orbit (Section 2.4), this quantity is approximately 5 parts/10^{10}.

3.1.3 Slave Frequency Open Loop

The master frequency loop places the reference frequency in the satellite with some error. Next the slave frequency open loop attempts to generate a transmitted slave frequency such that the slave frequency and the master frequency agree at the satellite. The error in the slave frequency open loop operation is the frequency difference between the slave frequency and the master frequency at the satellite.

The nominal slave frequency open loop is illustrated by Figure 3.1-[illegible] The slave station has a receiver at D that detects the master frequency. If the master frequency at the satellite is ω the receiver at D receives ω (1-d) to first order where d is the doppler coefficient for the slave station. In general, the master station and the slaves will be widely separated and have different doppler coefficients. The approximate slave transmit frequency is then generated by subtracting the master frequency at the slave station from the standard frequency 2ω to form the frequency ω (1 + d). This frequency is then transmitted to the satellite where it is received as w because of the doppler.

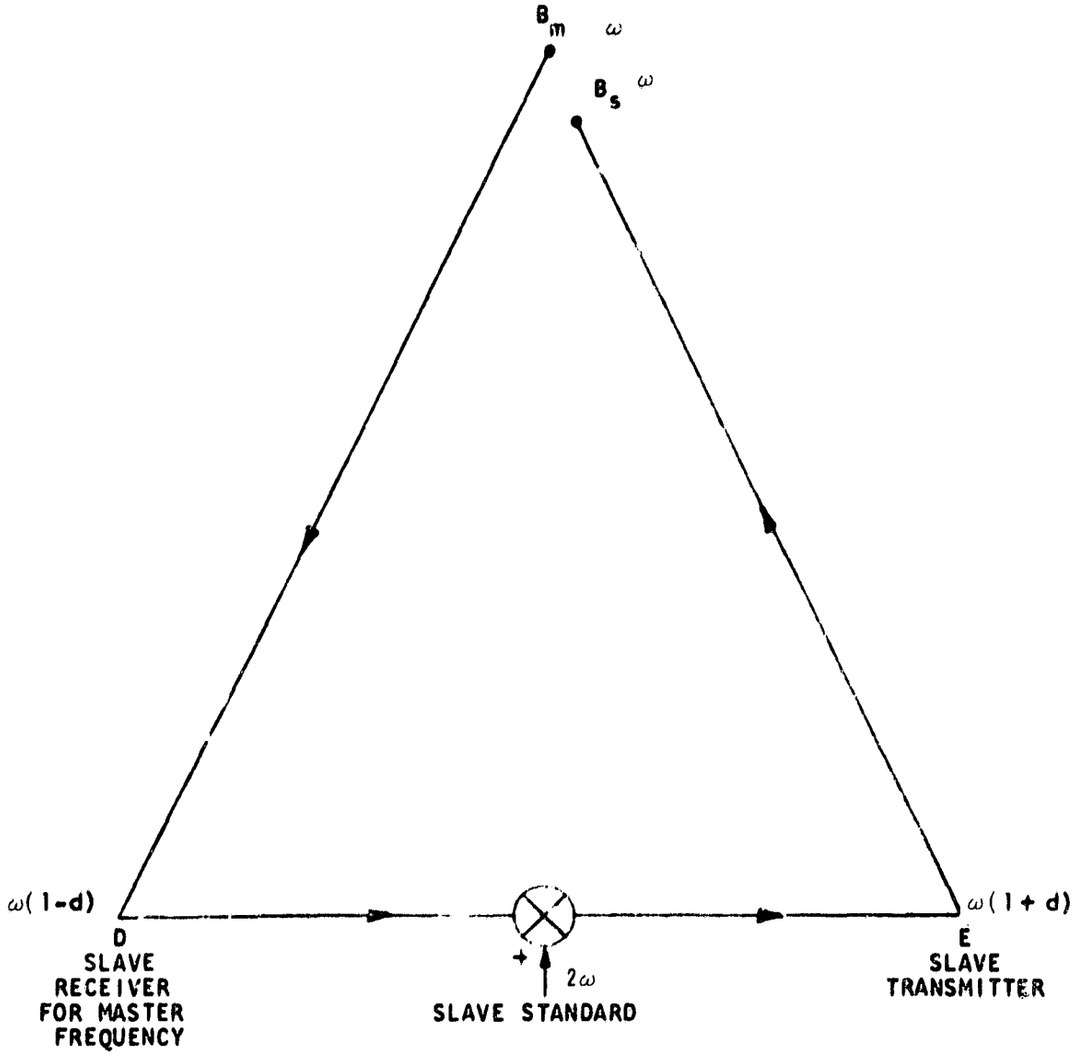

Figure 3.1-3. Nominal Slave Frequency Open Loop

There are several sources of frequency error measured at the satellite, in the slave open loop doppler compensation.

1. Frequency error in the satellite master frequency. An error in the master frequency at the satellite will cause an error in the slave frequency at the satellite.
2. Frequency error in the slave standard.
3. Satellite motion. Although first order doppler terms are cancelled by this loop, higher order error terms remain.
4. Phase shifts and delays at the satellite and the slave station.

The diagram in Figure 3.1-3 leaves out details of the loop covered in equipment diagrams and more detailed analysis. Also, a reference to Figure 3.1-1 will show that while Figure 3.1-3 is a convenient method of analyzing this part of the system; in practice, the slave frequency open loop and the slave frequency phase locked loop overlap each other and use the same transmitter.

The effect of satellite motion on the slave open loop is found in Section 3.4.4. In that section the idealized open loop shown in Figure 3.1-3 is used. Again the idealized case ignores errors due to 1, 2, and 4 above. The fractional frequency error of the slave open loop is shown to be (Equation 3.4-13):

$$\frac{\omega_s - \omega}{\omega} = -2\,\frac{\dot{r}_s^2 + r_s\,\ddot{r}_s}{c^2}, \qquad (3.1\text{-}3)$$

where

$\omega_s - \omega$ = slave open loop frequency error at satellite

$\dot{r}_s$ = satellite range from slave.

Except for the factor of two, this is the same, as Equation 3.1-1 and therefore can be evaluated using 3.1-2.

The combined effects of master frequency error and slave open loop error due to satellite motion are shown in Section 3.4.5 to be (Equation 3.4-14)

$$\frac{\Delta\omega}{\omega} = 2\,\frac{\omega_m - \omega}{\omega} + \frac{\omega_s - \omega}{\omega}, \qquad (3.1\text{-}4)$$

where

$\Delta\omega$ = open loop frequency error at satellite.

This is the frequency error due to satellite motion which must be tracked and corrected by the slave phase locked loop.

Another source of frequency error in the slave open loop doppler compensation is the difference between standard frequencies at the master and slave terminals. This is shown in Section 3.4.6 to be

$$\frac{\Delta\omega}{\omega} = 2(e_m - e_s) \quad , \tag{3.1-5}$$

where

e_m = fractional frequency error in master standard frequency

e_s = fractional frequency error in slave standard frequency .

The TDMA system uses frequency standards whose difference is less than 1 part/10^9.

The last source of error considered in the doppler compensation analysis is phase shifts in various parts of the system. One source of phase shift is the tracking error in either the receive or the transmit clock phase locked loop. Let Θ_k denote a typical such phase shift in the system. It is shown in Section 3.4.3 that this will result in a phase shift Θ_k between the sync signals at B_m and B_s. If this phase shift varies with time, it will cause a frequency error $\dot{\Theta}_k$; the total fractional frequency error due to time varying phase shifts is

$$\frac{\Delta\omega}{\omega} = \frac{1}{\omega} \sum_k \dot{\Theta}_k \quad . \tag{3.1-6}$$

It is shown in Section 3.6 (Equation 3.6-20) that the maximum $\dot{\Theta}_k/\omega$ due to doppler rate will not exceed 0.5 part/10^{10}.

The frequency errors given by 3.1-4, 3.1-5, and 3.1-6 are very small so that their combined effect is additive and therefore the slave phase locked loop must track and correct the sum of these three frequency errors. This total frequency error is thus seen not to exceed a few parts/10^9.

3.1.4 Slave Phase Locked Loop

In the absence of a phase locked loop, the master frequency and the slave frequency will differ slightly at the satellite and the relative phase of master timing and slave timing will slowly shift through all possible values. The slave phase locked loop adjusts the phase of the slave frequency so that at the satellite the slave timing and master timing coincide and the slave data bursts have the correct relation to master synch pulses.

Two ways of treating the slave phase locked loop are illustrated in Figure 3.1-4A and -4B. Figure 3.1-4A portrays the phase locked loop obtained by extracting from Figure 3.1-1 the appropriate system elements. In this diagram, the inputs to the loop are the master frequency and the approximate slave transmit frequency at the slave station. The loop signal is the slave transmit frequency. However, since the system is linear Figure 3.1-4B in which the loop signal is the slave phase correction, can be used. In Figure 3.1-4B, at the satellite the slave phase correction is subtracted from the phase error which would have occurred at the satellite between the master frequency and the slave frequency of the slave phase loop were disabled. The resulting phase error is transmitted from the satellite to the slave station at F. This phase error drives a motor which operates a phase shifter, the output of which is the slave phase correction then transmitted to the satellite.

3.2 ACCURACY OF IDEAL DOPPLER COMPENSATION SERVO

3.2.1 Introduction

In the TDMA system a master station servomechanism places a timing signal with exactly the correct frequency in the satellite. In principle, this servomechanism makes the sum of the timing frequency transmitted from the ground and the timing frequency received at the ground equal to twice the correct frequency. This system will have systematic errors because of the propagation time of the signal and the second derivative of the range with respect to time. It is shown in this section that this frequency error is approximately

$$-\frac{\omega}{c^2}\left[\left(\frac{dr}{dt}\right)^2 + r\,\frac{d^2r}{dt^2}\right],$$

where ω is the signal frequency, c the velocity of light, and r is the range.

A simple analysis for the case where the doppler is constant, which agrees with the more complicated analysis, is discussed first.

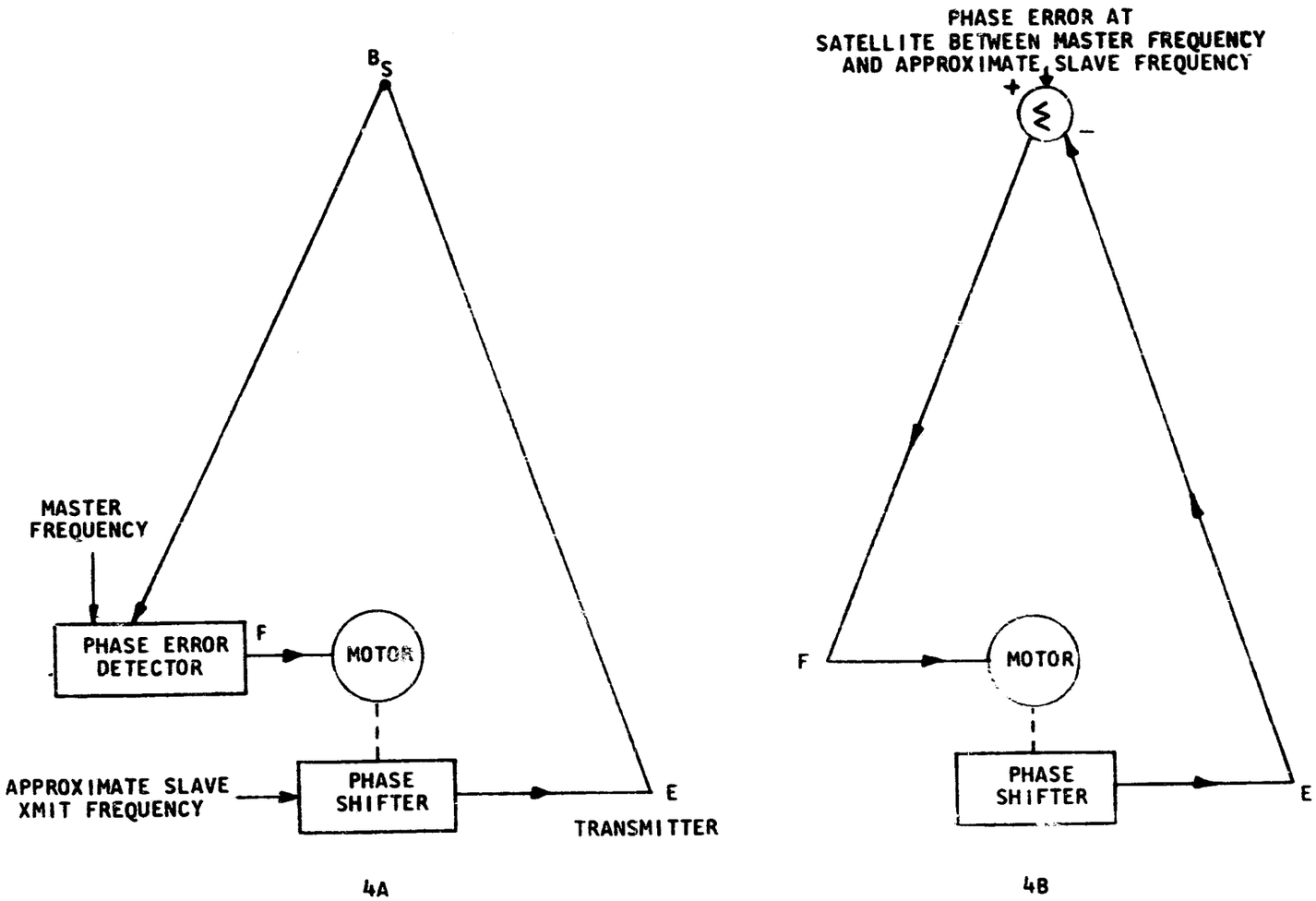

Figure 3.1-4. Nominal Slave Frequency Phase Locked Loop

3.2.2 Description of the Servomechanism

The system is shown in Figure 3.1-2. There is a master ground station which controls the timing signal with a transmitter A, and a receiver C. The satellite is denoted by B. The timing signal is transmitted to the satellite which amplifies and retransmits this signal back to the ground.

The heuristic reasoning behind the servomechanism is as follows: If the satellite has the correct frequency, ω, and there is doppler, d, because the satellite moves, the received frequency at the ground will be too high because of the doppler and have the value $\omega(1+d)$. On the other hand, the transmitted frequency will be too low and have the value $\omega(1-d)$. Thus the correct frequency can be placed in the satellite by adjusting the transmitted frequency so that the sum of the received frequency and transmitted frequency $\omega(1+d) + \omega(1-d)$ is twice the correct frequency.

3.2.3 Constant Doppler Case

This sub-section analyzes the simple case when the satellite doppler is constant. The analysis for this is exact and provides a check on the more complicated analysis for varying satellite doppler. There are known formulae for fixed and moving receivers and transmitters. Doppler is assumed positive if the range is increasing.

$$d = \text{doppler} = \frac{\text{relative velocity}}{\text{speed of light}} \qquad (3.2\text{-}1)$$

A fixed transmitted with frequency ω_1 is received by a moving receiver as a frequency $\omega_1(1-d)$ (3.2-2a)

A moving transmitter with frequency ω_2 is received by a fixed receiver as frequency $\omega_2/(1+d)$ (3.2-2b)

Assume that the satellite frequency is ω_B. Then using equations 3.2-2a and 2b the ground transmitted and received frequencies can be found.

$$\text{Ground transmitted frequency } \omega_A = \frac{\omega_B}{1-d} \qquad (3.2\text{-}3a)$$

$$\text{Ground receiver frequency} = \omega_c = \frac{\omega_B}{1+d} \qquad (3.2\text{-}3b)$$

The servomechanism makes the sum of ω_A and ω_C equal to twice the nominal frequency w. Thus w_B, the satellite frequency, can be solved. It differs from the nominal frequency by the error $-wd^2$ which agrees with the more general case if constant doppler is assumed.

$$\frac{\omega_B}{1-d} + \frac{\omega_B}{1+d} = \frac{2\,\omega_B}{1-d^2} = 2 \qquad (3.2\text{-}4)$$

$$\omega_B = \omega\,(1-d^2) \qquad (3.2\text{-}5)$$

3.2.4 Varying Doppler Case

Next make an exact analysis. The phase deviation of the signals at A, B, and C from the correct frequency are denoted by θ_A, θ_B, θ_C, respectively. If these angles grow linearly with time they will represent a frequency error.

$$\text{Signal at A} = S_A(t) = \sin(\omega t + \theta_A(t)) \qquad (3.2\text{-}6a)$$

$$\text{Signal at B} = S_B(t) = \sin(\omega t + \theta_B(t)) \qquad (3.2\text{-}6b)$$

$$\text{Signal at C} = S_C(t) = \sin(\omega t + \theta_C(t)) \qquad (3.2\text{-}6c)$$

The distance from the satellite to the ground station at time t is denoted by r(t).

$$\text{Range from satellite to ground at t} = r(t) \qquad (3.2\text{-}7a)$$

$$c = \text{velocity of light} \qquad (3.2\text{-}7b)$$

The signal at the satellite is a delayed version of the transmitted signal.

$$S_B(t) = \sin(\omega t + \theta_B(t)) \qquad (3.2\text{-}8a)$$

$$= S_A(t - \tau_{AB}(t)) = \sin\left[\omega\,(t - \tau_{AB}(t)) + \theta_A(t - \tau_{AB}(t))\right]$$

$$\tau_{AB}(t) = \text{the time of flight from A to B of the signal now arriving at B} \qquad (3.2\text{-}8b)$$

$$= \frac{r(t)}{c}$$

The signal at the receiver is a delayed version of the signal at the satellite.

$$S_C(t) = \sin(\omega t + \theta_C(t)) \qquad (3.2\text{-}9)$$

$$= S_B(t - \tau_{BC}(t)) = \sin\left[\omega(t - \tau_{BC}(t)) + \theta_B(t - \tau_{BC}(t))\right]$$

The time of flight from B to C is not easily calculated because when a given point on the signal arrives at C, the satellite is no longer at the place from which that point on the signal was sent. However, the time of flight τ_{BC} is implicitly defined since it is proportional to the range at time $t - \tau_{BC}(t)$.

$$\tau_{BC}(t) = \text{the time of flight from B to C of the signal now arriving at C} \qquad (3.2\text{-}10)$$

$$= \frac{r(t - \tau_{BC}(t))}{c}$$

Next relate the signal at C to the signal at A using equations 3.2-8 to 10.

$$S_C(t) = S_B(t - \tau_{BC}(t)) = S_A\left[t - \tau_{BC}(t) - \tau_{AB}(t - \tau_{BC}(t))\right]$$

$$= S_A\left[t - \frac{r(t - \tau_{BC}(t))}{c} - \frac{r(t - \tau_{BC}(t))}{c}\right] \qquad (3.2\text{-}11)$$

$$S_C(t) = S_A(t - 2\tau_{BC}(t))$$

Next relate θ_C to θ_A using equations 3.2-8, 9 and 11. Also $\tau_{BC}(t)$ is replaced by $\tau(t)$ as this will be the only propagation time used in the subsequent analysis.

$$\tau(t) = \tau_{BC}(t) \qquad (3.2\text{-}12)$$

$$\sin(\omega t + \theta_C(t)) = \sin\left[\omega(t - 2\tau(t)) + \theta_A(t - 2\tau(t))\right] \qquad (3.2\text{-}13a)$$

$$\theta_C(t) = -2\omega\tau(t) + \theta_A(t - 2\tau(t)) \qquad (3.2\text{-}13b)$$

Now a relation for θ_A alone is found using 3.2-13 and the servomechanism relationship that the sum of the frequencies at C and A equal 2ω.

$$2\,\omega t = \omega t + \theta_C(t) + \omega t + \theta_A(t) \qquad (3.2\text{-}14a)$$

$$\theta_A(t) = -\,\theta_C(t) \qquad (3.2\text{-}14b)$$

$$\theta_A(t) + \theta_A(t - 2\,\tau\,(t)) = 2\,\omega\,\tau\,(t) \qquad (3.2\text{-}15)$$

This is the key equation and its solution will be of major interest in the following pages.

At this point a relation will be found between θ_B and θ_A which will be needed to get the satellite frequency once θ_A is known. The derivation uses equation 3.2-8;

$$\omega t + \theta_B(t) = \omega t - \omega\,\tau_{AB}(t) + \theta_A\left[t - \tau_{AB}(t)\right] \qquad (3.2\text{-}16a)$$

$$\theta_B(t) = -\,\omega\,\frac{r(t)}{c} + \theta_A\left[t - \frac{r(t)}{c}\right] \qquad (3.2\text{-}16b)$$

3.2.5 Calculation of $\tau(t)$

Assume the r(t) is parabolic. This will then have two non-zero derivatives of time

$$\frac{r(t)}{c} = r_0 + r_1 t + r_2 t^2 \qquad (3.2\text{-}17)$$

The peak values of r_0, r_1 and r_2 for Relay will be on the order of 10^{-1}, 10^{-5}, and 10^{-7}, respectively, so that equation 3.2-17 will be a good description of the satellite range for intervals of time as long as a minute, if the appropriate values of r_0, r_1, r_2, are chosen. For longer intervals, equation 3.2-17 will be clearly inappropriate as the velocities and ranges in equation 3.2-17 become infinite with increasing time while both the velocity and the range of Relay are bounded.

The following discussion uses approximation methods in which only the more significant terms are retained. A few words as to how one determines which are the more significant terms will be helpful. Three sets of variables are used: r_n, τ_n, θ_n. The approximate orders of magnitude are as follows:

r_o, τ_o, θ_0 all have values on the order of 10^{-1}

r_1, τ_1, θ_1 all have values on the order of 10^{-5}

r_2, τ_2, θ_2 all have values on the order of 10^{-7}

This can be checked by examination of the various equations. The neglected terms in general have values less than or equal to 10^{-12} using the above values. Thus $r_1 r_2$, r_2^2 or $r_2 \tau_2$ or r_1^3 are usually neglected as they have values on the order of 10^{-12}, 10^{-13}, 10^{-14} and 10^{-15}, respectively. On the other hand r_1^2 and $r_o r_2$ are kept because they have values on the order of 10^{-10} and 10^{-8}, respectively.

Next a power series is found for $\tau(t)$ in terms of r_o, r_1, r_2. Using equations 3.2-10, 12 and 17.

$$\tau(t) = \frac{r(t - \tau(t))}{c} = r_o + r_1 \left[t - \tau(t)\right] + r_2 \left[t - \tau(t)\right]^2 \qquad (3.2\text{-}18)$$

Equation 3.2-18 is quadratic in $\tau(t)$ and can be solved for $\tau(0)$.

$$\tau(0) = r_o - r_1 \tau(0) + r_2 \tau^2(0) \qquad (3.2\text{-}19)$$

$$\tau(0) = \frac{1 + r_1 \pm \sqrt{(1+r_1)^2 - 4 r_2 r_o}}{2 r_2} \qquad (3.2\text{-}20)$$

There are two mathematical solution for $\tau(0)$ depending whether the plus or minus sign is used in equation 3.2-20. For the magnitude of r_o, r_1, and r_2 with which we are concerned, the plus sign solution can be neglected because of the following argument. Since r_1 and $r_o r_2$ are both much less than one, $\tau(0)$ with a plus sign is about $1/r_2$. Since the magnitude of r_2 is about 10^{-7} this means that the solution for $\tau(0)$ with the plus sign corresponds to a one-way path delay of over 10^7 seconds which is clearly unrealistic.

Next equation 3.2-18 is differentiated. Assume in the derivation that the unit of distance is the distance traveled by light in one second so that c can be ignored in the following:

$$\dot{\tau}(t) = \dot{r}(t - \tau(t))\ (1 - \dot{\tau}(t)) \tag{3.2-21}$$

$$\dot{\tau}(t) = \frac{\dot{r}(t - \tau(t))}{1 + \dot{r}(t - \tau(t))} = 1 - \frac{1}{1 + \dot{r}(t - \tau(t))} \tag{3.2-22}$$

$$1 - \dot{\tau}(t) = \frac{1}{1 + \dot{r}(t - \tau(t))} \tag{3.2-23}$$

Differentiating equation 3.2-22

$$\ddot{\tau}(t) = \frac{\ddot{r}(t - \tau(t))\,(1 - \dot{\tau}(t))}{\left[1 + \dot{r}(t - \tau(t))\right]^2} \tag{3.2-24}$$

Using the fact that $\ddot{r}(t) = 2\ r_2$ and equation 3.2-23

$$\ddot{\tau}(t) = \frac{2\ r_2}{\left[1 + \dot{r}(t - \tau(t))\right]^3} \tag{3.2-25}$$

By the use of induction, equation 3.2-23 and the fact that $\ddot{r}(t) = 2\ r_2$, it can be shown

$$\frac{d^n \tau(t)}{dt^n} = \frac{(-1)^n\ 2\,(2n-3)!\ r_2^{\,n-1}}{(n-2)!\ \left[1 + \dot{r}(t - \tau(t))\right]^{2n-1}} \tag{3.2-26}$$

for $n = 2, 3, 4, \ldots$

Expanding $\tau(t)$ in a power series and using equations 3.2-18, 20, 22 and 26.

$$\tau(t) = \tau_o + \tau_1 t + \tau_2 t^2 + \tau_3 t^3 \ldots \tag{3.2-27}$$

where

$$\tau_n = \frac{1}{n!} \left.\frac{d^n \tau(t)}{dt^n}\right|_{t=o}$$

$$\tau_o = \frac{(1 + r_1)\left[1 - \sqrt{1 - \frac{4\, r_2\, r_o}{(1 + r_1)^2}}\right]}{2\, r_2} \approx \frac{r_o}{1 + r_1}\left[1 + \frac{r_2\, r_o}{(1 + r_1)^2}\right]$$

$$\tau_1 = \frac{\dot{r}(-\tau_o)}{1 + \dot{r}(-\tau_o)} = \frac{r_1 - 2\, r_2\, \tau_o}{1 + r_1 - 2\, r_2\, \tau_o}$$

$$\tau_2 = \frac{r_2}{(1 + r_1 - 2\, r_2\, \tau_o)^3}$$

$$\tau_3 = \frac{(-1)^3 \cdot 2 \cdot 3! \cdot r_2^2}{3! \cdot 1! \cdot (1 + r_1 - 2\, r_2\, \tau_o)^5} = \frac{-2\, r_2^2}{(1 + r_1 - 2\, r_2\, \tau_o)^5}$$

3.2.6 Calculation of $\theta_A(t)$

Next an approximate solution of θ_A will be found. Repeating equation 3.2-15.

$$\theta_A(t) + \theta_A(t - 2\,\tau(t)) = 2\,\omega\,\tau(t). \qquad (3.2\text{-}28)$$

Now assume that $\theta_A(t)$ and $\tau(t)$ can be represented by a power series

$$\theta_A(t) = \omega\,\theta_o + \omega\,\theta_1\, t + \omega\,\theta_2\, t^2 \ldots \qquad (3.2\text{-}29a)$$

$$\tau(t) = \tau_o + \tau_1\, t + \tau_2\, t^2 + \tau_3\, t^3 \ldots \qquad (3.2\text{-}29b)$$

Substituting equation 3.2-29 into equation 3.2-28 and eliminating terms of t^3 and higher.

$$\omega\left\{\theta_o + \theta_1\, t + \theta_2\, t^2 + \theta_0 + \theta_1\left[t - 2\,\tau_o - 2\,\tau_1\, t - 2\,\tau_2\, t^2\right]\right. \qquad (3.2\text{-}30)$$
$$\left. + \theta_2 \cdot \left[t - 2\,\tau_o - 2\,\tau_1\, t - 2\,\tau_2\, t^2\right]^2 = \omega(2\,\tau_o + 2\,\tau_1\, t + 2\,\tau_2\, t^2)\right\}$$

$$2\theta_o - 2\theta_1 \tau_o + 4\theta_2 \tau_o^2 + t(2\theta_1 - 2\theta_1 \tau_1 - 4\theta_2 \tau_o + 8\theta_2 \tau_o \tau_1) + t^2(2\theta_2 - 2\theta_1 \tau_2 + 4\theta_2 \tau_1^2 - 4\theta_2 \tau_1 + 8\theta_2 \tau_o \tau_2) = 2\tau_o + 2\tau_1 t + 2\tau_2 t^2 \quad (3.2\text{-}31)$$

Setting coefficients of like powers of t equal we get three equations

$$\theta_o = \tau_o + \theta_1 \tau_o - 2\theta_2 \tau_o^2 \quad (3.2\text{-}32a)$$

$$\theta_1(1 - \tau_1) + \theta_2(-2\tau_o + 4\tau_o \tau_1) = \tau_1 \quad (3.2\text{-}32b)$$

$$-\theta_1 \tau_2 + \theta_2(1 + 2\tau_1^2 - 2\tau_1 + 4\tau_o \tau_2) = \tau_2 \quad (3.2\text{-}32c)$$

Solving for θ_1 and θ_2 using 3.2-32b and 32c and then substituting into equation 3.2-32a

$$\theta_2 = \frac{\tau_2}{1 - 3\tau_1 + 4\tau_1^2 - 2\tau_1^3 + 2\tau_o \tau_2} \quad (3.2\text{-}33a)$$

$$\theta_1 = \frac{\tau_1 - 2\tau_1^2 + 2\tau_1^3 + 2\tau_o \tau_2}{1 - 3\tau_1 + 4\tau_1^2 - 2\tau_1^3 + 2\tau_o \tau_2} \quad (3.2\text{-}33b)$$

$$\theta_o = \tau_o + \theta_1 \tau_o - 2\theta_2 \tau_o^2 \quad (3.2\text{-}33c)$$

Using equations 3.2-33 an approximation to θ_o, θ_1, θ_2 can be obtained

$$\theta_o = \tau_o + \tau_o \tau_1 + \tau_o \tau_1^2 \quad (3.2\text{-}34a)$$

$$\theta_1 = \tau_1 + \tau_1^2 + \tau_1^3 + 2\tau_o \tau_2 + 4\tau_o \tau_1 \tau_2 \quad (3.2\text{-}34b)$$

$$\theta_2 = \tau_2 + 3\tau_1 \tau_2 + 5\tau_1^2 \tau_2 - 2\tau_o \tau_2^2 \quad (3.2\text{-}34c)$$

Equations 3.2-34 and 29a give an approximation to θ_A (t) as a function of τ_o, τ_1, τ_2.

3.2.7 Calculation of Frequency Offset

Next the frequency offset at the satellite is calculated. Using equation 3.2-16, 17, and 29.

$$\theta_B(t) = -\omega(r_o + r_1 t + r_2 t^2) + \omega\theta_o \qquad (3.2\text{-}35)$$

$$+ \omega\theta_1(t - r_o - r_1 t - r_2 t^2) + \omega\theta_2(t - r_o - r_1 t - r_2 t^2)^2$$

$$\left.\frac{d\theta_B(t)}{dt}\right|_{t=o} = \omega\left[-r_1 + \theta_1(1-r_1) + 2\theta_2(t - r_o - r_1 t - r_2 t^2)(1-r_1)\right]$$

$$= \omega\left[-r_1 + (1-r_1)(\theta_1 - 2 r_o \theta_2)\right] \qquad (3.2\text{-}36)$$

Using equations 3.2-36, 34, and 27 and neglecting all items whose magnitude is 10^{-12} or smaller (i.e., terms such as r_1, r_2, r_1^3, $r_o\ r_1\ r_2$, etc.).

$$\left.\frac{d\theta_B(t)}{dt}\right|_{t=o} \approx -\omega(r_1^2 + 2 r_o r_2) \qquad (3.2\text{-}37)$$

Frequency offset at the satellite

$$\frac{d\theta_B(t)}{dt} \approx -\frac{\omega}{c^2}\left(\left(\frac{dr}{dt}\right)^2 + r\frac{d^2 r}{dt^2}\right) \qquad (3.2\text{-}38)$$

The minus sign means that if the first two derivatives of satellite range are positive, the satellite frequency will be lower than the ideal frequency w.

3.3 CALCULATION OF MAXIMUM FREQUENCY ERROR

The purpose of this section is to compute the maximum magnitude of the master frequency error determined in Section 3.2 from the parameters of the satellite orbit. The orbit parameters are defined in Figure 3.3-1 and the geometry for the problem is shown in Figure 3.3-2. The range of the satellite from the station, which is denoted r in other sections, will be denoted ρ for this section only.

The following assumptions are made in the calculation.

1. Stationary earth. It seems reasonable, since Relay II has a period 1/8 of of the earth and also has a much higher average velocity than the earth, that the results will be approximately correct.
2. Ground station lies on the plane of the satellite orbit which is an ellipse. We will also show that a calculation for an out-of-plane ground station gives a smaller peak frequency error.

The following four basic equations of an elliptical orbit are used to derive all the results of this section;

a. Equation of ellipse (polar coordinates):

$$r = \frac{\ell}{1 + e \cos \theta} \tag{3.3-1}$$

b. Relation between ℓ, e, a:

$$\ell = a(1 - e^2) \tag{3.3-2}$$

c. Kepler's second law:

$$r^2 \dot{\theta} = K = \sqrt{\mu \ell} \tag{3.3-3}$$

d. Period of orbit:

$$\tau = 2\pi \sqrt{\frac{a^3}{\mu}} \tag{3.3-4}$$

First show how a and e are related to r_{max} and r_{min}. Using 3.3-1

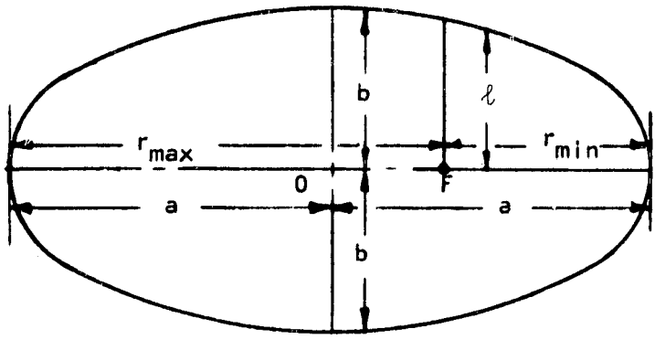

ℓ - SEMI-LATUS RECTUM
a - SEMI-MAJOR AXIS
b - SEMI-MINOR AXIS
e - ECCENTRICITY
μ - GRAVITATIONAL CONSTANT OF EARTH
τ - ORBIT PERIOD
F - FOCUS OF ELLIPSE

Figure 3.3-1. Ellipse Parameters

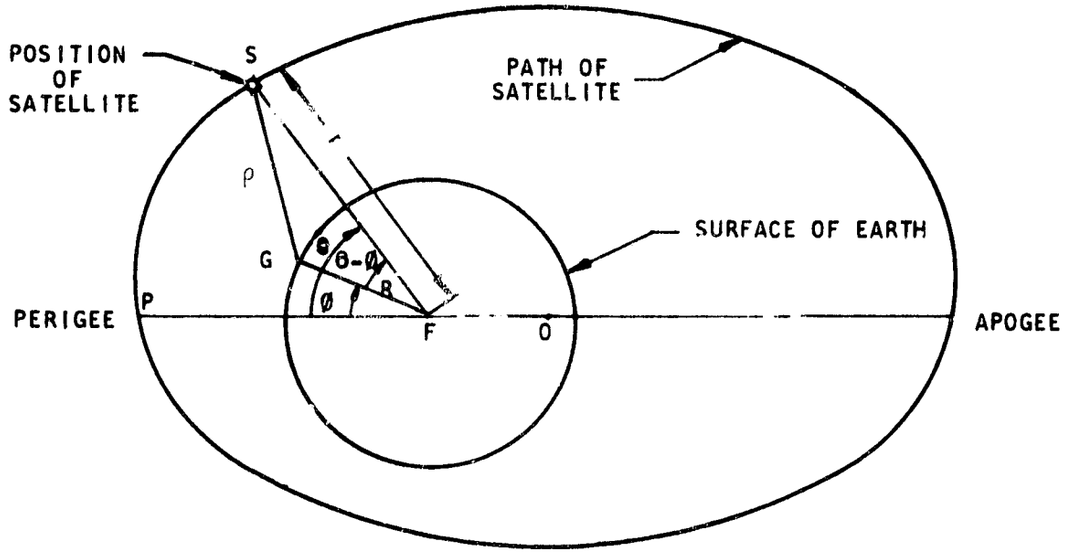

S - SATELLITE POSITION
G - GROUND STATION POSITION
F - FOCUS OF ELLIPSE
  - CENTER OF EARTH
R - DISTANCE FROM F TO G
ρ - DISTANCE FROM G TO S
r - DISTANCE FROM F TO S
O - CENTER OF ELLIPSE
P - PERIGEE
θ - ANGLE PFS
ϕ - ANGLE PFG

Figure 3.3-2. Satellite Orbit

$$r_{max} = \frac{\ell}{1-e} \quad ; \quad r_{min} = \frac{\ell}{1+e} \tag{3.3-5}$$

and 3.3-2 gives

$$a = \frac{\ell}{1-e^2} = \frac{\ell}{2} \frac{1+e+1-e}{(1+e)(1-e)} = \frac{r_{max} + r_{min}}{2} \tag{3.3-6}$$

$$r_{max} = \frac{a(1-e^2)}{1-e} = a(1+e) \tag{3.3-7}$$

$$e = \frac{r_{max}}{a} - 1 \ . \tag{3.3-8}$$

Next evaluate $\dot{\rho}^2 + \rho\ddot{\rho}$,

$$\frac{d^2}{dt^2}\left(\frac{1}{2}\rho^2\right) = \frac{d}{dt}(\rho\dot{\rho}) = \dot{\rho}^2 + \rho\ddot{\rho} . \tag{3.3-9}$$

Using the law of cosines in Figure 3.3-2 gives

$$\rho^2 = r^2 + R^2 - 2rR\cos(\theta - \varphi) \tag{3.3-10}$$

$$\frac{d}{dt}\left(\frac{1}{2}\rho^2\right) = r\dot{r} + R\left[-\dot{r}\cos(\theta-\varphi) + r\dot{\theta}\sin(\theta-\varphi)\right] \tag{3.3-11}$$

$$\begin{aligned}\frac{d^2}{dt^2}\left(\frac{1}{2}\rho^2\right) = {} & \dot{r}^2 + r\ddot{r} + R\left[-\ddot{r}\cos(\theta-\varphi)\right. \\ & + \dot{r}\dot{\theta}\sin(\theta-\varphi) + \dot{r}\dot{\theta}\sin(\theta-\varphi) \\ & \left. + r\ddot{\theta}\sin(\theta-\varphi) + r\dot{\theta}^2\cos(\theta-\varphi)\right]\end{aligned} \tag{3.3-12}$$

$$\begin{aligned}\frac{d^2}{dt^2}\left(\frac{1}{2}\rho^2\right) = {} & \dot{r}^2 + r\ddot{r} + R\left[\cos(\theta-\varphi)(-\ddot{r} + r\dot{\theta}^2)\right. \\ & \left. + \sin(\theta-\varphi)(2\dot{r}\dot{\theta} + r\ddot{\theta})\right] .\end{aligned} \tag{3.3-13}$$

The last equation will be simplified by showing that

$$\text{(i)} \quad \dot{r}^2 + r\ddot{r} = \frac{K^2}{\ell^2} \left(e^2 + e \cos\theta\right)$$

$$\text{(ii)} \quad 2\,\dot{r}\,\dot{\theta} + r\,\ddot{\theta} = 0$$

$$\text{(iii)} \quad -\ddot{r} + r\,\dot{\theta}^2 = \frac{K^2}{\ell^3} \left(1 + e \cos\theta\right)^2$$

When these relations are shown, 3.3-13 will become

$$\frac{d^2}{dt^2}\left(\frac{1}{2}\rho^2\right) = \frac{K^2}{\ell^2}\left[e^2 + c\cos\theta + \frac{R}{\ell}\cos(\theta-\phi)\,(1+e\cos\theta)^2\right] . \tag{3.3-14}$$

Relation (ii) follows from 3.3-3,

$$r^2\,\dot{\theta} = K \tag{3.3-15}$$

$$\frac{d}{dt}\left(r^2\,\dot{\theta}\right) = r^2\,\ddot{\theta} + 2\,r\,\dot{r}\,\dot{\theta} = r\left(2\,\dot{r}\,\dot{\theta} + r\,\ddot{\theta}\right) = 0 . \tag{3.3-16}$$

The other two relations will be shown next. To this end we evaluate $\dot{\theta}$, r, $\dot{r}$, $\ddot{r}$. From 3.3-1

$$r = \frac{\ell}{1 + e\cos\theta} . \tag{3.3-17}$$

Substituting 3.3-3 into this gives

$$\dot{\theta} = \frac{K}{r^2} = \frac{K\,(1 + e\cos\theta)^2}{\ell^2} \tag{3.3-18}$$

Differentiating 3.3-17 and using 3.3-18 gives

$$\dot{r} = \frac{-\ell\,(-e\sin\theta)\,\dot{\theta}}{(1 + e\cos\theta)^2} = \frac{el\sin\theta}{(1 + e\cos\theta)^2} \cdot \frac{K\,(1 + e\cos\theta)^2}{\ell^2} \tag{3.3-19}$$

$$\dot{r} = \frac{eK \sin \theta}{\ell} \tag{3.3-20}$$

Differentiating 3.3-20 and again using 3.3-18 gives

$$\ddot{r} = \frac{eK}{\ell} (\cos \theta)\dot{\theta} = \frac{eK^2}{\ell^3} \cos \theta \ (1 \pm e \cos \theta)^2 \tag{3.3-21}$$

The above equations are used to show relation (iii)

$$-\ddot{r} + r\dot{\theta}^2 = \frac{-eK^2}{\ell^3} \cos \theta (1 + e \cos \theta)^2$$

$$+ \frac{1}{1 + e \cos \theta} \frac{K^2}{\ell^4} (1 + e \cos \theta)^4$$

$$= \frac{K^2}{\ell^3} (1 + e \cos \theta)^2 (- e \cos \theta + 1 + e \cos \theta) \tag{3.3-22}$$

and also relation (i)

$$\dot{r}^2 + r\ddot{r} = \frac{e^2 K^2}{\ell^2} \sin^2 \theta + \frac{eK^2}{(1 + e \cos \theta)} \frac{}{l^3} \cos \theta \ (1 + e \cos \theta)^2$$

$$= \frac{K^2}{\ell^2} \left[e^2 \sin^2 \theta + e \cos \theta (1 + e \cos \theta)\right] \tag{3.3-23}$$

$$\dot{r}^2 + r\ddot{r} = \frac{K^2}{\ell^2} (e^2 + e \cos \theta) \tag{3.3-24}$$

Thus the three relations are shown and 3.3-14 follows from 3.3-13.

Next the constant K^2/ℓ^2 is evaluated from 3.3-2 and 3.3-3.

$$\frac{K^2}{\ell^2} = \frac{\mu l}{\ell^2} = \frac{\mu}{a(1 - e^2)} \tag{3.3-25}$$

and 3.3-4

$$\mu = \frac{4 \pi^2 a^3}{\tau^2} \tag{3.3-26}$$

$$\frac{K^2}{l^2} = \frac{4\pi^2 a^3}{\tau^2 a(1-e^2)} = \frac{4\pi^2 a^2}{\tau^2(1-e^2)} \qquad (3.3\text{-}27)$$

Finally, using 3.3-2, 14 and 27, 3.3-14 becomes

$$\dot{\rho}^2 + \rho\ddot{\rho} = \frac{4\pi^2 a^2}{\tau^2(1-e^2)}\left[e^2 + e\cos\theta + \frac{R\cos(\theta-\varphi)(1+e\cos\theta)^2}{a(1-e^2)}\right] \qquad (3.3\text{-}28)$$

The right hand side of 3.3-28 has maximum magnitude if each term is maximum. This occurs for $\theta = \varphi = 0$ (notice that $0 < e < 1$, $0 < \tau$, $0 < a$, $0 < R$). Thus

$$\left|\dot{\rho} + \rho\ddot{\rho}\right|_{\text{peak}} = \frac{4\pi^2 a^2}{\tau^2(1-e^2)}\left[e(1+e) + \frac{R}{a}\frac{1+e}{1-e}\right]$$

$$= \frac{4\pi^2 a^2}{\tau^2(1-e)}\left[e + \frac{R}{a(1-e)}\right] \qquad (3.3\text{-}29)$$

The case $\theta = \varphi = 0$ occurs at perigee and satellite overhead.

It remains to show that a ground station which is not in the plane of the orbit will have a smaller peak frequency error. Assume a new ground station G_1 not in the orbit plane shown in Figure 3.3-2 so that the line GG_1 is perpendicular to the orbit plane. If G_1 is on the surface of the earth, G must be on a sphere of radius smaller than R if GG_1 is to be perpendicular to the orbit plane. Let h denote the length of GG_1 and let ρ_1 denote the range of the satellite from G_1. Since SGG_1 is a right triangle,

$$\rho_1^2 = \rho^2 + h^2 \qquad (3.3\text{-}30)$$

Differentiating both sides twice with respect to time, and noting that h is a constant, shows that

$$\frac{d^2}{dt^2}\left(\frac{1}{2}\rho_1^2\right) = \dot{\rho}_1^2 + \rho_1\ddot{\rho}_1 = \dot{\rho}^2 + \rho\ddot{\rho} \qquad (3.3\text{-}31)$$

Thus G_1 and G will have exactly the same frequency error. However, the peak frequency error for G is given by 3.3-29 with a value of R smaller than the radius of the earth. Thus the peak frequency error for G_1 will be smaller than for a station in the orbit plane.

3.4 EFFECTS OF PHASE SHIFTS AND DOPPLER RATE ON DOPPLER COMPENSATION

3.4.1 Introduction

This section continues the description of the TDMA doppler compensation analysis started in sections 3.1 and 3.2. The effects of phase shifts in the various links are analyzed first. It will be shown that a phase shift anywhere in the system links must be compensated by the slave phase correction loop on a one-to-one basis.

Next, the effect of doppler rate on the slave open loop is considered. It is shown that the effect has the form

$$\frac{1}{c^2}\left[\left(\frac{dr}{dt}\right)^2 + r\left(\frac{d^2r}{dt^2}\right)\right]$$

just as in the master station loop (see section 3.2). The slave phase compensation servomechanism must compensate twice the difference between the doppler rate effect for the master loop and the doppler rate effect for the slave loop. This effect is no larger than 1×10^{-9} for Relay.

3.4.2 Phase Shifts In The System

In addition to the delays incurred when the signal goes from the ground to the satellite and back, there will be various phase shifts in the system. These phase shifts can occur in any of the filtering or mixing operations in the satellite or on the ground. In addition to this, the effect of the master frequency servomechanism in the signal can be described in terms of a phase shift. If the servo works perfectly, $wt + \theta_A + wt + \theta_C = 2\ wt$ or $\theta_A = -\theta_C$ (see Equation 3.2-14b). However, the servomechanism in practice will have a phase error and $\theta_A = -\theta_C + \theta_{err}$. Thus the servomechanism will in effect introduce a phase error θ_{err}.

One should be careful to distinguish between the timing signal and its carrier. The timing signal is represented either by an 800 khz sine wave or pulses with an 800 khz pulse repetition rate. Phase shifts or time delays in these signals will cause timing errors. However, when the timing signal is modulated on a carrier, the carrier can have phase shifts or frequency errors without affecting the timing of the signal. Thus, one should be careful to consider phase shifts in the timing signals and not phase shifts in the carriers.

The following discussion will consider the effect of a phase shift in the system on the phase error between the master timing signal and the slave open loop timing signal at the satellite. It will be shown that a unit phase shift in the system produces a unit phase error between the master timing signal and slave open loop timing signal at the satellite. This error must be compensated by the slave phase locked loop. If the phase errors are fixed, then this is an initial correction. If the phase error changes with time, the slave phase servo will have to follow it. An intuitive guess is that the total phase shift should be no more than a few radians in a half hour pass. This is an error of about one revolution compared to 800 khz for 1800 seconds or about 7×10^{-10}. Thus, this source of error puts a negligible load on the phase servo.

3.4.3 Calculation of Phase Errors Due To Phase Shifts

The basic method of calculation will be to assume a phase shift someplace in the system (see Figure 3.4-1) and then calculate the phase error that will appear between B_m and B_s. It is assumed that the system has been allowed to stabilize and thus the following describes only the incremental phase errors in the signal due to each of the assumed phase shifts.

The first case is a phase shift in the path from B_m to D in the slave open loop. This could be caused, for example, by a tracking error in the receive clock tracking phase locked loop in the slave terminal. In this case the signal at B_m is correct (0 degrees phase) and has an angle ϕ at D, E and B_s. See figure 3.4-1A. Thus, a phase advance of ϕ in the path B_m D causes the slave open loop signal at B_s to be retarded ϕ relative to the signal at B_m. Similarly a phase shift of ϕ anywhere in the path B_m D E B_s causes a phase error, whose magnitude is ϕ, between the signals at B_m and B_s. For example, a phase shift in the path EB_s can be caused by a phase error in the transmit phase locked loop at the slave terminal (see Section 3.6 for equations expressing tracking error of phase locked loops).

Next consider the effect on the slave open loop of a phase shift ϕ at B_m. As seen in figure 3.4-1B, this will cause an opposite phase shift $-\phi$ in B_s so that phase shift ϕ in B_m causes twice the phase difference, i. e., 2ϕ, to appear in the difference $B_m - B_s$. With this result the effect of a phase shift in the master frequency loop can be studied.

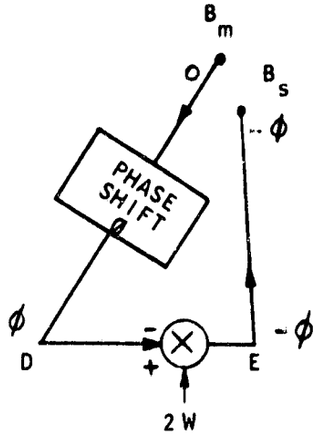

FIGURE a

NOMINAL SLAVE FREQUENCY OPEN LOOP WITH PHASE SHIFT IN PATH B_m D

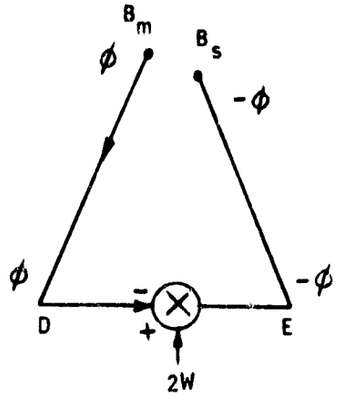

FIGURE b

NOMINAL SLAVE FREQUENCY OPEN LOOP WITH PHASE ERROR AT B_m

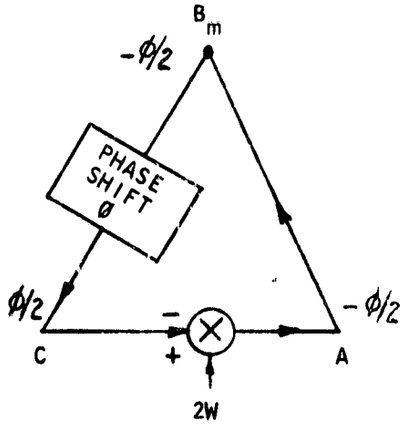

FIGURE c

MASTER FREQUENCY LOOP WITH PHASE SHIFT IN PATH BC

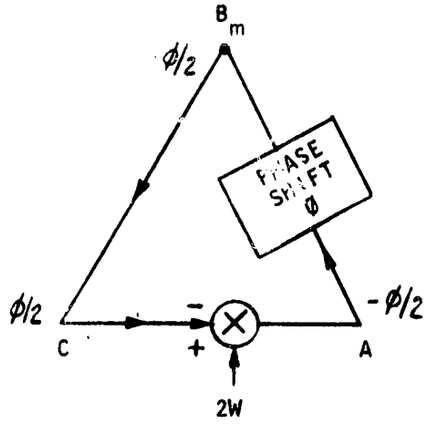

FIGURE d

MASTER FREQUENCY LOOP WITH PHASE SHIFT IN PATH A B_m

Figure 3.4-1. Phase Shifts in Master Loop

Assume a phase shift ϕ in the master frequency loop in the path B_m C, such as that due to receive clock tracking phase locked loop at master. Because of the servomechanism action of the loop; i.e., $\theta_c = -\phi_a$, this will result in a phase shift of 1/2 ϕ at B_m as seen in Figure 3.4-1C. Similarly, a phase shift ϕ in the path A B_m will cause the signal at B_m to have a phase shift of 1/2 ϕ as seen in Figure 3.4-1D. In general, a phase shift of ϕ the closed loop A B_m C will cause the signal at B_m to shift by an angle whose magnitude is 1/2 ϕ. The phase shift of 1/2 ϕ at B_m will cause a phase error $B_m - B_s$ of magnitude ϕ (see Figure 3.4-1B). Thus we have shown that a phase shift ϕ anywhere in the closed master loop A B_m C or the slave open loop B_m D E B_s causes a phase error of magnitude ϕ between the signals at B_m and B_s.

3.4.4 Calculation of Doppler Effects on the Slave Open Loop

The following will calculate the effects of doppler on the slave open loop. This calculation is similar to the calculation on the effects of doppler on the master closed frequency loop in Section 3.2. This calculation will include the effect of delays in the slave station and in the satellite. These delays will be assumed constant and of the same order of magnitude as the satellite to ground delay for all questions of retaining or dropping terms.

The diagram for this system is given in Figure 3.4-2. A delay D_2 is assumed to exist between the slave receiver at D and the input to the mixer which is denoted by D*. A delay D_1 is assumed to exist between B_s which is at the satellite output and B* which is at the satellite receiver.

The following quantities are defined as in Section 3.2.

Range from satellite to ground at time t = r (t) (3.4-1a)

$$\frac{r(t)}{c} = r_0 + r_1 t + r_2 t^2 \qquad (3.4\text{-}1b)$$

c = velocity of light

$\tau_{EB^*}(t)$ = the propagation time from E to B* of the signal now arriving at B* (3.4-2a)

$$= \frac{r(t)}{c}$$

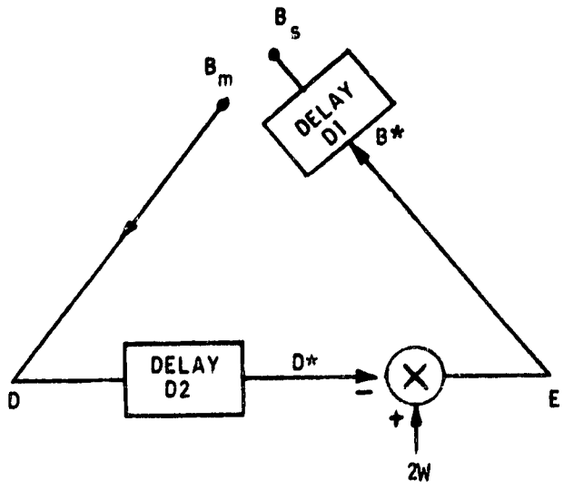

Figure 3.4-2. Delays in Slave Open Loop

$$\tau_{BmD}(t) = \text{the propagation time from } B_m \text{ to D of the signal now arriving at D} \quad (3.4\text{-}2b)$$

$$= \frac{r\left(t - \tau_{BmD}(t)\right)}{c}$$

$$\text{Signal at } B_m = S_{Bm}(t) = \sin\left(\omega t + \theta_{Bm}(t)\right) \quad (3.4\text{-}3a)$$

$$\text{Signal at D} = S_D(t) = \sin\left(\omega t + \theta_D(t)\right) \quad (3.4\text{-}3b)$$

$$\text{Signal at D*} = S_{D*}(t) = \sin\left(\omega t + \theta_{D*}(t)\right) \quad (3.4\text{-}3c)$$

$$\text{Signal at E} = S_E(t) = \sin\left(\omega t + \theta_E(t)\right) \quad (3.4\text{-}3d)$$

$$\text{Signal at B*} = S_{B*}(t) = \sin\left(\omega t + \theta_{B*}(t)\right) \quad (3.4\text{-}3e)$$

$$\text{Signal at } B_S = S_{BS}(t) = \sin\left(\omega t + \theta_{BS}(t)\right) \quad (3.4\text{-}3f)$$

Next, using the delays, one can interrelate most of the signals. The mixer equation at the slave station says that the sum of the frequency at D* and the frequency at E is 2ω.

$$S_D(t) = S_{Bm}\left(t - \tau_{BmD}(t)\right) \quad (3.4\text{-}4a)$$

$$S_{D*}(t) = S_D(t - D_2) = S_B\left[t - D_2 - \tau_{BmD}(t - D_2)\right] \quad (3.4\text{-}4b)$$

$$S_{B*}(t) = S_E\left(t - \tau_{EB*}(t)\right) \quad (3.4\text{-}4c)$$

$$S_{BS}(t) = S_{B*}(t - D_1) - S_E\left(t - D_1 - \tau_{EB*}(t - D_1)\right) \quad (3.4\text{-}4d)$$

$$\omega t + \theta_{D*}(t) + \omega t + \theta_E(t) = 2\omega t \quad (3.4\text{-}4e)$$

Using equations 3.4-3a, 3c and 4b, one can find θ_{D*}. Since this calculation is only considering the effects of the slave open loop, the satellite master frequency will be assumed to be correct - i.e., $\theta_{Bm} = 0$.

$$\sin(\omega t + \theta_{D^*}(t) = \sin\left\{\omega\left[t-D_2 - \tau_{BmD}(t-D_2)\right] + \theta_{Bm}\left[t-D_2 - \tau_{BmD}(t-D_2)\right]\right\} \quad (3.4\text{-}5a)$$

$$\theta_{D^*}(t) = -\omega D_2 = \omega\,\tau_{BmD}(t-D_2) \quad (3.4\text{-}5b)$$

Next using 4e

$$\theta_E(t) = \theta_{D^*}(t) = \omega D_2 + \omega D_2 + \omega\,\tau_{BmD}(t-D2) \quad (3.4\text{-}6)$$

Using equations 3.4.4e, 3e, 3f and a calculation similar to that of 3.4-5a we can find θ_{BS} in terms of θ_E

$$\theta_{BS}(t) = -\omega D_1 - \omega\,\tau_{EB^*}(t-D_1) + \theta_E\left[t-D_1 - \tau_{EB^*}(t-D_1)\right] \quad (3.4\text{-}7)$$

Using equations 6 and 7

$$\theta_{BS}(t) = -\omega D_1 - \omega\,\tau_{EB^*}(t-B_1) + \omega D_2 + \omega\,\tau_{BmD}\left[t-D_2 - D_1 - \tau_{EB^*}(t-D_1)\right] \quad (3.4\text{-}8)$$

Differentiating equation 3.4-8 with respect to t obtains the frequency error at the satellite due to the slave open loop

$$\frac{d\,\theta_{BS}(t)}{dt} = -\omega\,\dot{\tau}_{EB^*}(t-D_1) + \omega\left\{\tau_{BmD}\left[(t-D_2-D_1-\tau_{EB^*}(t-D_1)\right]\right\}\left[1-\tau_{EB^*}(t-D_1)\right] \quad (3.4\text{-}9)$$

Using 2a and 1b, evaluate $\dot{\tau}_{EB^*}(t-D_1)$

$$\tau_{EB^*}(t-D_1) = r_o + r_1(t-D1) + r_2(t-D_1)^2 \quad (3.4\text{-}10a)$$

$$\dot{\tau}_{EB^*}(t-D_1) = r_1 + 2\,r_2(t-D_1) \quad (3.4\text{-}10b)$$

Using equations 3.2-27 and 3.2-12 and realizing that the path BC there is analogous to path BMD one can find τ_{BMD}. Limit the calculation to second order terms just as in Section 3.2.

$$\tau_{BMD}(t) = \tau(t) - \tau_o + \tau_1 t + \tau_2 t^2 \ldots \quad (3.4\text{-}11a)$$

$$\tau_{BMD}(t) = \tau_1 + 2\tau_2 t \quad (3.4\text{-}11b)$$

$$\tau_o = \frac{r_o}{1 + r_1}\left(1 + \frac{r_2 r_o}{(1 + r_1)^2}\right) \approx r_o(1 - r_1 + r_1^2 + r_2 r_o) \quad (3.4\text{-}11c)$$

$$\tau_1 = \frac{r_1 - 2r_{2\,o}}{1 + r_1 - 2r_{2\,+\,0}} \approx r_1 - r_1^2 - 2r_2 r_o \quad (3.4\text{-}11d)$$

$$\tau_2 = \frac{r_2}{(1 + r_1 - 2r_{2\quad o})^3} \approx r_2 \quad (3.4\text{-}11e)$$

Inserting equations 3.4-10 and 11 into 3.4-9

$$\frac{d\theta_{BS}(t)}{dt} = \omega\left\{-r_1 - 2r_2(t - D_1) + \left[\tau_1 + 2\tau_2(t - D_2 - D_1 - \tau_{EB^*}(t - D_1)\right] (1 - r_1 - 2r_2(t - D_1))\right\} \quad (3.4\text{-}12)$$

$$= \left\{-r_1 - 2r_2 t + 2r_2 D_1 + \left[r_1 - r_1^2 - 2r_2 r_o + 2r_2(t - D_2 - D_1 - r_o - r_1(t - D_1) - r_2(t - D_1)^2)\right] \left[1 - r_1 - 2r_2(t - D_1)\right]\right\}$$

Setting t=0 and retaining terms of second order or less one finds:

Frequency offset at B_S due to doppler effects on slave loop

$$= \frac{d\theta_{BS}}{dt} = -2\omega\left(r_1^2 + 2r_2\left(r_o + \frac{D_2}{2}\right)\right) \quad (3.4\text{-}13)$$

$$= \frac{-2\omega}{c^2}\left[\frac{(dr)^2}{(dt)} + \frac{d^2 r}{dt^2}\left(r + \frac{cD_2}{2}\right)\right]$$

where the minus sign means that the frequency at B_S is lower than that at B_M.

3.4.5 Combined Master Frequency Loop And Slave Open Loop Frequency Errors

The above has calculated the effects of doppler on the slave open loop. In Section 3.2, the effects of doppler on the master closed loop were calculated. Next the combined effects of both loops will be calculated.

In this calculation, assume that there is no signal delay in the ground station and in the satellite. For the slave open loop this can be justified from equation 3.4-13 as long as the delays in the station and in the satellite (i.e., D1 and D2) are small compared to the propagation delay $\frac{r}{c}$. The justification for the master open loop would require a recalculation of Section 3.2 with additional terms analogous to D_1 and D_2. However, it seems intuitively clear that the satellite delay and the ground station delays produce negligible effects as long as they are small compared to the propagation delay.

There is a separate range for the master station which we denote by r_m and a separate range for the slave station which we denote by r_s. According to Section 3.2, the master frequency at B_m will be lower than the correct value by $\frac{\omega}{c^2}\left[\left(\frac{dr_m}{dt}\right)^2 + r_m \frac{d^2 r_m}{dt^2}\right]$ This will in turn cause the slave frequency at B_S to be raised by the same amount as can be seen by following the signal from B_m to B_S on Figure 3.1-3. Thus the master doppler causes the difference frequency $B_S - B_m$ to have the value $\frac{2\omega}{c^2}\left[\left(\frac{dr_m}{dt}\right)^2 + r_m\left(\frac{d^2 r_m}{dt^2}\right)\right]$. On the other hand, equation 13 shows that the slave doppler lowers the frequency at B_S by $\frac{2\omega}{c^2}\left[\left(\frac{dr_s}{dt}\right)^2 + r_s\left(\frac{d^2 r_s}{dt^2}\right)\right]$ while the slave doppler does not affect the frequency at B_m. Thus the net effect of both slave and master dopplers is to make the $B_m - B_S$ frequency have the value

$$\frac{2\omega}{c^2}\left[\left(\frac{dr_m}{dt}\right)^2 + r_m\left(\frac{d^2 r_m}{dt^2}\right) - \left(\frac{dr_s}{dt}\right)^2 - r_s\left(\frac{d^2 r_s}{dt^2}\right)\right] \qquad (3.4\text{-}14)$$

Several comments can be made about these effects. First, if the slave and master station are located at nearby installations the doppler effects will cancel as r_m will equal r_s. Second, the total effect of both dopplers is no worse than the sum of the magnitude of both effects. It was shown that the magnitude of $\frac{1}{c^2}\left[\left(\frac{dr}{dt}\right)^2 + \left(\frac{d^2r}{dt^2}\right)\right]$ for Relay is less than 5×10^{-10}. Thus the peak effect of both dopplers on $B_m - B_S$ is less than 2×10^{-9}. In fact, if equation 3.3-28 is examined only for the time when both stations can see the satellite, then the peak effect on both dopplers is less than 1×10^{-9}.

3.4.6 Effects of Frequency Standard Errors

In this section the effects of errors in the master and slave frequency standard are considered. It is shown that the resulting difference at the satellite between the master frequency and the approximate slave frequency is equal to twice the difference of the two standards if only first order error terms are considered.

Let ω_o be the ideal frequency. Assume that the master frequency standard and the slave frequency standard are $2\ \omega_o (1 + e_m)$ and $2\ \omega_o (1 + e_s)$.

Since the master frequency at the satellite is proportional to the master standard, the master frequency at the satellite will be $\omega_o (1 + e_m)$ if other sources of error and second order error terms are neglected. Next using Figure 3.1-3 calculate the frequencies in the slave frequency open loop. The slave receiver of the master frequency will receive due to doppler $\omega_o (1 + e_m)(1 - d) \approx \omega_o (1 + e_m - d)$. The slave transmitter will then transmit the frequency $2\ \omega_o (1 + e_s) - \omega_o (1 + e_m - d) = \omega_o (1 + 2\ e_s - e_m + d)$. The satellite will then receive the frequency $\omega_o (1 + 2\ e_s - e_m + d)(1 - d) \approx \omega_o (1 + 2\ e_s - e_m)$ because of doppler. The difference between the master frequency and the slave frequency will be $\omega_o (1 + \omega\ e_s - e_m) - \omega_o (1 + e_m) = 2\ \omega_o (e_s - e_m)$.

Two points of interest: First, if both standards have the same error, the effects cancel. Second, an error of $\Delta\ \omega$ cycles per second of master frequency at the satellite from any source will cause a difference of $2\Delta\ \omega$ cycles per second between the master frequency and the slave frequency.

3.5 PHASE LOCKED LOOP DESIGN PROCEDURE AND SUMMARY

The design of the phase locked loops used in the TDMA equipment was based on the linear model shown in Figure 3.5-1. The output, E_1, of the phase detector is assumed to be proportional to the phase difference between the input and output signals;

$$E_1 = K_E (\theta_1 - \theta_2), \tag{3.5-1}$$

where K_E is the phase detector gain in volts/radian. The frequency deviation, $\dot{\theta}_2$, of the voltage controlled oscillator output is assumed proportional to the control voltage E_2;

$$\dot{\theta}_2 = K_{VCO} E_2,$$

where K_{VCO} is the voltage controlled oscillator gain in rad/sec/volt.

The phase difference between two periodic signals each of whose period is $2\pi/\omega_o$ can be converted to a time difference by the relation

$$(\theta_1 - \theta_2) = \omega_o (t_1 - t_2) . \tag{3.5-2}$$

This is sometimes used to express the phase detector and voltage controlled oscillator gains more conveniently in terms of time rather than phase; e.g., the units of K_E can be volts/μs.

The loop filter has a transfer function

$$F(s) = K_F \frac{1 + T_2 s}{1 + T_1 s} , \tag{3.5-3}$$

where K_F is the d-c loop filter gain. The open loop gain of the phase locked loop is then

$$G(s) = \frac{K}{s} \frac{1 + T_2 s}{1 + T_1 s} , \tag{3.5-4}$$

where

$$K = K_E K_F K_{VCO} \tag{3.5-5}$$

is called the d-c loop gain.

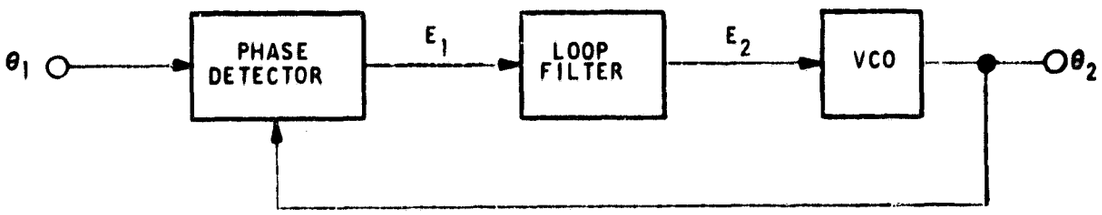

Figure 3.5-1. Linear Model of Phase Locked Loop

The loop filter is implemented by using an operational amplifier as shown in Figure 3.5-2. The input to this operational amplifier circuit may be arranged to obtain either an inverting or a non-inverting amplifier. If it is assumed that the gain of the operational amplifier is much greater than K_F, the following equations are valid for the inverting case:

$$K_F = R_F / R_1 \tag{3.5-6}$$

$$T_1 = (R_F + R_2)C \tag{3.5-7}$$

$$T_2 = R_2 C \quad . \tag{3.5-8}$$

Similar equations hold for the non-inverting case. In the case of the pseudo noise ranging loop, R_2 and C are omitted from the loop filter. This leads to a first order phase locked loop with open loop transfer function

$$G(s) = \frac{K}{s} \quad . \tag{3.5-9}$$

The propagation delays in the feedback paths of the master transmit phase locked loop and the pseudo noise ranging phase locked loop are ignored in the design procedure. Thus the loop bandwidths and damping factors specified are for zero propagation delay. The effect of propagation delay on the actual loop parameters is considered in Sections 3.7 and 3.8.

The closed loop transfer function corresponding to the open loop gain (3.5-4) is

$$H(s) = \frac{K}{T_1} \quad \frac{1 + T_2 s}{s^2 + \frac{1 + KT_2}{T_1} \quad s + \frac{K}{T_1}} \tag{3.5-10}$$

Defining the loop natural frequency $f_n = w_n \ /2\pi$ and damping factor ζ by the relations

$$\omega_n^2 = \frac{K}{T_1} \tag{3.5-11}$$

$$2\zeta w_n = \frac{1+KT_2}{T_1} \tag{3.5-12}$$

leads to the standard form of the denominator of H(s) for a second order loop

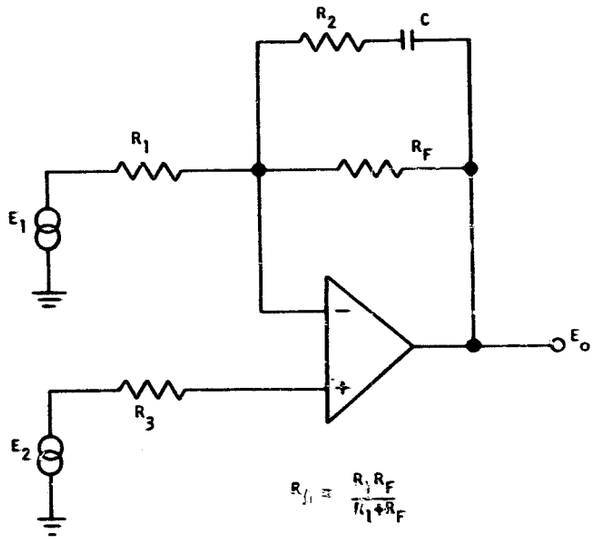

$R_{in} = \frac{R_1 R_F}{R_1 + R_F}$

E_1 = INVERTING INPUT

E_2 = NONINVERTING INPUT

FIGURE 3.5-2
IMPLEMENTATION OF LOOP FILTER

LOOP FILTER DESIGN CHART		
	INVERTING AMPLIFIER	NONINVERTING AMPLIFIER
1	$T_1 = K/\omega_n^2$	
2	$T_2 = \frac{2\zeta}{\omega_n} - \frac{1}{K}$	
3	$K_F = K/K_E K_{VCO}$	
4	$F(S) = -K_F \frac{1 + T_2 s}{1 + T_1 s}$	$F(S) = K_F \frac{1 + T_2 s}{1 + T_1 s}$
5	$R_1 = R_F/K_F$	$R_1 = R_F/(K_F - 1)$
6	$R_2 = \frac{R_F}{\frac{T_1}{T_2} - 1}$	$R_2 = \frac{R_F\left(1 - \frac{T_1}{T_2}\frac{1}{K_F}\right)}{\frac{T_1}{T_2} - 1}$
7	$C = \frac{T_2}{R_2}$	$C = \frac{T_2}{\frac{R_F}{K_F} + R_2}$

GIVEN: f_n, ζ, K, $K_E K_{VCO}$, R_F

Figure 3.5-2. Implementation of Loop Filter

$$H(s) = \frac{\omega_n^2 \ (1+T_2 s)}{s^2+2\zeta\omega_n s + \omega_n^2} \quad . \tag{3.5-13}$$

If T_1 is much less than T_2, the behavior of the loop for high frequencies is approximated by the second order loop with perfect integration whose open loop transfer function is

$$G(s) = \frac{H}{s} \ (1 + \frac{1}{T_2 s}) \quad , \tag{3.5-14}$$

where

$$H = K_E \ H_F \ K_{VCO} \tag{3.5-15}$$

and where

$$H_F = \frac{R_2 R_F / (R_2+R_F)}{R_1} \quad . \tag{3.5-16}$$

The quantity H is called the high frequency loop gain and is related to K by

$$\frac{K}{H} = \frac{T_2}{T_1} \quad . \tag{3.5-17}$$

If K is much greater than H, we obtain from (3.5-11) and (3.5-12) the approximate relations

$$H = 2\zeta \ \omega_n \tag{3.5-18}$$

and

$$T_2 = 2\zeta/\omega_n \quad . \tag{3.5-19}$$

These expressions are exact for the second order loop with ideal integration.

The design procedure will now be outlined. The phase locked loop designs are summarized in Table 3-1. The d-c loop gain is determined from the specified maximum phase error at the specified maximum input frequency offset; i.e., doppler shift plus oscillator stability.

$$K = \frac{\text{max. frequency offset (rad/sec)}}{\text{max. phase error (rad)}} \tag{3.5-20}$$

HOLDOUT FRAME /

Table 3-1. Summary of P

NAME OF LOOP	K_E ERROR DETECTOR SENSITIVITY	K_{VCO} VCO SENSITIVITY	$K_E K_{VCO}$	f_m MAXIMUM FREQUENCY OFFSET	MAXIMUM ERROR	K DC LOOP GAIN	f_n LOOP NATURAL FREQUENCY	B_L NOISE BANDWIDTH	SWITCH POSITIO
			SEC^{-1}			SEC^{-1}	HERTZ	HERTZ	
CARRIER TRACKING PLL	$\frac{0.050 \text{ VOLT}}{\pi \text{ RAD}}$	$\frac{2.5 \text{ MHz}}{\text{VOLT}}$	2.5×10^5	400 KC	9 DEG	16.0×10^6	100 300 1000	333 1000 3330	3 2 1
SUBCARRIER TRACKING PLL	$\frac{0.500 \text{ VOLT}}{\pi \text{ RAD}}$	$\frac{2.5 \text{ MHz}}{\text{VOLT}}$	2.5×10^6	400 KC	9 DEG	16.0×10^6	100 300 1000	333 1000 3330	3 2 1
RECEIVE CLOCK TRACKING PLL	$6.4 \frac{\text{VOLT}}{\mu S}$	$\frac{35.65 \frac{\mu S}{S}}{\text{VOLT}}$	228	$40 \frac{\mu S}{SEC}$	4 nS	10^4	100 300 1000	319 935 2790	0 1 2
TRANSMIT PLL	$45.2 \frac{\text{VOLT}}{\mu S}$	$\frac{35.68 \frac{\mu S}{S}}{\text{VOLT}}$	1610	$40 \frac{\mu S}{SEC}$	40 nS	10^3	0.5 1.0 2.0	1.66 3.33 6.66	3 2 1
PN RANGING PLL		$\frac{50 \frac{nS}{SEC}}{\text{VOLT}}$		$100 \frac{nS}{SEC}$					

DAMPING FACTOR = 0.707

FOLDOUT FRAME 2

3-1. Summary of Phase Locked

f_n LOOP NATURAL FREQUENCY	B_L NOISE BANDWIDTH	SWITCH POSITION	LOOP FILTER MODE	R_F	T_1	T_2	K_F DC GAIN OF LOOP FILTER	R_1	R_2	C
HERTZ	HERTZ				SEC	mS		OHM	OHM	uF
100	333	3	INVERT	4.05 MEG	40.5	2.25	100	40.5K	225	10
300	1000	2			4.50	0.75			683	1.1
1000	3330	1			0.405	0.225			2250	0.1
100	333	3	INVERT	4.05 MEG	40.5	2.25	10	405K	225	10
300	1000	2			4.50	0.75			683	1.1
1000	3330	1			0.405	0.225			2250	0.1
100	319	0	NON-INVERT	510K	2.54×10^{-2}	2.24	43.9	12K	39K	0.0442
300	835	1			2.82×10^{-3}	0.65			137K	0.004
1000	1790	2			2.54×10^{-4}	0.125			470K	0.00027
0.5	1.66	3	INVERTING (WITH DIFFERENTIAL INPUT)	2.5 MEG	101	449	0.62	4.0 MEG	11.2K	40
1.0	3.33	2			25.4	224			22.3K	10
2.0	6.66	1			6.24	112			45.6K	2.45

SEE TABLE IN FIGURE 3.5-2

It is assumed that the phase detector and voltage controlled oscillator gain are specified. It is also assumed that the loop natural frequency and damping factor are specified as shown in Table 3-1. The only parameter which is left to be specified is the impedance level of the loop filter circuit shown in Figure 3.5-2. This depends on source and load impedances, operational amplifier input offset current, and physical size and leakage current of the time constant capacitor C. The impedance level in Table 3-1 is implicit in the choice of R_F. The remaining element values are determined by the equations shown in Figure 3.5-2.

Table 3-2 summarizes the parameters of the first order pseudo noise ranging phase locked loop.

TABLE 3-2. PSEUDO NOISE RANGING PHASE LOCKED LOOP SUMMARY

Loop Filter Switch Position.	R_F Ohms	f_n - Loop Bandwidth = hertz (R_1 = 10 K)				
		Gate Selector position:	1	2	3	4	5
		Gate Width: us	1.25	3.75	6.25	8.75	1.25
0	200 k		0.509	0.170	0.102	0.0726	0.0566
1	390 k		0.994	0.332	0.198	0.142	0.110
2	620 k		1.58	0.528	0.315	0.225	0.176
3	820 k		2.08	0.698	0.417	0.298	0.232
4	1.2 meg		3.06	1.02	0.610	0.436	0.340
5	1.8 meg		4.59	1.53	0.918	0.654	0.510
6	2.4 meg		6.11	2.04	1.22	0.871	0.679
7	3.6 meg		9.16	3.06	1.83	1.31	1.02
8	5.6 meg		14.3	4.77	2.87	2.04	1.59
9	6.8 meg		17.3	5.78	3.56	2.47	1.92

3.6 PHASE LOCKED LOOP TRACKING PERFORMANCE

The effects of noise and doppler on phase locked loop tracking accuracy are considered in this section. The phase locked loops in the TDMA system are as shown in Figure 3.6-1A. The input contains a signal component s(t) and a noise component n(t). The phase detector is actually implemented with a multiplier in which the input signal is multiplied by a reference signal x(t) locally generated from the voltage controlled oscillator.

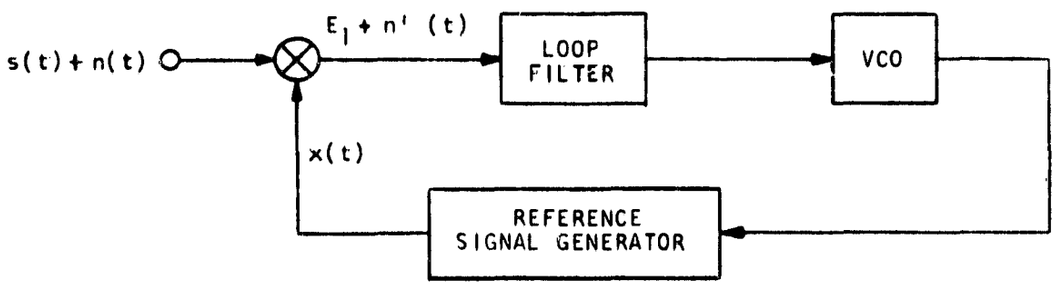

(A) PLL CONFIGURATION

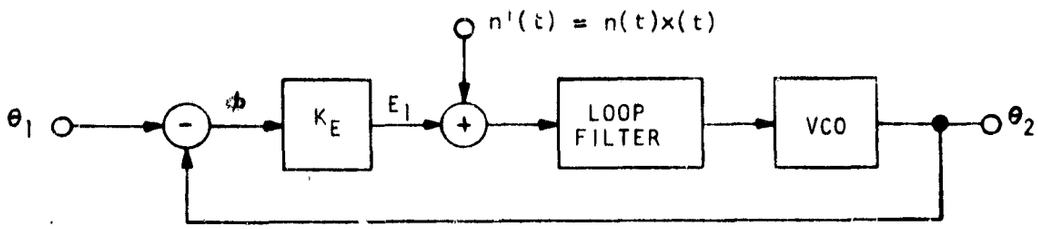

(B) LINEAR MODEL OF PLL

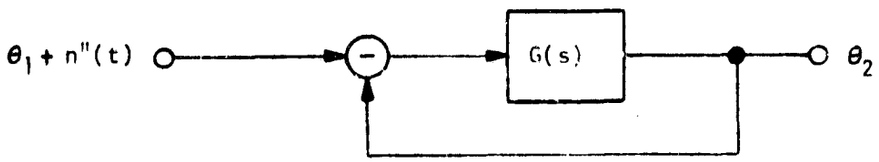

(C) SIMPLIFIED LINEAR MODEL OF PLL

Figure 3.6-1. Derivation of Linear Phase Locked Loop Model

The signals s(t) and x(t) may be sinusoids as assumed in Section 2.6, but in general are periodic signals each with period $2\pi/\omega_0$. These two signals must be chosen such that the d-c component E_1 of their product is an odd function $h(\Delta\theta)$ of the phase difference $\ell = \theta_1 - \theta_2$ between them. Then the linear model of Figure 3.6-1B is valid for small phase differences ℓ. The phase detector gain is the slope of $h(\ell)$ at the origin;

$$K_E = \left.\frac{dh(\ell)}{d\ell}\right|_{\ell = 0} \quad . \tag{3.6-1}$$

The noise

$$n'(t) = n(t)\,x(t) \tag{3.6-2}$$

at the loop filter input is the same in both Figures 3.6-1A and B. The linear model can further be simplified as shown in Figure 3.6-1C. Here the noise

$$n''(t) = \frac{n'(t)}{K_E} = \frac{x(t)}{K_E}\, n(t) \tag{3.6-3}$$

gives rise to n'(t) at the loop filter input also. The tandem connection of the amplifier K_E, the loop filter, and the voltage controlled oscillator is shown as the open loop gain G(s). Finally, the entire feedback network of Figure 3.6-1C can be replaced by a network with a transfer function equal to the closed loop gain H(s).

It will be assumed that the input noise n(t) has a bandwidth wide compared to that of s(t) and constant power density N_o watts/cps. It will also be assumed that the loop bandwidth is much less than the repetition rate $\omega_0/2\pi$ of s(t) and x(t). The effect of multiplying n(t) by x(t) is to translate components of n(t) which are close to harmonics of $\omega_0/2\pi$ down to components of n'(t) which are close to d-c.

The power density of n''(t) will also be constant (within the band of the loop filter) of magnitude

$$N_o'' = \frac{P_x}{K_E^2}\, N_o \quad , \tag{3.6-4}$$

where P_x is the average power of x(t).

The phase jitter on the phase locked loop output due to input noise can be expressed in terms of the loop noise bandwidth

$$B_L = \int_0^\infty \left| H(f) \right|^2 df \quad . \tag{3.6-5}$$

The noise bandwidth for a second order loop (Equation 3.5-10) is

$$B_L = \frac{K}{4} \quad \frac{1 + \frac{T_2^2}{T_1} K}{1 + KT_2} \tag{3.6-6}$$

and for a first order loop (Equation 3.5-9) is

$$B_L = \frac{K}{4} \quad . \tag{3.6-7}$$

In terms of B_L, the mean square phase jitter is

$$\sigma^2 = N_o'' B_L$$

$$= \frac{P_x}{K_E^2} \quad N_o B_L \quad . \tag{3.6-8}$$

For the carrier tracking phase locked loops, 3.6-8 becomes

$$\sigma^2 = \frac{1}{d} \quad \frac{N_o B_L}{P_c} \tag{3.6-9}$$

where

d = duty cycle of sync burst

= 1/12.375, for carrier tracking phase locked loop

= 1.0, for subcarrier tracking phase locked loop

$P_c = P_r \cos^2 p$ is the carrier power, (Section 2.5).

The units of σ^2 in this case are radians^2.

For the receive clock tracking phase locked loop, 3.6-8 becomes

$$\sigma^2 = \left(\frac{\pi}{2}\right)^2 \quad \frac{1}{d} \quad \frac{N_o B_L}{P_s} \quad , \tag{3.6-10}$$

where

d = duty cycle of sync burst = 1/12.375

$P_s = P_r \sin^2 p$

= Sideband power (Section 2.5).

The units of σ^2 in this case are (radians of 800 khz clock)^2. In obtaining 3.6-10 from 3.6-8, it is assumed that the carrier tracking phase locked loop phase error is negligible; i.e., cos ℓ = 1 in Equation 2.5-9.

For the PN ranging phase locked loop, 3.6-8 becomes

$$\sigma^2 = \frac{11}{24} \quad (t_g T) \quad \frac{N_o B_L}{P_S} \quad , \tag{3.6-11}$$

where

t_g = gate width (Section 4.10)

T = 11.25 μs

$P_s = P_r \sin^2 p$

= Sideband power (Section 2.5).

Again the subcarrier tracking phase locked loop phase error is ignored. The units of σ^2 are the same as those of the product (t_g T); e.g., us^2 if both t_g and T are expressed in us.

This completes the evaluation of the effect of noise on phase locked loop performance. The remainder of this section will be used to evaluate the tracking error due to doppler and doppler rate. The linear model of Figure 3.6-1C, neglecting noise, will be used.

The doppler will be represented by a quadratic polynomial of the form

$$\ell_1(\phi) = a_o + a_1 t + a_2 t^2 , \qquad (3.6\text{-}12)$$

where

a_o = constant phase shift

a_1 = doppler shift - rad/sec

a_2 = doppler rate - rad/sec^2 .

Numerical values for the maximum doppler and doppler rate were given in Section 2.5. The loops must also track the frequency error due to tolerances on the oscillators in the system. These tolerances can be including with the doppler as was done in Section 2.5.

With an input of the form of 3.6-12, the steady state tracking error for a first or second order loop will be (see Reference 3-1, Eq. 1.255).

$$\ell(\phi) = \frac{a1}{K_p} + \frac{2\,a\,2}{K_a} + \frac{2\,a\,2}{K_\nu}\, t , \qquad (3.6\text{-}13)$$

where

K_ν = velocity constant

K_a = acceleration constant .

These constants are defined and evaluated below. It can be seen from 3.6-13 that a constant phase shift a_o at the input causes no steady state tracking error for first or second order loops. (This is because the position constant Kp is infinite for such loops.)

The error constants can be defined as coefficients in the following series expansion (see Reference 3-2, Eq. 1.250)

$$\frac{1}{1+G(s)} = \frac{1}{1+Kp} + \frac{1}{K_\nu}\, s + \frac{1}{K_a}\, s^2 + \ldots . \qquad (3.6.14)$$

This definition is convenient because the coefficients can be evaluated directly from the open loop transfer function G(s).

For a first order loop, Eq. 3.5-9,

$$\frac{1}{1+G(s)} = \frac{1}{K}s - \frac{1}{K^2}s^2 + \frac{1}{K^3}s^3 + \dots \quad . \tag{3.6-15}$$

Thus

$$K_\nu = K \quad , \quad K_\alpha = -K^2 \quad . \tag{3.6-16}$$

For a second order loop, Eq. 3.5-4, a similar expansion yields

$$K_\nu = K \quad , \quad K_\alpha = \frac{K^2}{K(T_1 - T_2) - 1} \quad . \tag{3.6-17}$$

The tracking error due to doppler shift depends on the velocity constant which is simply K for the loops considered. This error was already considered in Section 3.5 (Eq. 3.5-20 and Table 3-1). It is, according to 3.6-13, a constant phase error.

The tracking error due to doppler rate, however, gives rise to a frequency error as well as a constant phase error. Such frequency errors were referred to as $\dot{\theta}_k$ in Section 3.1 (see esp. Eq. 3.1-6).

Now, using 3.6-13, 16 and 17,

$$\dot{\theta}_k = \frac{2a_2}{K} \quad . \tag{3.6-18}$$

The fractional frequency error in the doppler compensation system caused by either the receive clock tracking or the transmit phase locked loop will be

$$\frac{\Delta\omega}{\omega} = \frac{1}{K}\left(\frac{2a_2}{\omega}\right) \quad . \tag{3.6-19}$$

The maximum value of $(2a_2/\omega)$ is approximately, from Table 2.4-1, 5×10^{-8} Sec^{-1}. From Table 3-1, the smaller K occurs for the transmit phase locked loop gives

$$\frac{\Delta\omega}{\omega} = 0.5 \text{ part}/10^{10}. \tag{3.6-20}$$

The fractional frequency error due to the receive clock tracking phase locked loop is an order of magnitude less.

3.7 SIMULATION OF NONLINEAR PHASE LOCKED LOOP WITH PROPAGATION DELAY

The system used for fine synchronization slave stations is shown in Figure 3.7-1. The master station sends a series of 800 khz bursts. The slave station tries to adjust a pseudo noise code transmission so that it will appear at the satellite in the proper time slot relative to the master station. This is done by using the received master 800 khz transmission to generate a pseudo noise code which is compared with the slave's received pseudo noise code transmission in a cross correlator. The error signal from the correlator then controls a meter driven phase shifter which operates on the slave's uplink transmission. The satellite completes the loop forming a closed loop servo system. However, the system contains certain nonlinearities which could make its analysis difficult, and it was decided to simulate the system using the IBM electronic circuit analysis program. This program can perform a transient analysis on electrical networks and has provisions for switches to simulate non-linear devices. Also there are transfer elements which permit one to build the system up from smaller subsystem programs. The electrical network that was simulated is shown in Figure 3.7-2, and the program as fed to the computer is shown in Figure 3.7-3. A brief description of the subsystems follow.

3.7.1 Pseudo Noise Error Detector

The output of the error detector as a function of the phase difference between master and slave codes is a periodic trapezcidal wave. For small phase differences less than ±1 microseconds it behaves like a limiter. It is simulated by a current source feeding a resistor in parallel with a limiter, where the output of the current source is equal to the phase difference between master and slave pseudo noise codes.

3.7.2 Loop Filter

The loop filter considered in the simulation is a simple log-lead network with a transfer characteristic.

$$F(s) = \frac{1 + \tau_2 s}{1 + \tau_1 \frac{s}{s}}$$

where

$$\tau_1 = \frac{K}{\omega n^2} \qquad \tau_2 = \frac{2\xi}{\omega n} - \frac{1}{K}$$

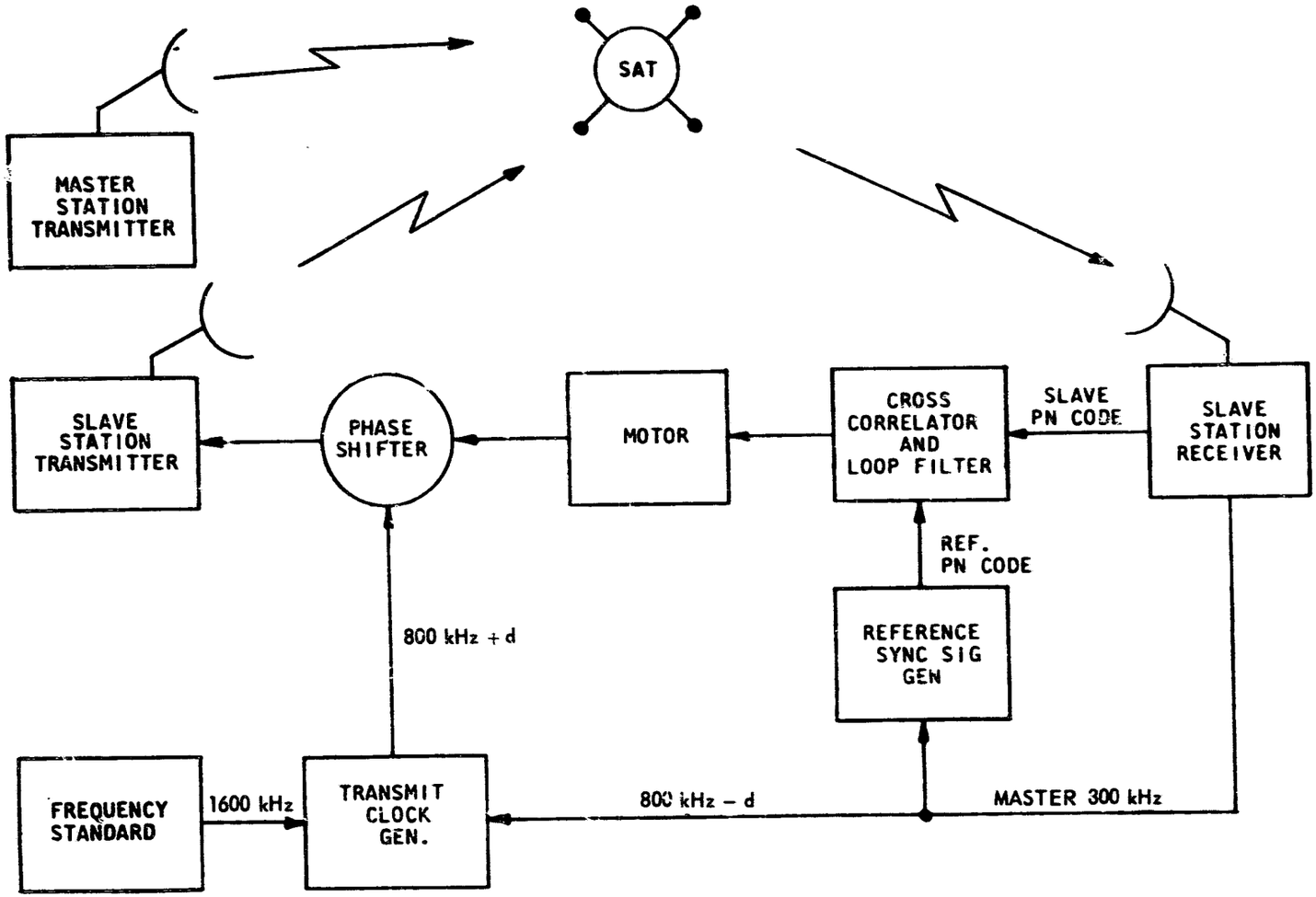

Figure 3.7-1. Fine Synchronization Servo Loop

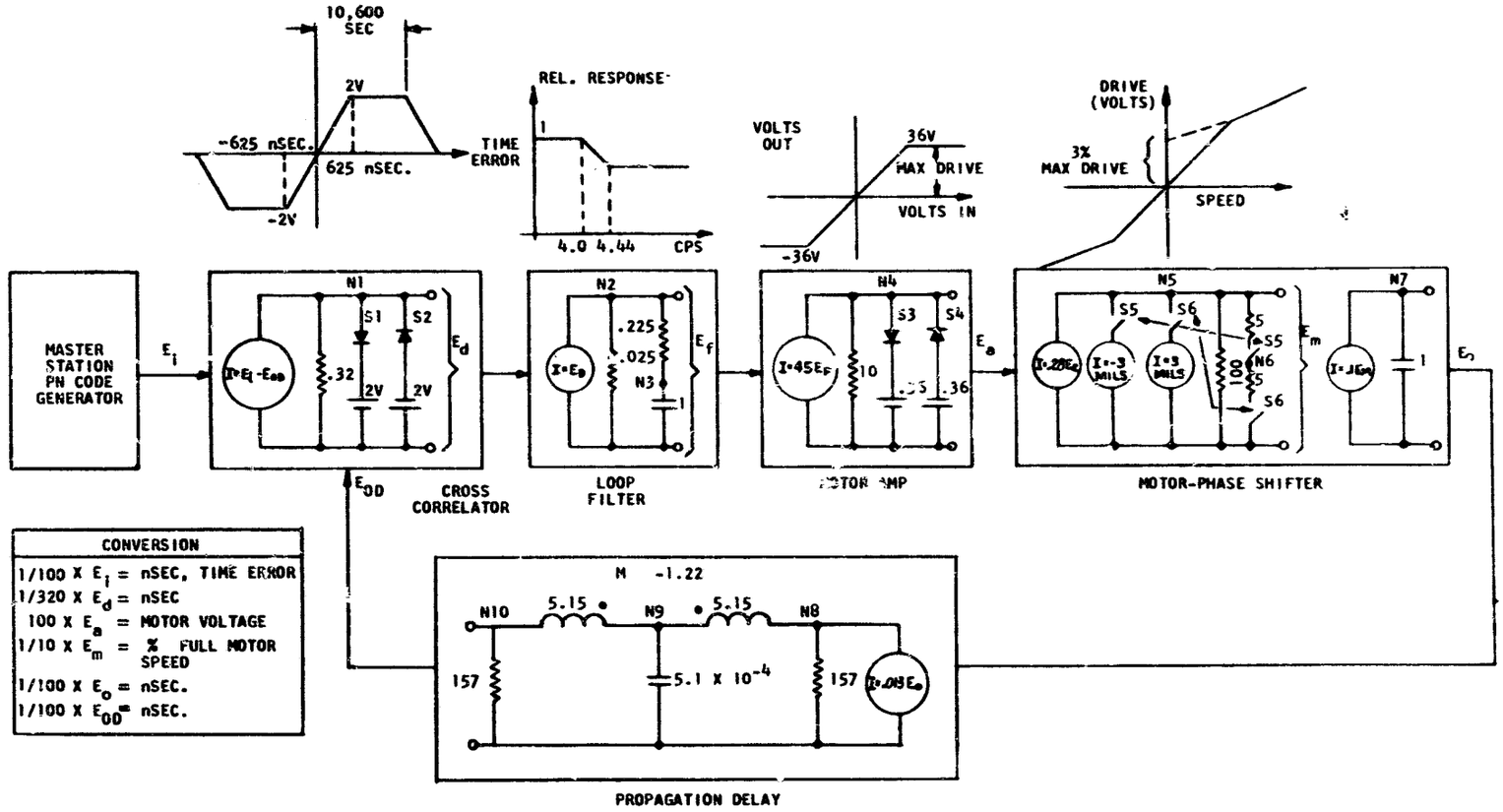

Figure 3.7-2. ECAP Simulation Model

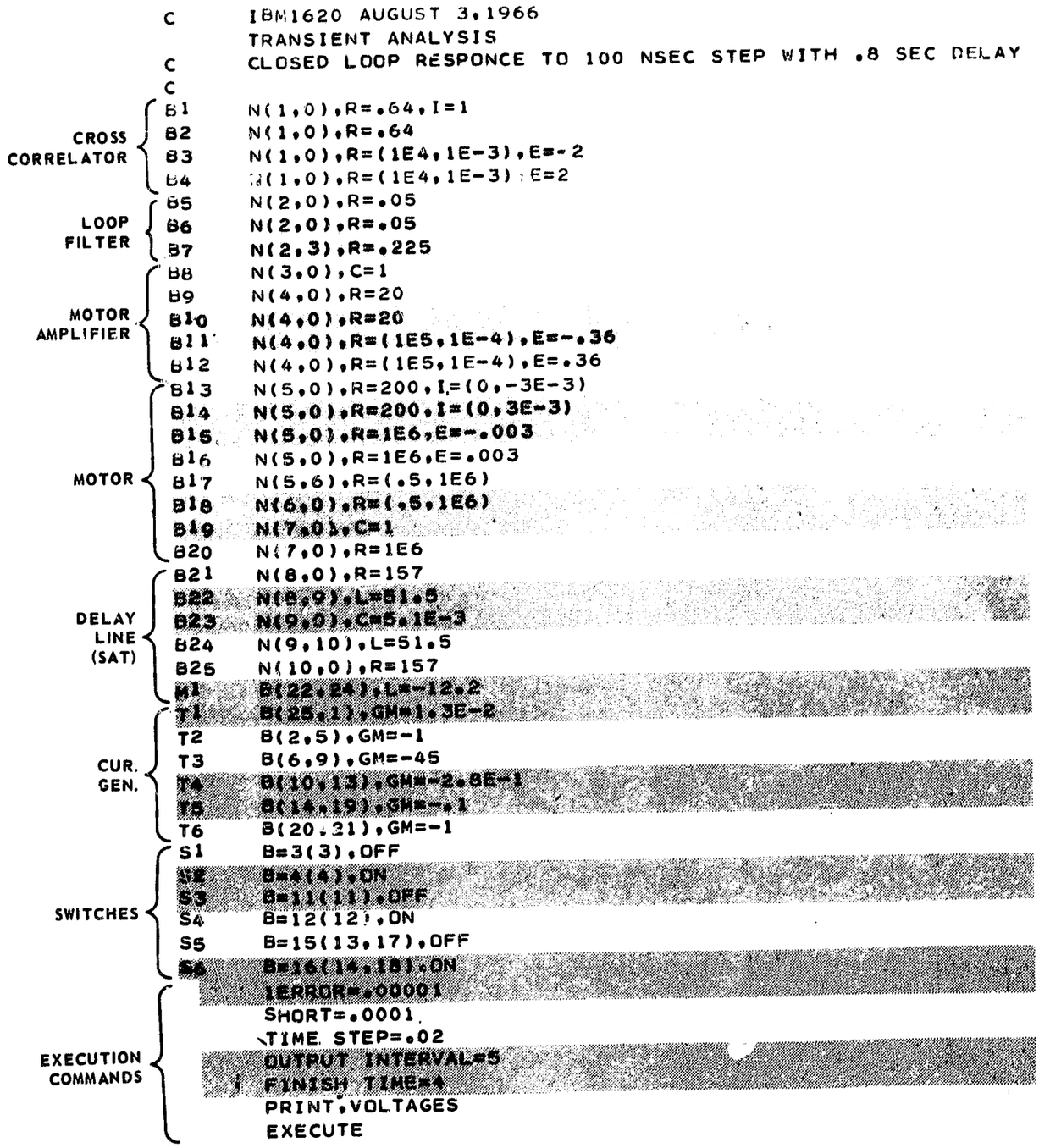

Figure 3.7-3. Simulation Program (Photo)

and ω_n = loop bandwidth

ξ = damping ratio

K = open loop DC gain

In this system

ωn = 6.28 rad/sec.

ξ = .707

K = 10/sec.

hence $F(s) = \frac{1 + .225s}{1 + .250s}$

A current source driving a simple r-c network is used to simulate the loop filter.

3.7.3 Motor Amplifier

The output of the loop filter is fed to an amplifier which is used to control the motor which in turn drives the phase shifter. The motor speed is proportional to the output of the amplifier. However, the amplifier has a non-linear characteristic and limits at 36 volts. This determines the maximum speed of the motor and the maximum rate of phase shift, 100 msec/sec. The motor amplifier simulation is essentially the same as the correlator and is a current source driving a resistor and limiter in parallel.

3.7.4 Motor Shifter

The differential equation for servo motor can be written in operational form as (Ref. 3-3, Eq. 1):

$$\text{Torque} = KmEa = Js\,\Omega + f\,\Omega = f\left[\frac{Js}{f} + 1\right]$$

where

E_a = applied control voltage

Km = motor constant

J = moment of inertia

f = windage friction

Ω = angular velocity

s = complex frequency .

In addition to the windage friction there is a bearing friction term which does not vary with speed. However, the bearing friction (coulomb friction) always opposes the direction of rotation and hence is discontinuous at $\Omega = 0$. The motor is then described by the following set of equations.

$$KmEa = Js\ \Omega + f\ \Omega - fb, \Omega > 0$$

$$= Js\ \Omega + f\ \Omega + fb, \Omega < 0$$

$$= \text{Starting Torque}, \Omega = 0$$

where fb = bearing friction.

There is a static bearing friction which is usually larger than the rotating bearing friction, fb. Hence, the torque required to start the motor is larger than the torque required to keep it moving. However, this effect was neglected.

For purposes of writing this program the following assumptions were made.

1. The moment of inertia was neglected since the motor's time constant, f/J, is several orders of magnitude smaller than the loop bandwidth.
2. The discontinuity at $\Omega = 0$ cannot be easily handled by the circuit analysis program so the equations were modified to give the voltage-speed transfer curve shown in Figure 3.7-4A.

In the program the analog of torque is current and the analog of speed is voltage. The non-linear torque-speed characteristic is simulated using switching elements to sense when the voltage passes through the switch points $\pm\omega s$ and then modifying the current sources and load resistances to duplicate the transfer characteristic.

3.7.5 Propagation Delay Line

The final elements in the servo loop are the satellite and propagation paths. For this analysis, these function merely as a delay line. Since it is impossible to program a distributed parameter delay line in the ECAP language, it was necessary to approximate the design with a lumped parameter model.

The design of lumped parameter delay lines are described in the literature (Ref. 3-4, Pg. 295) and the details will not be given here. The design chosen is essentially an m derived T network with m = 1.27 so as to minimize phase distortion.

The essential equations which determine the parameters are shown in Figure 3.7-4B (Ref. 3-4, Pg. 296).

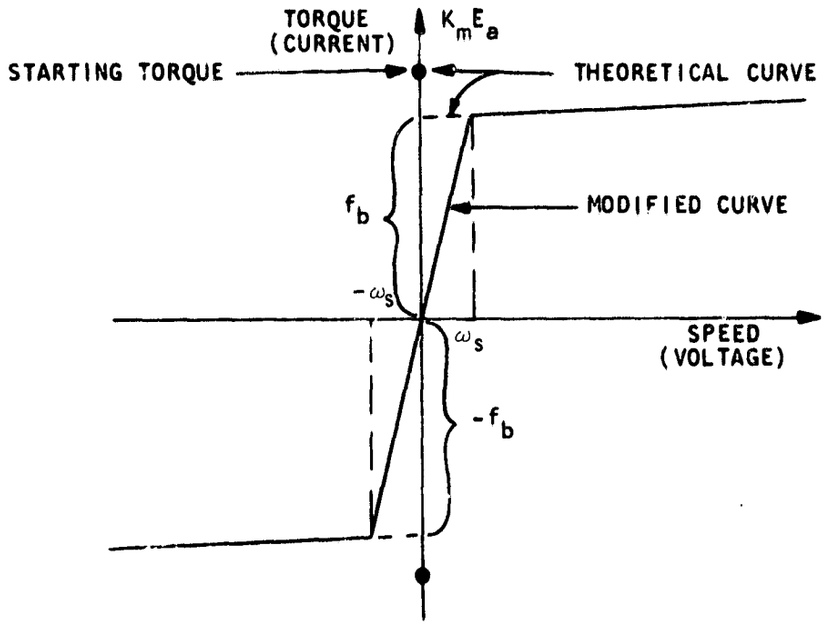

A - MOTOR TORQUE-SPEED CHARACTERISTIC

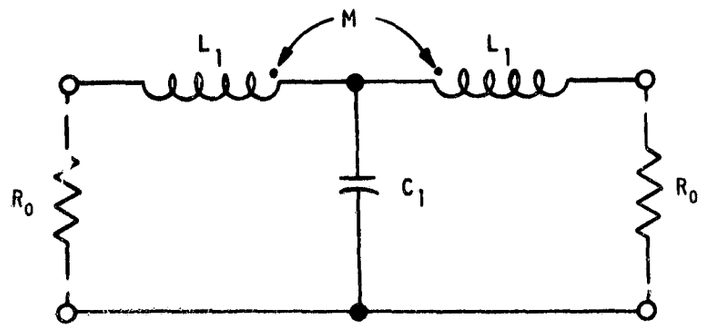

$L_1 = 0.515L$

$C_1 = 1.27C$

t_s = DELAY TIME = $1.27\sqrt{LC}$

$R_0 = \frac{1}{\sqrt{LC}}$

B - LUMPED PARAMETER DELAY LINE

Figure 3.7-4. Models for Simulation

3.7.6 ECAP Language

The basic element in the ECAP language is the network branch. Each branch must contain one passive circuit element; i.e., resistor, capacitor or inductor, and may also contain a voltage source, a current source, and a dependent current source, used as a transfer element from one subcircuit to another.

A branch may also contain a switch element which has two possible states, on and off, depending whether the branch current is positive or negative, respectively.

Two values may then be assigned to any branch element and the switch will choose one or the other value depending upon the instantaneous state of the switch; i.e., the direction of the branch current.

The ECAP program solves a transient analysis problem by converting it to a series of d-c analysis problems and solving these. At any time, $t_j + \Delta t$, where Δt is the specified time step, the branch currents are expressed in terms of the voltages and currents at time t_j, see Figure 3.7-5. The program then uses standard network equations to find all of the voltages at $t = t_j + \Delta t$.

If at some time the results indicate that a switch should have changed state in the interval t_j to $t_j + \Delta t$, then the program interpolates to find the point of switching and continues the solution from that point with the switch in the new state.

3.7.7. Performance Tests

One of the principal advantages of the computer simulation technique is that one can change system inputs and parameters by simply substituting a few cards.

There were three types of inputs used in these tests. 1) damped sinusoid, 2) step, and 3) ramp.

These were two values of d-c gain used: 10 and 1000; and two different delays through the satellite: 0.08, and 0.8 seconds.

Figure 3.7-6 shows the effect of a damped sinusoid with the system run as an open loop. The torque is proportional to the signal drive. When the torque drops below a certain value the motor stalls and will not move again until the torque rises above stall torque. Eventually, as the drive becomes smaller the motor remains stalled.

Resistor: $J^{j+1} = \frac{1}{R} \left[e^m - e^n\right]$

Capacitor: $J^{j+1} = \frac{C}{\Delta t} \left[e_m^{j+1} - e_n^{j+1} - (e_m^j - e_n^j)\right]$

Inductor: $J^{j+1} = \frac{\Delta t}{2L} \left[e_m^{j+1} - e_n^{j+1} + (e_m^j - e_n^j)\right] + J^j$

Figure 3.7-5. ECAP Branch Element

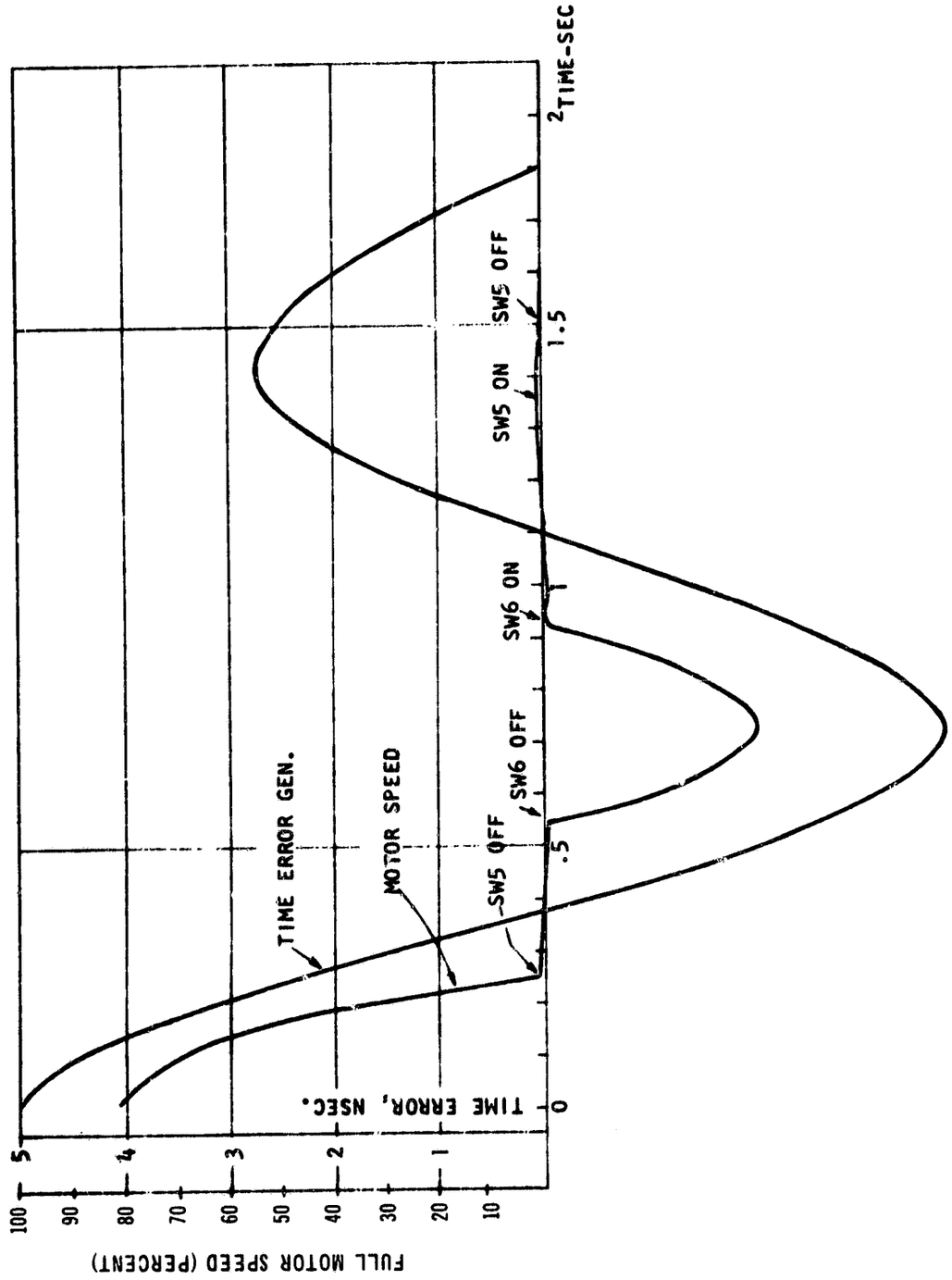

Figure 3.7-6. Open Loop Response

Figure 3.7-7 shows the effect of a step input into the closed loop system. The system does not react immediately due to 0.08 second delay through the satellite. Also, the error function will not go to zero since once the motor stalls the error function does not change.

Figure 3.7-8 shows the effect of a ramp with two different gains.

Figure 3.7-9 shows the effect of increasing the delay from 0.08 sec. to 0.8 sec. As might be expected, the system becomes unstable.

3.8 EFFECT OF PROPAGATION DELAY ON PHASE LOCKED LOOP NOISE BANDWIDTH AND STABILITY

The closed loop response and hence the noise bandwidth vary considerably with transport lag.

Figure 3.8-1 shows how the closed loop response varies with normalized transport lag KT, for a first order servo. For $KT = \frac{\pi}{2}$ the closed loop response becomes infinite at $\omega = 1$ indicating that the loop will oscillate at this frequency.

Figure 3.8-2 shows the closed loop response for the second order loop of Section 3.7-2. Here the loop becomes unstable at $T = 0.2$, $\omega = 2\pi$.

Figure 3.8-3 shows the variation of the noise bandwidth for the first order loop. For delays much smaller than the delays that would make the system unstable, there is still a significant increase in the noise bandwidth.

For example, with a KT of only 0.65, the noise bandwidth increases 3 db, hence the time jitter will be 1.414 times the jitter with no delay.

A time domain analysis of the servo is somewhat more involved than a frequency domain analysis. However, the overshoot in the time domain is related to the overshoot in the frequency domain.

Moreover the system will become unstable for a normalized delay of $\pi/2$ seconds in the case of the first order servo and 0.2 seconds in the case of the second order servo.

The closed loop frequency responses were determined from a Nichols' chart, modified Nyquist plot, of the open loop response given by Equations 3.5-9 and 3.5-4 multiplied by the delay factor exp (-KTs).

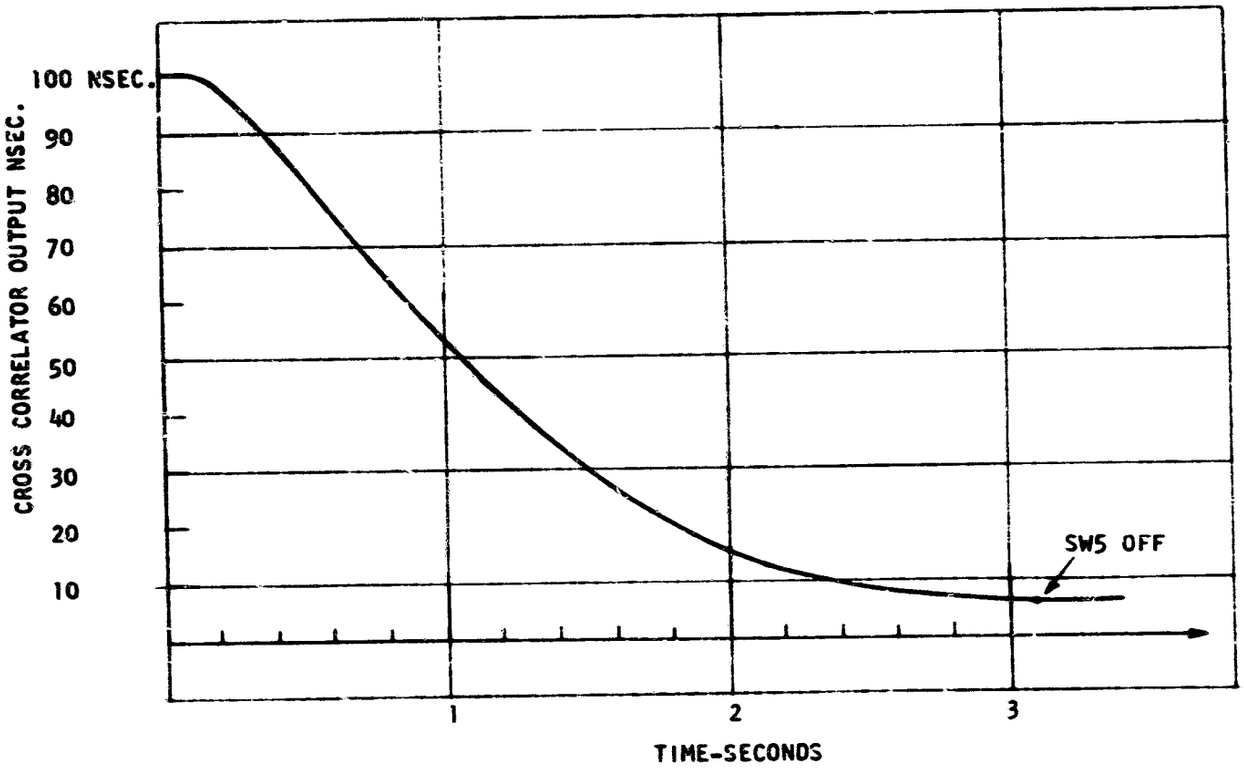

Figure 3.7-7. Response to 100 nsec Error

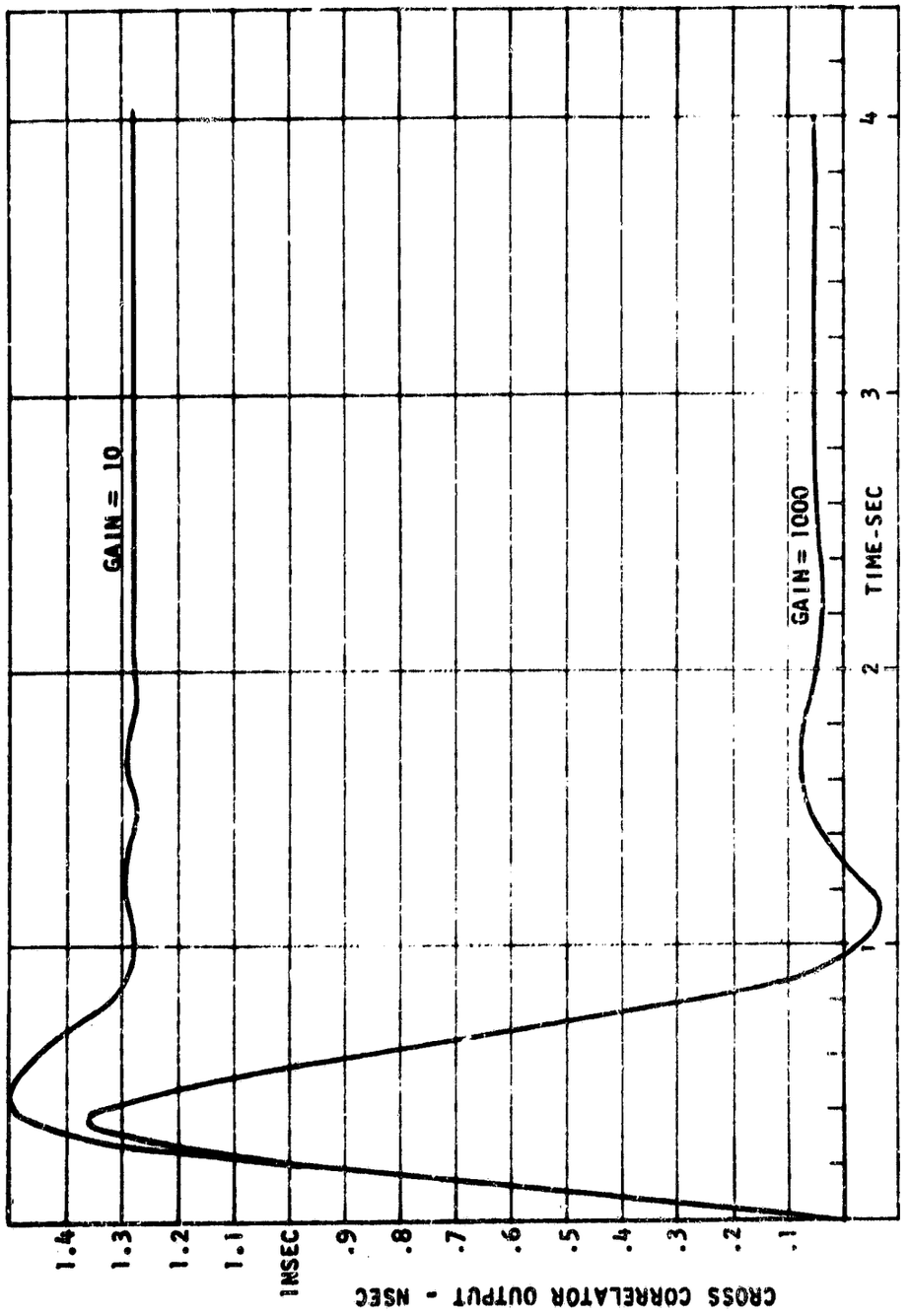

Figure 3.7-3. Response to 10 ns/sec Ramp

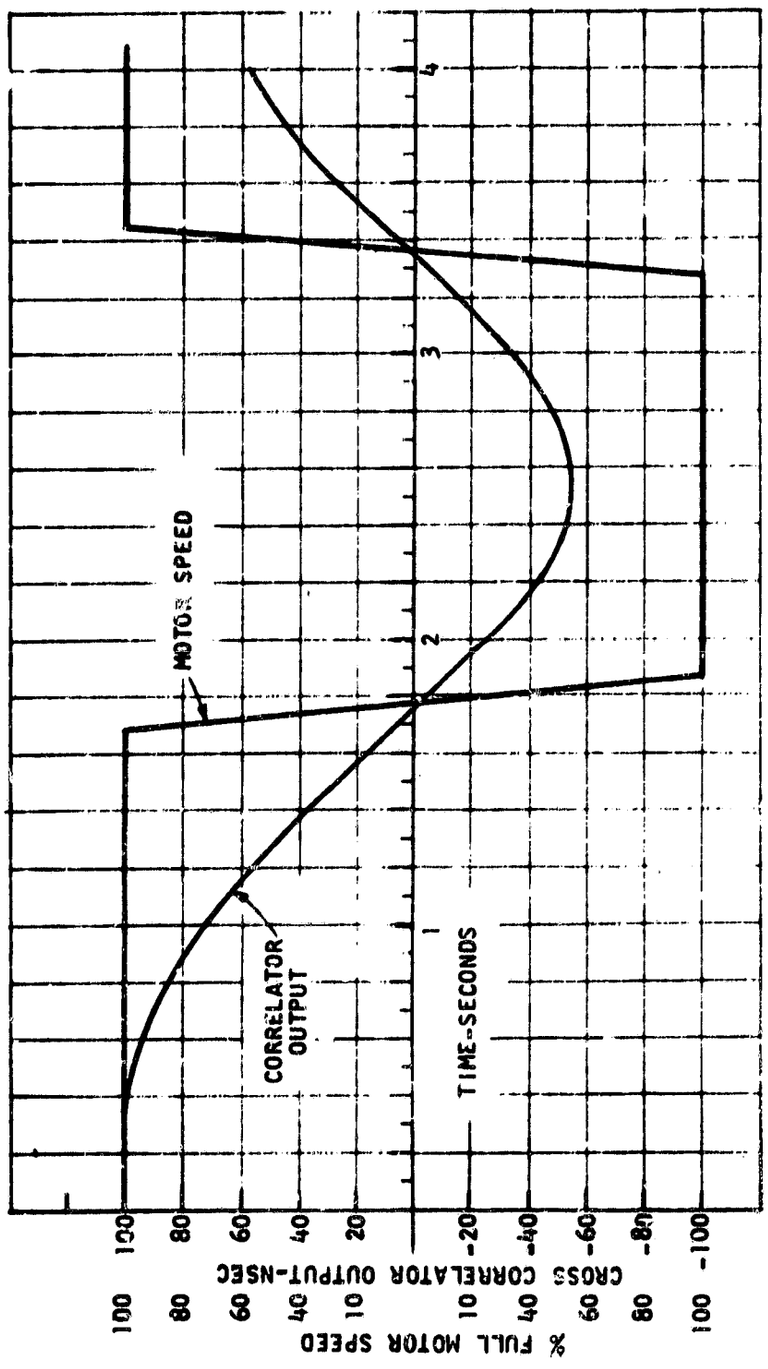

Figure 3.7-9. Response to 100 nsec Error

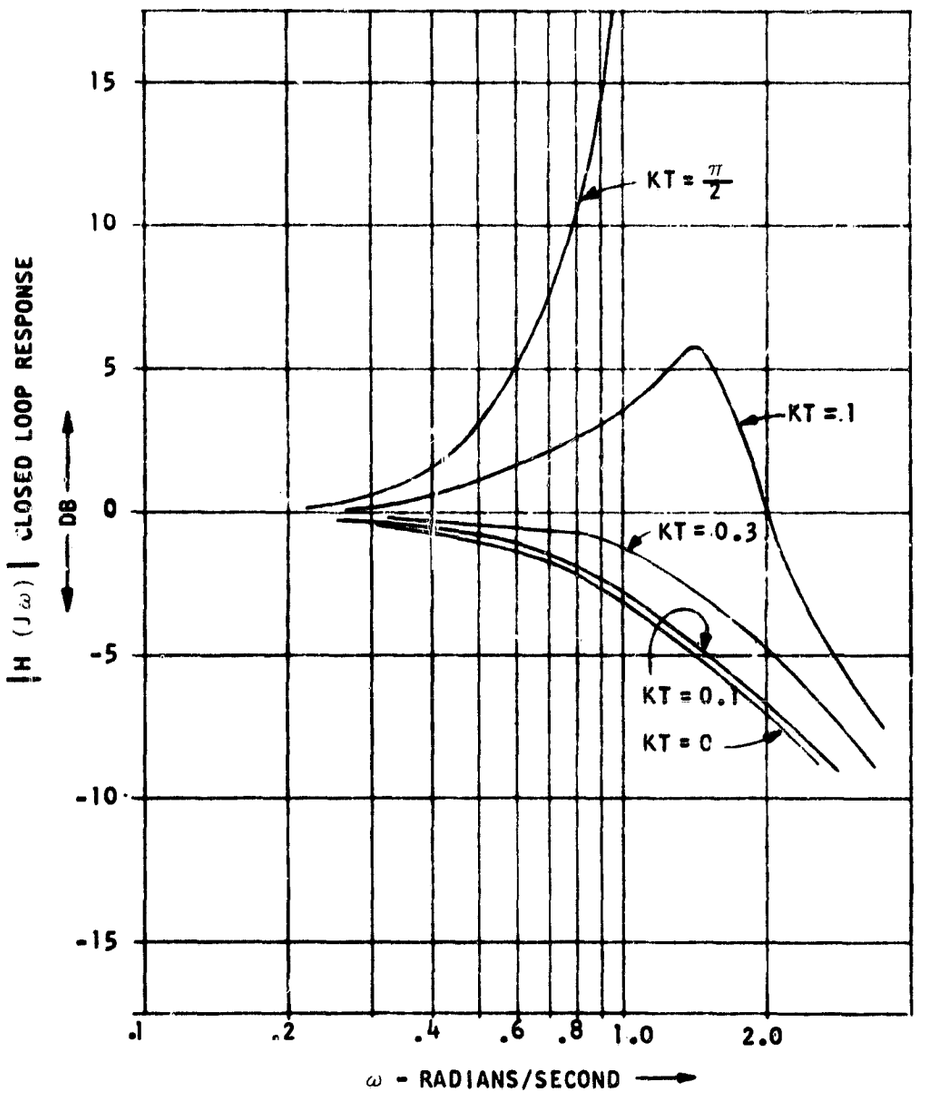

Figure 3.8-1. First Order Characteristic for Various Lags

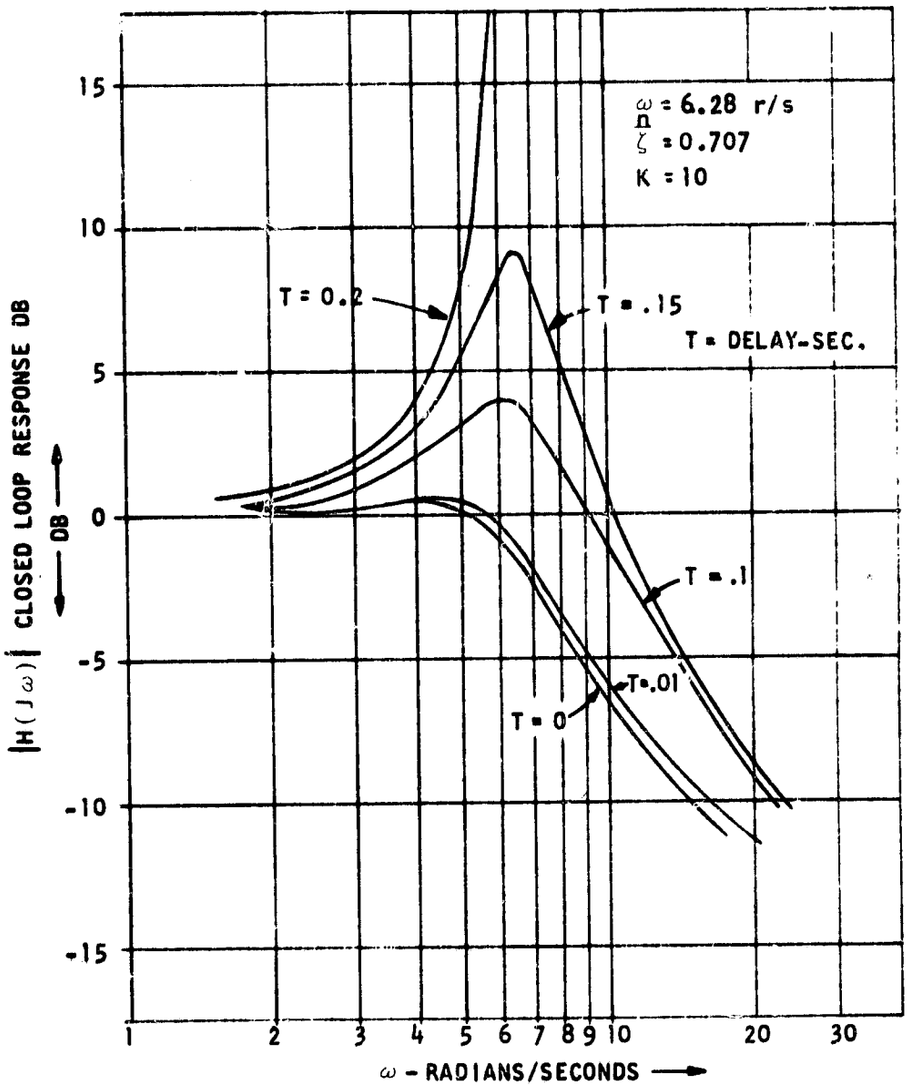

Figure 3.8-2. Second Order Characteristic for Various Lags

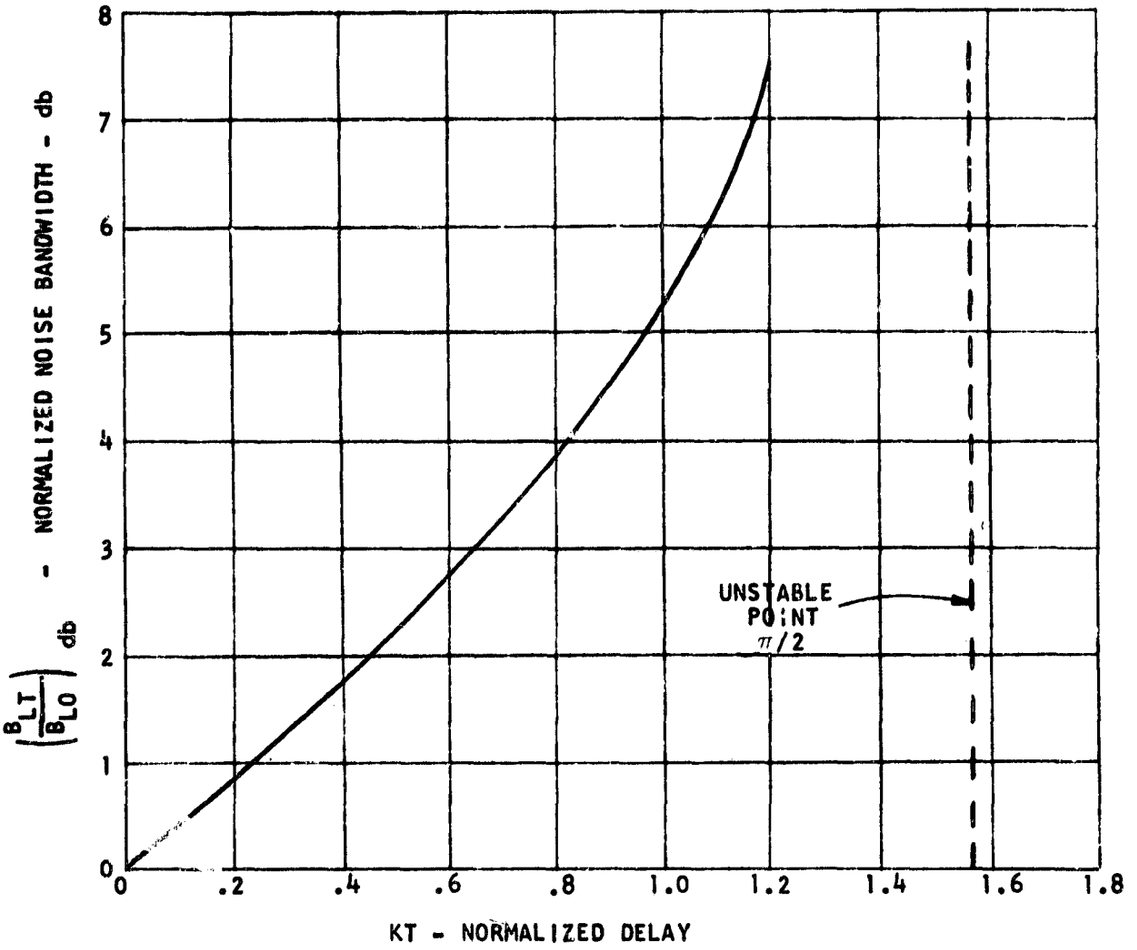

Figure 3.8-3. Noise Bandwidth Versus Propagation Delay

The noise bandwidth of the first order loop is defined by Equation 3.6-5. The closed loop response in this case is

$$H(s) = \frac{K}{s + K^{-K_1}} \qquad (3.8\text{-}1)$$

The integration was performed by approximating the exponential function with a rational function (Ref. 3-2, Table 9.3) and using known integrals.

3.9 RELAY SPACECRAFT SIMULATOR EXPERIMENT

These experiments were to investigate the change in relative signal levels on the output of the satellite as those signal levels were varied at its input. This was of interest in two cases: first where the input signals pass through a limiter and are then applied to the simulator; and second, where the input signals were directly applied to the simulator without any prior limiting operation.

The first experiment was performed using the test set-up shown in Figure 3.9-1A. The two CW signals C and S_2 were both held constant in frequency at 70 and 72 MHz. S_2 represents the carrier and C represents the transmitted subcarrier in the TDMA system. In the experiment, C was held constant in level (-10 dbm) while S_2 was varied in level so that carrier to subcarrier input ratio

$$R = (S_2/C)_{IN}$$

ranged from -20 to +20 db. The attenuator on the output of the summer, limiter, and power amplifier was inserted to provide the proper signal levels to the simulator and to prevent any non-linear operation of the microwave mixer due to over-drive. The local oscillator was varied in frequency so that one sideband of the mixed product was centered within the simulator bandwidth. The automatic gain control monitor on the simulator was noted to read constant in all tests (34 μa) to ensure a constant output level of the simulator automatic gain control amplifier. The output of the simulator was monitored using a spectrum analyzer. Photographs of the frequency spectrum on the output of the simulator were taken for each one db increment in R over the range -20 db to +20 db. Knowing the scale calibration on the analyzer permitted the reading of the relative amplitudes of all spectral lines on the output for each input ratio. The significant data found from this test is shown in Figure 3.9-2. These curves illustrate the relative amplitude of each spectral component on the output as a function of R.

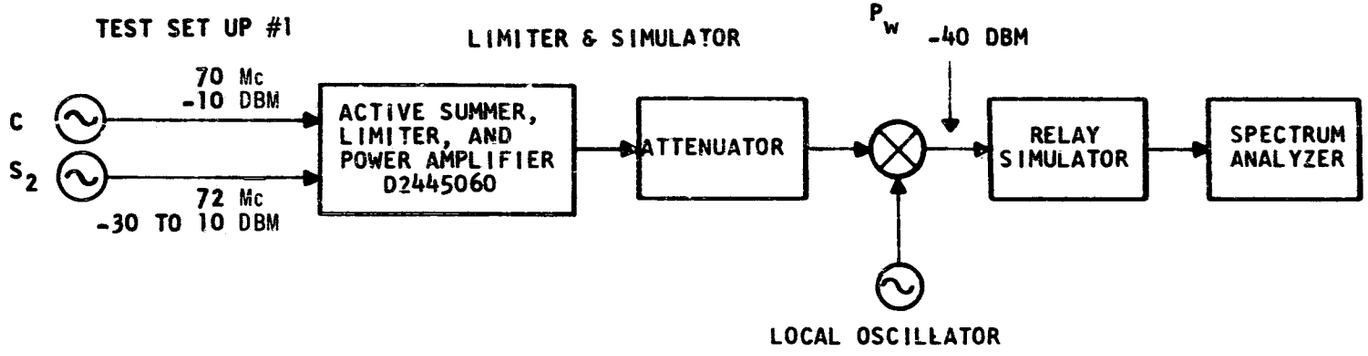

(a)

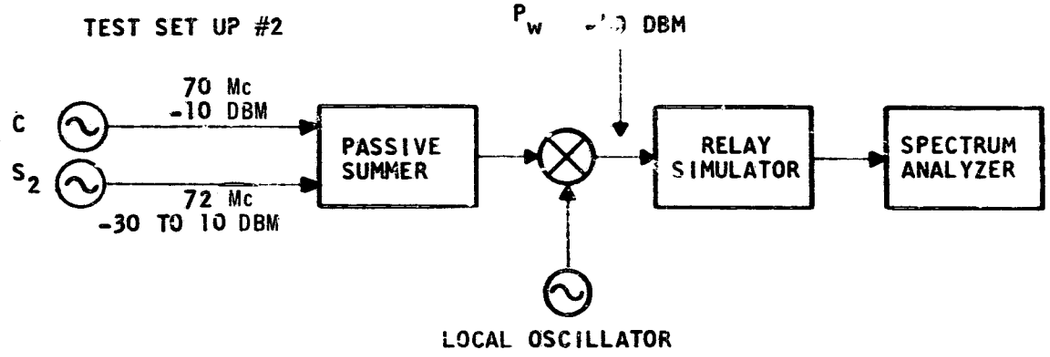

(b)

Figure 3.9-1. Simulator Experiment Test Set-Up

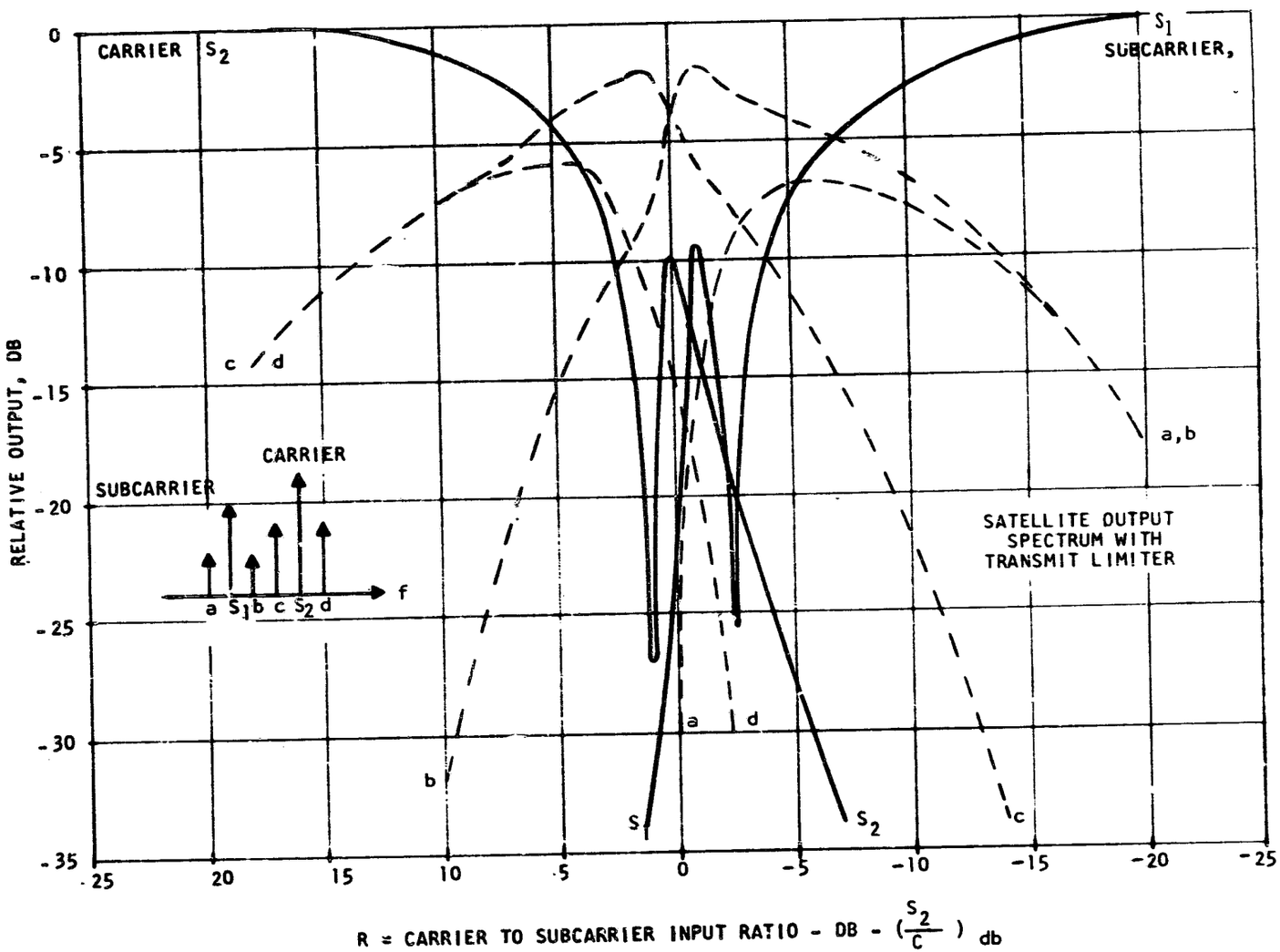

Figure 3.9-2. Output Spectrum Versus Input Level with Limiter

The 0 db relative amplitude point is a reference representing the single signal output under the conditions that only one signal is present on the input. The illustration found on this graph serves to identify the proper spectral line with its corresponding curve. The frequency difference between each spectral component is equal to the difference between C and S_2 on the inputs: 2 MHz. The 6 MHz difference between S_1 and S_2 on the simulator output is due to the tripler in the simulator, Figure 3.9-3.

The second experiment was performed in essentially the same way as the first, except that the summer, limiter, and amplifier was replaced by a passive summer (see Figure 3.9-1B). The results are shown in Figure 3.9-4.

Selected photographs of the simulator output spectrum are shown in Figures 3.9-5 and 3.9-6. Figure 3.9-5 pertains to the experiment performed on the limiter and simulator, and Figure 3.9-6 to the experiment performed on the simulator alone. The two extreme cases of input ratio for the limiter and simulator test can be described by noting that when $C \ll S_2$ or when $C \gg S_2$, the output of the limiter will be equivalent to a phase modulated signal with small deviation having as one of the sidebands either C or S_2 and the carrier as the stronger signal. The tripler will then triple the magnitude of phase deviation while not effecting the rate of phase deviation; 2 MHz in this case. Therefore, the output of the simulator should be closely approximated by a phase modulated signal. For the cases in which the level of C is on the order of S_2 there is no explanation as yet. To fully realize the performance in these regions would require a quite complicated mathematical investigation. Some of the inconsistencies in the values of levels pertaining to the phase modulation analog can be accounted for by noting the limiter output is filtered by the power amplifier causing one sideband to be weighted more heavily. Noting the close similarity between the results of the two tests it can be inferred that the non-linear operation of the tripler in the simulator is much the same as that of a limiter. Therefore, there is no need to precede the simulator by a limiter because both systems exhibit the same characteristics. Finally, it should be noted that to obtain a reasonable ratio of $\frac{S_1}{S_2}$ on the output of the simulator, the useful output level of the carrier S_2 must drop by drastic amount.

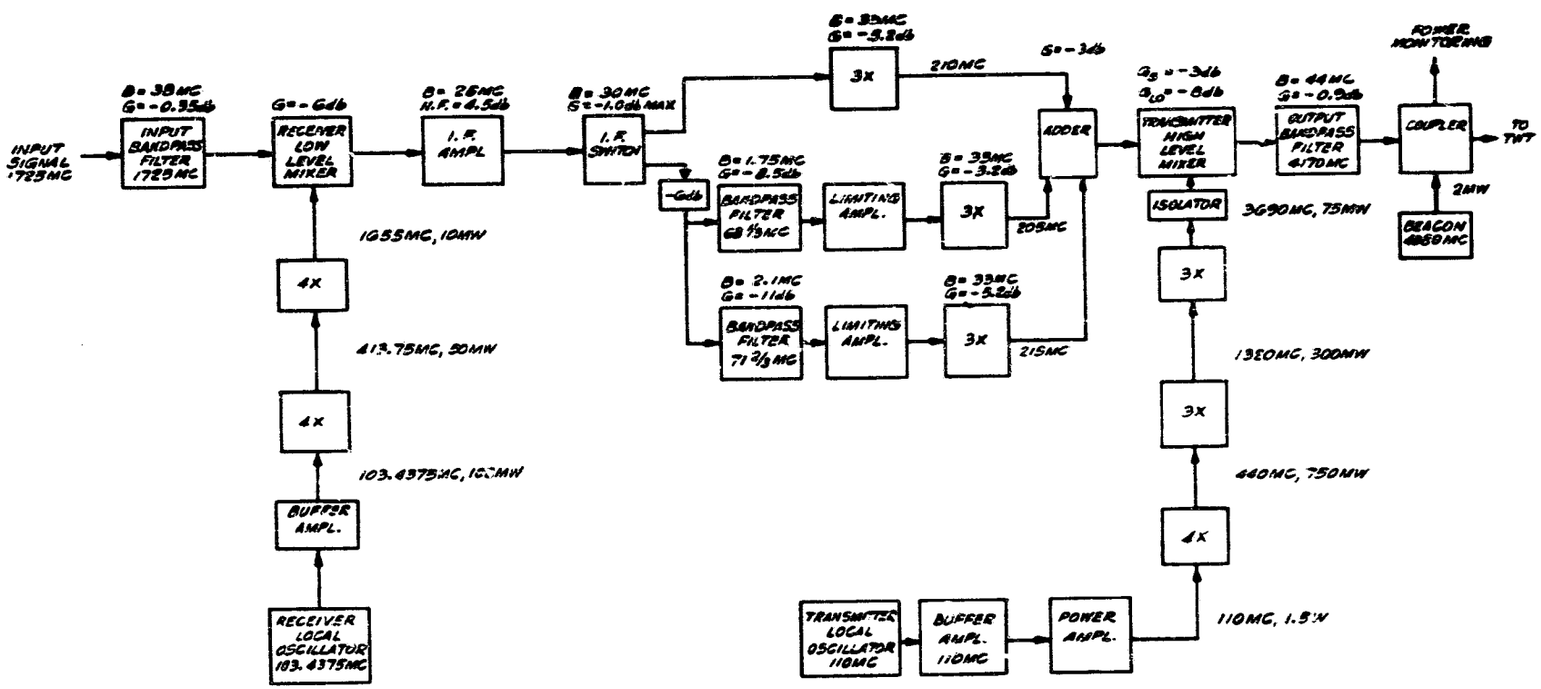

Figure 3.9-3. Block Diagram Relay Transponder

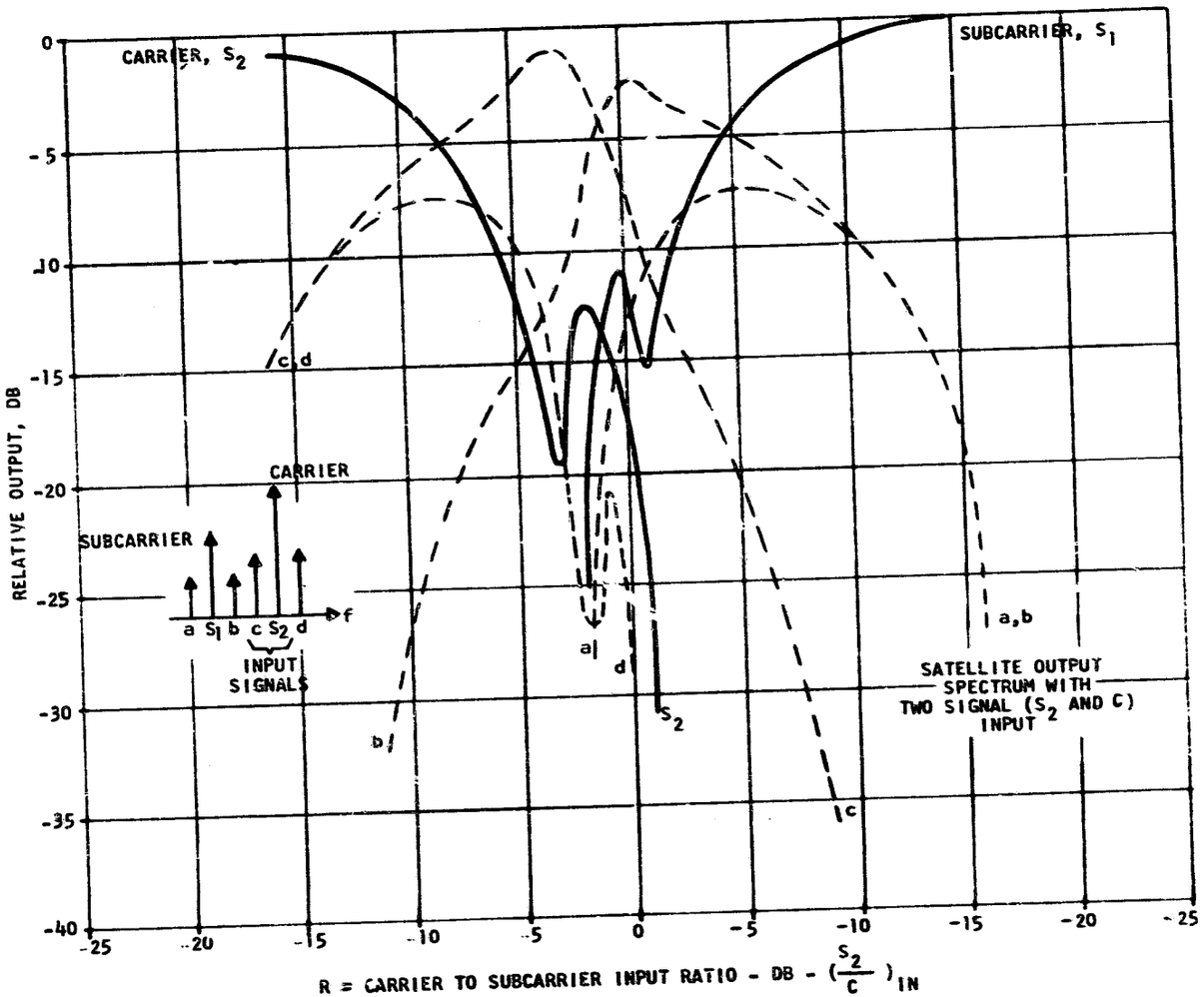

Figure 3.9-4. Output Spectrum Versus Input Level without Limiter

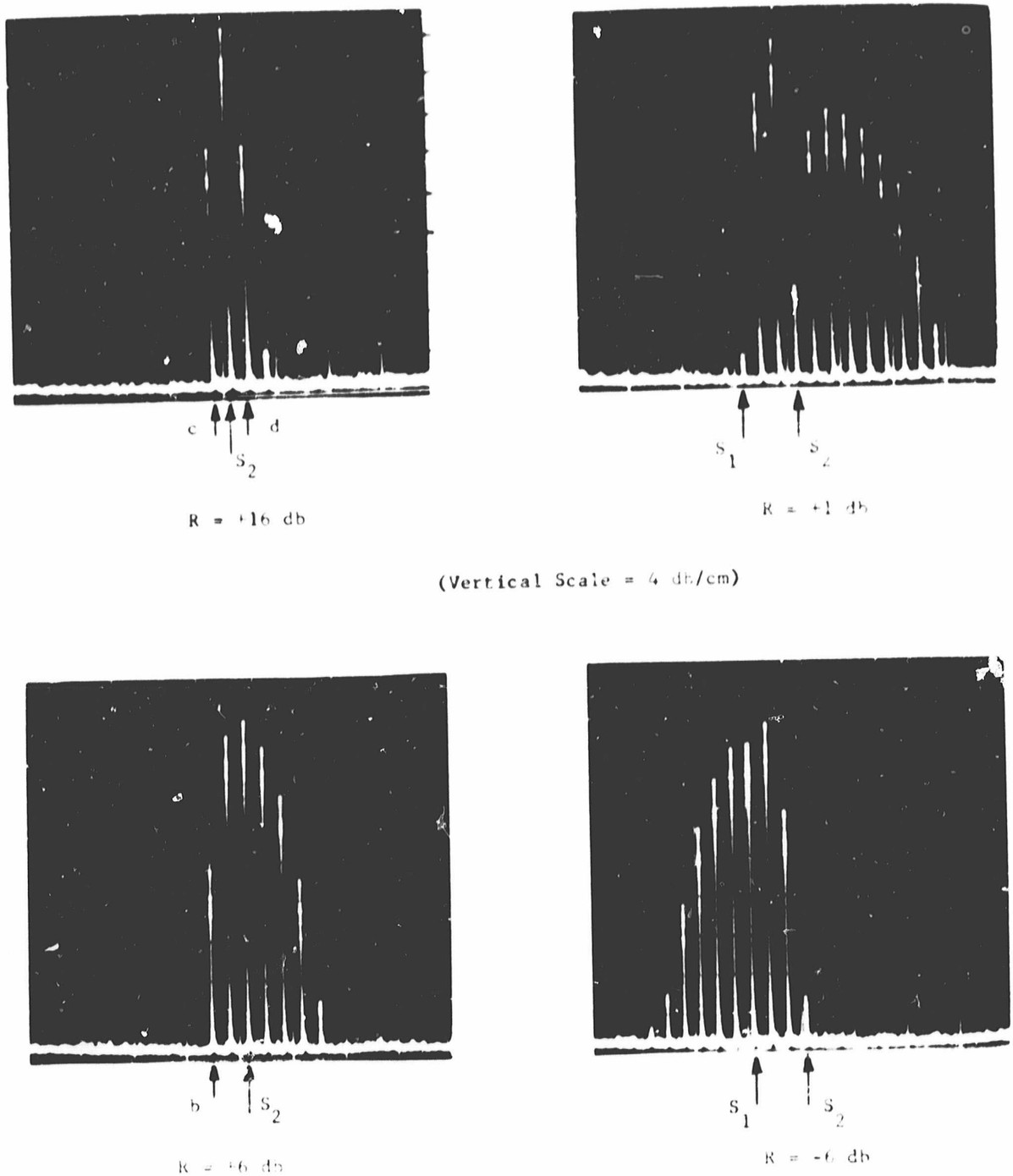

Figure 3.8-5. Output Spectrums with Limiter (Photo)

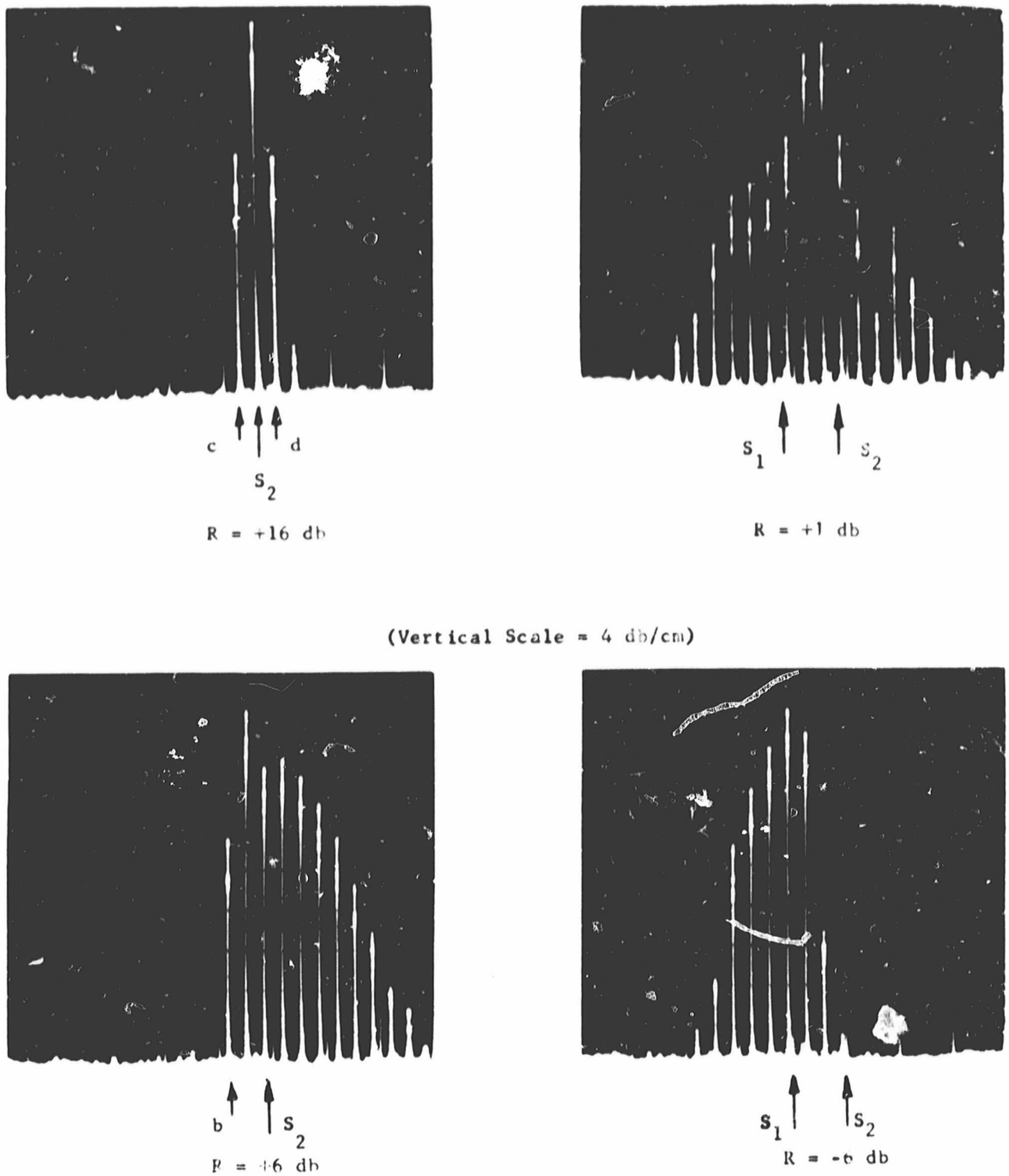

Figure 3.9-6. Output Spectrums without Limiter (Photo)

3.10 REFERENCES

3-1 P. E. O'Neill, Jr. Closed-Loop Doppler Correction Scheme, Document No. X733-67-281, Goddard Space Flight Center, Greenbelt, Md. June 1967

3-2 J. G. Truxal, Automatic Feedback Control System Synthesis, McGraw-Hill, New York, 1955.

3-3 Technical Note No. 1, Servo Motor, Kearfott Division, General Precision, Inc., Little Falls, N. J., September 1, 1961.

3-4 J. Millman and H. Taub, Pulse and Digital Circuits McGraw-Hill, New York, 1956.

4. DESCRIPTION OF TDMA EXPERIMENT

The experimental Phase of this program, was to demonstrate the feasibility of the TDMA system using a medium altitude satellite and a small ground station. The Relay II satellite was used for the tests; Table 2.5-1 summarizes the Relay II orbit parameters. The small ground station was defined as one having a 10 foot antenna and a 300°K system noise temperature.

The program was constrained to use one ground station for both the master and slave terminals. Two TDMA terminals were constructed and installed in the Nutley ground station. The electrical interface between the TDMA equipment and the ground station is described in Section 4.1.

The test set up and instrumentation is described in Section 4.2. The test set up was arranged so that both TDMA terminals were electrically independent except that they both received the same i-f input from the station receiver and their i-f outputs were summed to drive the station transmitter. The main part of the instrumentation was a chart recorder which had eight analog channels and five event markers.

The test program covered the period from January 15 to June 1, 1967. During this period all possible types of Relay II orbits of interest were observed from Nutley. These included maximum and minimum range, maximum doppler and maximum doppler rate. Experiments were performed during 55 passes and several other passes were also scheduled but were cancelled due to equipment malfunctions. A complete operations summary of all passes scheduled is contained in Section 4.4.

4.1 TDMA TO NUTLEY GROUND STATION INTERFACE

A block diagram of the transmit interface is shown in Figure 4.1-1. The i-f outputs of the two TDMA terminals are coupled to the summer/limiter and 0.8 watt amplifier. The output of the 0.8 watt amplifier is coupled to the high level mixer input of the AN/GRC-66 exciter. This input is available after disconnecting the 70 mhz frequency modulator internal to the exciter from the mixer.

The other input to the high-level mixer is from the exciter local oscillator at 1.5 watts. Thus, with 0.8 watt i-f to the mixer, the two signals are comparable in amplitude. It was found that with this amplitude, the exciter had a tendency to limit and degrade the on-to-off ratio in the pulsed mode. By attenuating the i-f signal, a more satisfactory on-to-off ratio was obtained without any noticeable sacrifice in exciter output power of 14 watts at the operating frequency. The exciter front panel meter in the MCO position monitors the i-f level from the TDMA. The attenuator preceeding the i-f mixer input is adjusted for 10 ua on this meter in the cw mode.

The exciter output is coupled to the 10 kw klystron power amplifier. The output is coupled to the antenna by waveguide. A waveguide switch is located at the base of the antenna tower to transfer the output to a water load. This waveguide switch is controlled from the console and must be set to ANTENNA, green indication, for normal operation. A previous waveguide switch for moon bounce operation was removed.

A coaxial directional coupler is used to couple a portion of the exciter output to the satellite simulator. The satellite simulator has an adjustable input attenuator which is normally set so that the agc voltage indicates 31 μa on the simulator panel meter. The simulator output is coupled to the receiver input as described below. Alternatively, the simulator input can be obtained from a directional coupler on the power amplifier output waveguide. This is usually done just prior to the beginning of a pass to provide a check on the klystron tuning. The output can also be monitored by the TDMA operator with a spectrum analyzer.

It is necessary to turn on the exciter power supply and also the moon bounce sequence switch in the small dome to operate the exciter. In addition, the 2 kmc exciter switch on the console must be on green indication. The exciter is interlocked with the power amplifier and antenna limits by breaking the 115 vac power to the exciter 800 volt supply. This interlock will only interrupt the exciter if the beam voltage is on.

When the antenna elevation is below limits, the exciter is interrupted as indicated by failure to obtain the green indication on the 2 kMc exciter switch on the console.

A block diagram of the receive interface is shown in Figure 4.1-2. The Nutley station previously had two receivers, the tracking receiver and the communications receiver. The tracking receiver is used as before, but the communications receiver has been replaced at i-f by the TDMA equipment. The antenna mounted front end components for the communications receiver are used as before. These components consist primarily of the uncooled paramp, the mixer and pre i-f, and the communications receiver local oscillator.

The sum channel waveguide from the antenna is coupled to a diplexer, one output of which drives the tracking receiver sum channel mixer. The other output is coupled to the paramp through a waveguide switch. The paramp varactor bias and pump level are adjusted from the communication receiver rack in the small dome. These are normally set to approximately 8 μa and 5 ma, respectively. The paramp output is coupled through a coax switch to the mixer and pre i-f. The switches at the input and output of the paramp are controlled from the console.

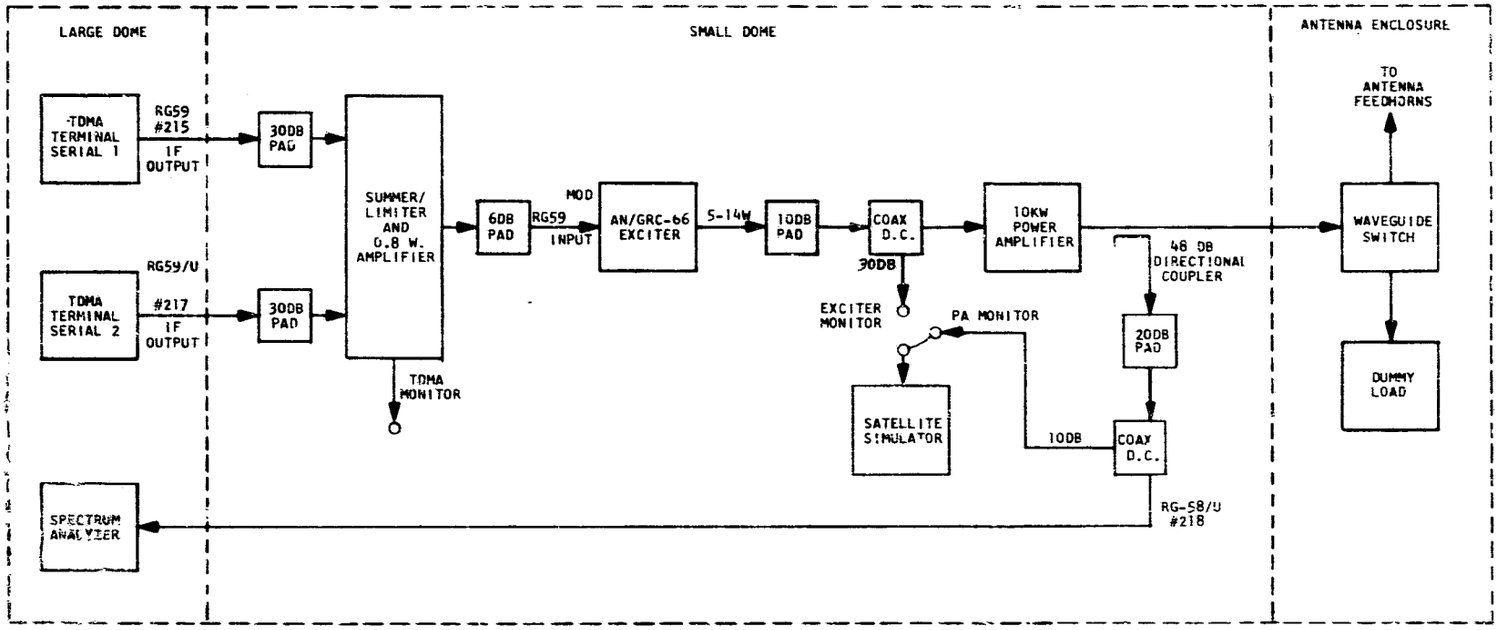

Figure 4.1-1. Transmit interface Block Diagram

The paramp was measured on the bench to have a noise figure of 3.5 db. The nominal gain of the paramp, mixer and pre i-f is 45 db but was measured as 50 db. This is consistent with previous measurements made on the station. A Hewlett-Packard G347A argon gas noise tube is coupled to the sum channel waveguide to make system noise temperature measurements (this is also coupled to the tracking receiver difference channels waveguides). The coupling loss is 18.2 db. A test signal input to the noise tube waveguide is also available and this is coupled to the small dome by coaxial cable. This is used to couple signals from the beacon simulator for testing the tracking receiver and from the satellite simulator for loop back testing of the TDMA equipment.

The pre i-f amplifier is followed by a 37 db linear amplifier, located in the antenna compartment. The output is coupled to the TDMA patch panel by 50-ohm RG-214/U coaxial cable. The gain of this amplifier was chosen so that no limiting would occur on the strongest background interference measured. The signal levels indicated in Figure 4.1-2 are for minimum predicted signal strength for the Relay II satellite.

A patch panel was constructed for mounting the i-f filters and amplifiers in the large dome. Numerous BNC connectors are available for convenience in modifying connections to the TDMA terminal i-f inputs. The broadband received i-f from the antenna amplifier is coupled through a 3 MHz bandwidth 5 pole gaussian approximate bandpass filter centered at 76 MHz, which is sufficiently wide to pass the 800 kHz sidebands of the master sync burst.

A problem in the system design for the TDMA interface is how to keep the signal input level to the 76 MHz phase locked loops constant at the design level of 0 dbm. The two approaches considered were the use of a bandpass limiter and agc operated from the pulsed signal.

It was felt that agc would be excessively complicated with the variable TDMA format used. Therefore, the 76 MHz bandpass filter is followed by a wideband limiter with dual outputs at 0 dbm. The limiter will go into full limiting with noise alone. The tests with this approach have been highly successful and the fact that noise fills the output during intervals between signal pulses appears to cause no difficulty.

The broadband i-f signal from the antenna is coupled through a 750 kHz bandwidth 5 pole gaussian approximate bandpass filter centered at 70 MHz, which is sufficient to pass the 100 kHz sidebands of the psuedo noise modulation and still narrow enough to avoid the local interference. Since the TDMA terminals already have limiters at the input of the 70 MHz phase locked loops, it is only necessary to amplify the filter output by 15 db to ensure full limiting. The 70 MHz filter output is a convenient point to make noise figure measurements. A patch can be made by a cable, to the 70 MHz input of the noise figure meter located in the small dome.

FOLDOUT FRAME 1

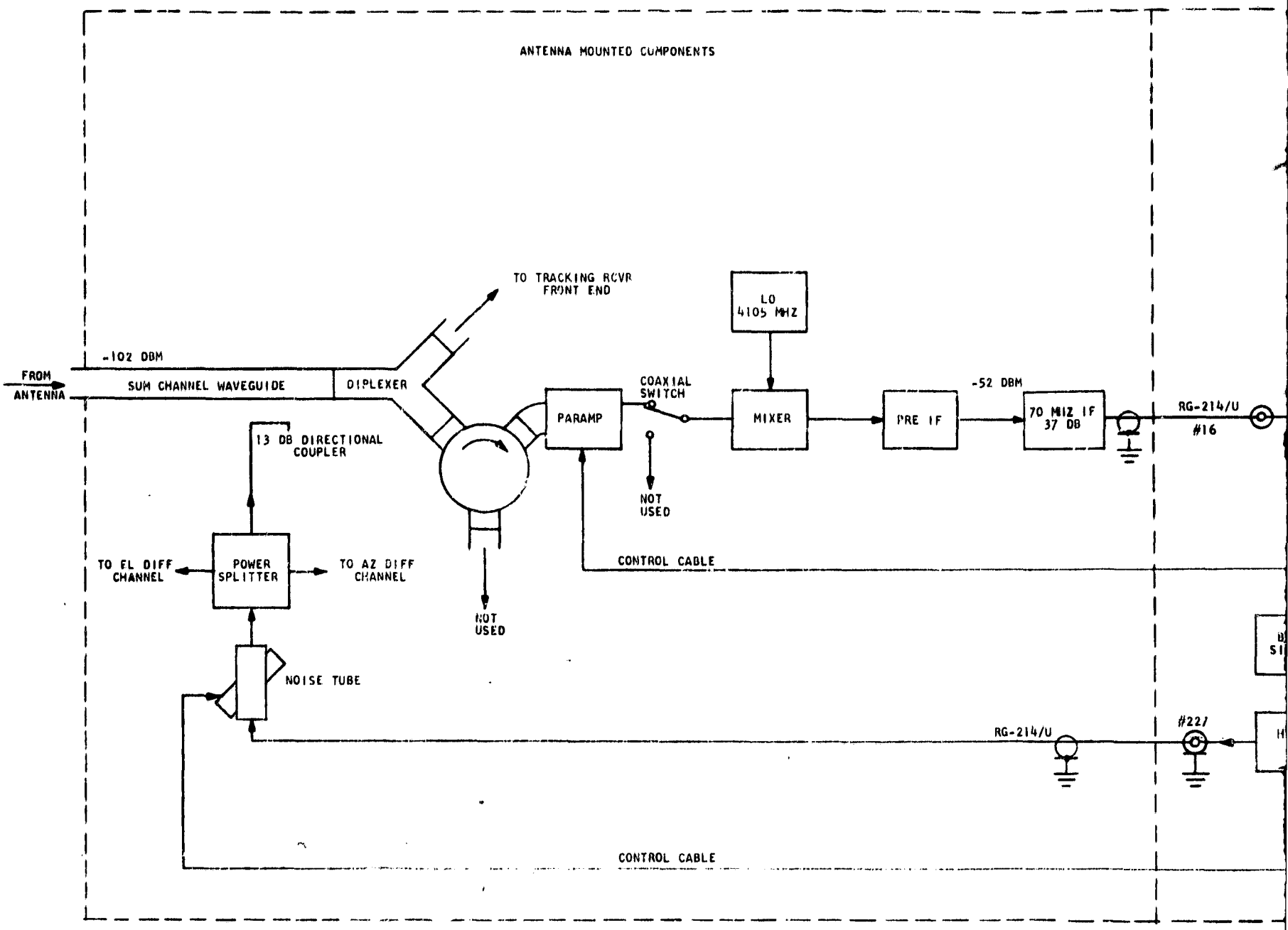

NOTE: SIGNAL LEVELS SHOWN ARE MINIMUM EXPECTED SIGNAL STRENGTH

FOLDOUT FRAME 2

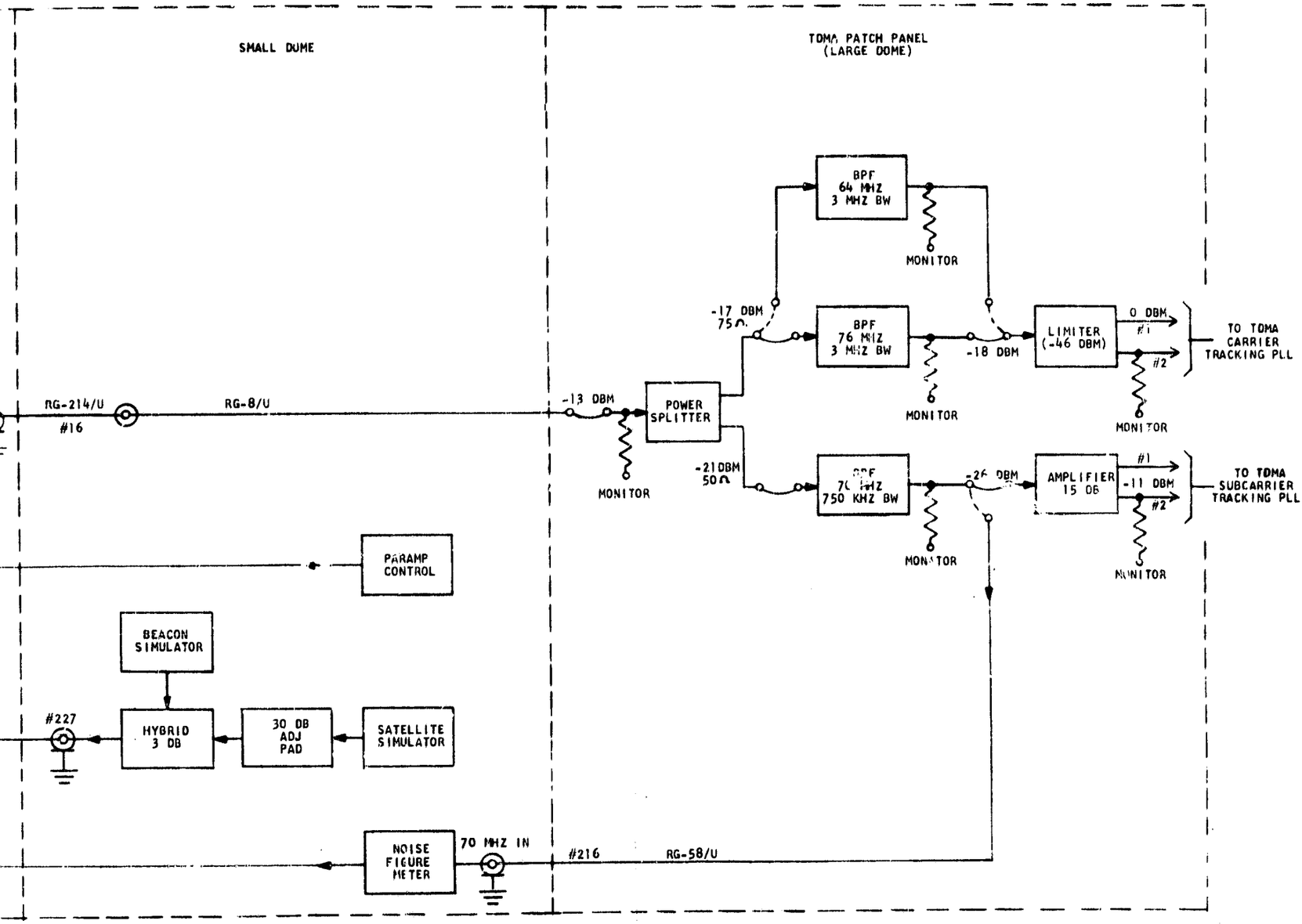

Figure 4.1-2. Receive Interface Block Diagram

A problem was encountered in the operation of the 10 kw klystron power amplifier in the pulsed mode. Before each pass, it was tuned while transmitting a cw carrier. In addition, the output power was adjusted to the correct value in the cw mode because the power meters respond to average power and are not accurately calibrated at the low average power which results in the pulsed mode. It was discovered that if the klystron was not tuned properly for wideband operation the actual peak power in the pulsed mode was several db below that measured in the cw mode due to the drift of the klystron tuning with time.

4.2 TEST SETUP AND INSTRUMENTATION

A block diagram of the test setup is shown in Figure 4.2-1. The i-f outputs of each TDMA terminal are summed to drive the station transmitter and the i-f output of the station receiver drives both terminal inputs. The chart recorder is used to record the following types of data:

- Real time
- Loop lock signals
- Acquisition mode signals
- Range modulo 18.56 Km
- Timing error

An event marker was used to record second and minute ticks from the station clock. The clock time was checked before and after each pass with standard time broadcasts from CHU, Ottawa, Canada. Occasionally, WWV, Fort Collins, Colorado was used instead. The clock setting was kept with 0.1 second of correct time, and in addition, the clock error was recorded before and after each pass to within 10 milliseconds. Except for a few passes of duration greater than about one half hour, a one cm/sec chart speed was used. This permitted reliable measurement of event times to within 0.1 second.

The phase difference between the transmitted and received TDMA signal provides a direct measurement of satellite range modulo 18.56 Km. The ambiguity results from the approximately 8 kHz frame repetition rate. A more detailed discussion of this range measurement is contained in Section 9.2. A phase detector is connected between the transmit and receive timers in the master terminal to provide this measurement.

The colocation of the two TDMA terminals at the same ground station provides a convenient way of measuring timing error. After the master and slave terminals have acquired, both should be transmitting their formats in phase. Timing error is then measured by comparing the phases of the two transmit timers. By connecting the phase detector to different points in the divider chain in the timer, various resolutions in this measurement can be obtained.

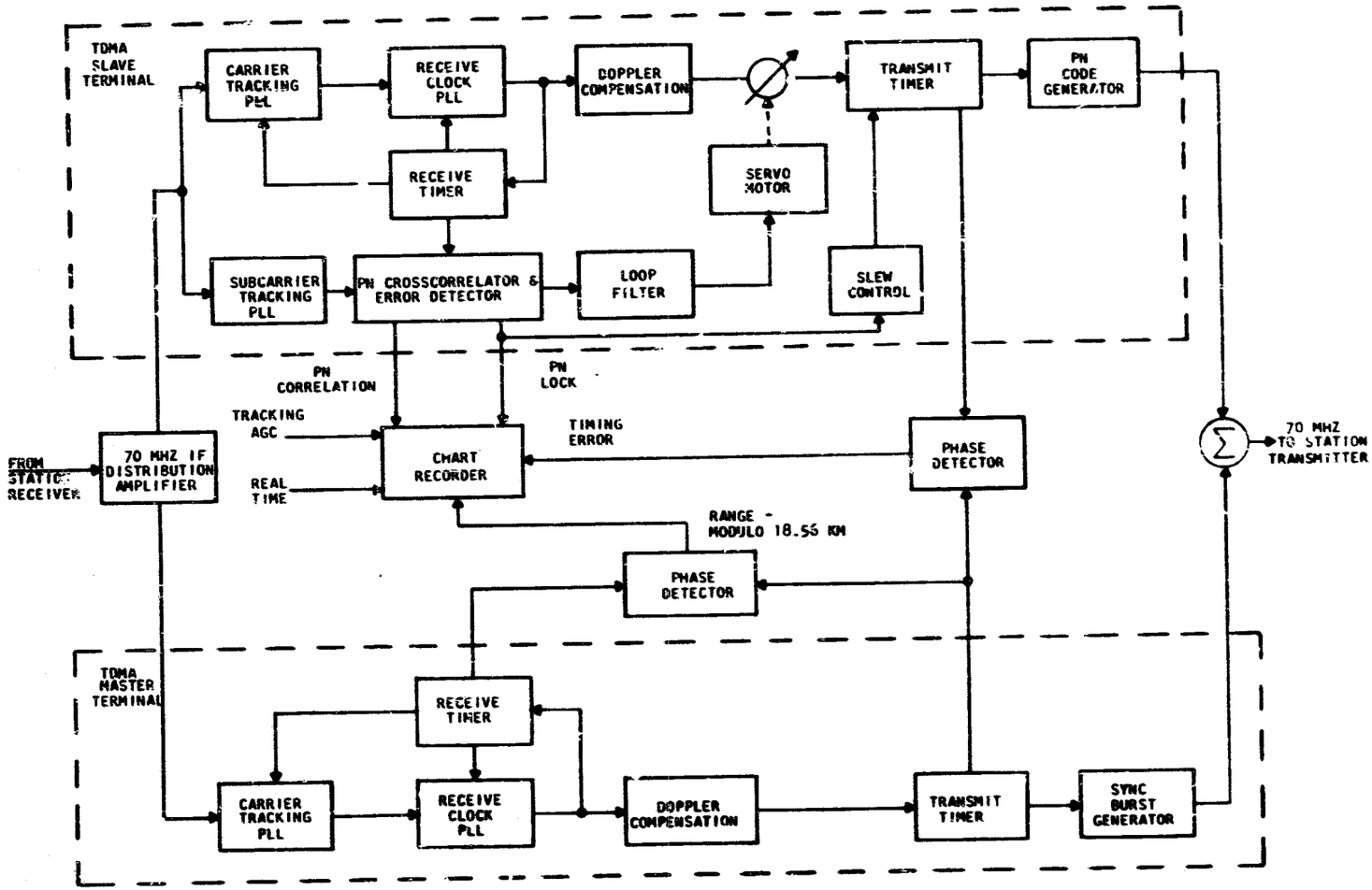

Figure 4.2-1. Test Setup Block Diagram

Figure 4.2-2 shows a portion of a typical chart recording obtained. This shows one run of the slave acquisition experiment. The data recorded on the various channels is as follows:

Number	Analog Channel	Event Marker
1	Slave transmit mode status	Master terminal transmit phase locked loop lock
2	Motor driven phase correction to slave transmit clock	Slave terminal carrier tracking phase locked loop lock
3	Tracking receiver agc	Slave terminal receive clock tracking phase locked loop lock
4	Slave receive mode status	Slave terminal transmit phase locked loop
5	Timing error - 123.75 μs full scale	Not used
6	Timing error - 11.25 μs full scale	Pseudo noise ranging phase locked loop lock
7	Pseudo noise cross correlator output	Real time
8	Range modulo 18.56 Km	Not used

To illustrate the meaning of this recording, the slave acquisition procedure will be described briefly.

The slave terminal must first acquire the sync burst received via the satellite from the master terminal by locking the phase locked loops for carrier tracking, receive clock tracking, and transmit doppler compensation. After the receive acquisition is completed, the slave begins transmit acquisition by transmitting a ranging signal. The ranging signal is then acquired by locking the subcarrier tracking and the pseudo noise ranging loops. The transmit clock phase is further adjusted by the fine slew which completes the transmit acquisition.

The start of the receive acquisition experiment occurs when the operator steps the receive mode from 0 (step) to 1. This occurred at $20^h\ 15^m\ 26.9^s$ for the run shown in Figure 4.2-2. The carrier tracking loop acquisition time is measured from this starting time until the carrier tracking loop lock time which is at $15^m\ 37.0^s$ in Figure 4.2-2. The total receive acquisition time is measured from the starting time until the transmit loop lock, $16^m\ 44.4^s$ in Figure 4.2-2.

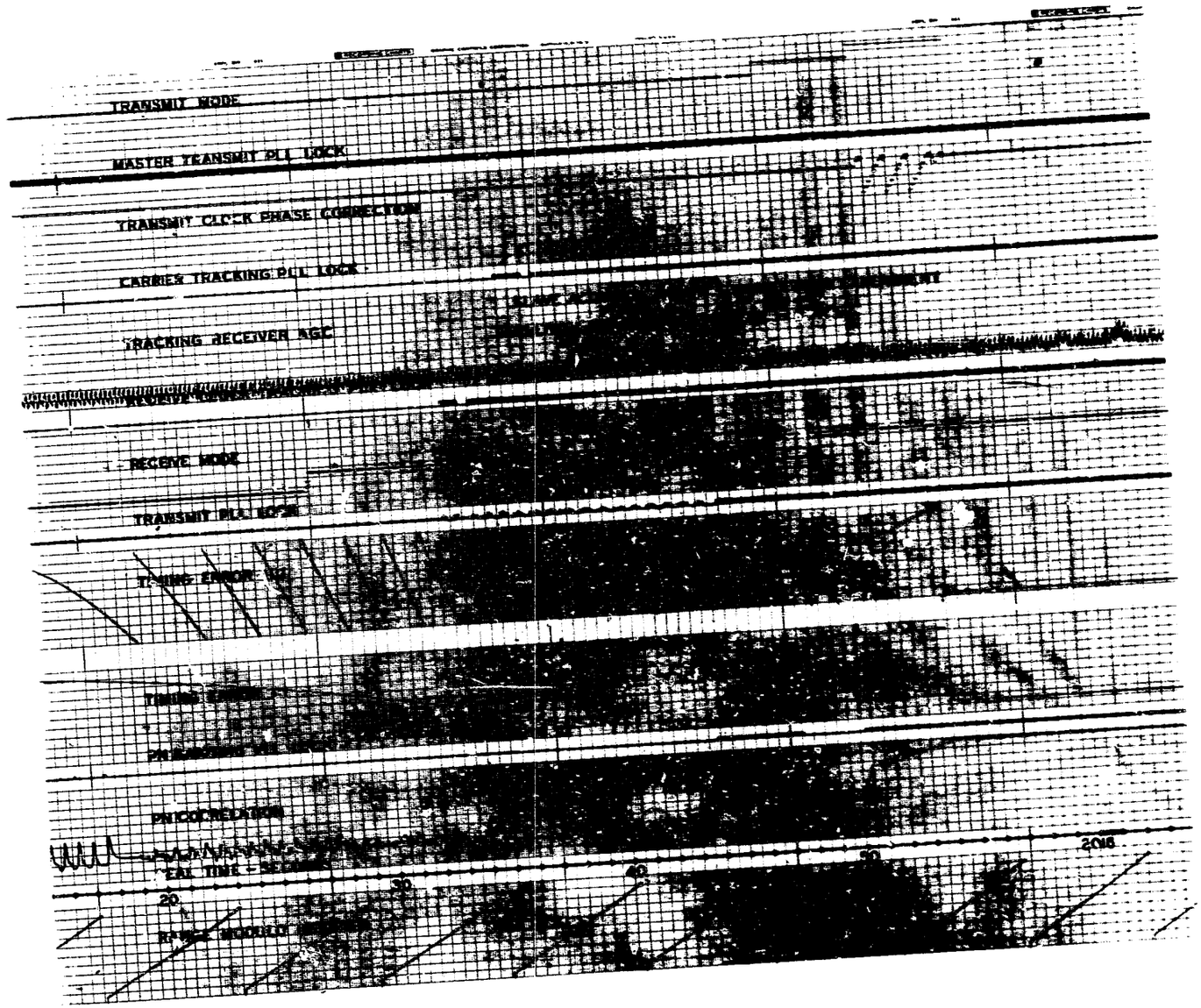

Figure 4.2-2. Slave Acquisition Experiment Chart Recording

The carrier tracking loop is acquired by using a manual procedure for assuring lock to the correct spectral line. This procedure is discussed in Section 5. The receive clock tracking loop usually locks at about the same time as the carrier loop.

The start of the transmit acquisition experiment occurs when the operator steps the transmit mode from 0 (stop) to 1, 15^m 47.0^s in Figure 4.2-2. The transmit fine slew starts when the operator steps the transmit mode from 1 to 2 and ends when he steps from mode 2 to 3. These occurred at 15^m 51.1^s and 15^m 55.2^s respectively, in Figure 4.2-2.

It was recognized during the test period that a doppler preset was required for the transmit phase locked loop. Previously, the doppler preset for the receive clock loop was used to preset the transmit loop as well, since the transmit loop is normally locked to the receive loop. It was found that the receive loop locked too quickly for the transmit loop to follow and frequently difficulty was experienced in subsequently locking it.

It was therefore decided to use the same voltage preseting both the receive and transmit loops. The present voltage drives the two loops in opposite directions in frequency to correspond to the foldover action of the transmit phase locked loop. This modification has been entirely satisfactory and no further difficulty with the doppler preset has been experienced.

The TDMA terminal has four transmit and four receive acquisition modes. It was desired to record the acquisition mode on a single analog channel rather than using several event markers. For this purpose a mode status decoder circuit was designed and used for indicating the mode status on the chart recorder.

5. CARRIER TRACKING PHASE LOCKED LOOP

As discussed in Section 2.3, the carrier tracking loop locks to the periodic sync burst received from the master. It operates in conjunction with the receive clock tracking phase locked loop and the sync burst detector. This turned out to be one of the most difficult areas of the system to implement. Since the sync signal is periodic, its spectrum consists of a number of discrete spectral lines spaced at the repetition frequency which is approximately 8 kHz. The carrier tracking phase locked loop then can lock to any of these spectral lines and initially acquires a multiple of 8 kHz from the incoming frequency.

A manual acquisition procedure was used to insure that the loop locks to the correct spectral line. This procedure is described in Section 5.1. The acquisition time is fairly long because of this manual procedure. Section 5.2 contains a summary of the carrier tracking phase locked loop acquisition time. Possible techniques for making this acquisition procedure automatic were studied and are discussed in Section 5.3.

An alternate method of making the carrier tracking phase locked loop automatic would be to widen the loop bandwidth to the point where it could not lock to the wrong spectral line. Since the bandwidth at which this occurs was not known, an experiment was conducted using various loop bandwidths wider than the 1000 Hz used in the original design. The results of these tests are described in Section 5.4.

5.1 CARRIER TRACKING LOOP ACQUISITION

The carrier tracking loop function is to demodulate the 800 kHz sync burst. The acquisition of the pulsed signal with this loop is quite tricky and various techniques were tried with varying degrees of success.

The following methods were tried for acquisition in the pulsed mode:

1. Preset frequency method.
2. Sweep method.

The pulsed mode represents the acquisition problems encountered by a slave station trying to come in sometime after the master station is operational.

In the preset method, the frequency of the loop is preset to the expected return frequency based on predicted doppler shifts vs time. For this method to work perfectly, the preset frequency must be within ±4 kHz of the received frequency and this frequency not only includes doppler shift but all frequency errors introduced by any of the oscillators in the system; i.e., transmitter up-conversion oscillator, transmitter i-f oscillator, conversion oscillators in the satellite, and the down-conversion oscillator in the receiver. Because this is a gated loop, and the gate timing has not yet acquired, the first few samples most probably occur at the wrong time. This admits noise into the loop which throws the preset frequency off.

In general it was found that the loop would acquire several spectrum lines off using this technique. The signal could be jogged in by momentarily shorting out the error signal with loop error shorting switch and by observing the output signal on a scope. If the error is ±1 or 2 lines, the slope of the signal on the scope indicates the direction to turn preset dial to find the carrier and the acquisition is rapid. More often, the loop is many lines out and some trial and error is involved slowing down the acquisition process.

In the sweep method, the confusion of which way to turn the dial is largely removed and leads to the fastest acquisition. In this method the preset dial is turned to an extreme position, e.g., clockwise. The operator now knows regardless of where he is in the time of the pass that he must turn the dial counter clockwise to acquire the signal. Doing this at a rate of about 2 turns per second he will acquire within a few lines, i.e., within 5 turns or 2 1/2 seconds. At this point he uses the shorting switch, except that now he knows that the dial must continue counter clockwise. With an experienced operator, acquisition of the carrier line would take place within 3 or 4 jogs. This method worked out to be the best manual method in practice.

In the master station and in a slave, which can track at the beginning of a pass, lock up on carrier can be automatic, by shorting out the gate, which makes the loop a full time loop. At first, cw carrier and pulsed modulation is transmitted. The loops automatically acquire within 0.1 second when preset to 76MHz. As soon as the loops have been locked up, the shorting switch is opened. This allows the loops to continue tracking in pulsed mode. Next, the master station transmits in pulsed mode and the loops continue to track.

The Sub-Carrier Tracking Loop has the ambiguity problem of locking to the wrong spectrum line, even though the loop is ungated. This is due to the spectrum lines of the pseudo noise signal itself. To acquire this signal, the modulation is turned off, and the loop walks over to the carrier; the modulation is now turned back on and the loop continues tracking the carrier.

5.2 ACQUISITION TIME MEASUREMENTS

The carrier tracking phase locked loop acquisition time was measured as part of the master acquisition in cw mode experiment, the master acquisition in pulsed mode experiment and the slave receive acquisition experiment. The most extensive data was taken for the latter experiment. Little difference was noted between the slave receive acquisition and the receive portion of the master acquisition in the pulsed mode. For this reason more time was spent on the slave acquisition experiments because they provide much additional information not obtained in the master acquisition experiments.

When the master terminal acquires in the cw mode, the carrier tracking phase locked loop is operated cw also. This removes the spectral line ambiguity problem and the loop acquires automatically and within a relatively short time as shown below. Table 5-1 summarized the acquisition time measurements for the carrier tracking phase locked loop.

TABLE 5-1. SUMMARY OF CARRIER TRACKING PHASE LOCKED LOOP ACQUISITION TIME

Exp. No.	Experiment	Average	Std. Dev.	Trials
1A	Master Acquisition - CW Mode			
	Average for all loop bandwidth	1.40 sec	-	17
	Average for 1000 Hz loop bandwidth	0.47	-	14
1B	Master Acquisition - Pulsed Mode	8.65	-	6
2	Slave Receive - over-all	12.73	8.66 sec.	106
	- standard parameters	10.88	6.32	41

Histograms showing the distributions of the acquisition times for slave experiments are shown in Figures 5.2-1 and 5.2-2. The method of tabulating the data for these experiments is discussed in detail in Chapters 6 and 7. For the present, it suffices to note that the manual acquisition procedure requires from about 5 to 25 seconds.

5.3 AUTOMATIC ACQUISITION OF THE CARRIER PLL

It was pointed out earlier that the gated phase locked loop is subject to spectral line ambiguity problems. These were resolved in the experimental equipment by a skilled operator employing an oscilloscope display, a loop error shorting switch, and the preset frequency dial. A brute force solution to the problem of automatic acquisition would be to replace the operator function electronically. This would lead to shorter and more consistent acquisition time.

The operator uses the slope of the gated phase detector output to determine which direction to stress the loop before depressing the shorting switch. This suggests that a double feedback loop could automatically lock to the right spectral line. Such a system might be implemented as shown in figure 5.3-1.

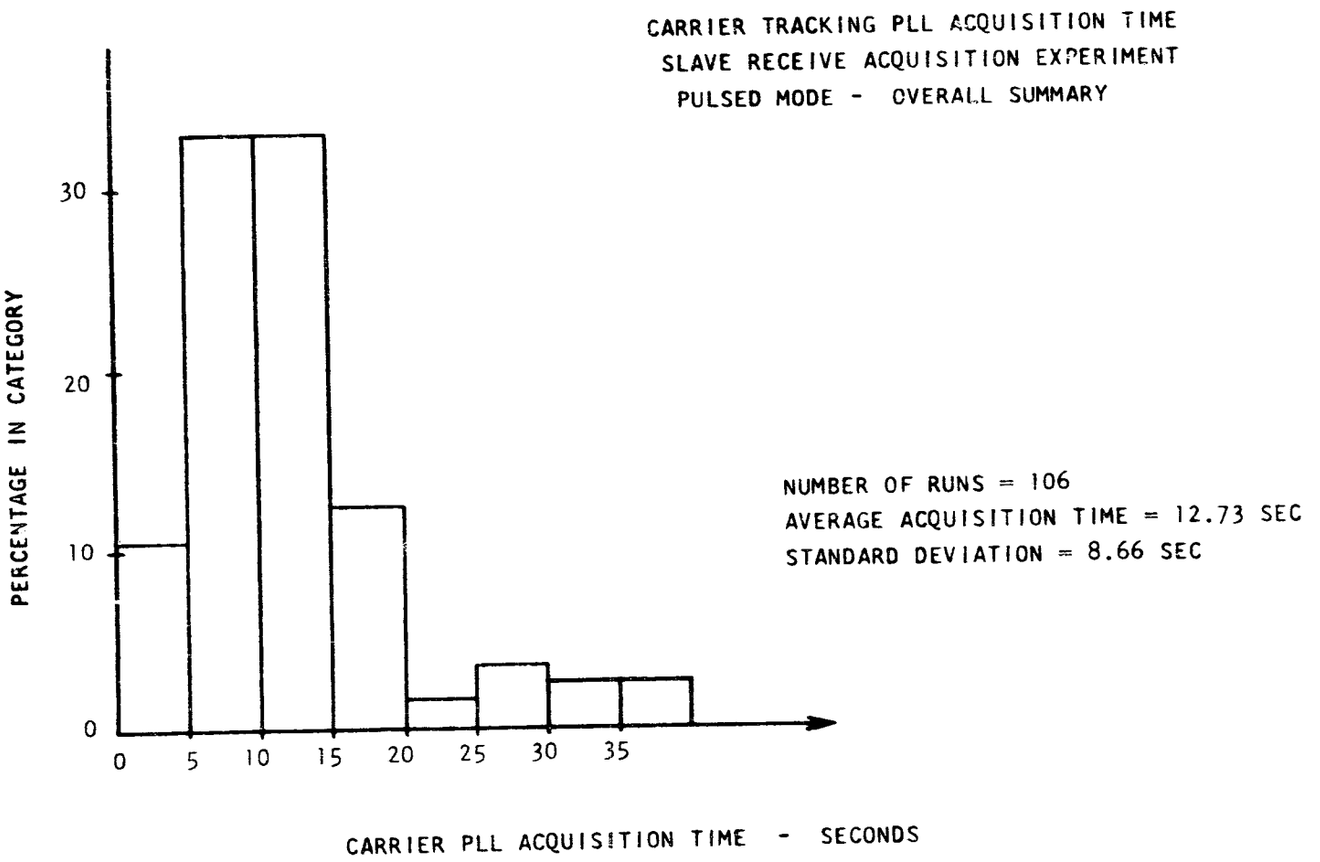

Figure 5.2-1. Carrier Tracking PLL Acquisition Times - Overall Summary

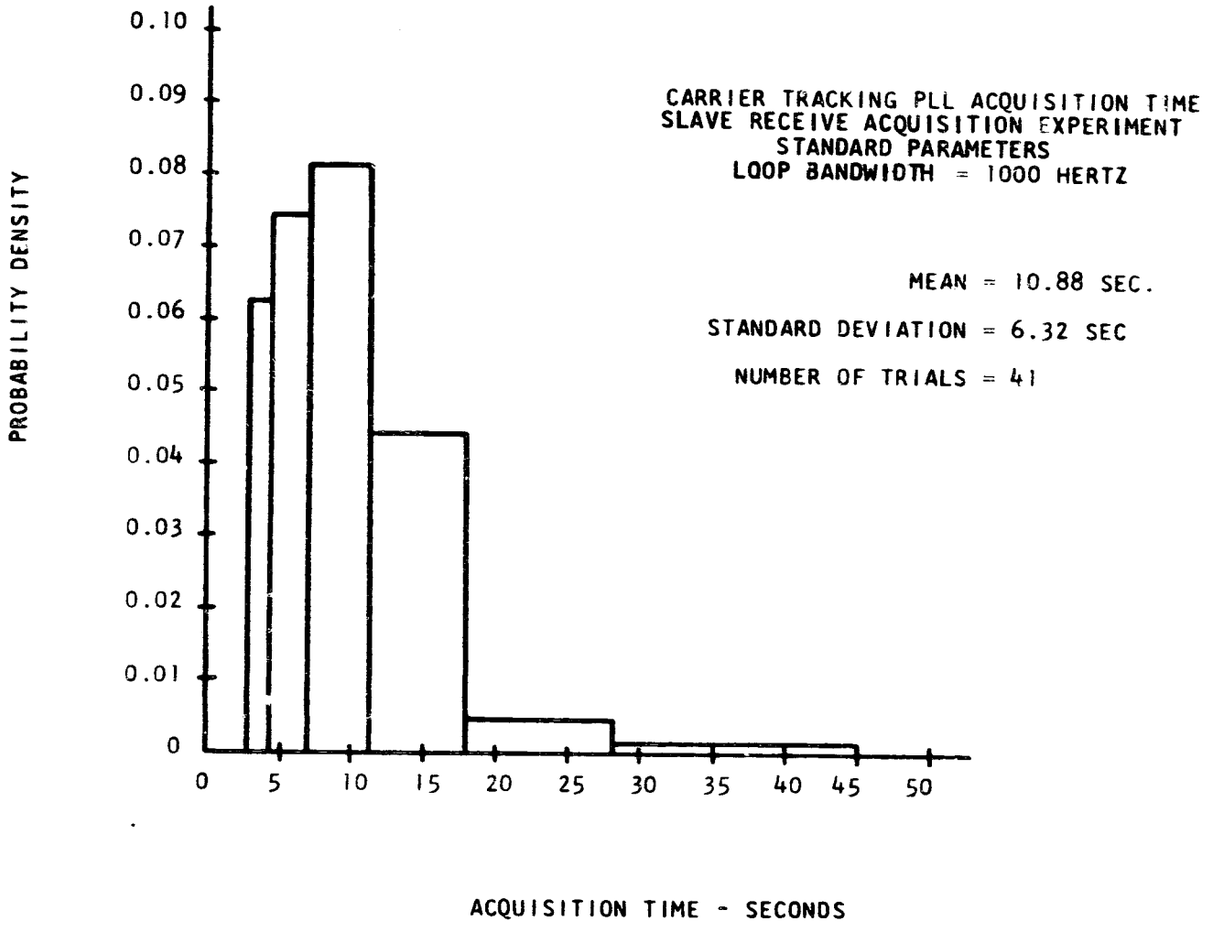

Figure 5.2-2. Carrier Tracking PLL Acquisition Times - Standard Parameters

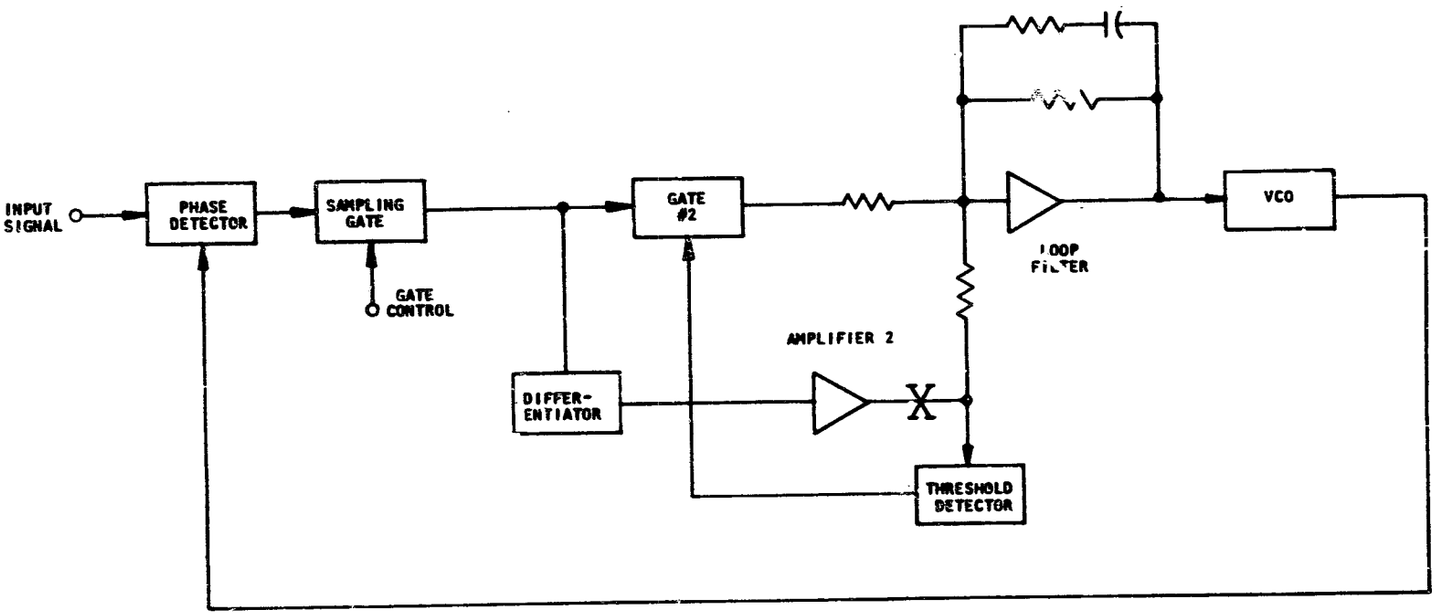

Figure 5.3-1. Method of Automatic Carrier PLL Acquisition

As shown in block form, this circuit consists of the original phase locked loop components shown in Figure 2.4-2 with the addition of four blocks in the lower right of the diagram. These components are gate 2, a differentiator, an amplifier, and a threshold detector. The circuit performs as follows: Assume that the operator has preset the loop to ±3 lines of the correct frequency. Assume that the output of amplifier 2 is 0.1 volt per line of error; that is, an error of -0.3 volts for -3 line error, 0 volts for 0 error, to +0.1 volt for 1 line of error.

Assume that the threshold detector opens gate 2 if the differentiator signal is greater than ±0.05 volts. If the operator had preset the loop to the carrier the differentiator output would be zero and the loop would lock up to the carrier, gate 2 remaining closed at all times. If the operator missed the preset frequency by -3 lines, the differentiator output would be -0.3 volts. This opens gate 2 and the loop is driven closer to the carrier line. When the error has dropped below 0.05 volts, the loop is running at less than half a line away from carrier and gate 2 closes. At this point the normal loop is cut in and since it is less than 1/2 line away from carrier, it will continue to lock in to carrier by itself.

A similar operation takes place if a +3 line error was made except that the voltages are reversed and the loop moves in the opposite direction. After the acquisition has taken place, the circuit may be broken at point X to prevent a noise pulse from re-activating the acquisition cycle.

5.4 WIDEBAND CARRIER PLL

The gated 70 MHz PLL was originally designed for a choice of three loop natural frequencies, 100, 300, and 1000 hertz. The loop is gated at an 8000 hertz rate and will lock an integral number of 8000 hertz from the incoming carrier frequency. Also, the output of the sampling gate had a holding capacitor to hold the value of the error voltage between samples.

A phenomenon was consistently observed with the 1000 hertz bandwidth loop which is not understood. This phenomenon could be observed when the input signal was applied at a low level and the loop was locked to the correct spectral line (i.e., the difference between the input and VCO frequencies is zero and not any multiples of 8000 hertz off). As the amplitude of the input was increased, a point was reached where the loop changed to a lock point 4000 hertz from the input frequency. When the input signal was initially applied with normal amplitude, it was impossible to lock the loop to the correct spectral line. It was felt that this must be a result of using the holding capacitor because the theory of the gated PLL without a holding capacitor does not predict such performance.

The circuit was modified by removing the holding capacitor and adjusting the gain of the loop filter accordingly. Also, capabilities for loop natural frequencies of 2000 and 5000 hertz (damping factor = 0.707) were added.

The open loop gain for the phase locked loop with various f_n is shown in Figure 5.4-1. A simplified schematic diagram of the modified loop filter is shown in Figure 5.4-2. Because the error signal into the loop filter is gated, step inputs are applied to the operational amplifier filter circuit. A rise time filter is placed ahead of the operational amplifier to prevent these step inputs from causing the amplifier output to exceed its maximum slew rate.

The rise time filter has the same response as a low pass r-c circuit with 3 db loss at 700 kHz and a rise time of 0.5 μs. Because the source impedance of the gate circuit is time varying, i.e., switching between essentially an open and short circuit, the low pass filter used is a constant resistance bridged tee configuration. This prevents the time varying source impedance from effecting its frequency response.

This low pass filter appears on the open loop gains as a breakpoint at 700 kHz (not shown in Figure 5.4-1). This breakpoint, which was determined by the maximum slew rate of the present operational amplifier, places an upper limit of approximately 50 kHz on the loop natural frequency.

The solid curves shown in Figure 5.4-1 are really loop gains averaged over one sampling period. They are determined by multiplying the gain when the gate is closed by the duty factor of the gate. This procedure is only valid when the loop bandwidth is much less than the sampling rate. The instantaneous loop gain (during the time the gate is closed) for the 5000 hertz loop is shown by the dotted line in Figure 5.4-1. This corresponds to a loop natural frequency:

$$f'_N = f_N / d^{1/2} = 17,500 \text{ hertz}$$

and damping factor

$$\zeta' = \zeta / d^{1/2} = 2.48,$$

where d is the duty factor for the gate.

For frequencies above about 10 kHz, the instantaneous closed loop appears as a first order loop with radian bandwidth equal to 547 Kilo radians/sec. During the time the gate is open, the loop will accumulate some phase error due to instability of the voltage controlled oscillator. When the sampling gate closes, the accumulated phase error will appear to the loop as a step phase error. The response of a first order loop is such that the phase error will decay exponentially with a time constant equal to the reciprocal of the radian bandwidth. For the 5000 hertz loop discussed, this time constant is approximately 2 μs compared with the period of 10 μs during which the sampling gate is closed.

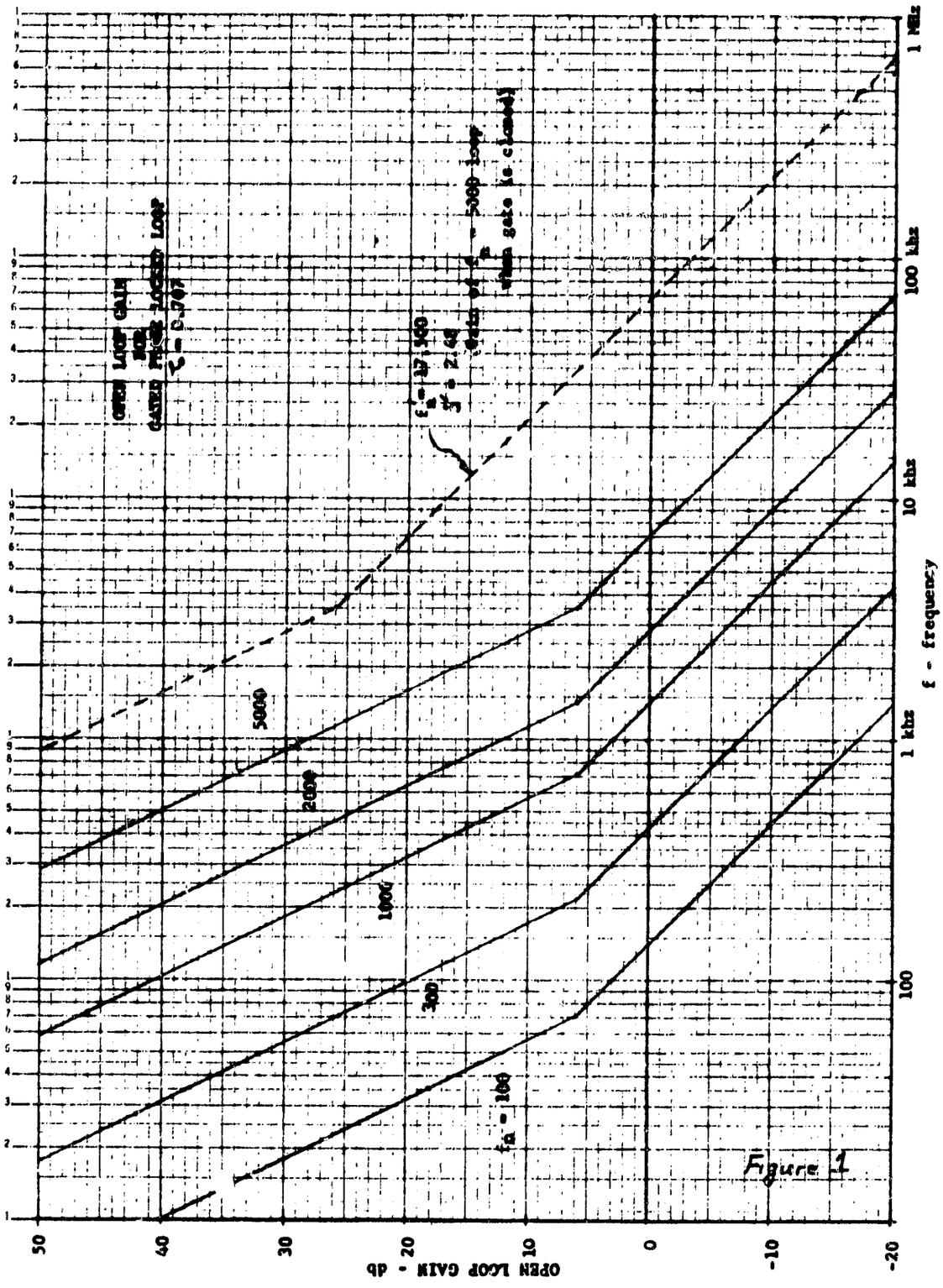

Figure 5.4-1. Open Loop Gain for Gated PLL

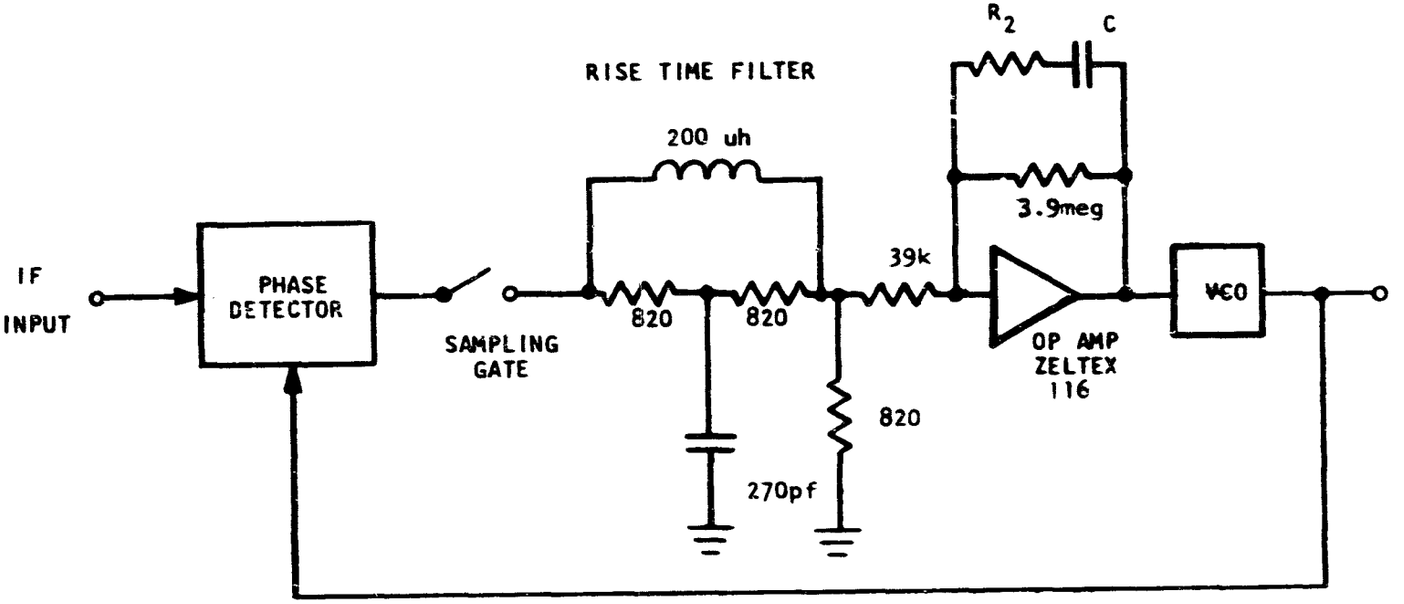

fn	R_2	C
100	220	10 uf
300	680	1.1
1000	2200	0.1
2000	4700	0.027
5000	11,000	3900 pf

SIMPLIFIED SCHEMATIC DIAGRAM
GATED CARRIER TRACKING PLL

Figure 5.4-2. Gated PLL - Schematic Diagram

This behavior was actually observed with the 2000 and 5000 hertz loop natural frequencies. The accumulated phase error at the start of the sync burst appeared to be distributed over ±90 degrees and decayed during the first few microseconds of the burst.

One of the reasons for trying the wider bandwidth loops was to see if they would still lock an integral multiple of 8000 hertz from the input frequency. It was found that the 2000 hertz loop still locked to the wrong spectral line but that the 5000 hertz loop did not.

Another reason for the experiment was to see if the effect of power supply hum on the input signal phase or on the voltage controlled oscillator output could be reduced. Originally the receiver local oscillator in the Nutley ground station had an afc control. It was found that power supply hum was picked up on the afc control lead which ran from the small dome to the antenna compartment. With this condition, the 1000 hertz loop reduced the hum on the demodulated signal to an acceptable level. The 2000 and 5000 hertz loops offered little advantage because of the increased phase jitter during the beginning of the sync burst. The 100 and 300 hertz loops could not be used because the hum caused a phase error greater than 90 degrees over most of the hum period. It is of interest that the loops even locked in this condition.

The voltage controlled local oscillator in the receiver was then connected to a fixed crystal oscillator. This essentially eliminated the hum and also improved the frequency stability by an order of magnitude. After this modification, any of loop bandwidths could be used. Only the 100 hertz loop showed evidence of hum and this is believed to be due to the voltage controlled oscillator.

A further experiment with the 5000 hertz loop bandwidth during orbit number 8700 was conducted. As discussed above, there is in this case considerable noise on the demodulated sync burst because the loop loses phase coherence between successive sync bursts and takes several microseconds at the beginning of each burst to reacquire. Because of this high noise level, the TDMA terminal will not hold lock for more than a few minutes with the 5000 Hz bandwidth. It reacquires quickly, but the operation is not satisfactory.

An experiment with the satellite was tried while operating the master terminal with a 5000 Hz carrier tracking phase locked loop bandwidth. The performance was the same as found with the satellite simulator; i.e., the terminal immediately locks to the correct line but experiences dropouts every minute or so.

6. RECEIVE ACQUISITION TEST RESULTS

The results of three types of experiments are presented in this chapter;

Exp. 1A - Master acquisition time - cw mode

Exp. 1B - Master acquisition time - pulsed mode

Exp. 2 - Slave receive acquisition time

Although the first two of these are total terminal acquisition times, they are presented with the slave receive acquisition time because there is practically no difference between total master acquisition and slave receive acquisition. In fact, the only difference is that the dopplier compensation is a closed loop operation in the case of the master and is an open loop operation for the slave. However, since the transmit phase locked loop bandwidth is small compared with the reciprocal of the propagation delay, the acquisition time does not depend on whether the doppler compensation is open or closed loop.

The master terminal was designed to permit it to acquire in either the cw or pulsed mode. The slave terminal always operates in the pulsed mode.

The various terminal parameters such as loop bandwidths were varied during the experiments. A large number of runs using a fixed set of parameters were also made to provide a standard of comparison for the varied parameter runs. The parameters chosen for this fixed set were felt to provide the best normal operation and are referred to as the standard parameters.

6.1 MASTER SYNC ACQUISITION - CW MODE

A total of 17 runs of the master sync acquisition experiment in the cw mode were conducted. The results are summarized in Table 6-1. In this experiment the carrier tracking phase locked loop is operated ungated, the receive clock tracking phase locked loop is operated gated and the doppler is preset prior to the run for all loops.

The run is started by transmitting carrier from the master terminal. The time the carrier on-off switch is turned on is recorded on an event marker channel of the chart recorder. The carrier is transmitted cw and is modulated by pulsed 800 kHz. The acquisition time for the carrier tracking phase locked loop is measured from the time the carrier is transmitted until the time the carrier loop locks.

The receive clock tracking phase locked loop acquisition time is measured from the time the carrier loop locks until the time the receive loop locks. The transmit phase locked loop acquisition time is measured from the time the receive loop locks until the time the transmit loop locks. The total master acquisition time is measured from the time carrier is transmitted until the transmit loop locks.

TABLE 6-1. MASTER SYNC ACQUISITION TIME SUMMARY EXP. 1A - CW MODE

Orbit Number	Date	Run Number	Carrier Track	Receive Clock	Transmit Clock	Total
8619	3-31-67	1	0.1 sec	0.1 sec.	8.4 sec.	8.6 sec
		2	0.5	0.2	5.9	6.6
		3	0.1	0	1.6	1.7
8641	4-3-67	1	0.2	0	21.2	21.4
		2	1.9	0	1.3	3.2
		3	8.2	0	7.1	15.3
		4	7.0	0.1	2.3	9.4
		5	0.4	0	4.4	4.8
		6	0.3	0.1	0.1	0.5
8642	4-3-67	1	0.1	0.3	1.2	1.6
		2	0.5	0.1	0.7	1.3
		3	0.5	0.1	0.1	0.7
		4	0.8	0	0.1	0.9
		5	0.5	0	1.0	1.5
		6	0.5	0	1.0	1.5
		7	0.9	0.1	2.0	3.0
		8	1.0	0	0.9	1.9
		Average	1.40	0.065	3.47	4.94

After the run the carrier tracking phase locked loop is switched to gated operation and then the transmitted carrier is switched to pulsed mode. Since the 800 kHz modulation was already gated, this pair of changes does not effect the acquisition already obtained.

In the cw mode experiment as described, it is possible for the carrier loop to lock a considerable time before the receive loop. This is not true in the pulsed mode when these two loops must lock at essentially the same time. It is conceivable, for example, that after the carrier loop has acquired, the receive loop is gated on during an interval of no 800 kHz clock modulation. This condition could persist if the master sync envelope detector failed to reset the receive timer so that the receive loop gate time overlaps the received modulation burst.

On the other hand, it is also conceivable, but less likely, for the receive loop to lock somewhat before the carrier loop. In this case an entry in the column for receive clock loop acquisition time in Table 6-1 would be negative.

It is interesting to observe that neither of these conditions actually occurred. As seen in Table 6-1, the receive loop locked an average of 65 milliseconds after the carrier loop. This demonstrates that the master sync envelope detector was effective in resetting in the receive timer.

The results in Table 6-1 summarize all runs of this experiment. Table 6-2 shows the average acquisition times of the various loops for specific loop bandwidths. It can be seen that the average acquisition time for the carrier loop with the 1000 Hz bandwidth is much less than that shown in Table 6-1. In the latter table, runs 2, 3 and 4 of orbit 8641 correspond to loop bandwidths narrower than 1000 Hz and required a longer time to acquire. The 100 Hz loop bandwidth was used on run 3 but did not provide satisfactory operation because it could not follow the local oscillator variations as discussed in Chapter 5.

TABLE 6-2. MASTER TERMINAL LOOP ACQUISITION TIMES
EXP. 1A - CW MODE

Name of Loop	Loop Bandwidth	Number of Runs	Average Acquisition Time
Carrier Tracking	1000 Hz	14	0.47 sec.
Receive Clock Tracking	100	10	0.10
	300	4	0
	1000	3	0.03
Transmit	0.5	8	2.34
	1	3	1.0
	2	6	6.2

Generally it was found that for this experiment the acquisition time was partly dependent on loop bandwidth but was more dependent on the accuracy to which the doppler was preset. This can be seen for the transmit phase locked loop in which the average acquisition time for the 2 Hz loop bandwidth was greater than that for the 0.5 Hz loop bandwidth.

6.2 MASTER SYNC ACQUISITION - PULSED MODE

Seven runs of the master sync acquisition experiment in the pulsed mode were conducted. The results are summarized in Table 6-3. The experiment is conducted the same as the cw mode described in Section 6.1 except that the carrier is in the pulsed mode.

The longer time for the carrier loop acquisition was discussed in Chapter 5. The data in Table 6-3 is not considered as useful as that obtained for the slave receive acquisition experiment because the former was obtained at the beginning of the test period when the experimental technique was still in the process of improvement. In addition, it was obtained before the doppler preset for the transmit phase locked loop was added. However, it was not found to be necessary because of the relatively low doppler experienced at that time.

The data does verify that the acquisition time does not depend on whether the doppler compensation is open or closed loop as can be seen by comparing it with that of the next section.

6.3 SLAVE RECEIVE ACQUISITION

A total of 106 runs of the slave receive acquisition experiment were conducted and the results are summarized in Tables 6-4, 6-5 and 6-6. In this experiment the master terminal is acquired at the beginning of a pass and tracks the remainder of the pass in receive and transmit modes three. Table 6-7 lists the master terminal parameters used during the slave acquisition experiments.

TABLE 6-3. MASTER SYNC ACQUISITION TIME SUMMARY EXP. 1B - PULSED MODE

Orbit Number	Date	Carrier Track	Receive Clock	Transmit Clock	Total
8339	2-21-67	35.6 sec.	4.8 sec.	1.5 sec.	41.9 sec.
8354	2-23-67	See Note	14.3	0.1	14.4
8387	2-28-67	9.9	0.1	0.2	10.2
8394	3-1-67	0.2	0	3.6	3.8
8443	3-8-67	0.4	0	19.5	19.9
8458	3-10-67	13	-2	4	15
8501	3-15-67	4.4	0.1	-0.1	4.4
	Average	8.65	2.73	4.11	15.65

Note: Due to PA klystron tuning experiment, carrier was transmitted CW. Acquisition time was measured from time pulsed modulation was turned on.

TABLE 6-7. MASTER TERMINAL PARAMETERS FOR SLAVE ACQUISITION

Carrier tracking loop bandwidth	1000 Hz
Receive clock loop bandwidth	100 Hz
Transmit loop bandwidth	1 Hz

FOLDOUT FRAME 1

PRECEDING PAGE BLANK NOT FILMED.

ORBIT NUMBER	DATE	RUN NUMBER	START TIME (GMT)	RANGE KM	RANGE RATE M/SEC	SLAVE TERMINAL PARAMETERS (SWITCH POSITIONS)								FILL BURSTS	ACQUI		
						CARRIER PLL	SUB CARRIER PLL	RECEIVE PLL	TRANSMIT PLL	PN GATE WIDTH	PN GAIN	COARSE SLEW	FINE SLEW		CARRIER PLL	RECEIVE PLL	TRA
8657	4/5/67	1	23:12:42.8	3146	2140	1	1	0	1	1	0	4	0	-	8.1	-0.2	
		2	23:14:04.4	2985	1316	1	1	0	2	1	0	4	0	-	14.6	-0.4	
		3	23:15:40.0	2923	0240	1	1	0	3	1	0	4	0	-	13.2	0	
		4	23:17:37.1	2965	1090	1	1	0	2	1	0	4	0	1,4,8	26.1	0	
		5	23:19:23.5	3160	7120	1	1	0	2	1	0	4	0	1,4,8	5.8	0	
		6	23:21:40.6	3496	3020	1	1	0	2	1	0	4	4	1,4,8	8.9	-0.1	
		7	23:23:16.2	3810	3460	1	1	0	2	1	0	4	4	1,4,8	35.6	0	
8671	4/7/67	1	20:25:33.6	3478	4820	1	1	0	3	1	0	7	0	-	2.9	-0.3	
		2	20:26:58.0	3090	4317	1	1	0	3	1	0	7	0	-	13.0	+22	
		3	20_28:58.0	2748	3527	1	1	0	3	1	0	7	0	-	33.7	-0.3	
		4	20:37:10.2	2866	3816	1	1	0	3	1	0	7	0	-	11.1	-2.1	
		5	20:39:37.1	3485	4590	1	1	1	3	1	0	7	0	-	22.6	-0.2	
		6	20:42:05.0	4202	4956	1	1	1	3	1	0	7	0	24.7	28.5	-1.7	
8700	4/11/67	1	18:25:15.1	3904	5206	1	1	2	3	0	5	7	0	-	12.4	-0.2	
		2	18:28:29.9	2978	4220	1	1	0	3	0	5	7	0	-	11.6	-1.6	
		3	18_35:07.6	2341	1674	1	1	0	3	0	5	7	0	-	33.6	-21.6	
		4	18:36:45.3	2575	3077	1	1	0	3	0	5	7	0	-	16.6	-1.3	
		5	18:38:48.7	3032	4260	1	1	0	3	0	5	7	0	3,4,5,6	22.7	-0.2	
8708	4/12/67	1	20:30:50.2	3542	4700	1	1	1	2	0	5	7	0	-	6.2	-0.4	
		2	20:32:41.2	3086	3990	1	1	1	2	0	5	0	0		13.4	-0.3	
		3	20:34:05.7	2758	3192	1	1	1	2	0	5	0	0	-	18.0	-0.3	
		4	20:36:00.0	2470	2000	1	1	1	2	0	5	4	0	-	25.1	-0.1	
		5	26:37:22.2	2356	0500	1	1	1	2	0	5	4	0	-	8.4	-0.1	
		6	20:40:17.6	2548	2210	1	1	1	2	0	5	4	0	3,4,5,6	61.2	+0.2	
		7	20:42:38.2	2970	3646	1	1	1	2	0	5	4	0	3,4,5,6	13.0	-0.3	
		8	20:45:28.9	3670	4556	1	1	1	2	0	5	4	0	3,4,5,6	14.0	-1.6	
		9	20:47:12.3	4145	4812	1	1	1	2	0	5	4	0	2,4,6,8	35.0	-0.1	
		10	20:48:49.6	4634	4932	1	1	1	2	0	5	4	0	2,4,6,8	15.5	-0.4	
8723	4/14/67	1	21:13:32.8	3872	4668	1	1	0	2	0	5	7	0	-	8.3	-0.3	
8723		2	21:16:21.4	3165	3665	1	1	0	2	0	5	7	0	-	3.4	-0.8	
		3	21:17:55.8	2846	2786	1	1	0	2	0	5	7	0	-	14.4	-0.7	
		4	21:23:52.1	2702	2020	1	1	0	2	0	5	7	0	-	4.4	-0.2	
		5	21:26:26.1	3128	3400	1	1	0	2	0	5	7	0	-	11.7	-5.4	
		6	21:28:50.3	3684	4144	1	1	0	2	0	5	7	0	-	28.1	-5.4	
		7	21:31:26.0	4366	4550	1	1	0	2	0	5	7	0	-	10.4	-1.0	
		8	21:33:02.4	4812	4671	1	1	0	2	0	5	7	0	-	10.2	-0.5	
		9	21:35:05.2	5390	4736	1	1	0	2	0	5	7	0	-	8.8	-0.1	
8745	4/17/67	1	20:37:07.0	3370	4308	1	1	0	2	0	5	7	0	-	34.3	-0.8	
		2	20:40:56.7	2610	2070	1	1	0	2	0	5	7	0	3	9.4	-1.1	
		3	20:46:21.2	2712	2512	1	1	0	2	0	5	7	0	3	4.0	-0.2	
		4	20:48:29.2	3118	3650	1	1	0	2	0	5	7	0	3,1	7.6	-2.7	
		5	20:49:43.2	3340	4094	1	1	0	2	0	5	7	0	3,1,4	8.2	-1.4	
		6	20:51:17.3	3800	4470	1	1	0	2	0	5	7	0	3,1,4,5	12.7	-4.3	

SWITCH POSITION	0	1	2	3	4	5	6	7
CARRIER AND SUBCARRIER PLL BW-HZ		1000	300	100				
RECEIVE CLOCK TRACKING PLL BW-HZ	100	300	1000					
TRANSMIT PLL BW-HZ		0.5	1	2				
PN COARSE SLEW STEP - μS	1.25	2.5	3.75	5	6.25	7.5	8.75	10
PN FINE SLEW STEP - μS	.156	.312	.468	.625	.780	.938	1.092	1.25

FOLDOUT FRAME 2

ETERS NS)			FILL BURSTS	ACQUISITION TIME - SECONDS								REMARKS
PN AIN	COARSE SLEW	FINE SLEW		CARRIER PLL	RECEIVE PLL	TRANSMIT PLL	TOTAL RECEIVE	SUBCARRIER AND PN COARSE	PN FINE	TOTAL TRANSMIT	TOTAL TERMINAL	
0	4	0	-	8.3	-0.2	0.5	9.8	8.5	2.0	11.3	30.5	
0	4	0	-	14.6	-0.4	4.6	18.8	3.4	2.4	6.4	38.3	SUBCARRIER UNLOCKED AFTER ACQUISITION
)	4	0	-	13.2	0	+25.9	39.1	18.6	5.0	29.7	47.8	TRANSMIT PLL NET LOCKED INTERNALLY
0	4	0	1,4,8	26.1	0	0.1	26.2	7.2	3.6	11.6	42.9	
0	4	0	1,4,8	5.8	0	1.7	7.5	4.2	1.4	6.8	20.4	
0	4	4	1,4,8	8.9	-0.1	1.8	11.0	3.3	1.3	5.9	18.1	
0	4	4	1,4,8	35.6	0	-0.1	35.5	3.8	1.4	6.1	48.1	
0	7	0	-	2.9	-0.3	22.9	25.5	23.1	4.3	28.6	39.5	XMT PLL SLOW & OPERATOR ERROR
0	7	0	-	13.0	+22	-0.1	15.1	3.2	3.9	8.7	28.3	
0	7	0	-	33.7	-0.3	1.0	34.6	7.5	4.1	12.3	49.9	SLOW CARRIER LOCK
0	7	0	-	11.1	-2.1	10.9	19.9	21.7	3.3	20.8	38.1	OPERATOR ERRORS
0	7	0	-	22.6	-0.2	-0.2	22.2	3.2	3.4	7.7	35.5	
0	7	0	24,7	28.5	-1.7	8.9	35.7	2.5	1.6	4.7	44.5	
5	7	0	-	12.4	-0.2	19.7	21.9	21.4	1.7	24.0	33.7	FIRST TIME MOTOR GAIN ADJUSTED
5	7	0	-	11.6	-1.6	-0.1	9.9	3.4	4.0	9.6	25.7	
5	7	0	-	33.6	-21.6	14.3	26.3	2.5	3.4	6.8	38.6	FORGOT TO USE AUTO SLEW
5	7	0	-	16.6	-1.3	13.1	28.4	2.1	5.9	9.7	39.2	
5	7	0	3,4,5,6	22.7	-0.2	6.9	29.4	2.2	4.8	9.4	42.9	
5	7	0	-	6.2	-0.4	8.0	13.8	4.5	1.6	7.9	26.6	
5	0	0	-	13.4	-0.3	0	13.1	1.7	6.5	10.2	28.4	
5	0	0	-	18.0	-0.3	2.8	17.8	12.3	4.8	17.7	40.1	
5	4	0	-	25.1	-0.1	-0.1	24.9	3.1	3.4	7.0	34.6	
5	4	0	-	8.4	-0.1	-0.1	8.2	1.9	2.2	5.8	17.5	
5	4	0	3,4,5,6	61.2	+0.2	-0.1	61.3	2.3	2.9	6.3	72.8	
5	4	0	3,4,5,6	13.0	-0.3	10.8	23.5	12.5	2.0	16.4	36.8	
5	4	0	3,4,5,6	14.0	-1.6	0	12.4	2.2	1.7	4.5	24.6	
5	4	0	2,4,6,8	35.0	-0.1	0.8	35.7	5.3	1.6	7.3	45.8	
5	4	0	2,4,6,8	15.5	-0.4	8.7	23.8	6.8	2.0	10.8	28.7	
5	7	0	-	8.3	-0.3	-0.1	7.9	5.8	6.1	12.7	36.8	AUTO ON SLAVE HAD TO BE TURNED OFF AFTER ACQUISITION
5	7	0	-	3.4	-0.8	1.5	4.1	1.8	4.0	7.4	19.1	
5	7	0	-	14.4	-0.7	-0.1	12.8	6.4	2.5	12.0	34.8	
5	7	0	-	4.4	-0.2	4.6	8.8	-	-	-	-	
5	7	0	-	11.7	-5.4	12.0	19.3	2.5	2.6	5.7	27.7	WENT TO RECEIVE LOOP BW1 AFTER RUN,5 NO EFFECT ON NOISY PN, WENT BACK TO BW0 BEFORE NEXT RUN
5	7	0	-	28.1	-5.4	6.6	31.3	3.8	5.1	9.5	42.2	
5	7	0	-	10.4	-1.0	9.4	18.0	5.2	2.7	10.5	31.5	
5	7	0	-	10.2	-0.5	6.2	15.9	3.6	2.6	6.1	24.3	
5	7	0	-	8.8	-0.1	3.8	12.5	4.5	7.0	13.7	30.1	
5	7	0	-	34.3	-0.8	0	33.5	20.9	2.2	22.5	78.7	
5	7	0	3	9.4	-1.1	1.0	9.3	1.4	5.3	6.4	23.6	FORGOT TO AUTO SLEW
5	7	0	3	4.0	-0.2	5.9	9.7	2.4	1.9	5.6	20.3	
5	7	0	3,1	7.6	-2.7	9.6	14.5	2.1	5.8	9.3	37.1	
5	7	0	3,1,4	8.2	-1.4	7.7	14.1	2.3	1.7	4.7	22.1	
5	7	0	3,1,4,5	12.7	-4.3	5.1	23.5	1.3	1.5	4.5	22.	

Table 6-4. Slave Receive Acquisition (Orbit 8657 to 9745) Summary

FOLDOUT FRAME

ORBIT NUMBER	DATE	RUN NUMBER	START TIME (GMT)	RANGE KM	RANGE RATE M/SEC	SLAVE TERMINAL PARAMETERS (SWITCH POSITIONS)								FILL BURSTS	ACQU	
						CARRIER PLL	SUB CARRIER PLL	RECEIVE PLL	TRANSMIT PLL	PN GATE WIDTH	PN GAIN	COARSE SLEW	FINE SLEW		CARRIER PLL	REC PL
		7	30:53:00.8	4274	4706	1	1	0	2	0	5	7	0	3,1,4,5,9	6.5	+1
8752	4/18/67	1	19:13:16.3	3918	5238	1	1	0	2	1	0	7	0	-	16.2	0
		2	19:16:00.0	3103	4542	1	1	0	2	1	0	7	0	-	13.2	-1
		3	19:18:21.5	2560	3220	1	1	0	2	3	3	7	0	-	11.4	-4
		4	19:20:27.6	2264	1494	1	1	0	2	1	0	7	0	-	6.9	-0
		5	19:23:57.3	2354	2310	1	1	0	2	1	0	7	0	-	17.7	-2
		6	19:26:45.7	2912	4060	1	1	0	2	1	0	7	0	-	10.0	-0
8759	4/19/67	1	17:52:29.3	4014	5382	1	1	0	2	1	0	5	0	-	2.8	-0
		2	17:53:59.0	3550	5110	1	1	0	2	1	0	7	0	-	8.3	-4
		3	17:55:55.6	2990	4530	1	1	0	2	1	0	7	0	-	12.1	-6
		4	17:57:58.6	2492	3360	1	1	0	2	3	3	7	0	-	6.9	-0
		5	18:01:06.5	2132	0950	1	1	0	2	3	3	7	0	-	3.3	-0
		6	18:03:58.9	2360	2750	1	1	0	2	3	3	7	0	-	9.2	-0
		7	18:06:07.1	2812	4210	1	1	0	2	1	3	7	0	-	5.3	-0
8760	4/19	1	21:23:48.0	3198	2932	1	1	0	2	1	3	7	0	-	14.1	-0
		2	21:29:10.2	2640	1160	1	1	0	2	1	3	7	0	-	12.8	-0
		3	21:31:24.7	2918	2695	1	1	0	2	1	3	7	0	-	5.8	-0
		4	21:33:11.4	3254	3490	1	1	0	2	1	3	7	0	-	9.0	-4
		5	21:36:20.3	4000	4270	1	1	0	2	1	3	7	0	-	10.7	-5
		6	21:37:54.1	4480	4470	1	1	0	2	1	3	7	0	-	9.9	-0
8774	4/21	1	18:33:51.0	4622	5538	1	1	0	2	1	1	7	0	-	3.5	-0
		2	18:35:44.7	4008	5342	1	1	0	2	1	1	7	0	-	16.0	-0
		3	18:42:57.3	2232	1680	1	1	0	2	1	1	7	0	-	17.7	-0
8775	4/21	1	22:08:56.4	2878	1800	1	1	0	2	1	1	7	0	-	3.5	-0
		2	22:12:35.0	2770	0860	1	1	0	2	1	1	7	0	-	10.0	-0
		3	22:14:20.7	2920	2040	1	1	0	2	1	1	7	0	-	7.8	-1
8803	4/25	1	16:34:30.9	4800	5450	1	1	0	2	1	1	7	0	-	5.0	-0
		2	16:36:15.4	4220	5316	1	1	0	2	1	1	7	0	-	9.2	-0
		3	16:38:32.3	3516	4960	1	1	0	2	1	1	7	0	-	18.4	-0
		4	16:41:20.2	2770	4700	1	1	0	2	1	1	7	0	-	10.8	-0
		5	16:45:27.1	2216	1150	1	1	0	2	1	1	7	0	-	15.0	-0
		6	16:46:41.3	2218	1148	1	1	0	2	1	1	7	0	-	10.9	-0
		7	16:47:52.7	2356	2300	1	1	0	2	1	1	7	0	-	8.9	-0
		8	16:49:04.4	2568	3410	1	1	0	2	1	1	7	0	-	12.3	-0
8804	4/25	1	20:08:54.1	2630	2400	1	1	0	2	1	1	7	0	-	16.9	-0
		2	20:11:00.9	2440	0550	1	1	0	2	1	1	7	0	-	14.4	-2
		3	20:12:57.4	2486	1340	1	1	0	2	1	1	7	0	-	9.4	-0
		4	20:15:26.9	2820	3090	1	1	0	2	1	1	7	0	-	10.0	-2
		5	20:17:55.7	3355	4110	1	1	0	2	1	1	7	0	-	6.2	-0
		6	20:20:02.1	3905	4580	1	1	0	2	1	1	7	0	-	12.1	-0
8819	4/27	1	20:47:45.5	3756	4570	1	1	0	2	1	1	7	0	-	19.9	-0
		2	20:49:25.2	3316	4060	1	1	0	2	1	1	7	0	-	12.4	-0
		3	20:50:59.1	2972	3270	1	1	0	2	1	1	7	0	-	5.3	-0
		4	20:53:03.5	2645	1880	1	1	0	2	1	1	7	0	-	4.4	-0

SWITCH POSITION	0	1	2	3	4	5	6	7
CARRIER AND SUBCARRIER PLL BW-HZ		1000	300	100				
RECEIVE CLOCK TRACKING PLL BW-HZ	100	300	1000					
TRANSMIT PLL BW-HZ		0.5	1	2				
PN COARSE SLEW STEP - μS	1.25	2.5	3.75	5	6.25	7.5	8.75	10
PN FINE SLEW STEP - μS	.156	.312	.468	.625	.780	.938	1.092	1.25

FOLDOUT FRAME 2

COARSE SLEW	FINE SLEW	FILL BURSTS	ACQUISITION TIME - SECONDS								REMARKS
			CARRIER PLL	RECEIVE PLL	TRANSMIT PLL	TOTAL RECIEVE	SUBCARRIER & PN COARSE	PN FINE	TOTAL TRANSMIT	TOTAL TERMINAL	
7	0	3,1,4,5,2	6.5	+1.9	-0.1	8.3	-	-	-	-	WOULD NOT LOCK, WENT TO COARSE STEP 1.0 NO LOCK
7	0	-	16.2	0	0.8	17.0	2.4	4.1	11.9	33.3	
7	0	-	13.2	-1.4	0.1	11.9	3.2	4.0	9.0	27.5	
7	0	-	11.4	-4.1	-0.2	7.1	0.8	1.9	5.0	21.8	
7	0	-	6.9	-0.3	0.8	7.4	2.9	4.2	7.7	19.1	
7	0	-	17.7	-2.4	11.0	26.3	2.5	4.9	8.1	37.5	
7	0	-	10.0	+0.2	4.5	14.3	5.5	2.5	8.8	27.4	
5	0	-	2.8	-0.6	0	2.2	4.7	2.1	7.5	16.9	
7	0	-	8.3	-4.9	4.8	8.2	1.7	8.8	11.8	25.1	
7	0	-	12.1	-0.7	0	11.4	3.2	2.8	7.1	23.7	
7	0	-	6.9	-0.2	0	6.7	2.8	4.6	9.0	21.8	DROPOUT AT 18:00:30
7	0	-	3.3	-0.1	13.4	16.6	2.6	10.8	14.4	23.7	RUN NO. 5 WAS DURING ZERO DOPPLER TIME.
7	0	-	9.2	-0.8	9.0	17.6	11.0	5.0	16.5	37.8	
7	0	-	5.3	-0.2	6.0	11.1	1.7	4.6	7.4	22.7	
7	0	-	14.1	-0.3	-0.1	13.7	2.7	2.4	7.3	28.1	
7	0	-	12.8	-0.3	12.0	24.5	1.8	2.2	5.2	36.1	
7	0	-	5.8	-0.1	4.9	10.6	2.3	2.0	4.8	20.3	
7	0	-	9.0	-4.0	4.7	9.7	1.3	3.7	7.4	27.1	
7	0	-	10.7	-5.7	7.9	12.9	2.8	5.0	8.2	23.7	
7	0	-	9.9	-0.2	4.9	14.6	2.3	3.8	6.8	23.5	
7	0	-	3.5	-0.4	-0.1	3.0	8.5	3.2	2.9	23.5	
7	0	-	16.0	-0.7	0	15.3	1.8	2.9	6.4	34.7	
7	0	-	17.7	-0.2	-0.1	17.4	1.5	1.8	3.8	23.7	
7	0	-	3.5	-0.8	1.4	4.1	2.8	2.5	5.9	14.7	
7	0	-	10.0	-0.3	5.8	15.5	1.8	1.7	4.4	23.7	
7	0	-	7.8	-1.7	7.2	13.3	3.3	2.4	6.3	21.5	
7	0	-	5.0	-0.3	0	4.7	5.1	5.5	11.2	21.9	
7	0	-	9.2	-0.6	-0.2	8.4	1.6	1.9	4.0	17.2	
7	0	-	18.4	-0.6	-0.1	17.7	3.2	5.2	8.4	32.7	
7	0	-	10.8	-0.1	0	10.7	1.6	3.7	6.4	20.8	
7	0	-	15.0	-0.6	4.1	18.5	2.2	2.5	5.1	27.0	
7	0	-	10.9	-0.2	3.1	13.8	1.3	4.1	7.4	26.0	
7	0	-	8.9	-0.4	4.1	12.6	2.3	2.5	5.5	20.5	
7	0	-	12.2	-0.1	5.1	17.3	4.0	3.7	8.3	28.9	
7	0	-	16.9	-0.2	-0.1	16.6	1.9	3.9	6.6	28.5	
7	0	-	14.4	-2.2	6.3	18.5	1.3	4.8	6.9	29.9	
7	0	-	9.4	-0.1	3.2	12.5	6.3	4.5	11.5	28.2	
7	0	-	10.0	-2.9	10.3	17.5	3.2	4.1	8.2	28.3	
7	0	-	6.2	-0.3	2.8	8.7	1.3	5.2	7.3	20.5	
7	0	-	12.1	-0.2	4.3	16.2	0.9	2.8	5.1	25.0	
7	0	-	19.9	-0.1	0	40.0	5.9	3.6	11.3	58.6	
7	0	-	12.4	-0.1	0	12.3	3.5	4.5	9.1	25.0	
7	0	-	5.3	-0.2	0.4	5.5	3.1	4.9	9.4	17.2	
7	0	-	4.4	-0.1	3.7	8.0	1.3	1.4	3.9	14.7	

Table 6-5. Slave Receive Acquisition (Orbit 8752 to 8819) Summary

FOLDOUT FR... PRECEDING PAGE BLANK NOT FILMED.

ORBIT NUMBER	DATE	RUN NO.	START TIME (GMT)	RANGE KM	RANGE RATE M/SEC	SLAVE TERMINAL PARAMETERS (SWITCH POSITION)							
						CARRIER PLL	SUB CARRIER PLL	RECEIVE PLL	TRANSMIT PLL	PN GATE WIDTH	PN GAIN	COARSE SLEW	FINE SLEW
		5	20:59:29.9	2950	3076	1	1	0	2	1	1	7	0
		6	21:00:59.7	3255	3700	1	1	0	2	1	1	7	0
		7	21:02:06.3	3510	4016	1	1	0	2	1	1	7	0
		8	21:03:29.3	3855	4336	1	1	0	2	1	1	7	0
		9	21:04:35.4	4140	4480	1	1	0	2	1	1	7	0
8826	4/28	1	19:25:03.0	4006	5092	1	1	0	2	1	1	7	0
		2	19:27:00.5	3434	4600	1	1	0	2	1	1	7	0
		3	19:28:39.3	3000	3970	1	1	0	2	1	1	7	0
		4	19:31:40.7	2476	1824	1	1	0	2	1	1	7	0
		5	19:34:04.8	2373	1026	1	1	0	2	1	1	7	0
		6	19:35:25.5	2460	1700	1	1	0	2	1	1	7	0
		7	19:36:58.5	2670	2910	1	1	0	2	1	1	7	0
8848	5/1	1	18:47:09.4	3880	5100	1	1	0	2	1	1	7	0
		2	18:49:56.0	3100	4260	1	1	0	2	1	1	7	0
		3	18:52:39.4	2510	2635	1	1	0	2	1	1	7	0
		4	18:52:23.4	2320	0990	1	1	0	2	1	1	7	0
		5	18:56:05.1	2321	1170	1	1	0	2	1	1	7	0
		6	18:58:24.1	2567	2810	1	1	0	2	1	1	7	0
		7	19:01:34.6	3270	4360	1	1	0	2	1	1	7	0

SWITCH POSITION	0	1	2	3	4	5	6	7
CARRIER AND SUBCARRIER PLL BW-HZ		1000	300	100				
RECEIVE CLOCK TRACKING PLL BW-HZ	100	300	1000					
TRANSMIT PLL BW-HZ		0.5	1	2				
PN COARSE SLEW STEP - μS	1.25	2.5	3.75	5	6.25	7.5	8.75	10
PN FINE SLEW STEP - μS	.156	.312	.468	.625	.780	.938	1.092	1.25

FINE SLEW	FILL BURSTS	ACQUISITION TIME - SECONDS								REMARKS
		CARRIER PLL	RECEIVE PLL	TRANSMIT PLL	TOTAL RECIEVE	SUB CARRIER AND PN COARSE	PN FINE	TOTAL TRANSMIT	TOTAL TERMINAL	
0	-	5.9	-0.3	3.9	9.5	10.0	4.2	14.3	27.3	
0	-	13.4	-0.3	-0.1	13.0	1.5	1.6	3.7	21.1	
0	-	8.5	-3.2	1.0	6.3	3.1	2.7	6.2	20.6	
0	-	9.0	-0.4	0	8.6	3.1	2.6	6.0	18.7	
0	-	6.9	-0.9	-0.1	5.9	5.5	6.0	8.3	20.8	
0	-	11.9	-0.2	-0.2	11.5	5.3	1.0	7.3	26.2	
0	-	8.4	-0.8	-0.1	7.5	10.9	1.9	14.2	29.8	
0	-	10.0	-0.3	0	9.7	1.5	2.6	4.7	19.7	
0	-	17.3	-4.0	8.1	21.4	1.3	1.8	4.0	30.4	
0	-	4.7	-0.3	5.3	9.7	2.4	3.9	6.8	19.6	
0	3.8	13.9	0	5.9	19.8	3.1	4.9	7.5	31.0	
0	3.8	9.8	+0.4	7.0	17.2	1.9	6.1	8.5	28.8	
0	-	19.2	-0.2	0	19.0	13.6	3.2	17.5	40.2	
0	-	5.5	-0.2	-0.1	5.2	3.0	2.2	5.8	17.6	
0	-	4.2	-0.1	1.4	5.5	1.4	4.0	6.6	16.0	
0	-	9.4	-0.7	12.3	21.0	3.5	3.5	7.7	31.5	
0	-	6.5	-0.3	7.0	13.2	2.0	2.0	4.3	20.2	
0	-	14.7	-3.1	7.0	18.6	1.7	3.6	5.9	28.0	CORRECTED EARLY/LATE ERRORS IN MASTER AND SLAVE.
0	-	10.5	-4.5	8.8	14.8	3.2	3.7	7.5	26.9	

Table 6-6. Slave Receive Acquisition (Orbit 8826 to 8848) Summary

Prior to a run, the operator breaks all slave terminal loop locks which were acquired during a previous run. The slave acquisition begins when the operator steps the receive mode from zero to one. He then acquires the carrier tracking loop to the correct spectral line by the procedure described in Section 5.1. The receive clock loop acquires at nearly the same time as the carrier loop. The operator then checks for transmit loop lock. This loop acquires by itself if the doppler preset is accurate, however, in cases where the doppler rate is high, it is sometimes necessary for the operate to adjust the preset to speed up transmit loop acquisition.

The definitions of loop acquisition times are the same as described in Section 6.1 except that the starting time of the run is measured from the time the receive mode is stepped from zero to one. After the transmit loop has acquired, the operator steps the receive mode to three (it goes to mode two automatically during receive acquisition).

The acquisition time for the carrier tracking phase locked loop was presented in Figure 5.2-1. A summary of the total receive acquisition is shown in Figure 6.3-4. It can be seen that average receive acquisition time was 16.08 seconds while the average carrier loop acquisition time was 12.73 seconds. It can be concluded then that most of the receive acquisition time is required for coding the carrier tracking phase locked loop.

As mentioned previously, a number of runs using fixed standard parameters for the slave terminal were made. The results are summarized in Table 6-8. A histogram for the carrier loop was shown in Figure 5.2-2 and histograms for the transmit phase locked loop and the slave receive acquisition times are shown in Figures 6.3-6 and 6.3-3.

As a general observation, the orbit parameters under which an experiment was conducted had no noticeable effect on the results. As an example, Table 6-9 shows the effect of doppler on slave acquisition time. In each case the eight runs with the lowest and highest doppler in the standard parameter case were picked. No significant difference appears, especially when compared with Table 6-8 which gives the standard deviation for these runs.

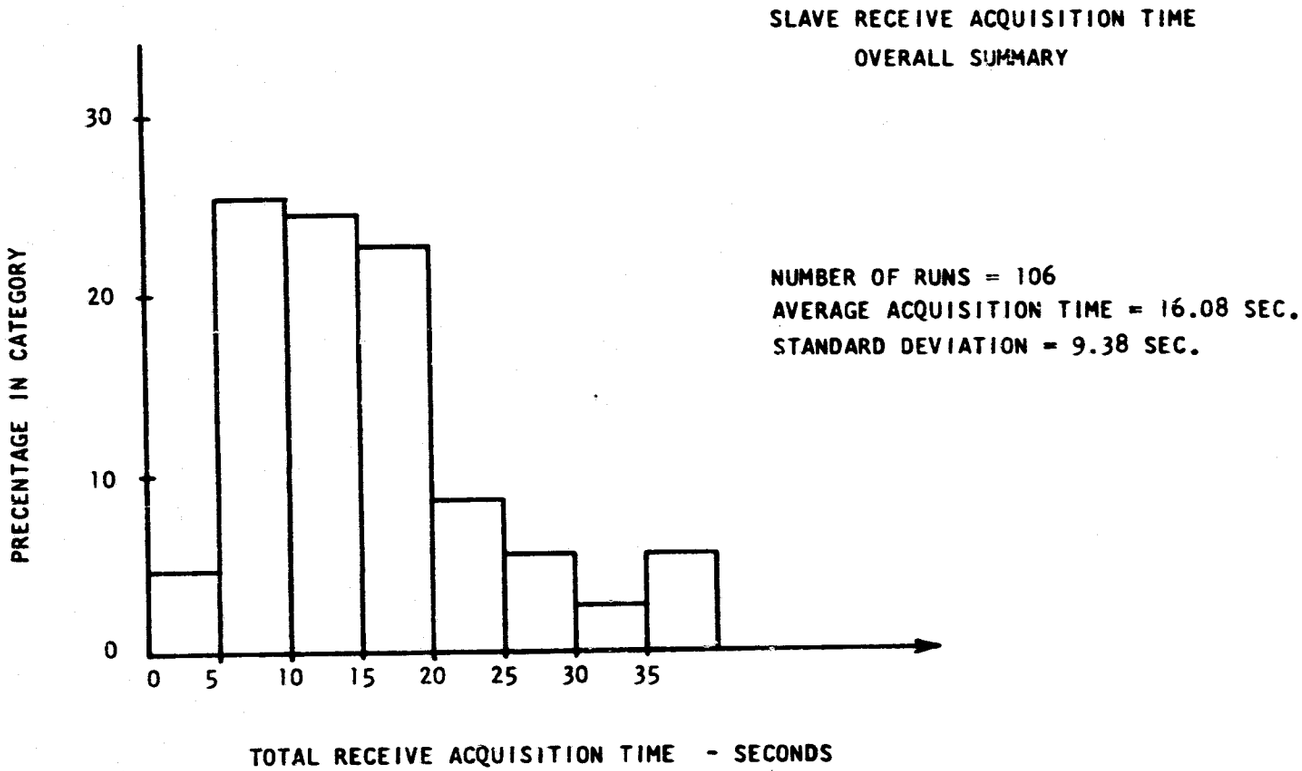

Figure 6.3-1. Slave Receive Acquisition Time - Overall Summary

SLAVE TERMINAL ACQUISITION TIME
STANDARD PARAMETERS

	AVERAGE	STANDARD DEVIATION
RECEIVE ACQUISITION		
CARRIER TRACKING PLL (1000 HZ)	10.88 SEC.	6.32 SEC.
TRANSMIT PLL (1 HZ)	2.81	3.38
TOTAL	12.89	6.60
TRANSMIT ACQUISITION		
SUBCARRIER TRACKING PLL (1000 HZ) AND PN COARSE SLEW (64 μS/SEC)	3.38	2.80
PN FINE SLEW (1 μS/SEC)	3.26	1.23
TOTAL	7.44	3.12
TOTAL SLAVE ACQUISITION TIME	25.0	7.80

NOTES: (1) 41 TRIALS
(2) PN COARSE SLEW STEP = 10μS
(3) PN FINE SLEW STEP = 156 ηS

Table 6-9. Slave Terminal Acquisition Times - Standard Parameters

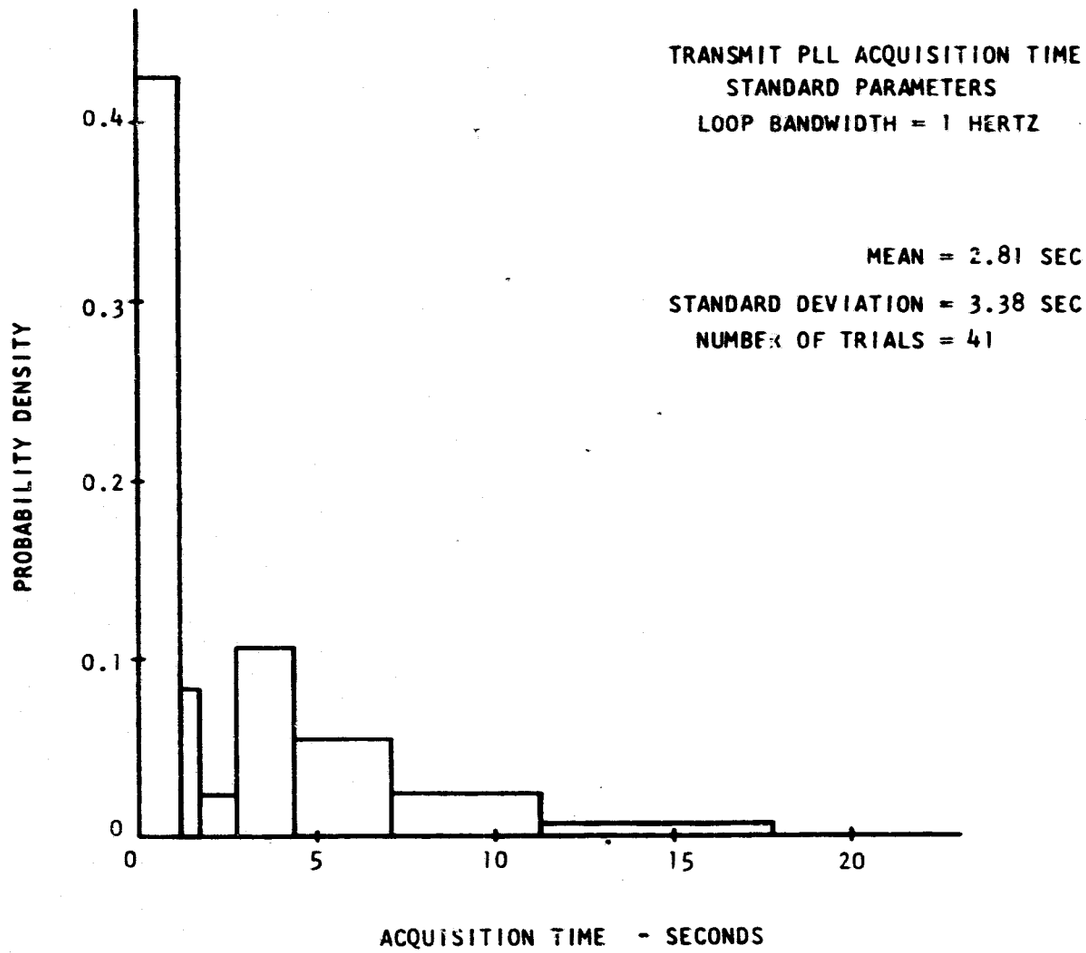

Figure 6.3-2. Transmit PLL Acquisition Time - Standard Parameters

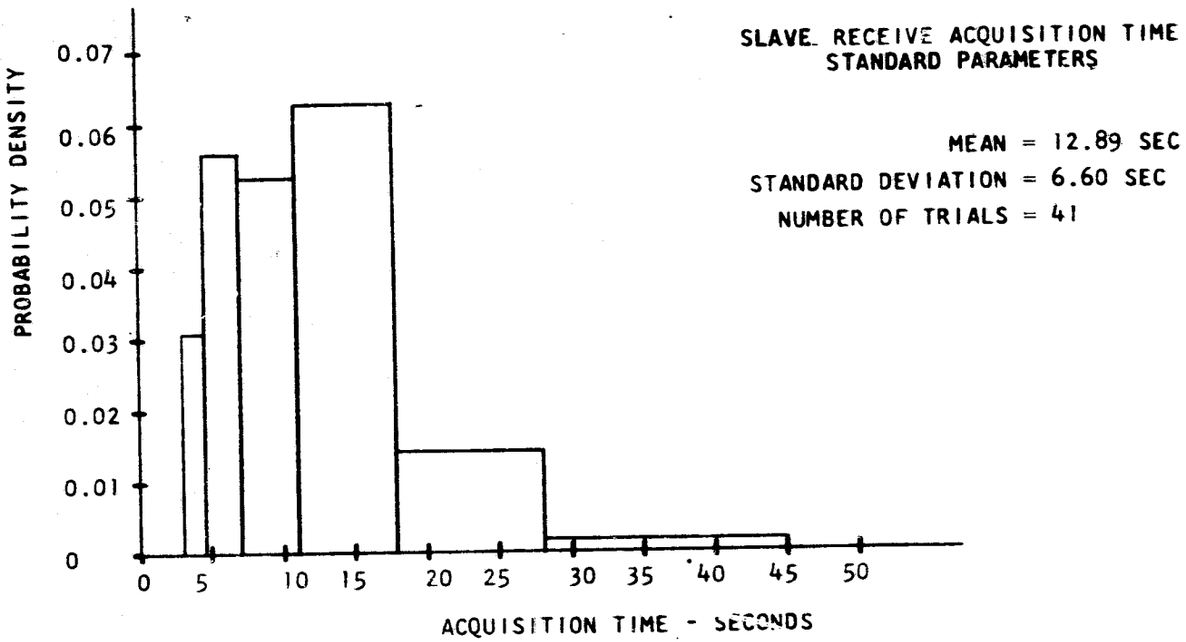

Figure 6.3-3. Slave Receive Acquisition Time - Standard Parameters

TABLE 6-9. SLAVE ACQUISITION VERSUS DOPPLER STANDARD PARAMETERS

	Average Acquisition Times	
	Low Doppler	High Doppler
Carrier tracking phase locked loop	10.0 sec.	11.75 sec.
Total receive	15.3	11.3
Subcarrier phase locked loop and pseudo noise coarse slew	2.0	5.0
Pseudo noise fine slew	2.75	3.2
Total transmit	5.8	9.1

Note: Low doppler - 8 runs: range rate 0 - 1500 m/sec
High doppler - 8 runs: range rate 4600 - 5600 m/sec

7. SLAVE TRANSMIT ACQUISITION TEST RESULTS

After a slave terminal acquires the sync burst from the master; i.e., receive sync, it transmits a cw ranging signal. The process of adjusting the phase of the transmitted ranging signal to bring the received ranging signal into proper phase with respect to the received sync burst is called transmit sync acquisition.

The ranging signal is transmitted at a low level to avoid interference with occupied time intervals. On the other hand, occupied time intervals will interfere with the ranging signal. This interference amounts to complete suppression in the case of the relay transponder and therefore it can be expected that the number and disposition of interferring bursts will have an effect on the transmit acquisition.

The master terminal has provision for simulating interferring bursts with unmodulated carrier bursts. These simulated bursts are called fill bursts and are numbered from 1 to 10 according to the time interval during which they occur. The eleventh time interval is always occupied by the sync burst so that the ranging signal can never be completely free from interference.

It was found that the most serious effect of the suppression of the ranging signal by interferring bursts was to reduce the outputs of the lock detectors for the subcarrier tracking and pseudo noise ranging phase locked loops. That is, these lock detectors consist of phase detectors followed by threshold comparators. The thresholds are normally adjusted to indicate lock when the phase detector output exceeds one half its maximum value. A sufficient number of fill bursts causes the phase detector output to fall below the threshold and the detector then indicates no lock. This causes improper acquisition because the pseudo noise slew operation depends on correct lock indications.

It was found that satisfactory operation with less than approximately five fill bursts could be obtained by wiring the logic to permanently indicate subcarrier tracking loop lock. The results of Section 7.1 were taken under this condition. Because the lock indication of the subcarrier loop was inoperative, the acquisition time of this loop could not be measured directly. Instead, the combined acquisition time of this loop and the pseudo noise coarse search was measured.

Basically the terminal was designed for a satellite transponder which can be characterized as a hard limiter. In this case there should be no serious problem with fill bursts. However, the Relay transponder contains an i-f tripler which causes the complete suppression effect mentioned above. A detailed analysis of this suppression effect is contained in Section 7.2.

In order to demonstrate operation with greater than five fill bursts while using the Relay satellite, a modification to the pseudo noise lock detector was made. This modification is described in Section 7.3 and permitted satisfactory operation with any number of fill bursts provided the 1.25 microsecond pseudo noise gate

width is used. With this modification the pseudo noise ranging signal is observed during the 1.25 microsecond guard times and during the empty time interval the slave is acquiring to.

7.1 SLAVE TRANSMIT ACQUISITION

A total of 104 runs of the slave transmit acquisition experiment were conducted prior to the modification for fill burst operation. The results are summarized in Tables 6-4, 6-5, and 6-6. This experiment was conducted following each run of the slave receive acquisition experiment described in Section 5.3. This permits a measure of total slave terminal acquisition time as well as individual acquisition times.

The slave transmit acquisition begins when the operator steps the transmit mode from zero (stop) to one. The subcarrier and pseudo noise coarse slew acquisition ends with pseudo noise lock. When the operator observes this lock he steps the transmit mode to two which starts the pseudo noise fine slew. The fine slew steps in the direction to reduce the pseudo noise error. Eventually the fine slew reaches a point where it oscillates between two steps, reversing direction each time.

The operator observes this on the panel display and steps the transmit mode to three. The pseudo noise fine slew and also the slave transmit acquisition time end when the transmit mode goes to three.

Occasionally the operator stepped the modes at the wrong time. For example, several times the operator started transmit acquisition before the transmit loop locked; i.e., before the receive acquisition was completed. This causes delay before the operator recognizes the trouble and corrects it. For this reason it was decided to edit the data to see if the incorrect procedure had any effect on the results. The results using both gross and edited data are presented below. The edited data consists of omitting five runs during which such improper procedure occurred.

The acquisition time as defined above does not include settling time for the fine phase adjustment pseudo noise ranging loop using the motor driven phase shifter. The motor is enabled when the transmit mode is stepped to three. It first corrects initial phase error remaining after the pseudo noise fine slew and then maintains sync by tracking the timing error. This time is considered, however, in the discussion of the results below.

The total slave terminal acquisition time is measured from the time the receive mode is stepped to one until the time the transmit mode is stepped to three. This includes, then, the time required for the operator to recognize completion of receive acquisition and to begin transmit acquisition. As discussed below, this reaction time is approximately one second and occurs several times in the acquisition procedure.

Table 7-1 summarizes the transmit acquisition times and compares the results using the gross data with that using the edited data. The average acquisition time was not changed very much by the editing, but the standard deviation was reduced significantly. Histograms for coarse, fine and total acquisition times using the gross data are shown in Figures 7.1-1, 7.1-2 and 7.1-3, respectively.

The acquisition times for the standard parameters are shown in Table 6-7. Histograms for the coarse, fine and total acquisition times are shown in Figures 7.1-4, 7.1-5 and 7.1-6, respectively. A histogram for the total slave terminal acquisition time is shown in Figure 7.1-7 for the standard parameter case.

As mentioned previously, the standard parameters used, which are shown in Table 7-2, are considered the best choice for normal operation. The reasons for choosing these particular values will now be discussed. The optimum loop bandwidth for the carrier and subcarrier loops was found to be 1000 hertz. As discussed in Section 5.4, these loops could not track satisfactorily with the 100 and 300 hz loop bandwidths because of the poor local oscillator stability in the ground station. Also as discussed in that section, loop bandwidths greater than 1000 Hz did not provide satisfactory phase coherence between successive sync bursts. Therefore these loops were almost always operated with the optimum value of 1000 Hz for the loop bandwidth. Nearly the same performance could be obtained with a 2000 Hz bandwidth but performance degraded rapidly below 1000 and above 2000 Hz.

The receive clock loop bandwidth was not critical; it acquired rapidly with any of the bandwidths used. The narrowest bandwidth, 100 Hz, was selected to reduce receive clock jitter due to noise. One effect was noticed which indicates that this narrower bandwidth is desirable. The transmit phase locked loop, which has a much narrower bandwidth, must track the receive clock. Under noisy conditions, the receive clock jitter with the 1000 Hz bandwidth was sufficient to cause the transmit loop tracking error to exceed about 60 degrees fairly often. This caused the transmit loop lock indication to flicker since the lock detector threshold corresponds to 60 degrees phase error.

The standard transmit loop bandwidth was chosen as one Hz. This was a compromise between the 0.5 Hz bandwidth with somewhat longer acquisition time and the 2 Hz bandwidth with higher transmit clock jitter. This choice was not critical however since performance differed only slightly with different bandwidths. The pseudo noise ranging loop bandwidth was chosen as one Hz for the same reasons.

The pseudo noise gate width was selected as 1.25 μs because it was the narrowest and can be used to measure pseudo noise tracking during the guard time between bursts. This choice and the choice of loop bandwidth determine the pseudo noise gain switch setting of 1 according to Table 2-2.

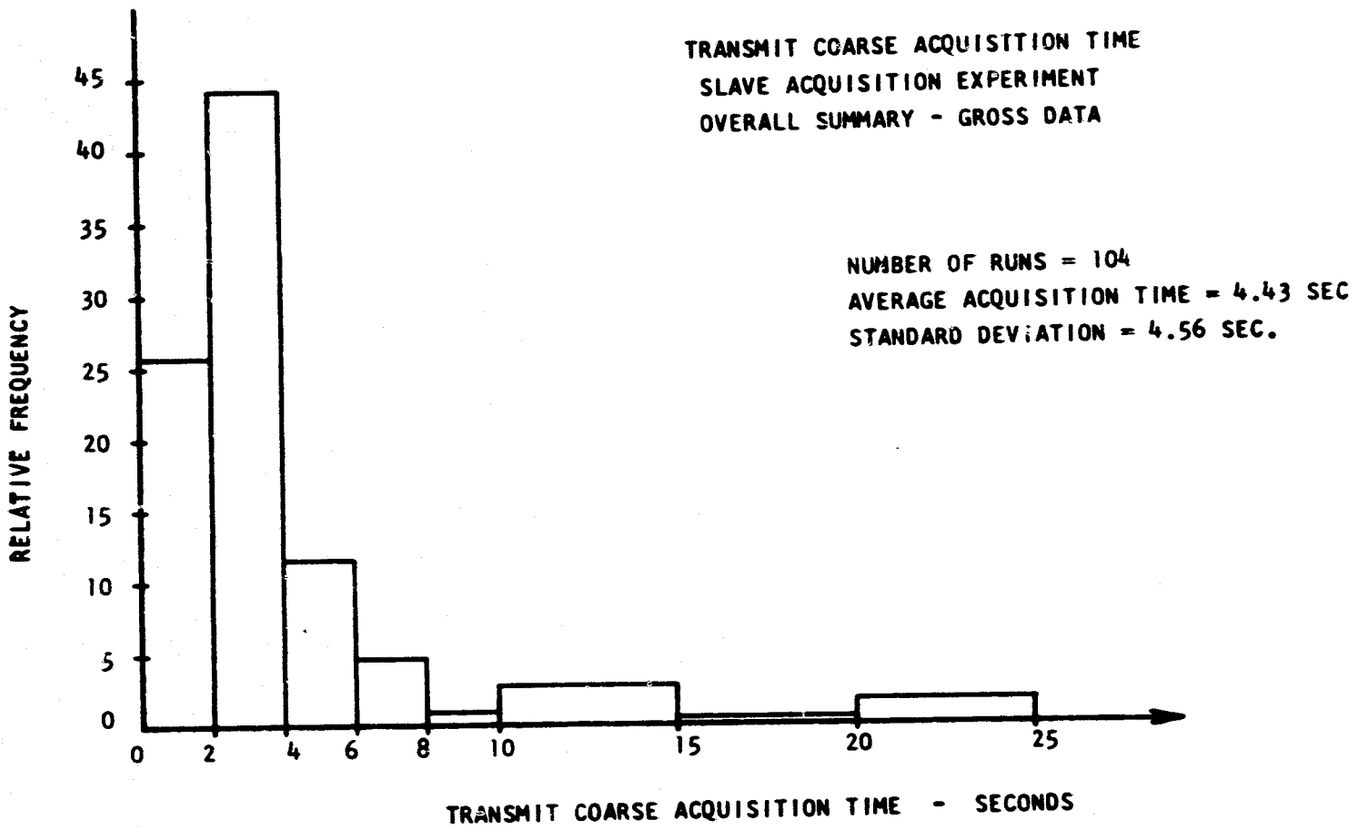

Figure 7.1-1. Transmit Coarse Acquisition Time - Overall Summary

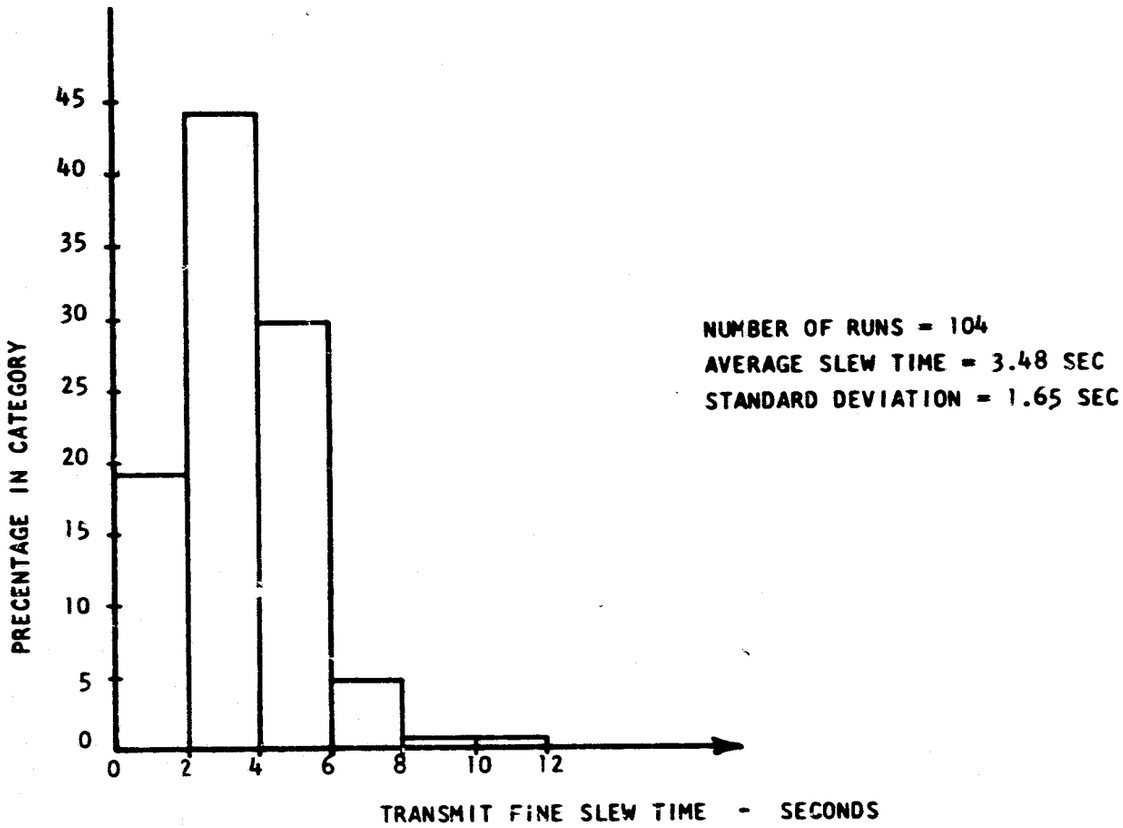

Figure 7.1-2. Transmit Fine Slew Acquisition Time - Overall Summary

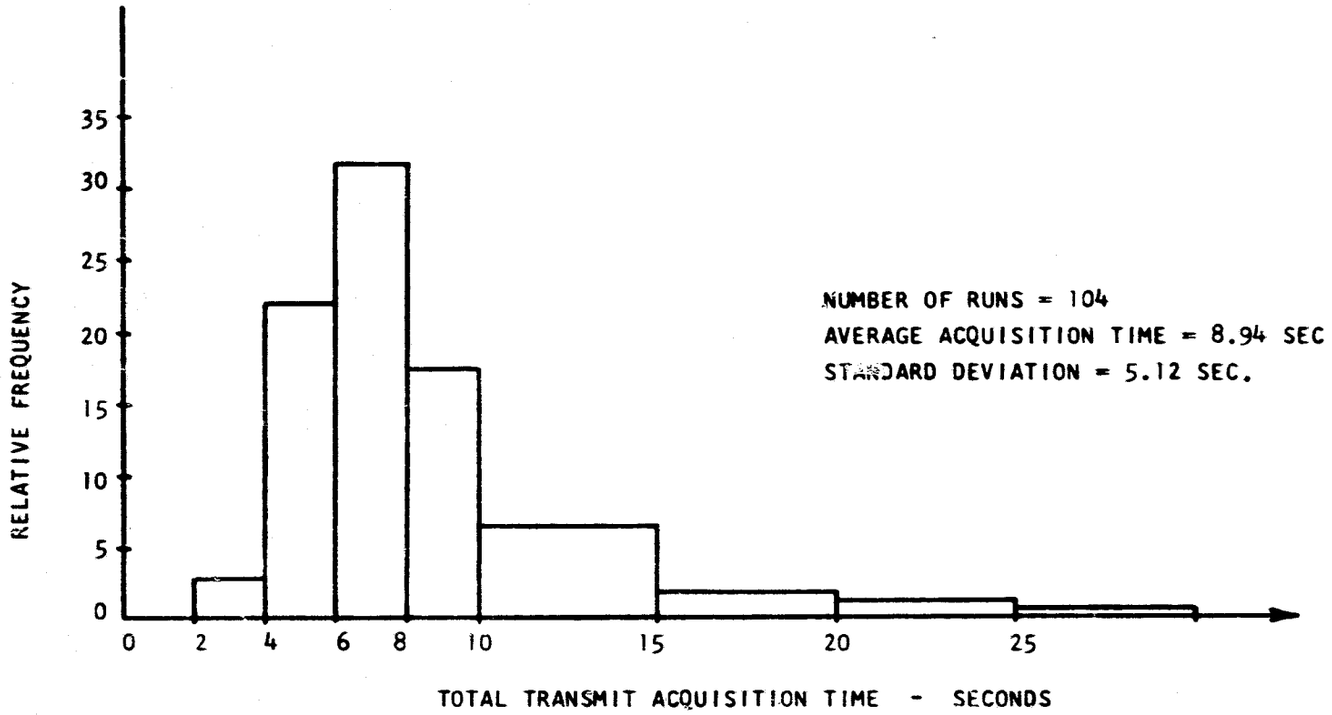

Figure 7.1-3. Slave Transmit Acquisition Time - Overall Summary

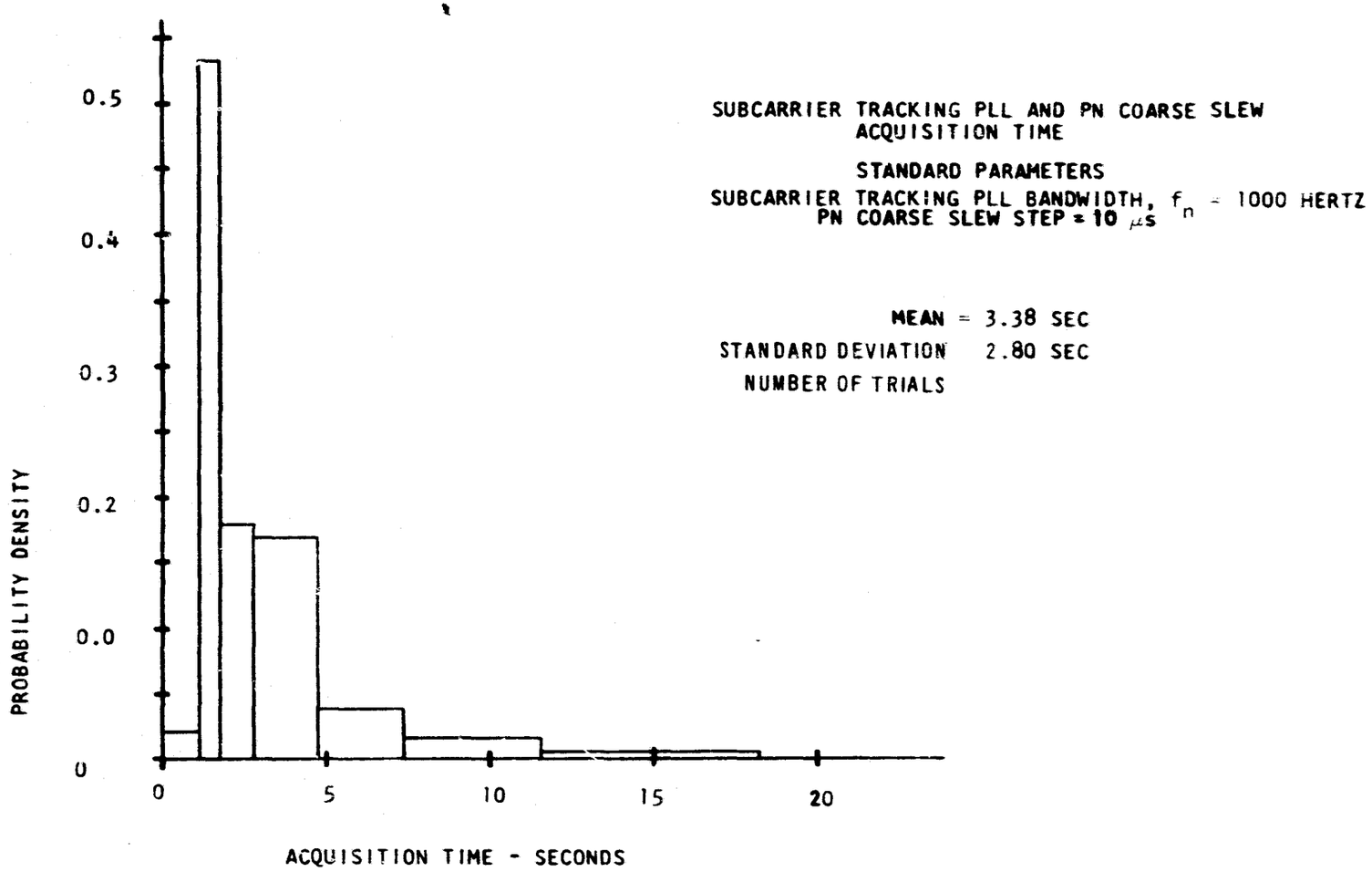

Figure 7.1-4. Transmit Coarse Acquisition Time - Standard Parameters

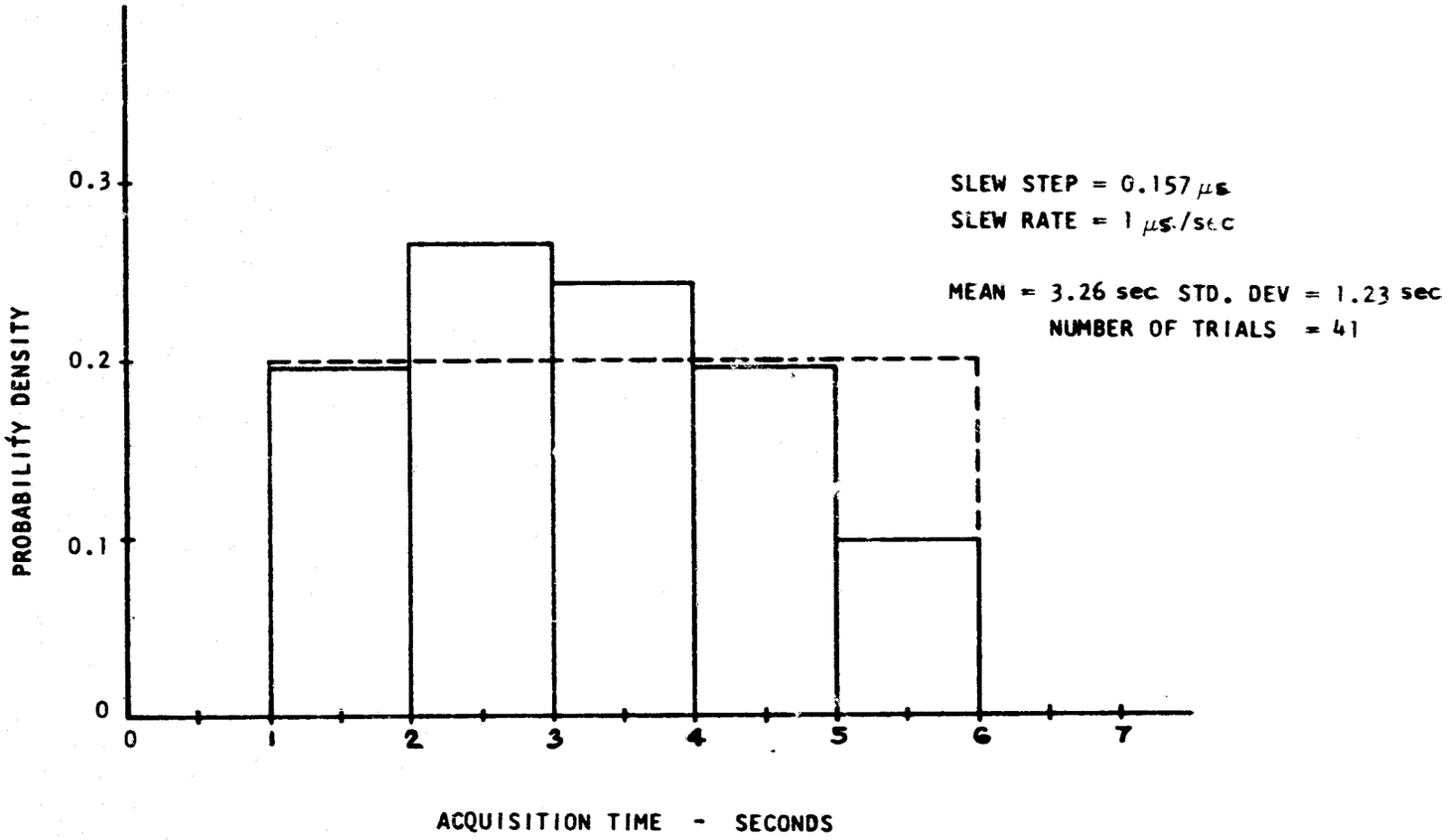

Figure 7.1-5. PN Fine Slew Acquisition Time - Standard Parameters

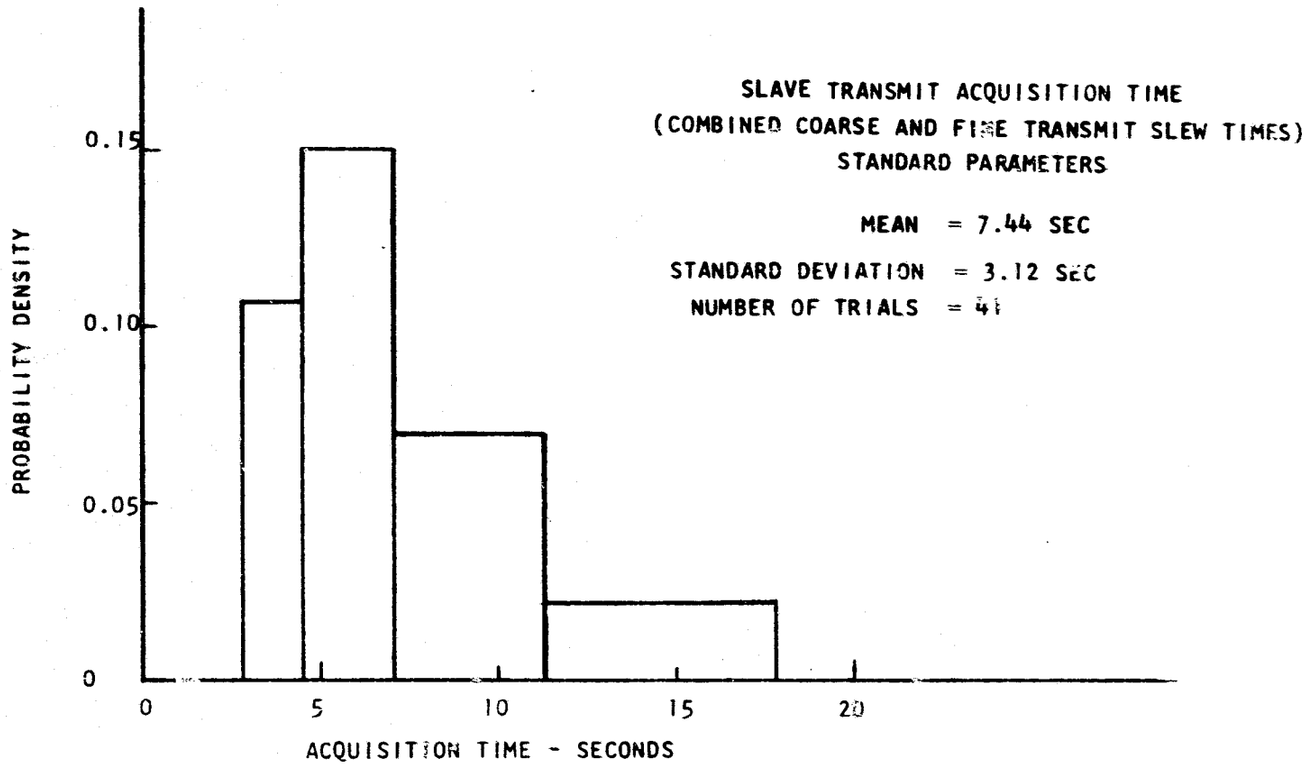

Figure 7.1-6. Slave Transmit Acquisition Time - Standard Parameters

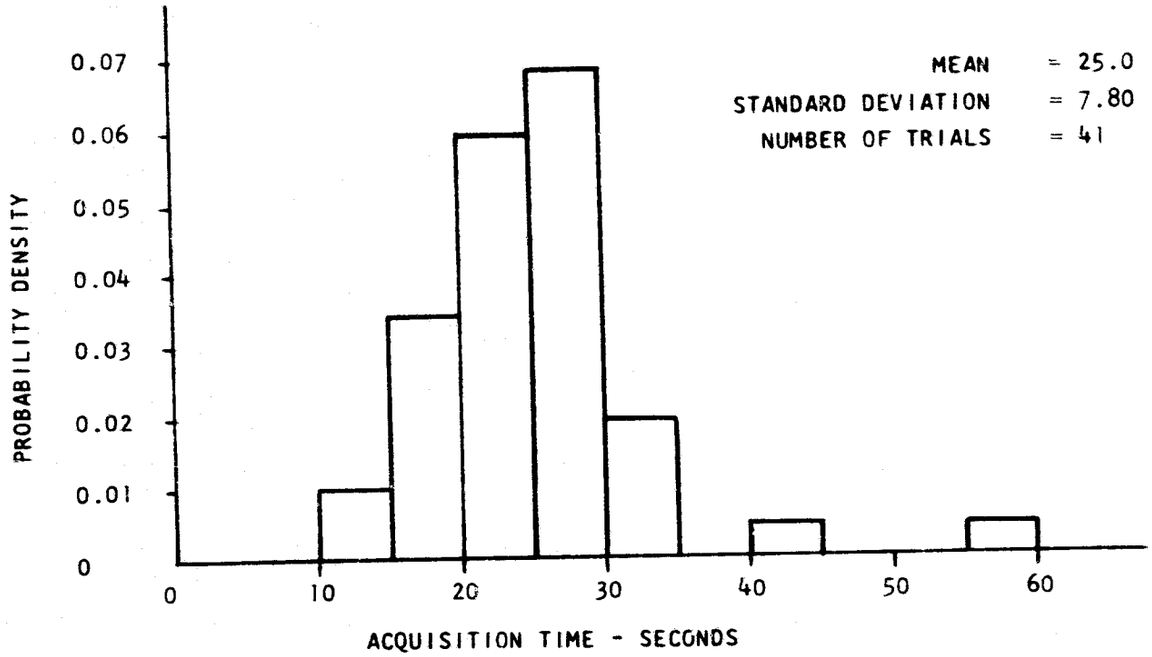

Figure 7.1-7. Total Slave Terminal Acquisition Time - Standard Parameters

TABLE 7-1. SLAVE TRANSMIT ACQUISITION TIME

OVERALL SUMMARY

	Gross Data (104 runs)		Edited Data (99 runs)	
	Average	Standard Deviation	Average	Standard Deviation
Subcarrier Loop and Pseudo Noise Coarse Slew	4.43 sec	4.56 sec	3.57 sec	2.66 sec
Pseudo Noise Fine Slew	3.47	1.65	—	—
Total	8.94	5.12	8.12	3.16

Note: Edited data same as gross data except following runs deleted - 8657, run 3; 8671, runs 1 and 4; 8700, run 1; 8745, run 1.

TABLE 7-2. STANDARD PARAMETERS

Parameter	Switch Position	Value
Carrier and Subcarrier Loop Bandwidth	1	1000 Hz
Receive Clock Loop Bandwidth	0	100 Hz
Transmit Loop Bandwidth	2	1 Hz
Pseudo Noise Ranging Loop Bandwidth	-	1 Hz
Pseudo Noise Gate Width	1	1.25 μs
Pseudo Noise Gain	1	—
Pseudo Noise Slew Step	7	10 μs (64 μs/sec)
Pseudo Noise Fine Slew Step	0	0.156 μs (1 μs/sec)

The pseudo noise coarse slew step was chosen as 10 microseconds because it is the largest and provides the fastest search of the frame. There was some question as to whether this was too large since the lock range is only 10 microseconds. However, no difficulty with missing the lock range was experienced. Since the step is made every 156 milliseconds, this step size gives a search rate of 64 μs/sec. At this rate one would expect a 1 sec average acquisition time which is what was observed.

It should be noted that with this large a step size the phase error after lock occurs is uniformly distributed over the full ±5 microsecond range. On the other hand, if a much smaller step size were used, the phase error after lock would be concentrated near the maximum error of 5 microseconds. This results because the search is in one direction and ends as soon as the edge of the lock range is found. This means that the initial phase error for the fine slew mode would average much higher than with 10 microsecond coarse step and would increase the fine slew acquisition time.

Similar reasoning indicates that the smallest fine slew step, 156 nanoseconds, is the best choice. This is because of the relatively low slew rate of 100 ηs/sec for the motor driven phase shifter. Even the smallest fine slew step gives a much higher slew rate (1 μs/sec) than the motor driven phase shifter. If the fine slew step is A microseconds, than the magnitude of the initial phase error for the

motor driven phase shifter will be uniformly distributed over the range from zero to A microseconds. Thus the average initial phase error is minimized by picking the smallest fine slew step. The 156 nanosecond step is chosen for the standard parameter so that most of phase error resulting from the coarse slew is slewed by the higher speed digital slew rather then the motor slew.

As mentioned above, the magnitude of the initial phase error for the pseudo noise fine slew is uniformly distributed from zero to 5 microseconds. With a slew rate of 1 μs/sec, we would expect the pseudo noise fine slew acquisition time to be uniformly distributed between zero and 5 seconds. However, this neglects the time it takes the operator to recognize that the fine slew is finished and to step the transmit mode to three. Thus we expect the uniform distribution for the pseudo noise fine slew time to be displayed by the operators reaction time. As seen in Figure 7.1-5, the pseudo noise fine slew acquisition time is close to a uniform distribution over the range of one to six seconds. The uniform distribution is shown by the dotted line. Thus we can conclude that the operator reaction time is close to one second.

Other acquisition time measurements also include the operator reaction time but the nature of the acquisition time distribution does not permit such an accurate measurement of this reaction time.

7.2 SIGNAL SUPPRESSION WITH RELAY TRANSPONDER

Several experiments were conducted to determine the effect of fill bursts on the performance of the pseudo noise ranging phase locked loop. It was found that the loop would not hold lock if too many fill bursts were added. However, this is to be expected with the Relay satellite. The reasons for this are described in this section.

The ranging signal is a continuous carrier which is phase modulated by a periodic pseudo noise code. Two means are provided to reduce the interference caused by this ranging signal to the sync burst and occupied time intervals. The most important is that the power of the ranging signal is chosen to be well below, by 10 to 20 db, that of the sync burst. The other is that the frequency of the ranging signal is displayed 2 MHz from the frequency of the transmitted sync burst.

Since the power of the ranging signal at the satellite input is much less than the power of the sync burst or a data burst, the hard limiter in the satellite causes the composite output signal to consist of the sync and data burst carriers with phase modulation sidebands due to the ranging signal displaced 2 MHz from the carrier. The ranging signal is thus called the subcarrier to distinguish it from the carrier of the sync or data bursts.

Although the ranging signal does not interfere with the sync burst and occupied time intervals, the latter signals do interfere with the ranging signal. The non-linear transfer characteristic of the satellite transponder generally will result in the stronger signal having a suppression effect on the weaker ranging signal.

The concept behind the ranging technique under consideration is that the satellite transponder can be characterized as a hard limiter.

The signal out of such a transponder depends on the relative input power levels of the ranging signal, interfering burst and noise. It is assumed that in the interest of system efficiency, the interfering burst, which is actually the main signal sync burst and data bursts for the system, is at least 10 db greater than the other two inputs so that it dominates the limiter and uses most of the satellite output power. The ranging signal power at the satellite output will then fluctuate depending on whether the interfering signal is present or not.

The most extreme fluctuation will occur if the ranging signal power is much stronger than the noise at the transponder input. Suppose, for example, that the interfering signal is 10 db above the ranging signal. Then when an interfering burst is present, the ranging signal will be 16 db down at the satellite output. However, when there is no interfering burst, and neglecting noise, the ranging signal will dominate the limiter and will take the full satellite output power. Thus, the ranging signal power will fluctuate 16 db depending on whether or not an interfering burst is present.

This fluctuation will be reduced somewhat if the noise power is comparable to or greater than the ranging signal power. For example, suppose the noise power equals the ranging signal and both are 10 db below an interfering burst. Then the ranging signal power will be 16 db down with the interfering burst present and about 3 db down with noise only present.

The input to the subcarrier tracking phase locked loop has a bandpass filter which passes only the ranging signal. This is followed by a hard limiter to eliminate the amplitude fluctuation during a frame period due to interfering bursts.

The Relay satellite which was used for this experimental program cannot be simply characterized as a hard limiter, however. Tests on the Relay simulator have shown that the transponder acts as a hard limiter followed by a tripler. The following analysis shows that an interfering burst has a far more serious suppression effect than that described above. In fact, for practical purposes it can be assumed that an interfering burst completely suppresses the ranging signal.

Let the transponder input be denoted:

$$x(t) = m(t) \cos \omega_o t + p \cos (\omega_o + \omega_m)t, \qquad (7.2\text{-}1)$$

where:

$m(t) = 1$, during interfering burst

$= 0$, otherwise

p^2 = ratio of ranging signal carrier power to interfering burst power.

ω_o = interfering burst angular frequency

ω_m = angular frequency difference between interfering burst and ranging carrier.

The modulation sidebands on the ranging signal are ignored in writing Equation 7.2-1. Expanding the second trigonometric function in 7.2-1, we obtain:

$$x(t) = \left[m(t) + p \cos \omega_m t\right] \cos \omega_o t - p \cos \omega_m t \sin \omega_o t \qquad (7.2\text{-}2)$$

This can be written in the form:

$$x(t) = A(t) \cos \left[\omega_o t + \theta(t)\right], \qquad (7.2\text{-}3)$$

where:

$$A^2(t) = \left[m(t) + p \cos \omega_m t\right]^2 + p^2 \sin^2 \omega_m t \qquad (7.2\text{-}4)$$

$$\tan \theta(t) = \frac{p \sin \omega_m t}{m(t) + p \cos \omega_m t} \qquad (7.2\text{-}5)$$

Since the interfering burst power is at least 10 db above that of the ranging signal, we assume $p << 1$ and use the small angle approximation for $\tan \theta$ in 7.2-5 to obtain,

$$\theta(t) = p \sin \omega_m t \quad \text{, during interfering burst} \qquad (7.2\text{-}6)$$

$$= \omega_m t \quad \text{, otherwise.}$$

The effect passing x(t) through a hard limiter and tripler is to give,

$$y(t) = A_o \cos \left[3\omega_o t + 3\theta(t) \right] \qquad (7.2\text{-}7)$$

at the satellite output, or, using 7.2-6

$$y(t) = A_o \cos (3\omega_o t + 3p \sin \omega_m t), \text{ during interfering burst} \qquad (7.2\text{-}8a)$$

$$= A_o \cos (3\omega_o + 3\omega_m)t \quad , \text{otherwise.} \qquad (7.2\text{-}8b)$$

Thus, when the interference is absent, the ranging signal angular output frequency will be $(3\omega_o + 3\omega_m)$. On the other hand, during the interfering burst the output frequency will be $3\omega_o$ phase modulated by a sinusoid or angular frequency ω_m with peak phase deviation of 3p radians. The output in this case is at an angular frequency of $3\omega_o$ with sidebands at $3\omega_o \pm \omega_m$, i.e., no significant output appears at $3\omega_o + 3\omega_m$.

The conclusion of this analysis of the tripler is that the ranging signal power is completely suppressed by an interfering burst. Of course, this complete suppression is a result of the small angle approximation in the analysis. On the other hand, experiments with the Relay transponder generally agree with the analysis and show that this suppression effect is, for practical purposes, essentially complete.

In the slave sync acquisition experiments described in the previous section, the data bursts in the format were simulated by fill bursts which are unmodulated 10 μs burst of carrier generated by the master terminal at the same frequency and level as the sync burst. The number of fill bursts present is selectable and can vary from zero to ten. Counting the sync burst which is always present, the number of interfering bursts can then vary from one to eleven.

The output of the bandpass filter and limiter at the subcarrier tracking loop input is only noise during an interfering burst. The lock detector in the subcarrier tracking loop has its threshold adjusted at 50 per cent of that lock phase detector output which occurs with full signal input. It should be expected then, that lock will not be indicated when approximately 50 per cent of the full input signal is suppressed by interfering bursts. The same situation occurs with the pseudo noise cross correlator lock detector.

Thus, the Relay transponder behaves quite differently than the hard limiting satellite assumed for system design. The problem which then arises is how to design the experimental program using the Relay satellite to reasonably simulate a system designed for a hard limiting satellite. The simplest approach and the approach, initially followed was to go ahead and use the system with Relay as is. Satisfactory results were obtained except when a large number of fill bursts are added.

However, there was also another approach which was in fact implemented after the test program started. This approach made use of the ranging signal during the 1.25 microsecond guard time between data bursts and the modification which was made to do this is described in the next section.

7.3 MODIFICATION FOR OPERATION WITH FILL BURSTS

As described at the beginning of this chapter, the lock signal for the subcarrier tracking phase locked loop was wired to indicate lock at all times. The actual operation of the subcarrier tracking phase locked loop was observed as fill bursts were added. It was found that the loop would retain lock even with all fill bursts in.

The case of all fill bursts in is an extreme which cannot occur in practice because at least the burst in which the slave station will transmit data must be unoccupied prior to the slave acquisition. This is important because it was found that although the subcarrier loop would hold lock with all fill bursts, it could only be acquired if there was at least one unoccupied time interval. The reason for this is that the operator needed this time interval in order to be able to observe when the loop was locked to the correct spectral line.

With no fill bursts it was found that the problem of locking the subcarrier loop to the correct spectral line could be resolved by removing the pseudo noise modulation. However, with a large number of fill bursts, the periodic suppression of the subcarrier generates spectral lines in the unmodulated ranging signal. The procedure used to lock the subcarrier loop with nine fill bursts; i.e., one unoccupied time interval, was the same as used for locking the carrier loop to the correct spectral line. The average acquisition time for the subcarrier loop then becomes the same as required for the carrier loop rather than the shorter time presented in the previous section.

Since the pseudo noise timing error detector could be operated with a 1.25 microsecond gate width, the only modification required for fill burst operation was to the pseudo noise lock detector. It was desired, therefore, to add the 1.25 microsecond gating pulse used for the timing error detector to lock detector reference signal. This was very easily done by adding a jumper on a printed circuit card.

This modification was made at the time the instrumentation was setup for the timing error experiment. During the period of these latter experiments, the slave acquisition was tried to large number of times using nine fill bursts. Except for the longer subcarrier loop acquisition time, results similar to those described in Section 7.1 were obtained.

8. TIMING ERROR TEST RESULTS

The slave acquisition experiments were initially run with instrumentation with sufficient resolution to accurately measure timing error which had a magnitude comparable with the 1.25 microsecond guard time. However, this was not sufficient to measure the timing error which actually occurred because it was found to be much less than the guard time.

A phase detector was then used to measure the phase difference between the master and slave 800 kHz transmit clocks which gives a full scale resolution of 1.25 microseconds. Furthermore, the chart recorder gain was adjusted so that 1 mm corresponded to about 25 nanoseconds timing error. This, however, was still not sufficient resolution to measure jitter due to noise.

No attempt was made to increase the resolution beyond this because of timing variations due to other causes besides noise. That is, variations in timing error on the order of 25 nanoseconds were observed due mainly to changes in signal strength and to adding or subtracting fill bursts. These variations which are called bias errors were found to be more significant than timing jitter due to noise.

Figures 8.0-1 and 8.0-2 illustrate the type of timing errors encountered. These figures show the timing error measured during two typical orbits. The 1.25 microsecond phase detector output was recorded on the chart recorder during the pass and was calibrated before and after each pass using the simulator for loop back. The pre and post calibrations were usually different (see Figure 8.0-2) so that timing error was defined as the difference between the phase detector reading and the average of the pre and post pass phase detector outputs. The fact that the pre and post calibrations were different indicates some bias drift with time. This is understandable since the amount of drift is only about one percent of the 1.25 microsecond pulse used for sync.

It can be seen that there is still a timing error during the pass which is greater than the calibration drift. This was found to be due to the difference in signal strength and is again a bias effect. The other main source of these bias errors was the addition or deletion of fill bursts. Figures 8.0-1 and 8.0-2 shows the effect of adding successive fill bursts and of then removing all of them.

In the orbits shown, the fill bursts were added one at a time but were not removed until all were removed together. This shows that the fill bursts do not give an additive effect, that is, there may be no significant difference whether one or nine fill bursts is added.

An overall summary of the timing error measurements is shown in Table 8-1. This compares the measured errors with the target specifications which were used in the design phase. It can be seen that these specifications were met; the maximum timing error never exceeded 75 nanoseconds.

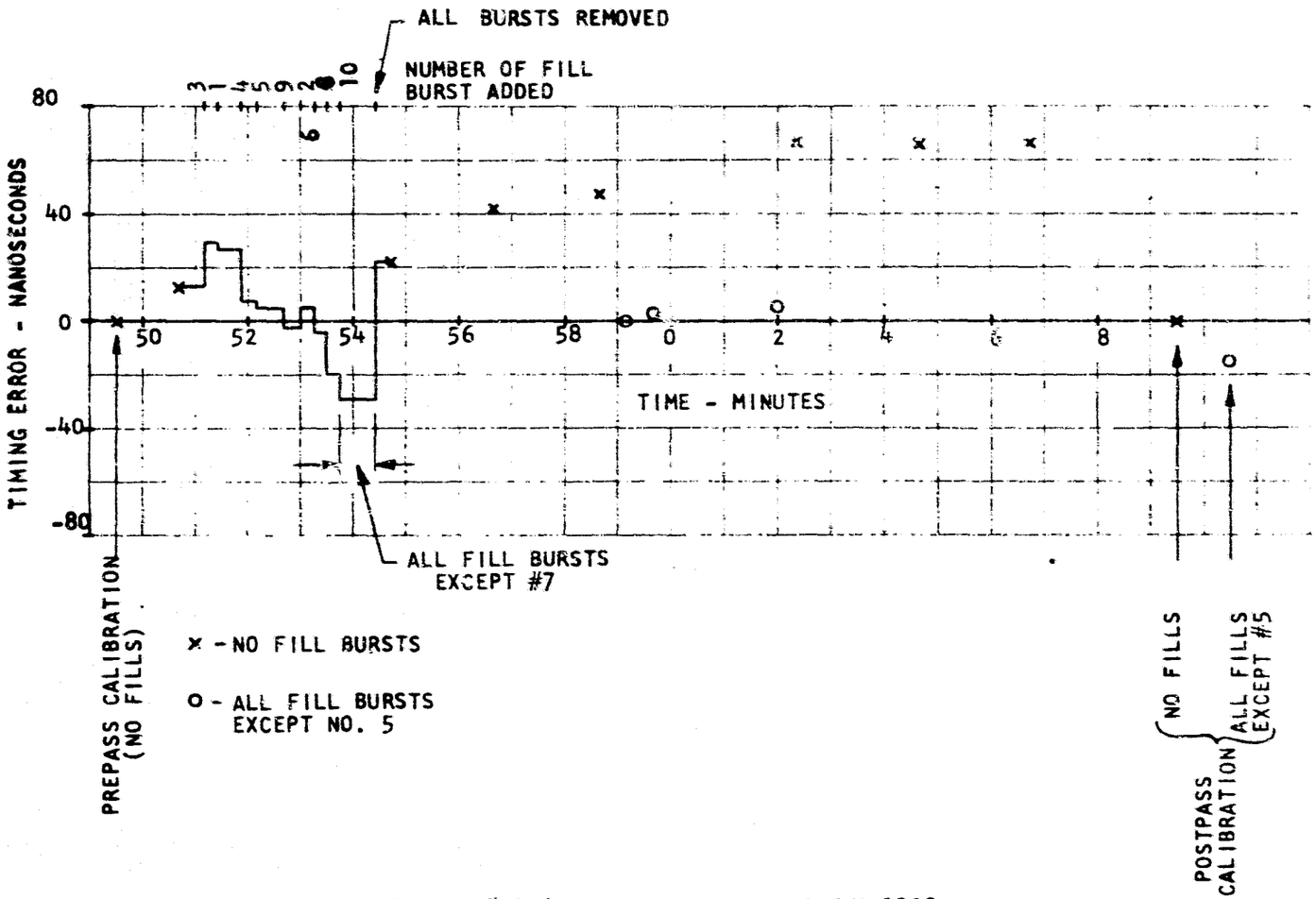

Figure 8.0-1. Timing Error - Orbit 9003

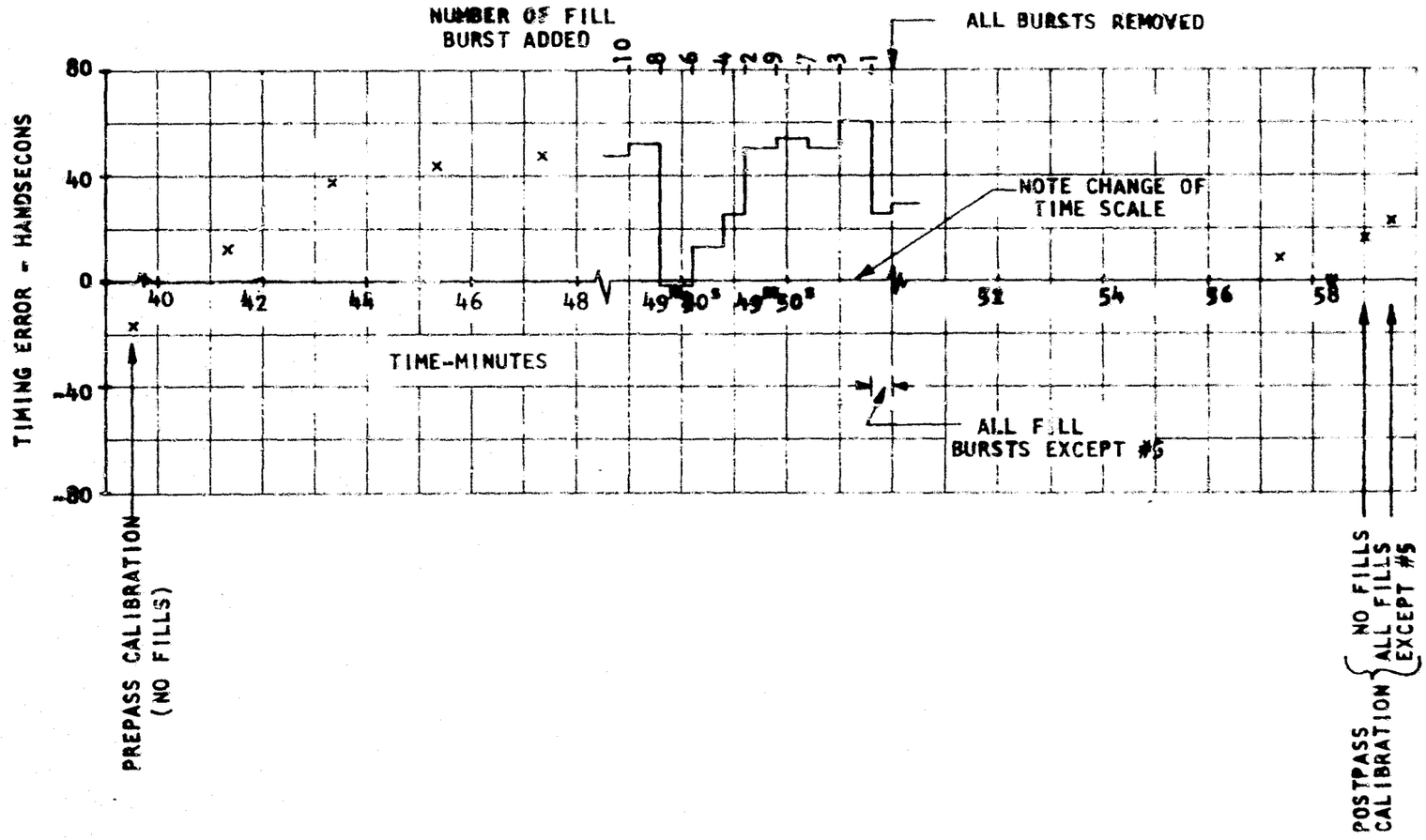

Figure 8.0-2. Timing Error - Orbit 9055

TIMING ERROR SUMMARY

TYPE OF ERROR	TARGET-SPECIFICATION	MEASURED
BIAS	200 NS	25 NS, TYPICAL 75 NS, MAX.
JITTER	20 NS, RMS	25 NS, MAX.

CAUSES OF BIAS ERROR: (i) VARIATIONS IN SIGNAL STRENGTH

(ii) INTERFERENCE FROM OCCUPIED TIME INTERVALS

Table 8-1. Timing Error Summary

9. ADDITIONAL RESULTS

9.1 RANGE MEASUREMENTS

As will be discussed in Appendix II the instrumentation for the master terminal provides for the measurement and recording of the satellite range, module 18.56 Km. The measured range was compared with the predicted range for a number of passes. After discussion with the technical officer, it was decided not to continue the reduction of these measurements since it was felt that they were not an essential part of the TDMA test program. The raw data is recorded in any event on all passes and could always be reduced at some future time if this was found to be desirable.

The results for those cases in which the data was reduced are summarized in Table 9-1. Plots of range residuals for two orbits are shown in Figures 9.2-1 and 9.2-2. An estimate of the bias error which could be caused by signal path delay in the station was made and indicated that such a bias error should not exceed 0.5 Km. Based on the data in Table 9-2, there appears to be a bias on this order of magnitude.

TABLE 9-1. COMPARISON OF RANGE MEASUREMENTS WITH PREDICTED RANGE

Orbit Number	Date	Range Residuals (Predict)		Range Residuals (Postdict)	
		Min.	Max.	Min.	Max.
8354	2-23-67	-1.54 km	1.17 km	-2.24	-0.2
8387	2-28-67	-4.24	-2.24	-1.00	-0.07
8394	3-1-67	-3.26	-1.29	-1.76	0.03
8487	3-13-67	-3.90	1.90		
8501	3-15-67			-0.87	0.24
8516	3-17-67	-2.90	2.81		
8538	3-20-67	-1.05	1.58		

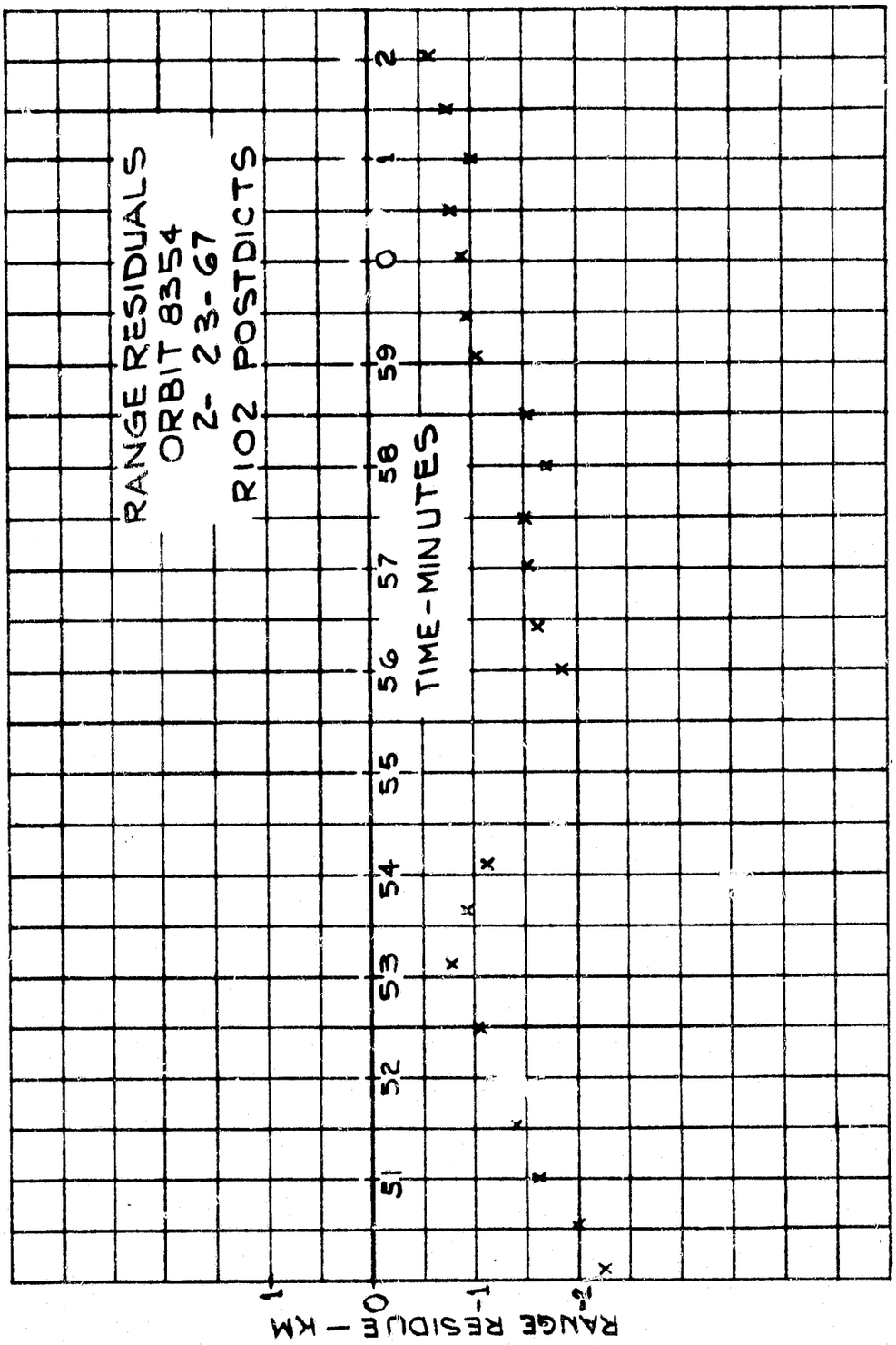

Figure 9.2-1. Range Residuals - Orbit 8354

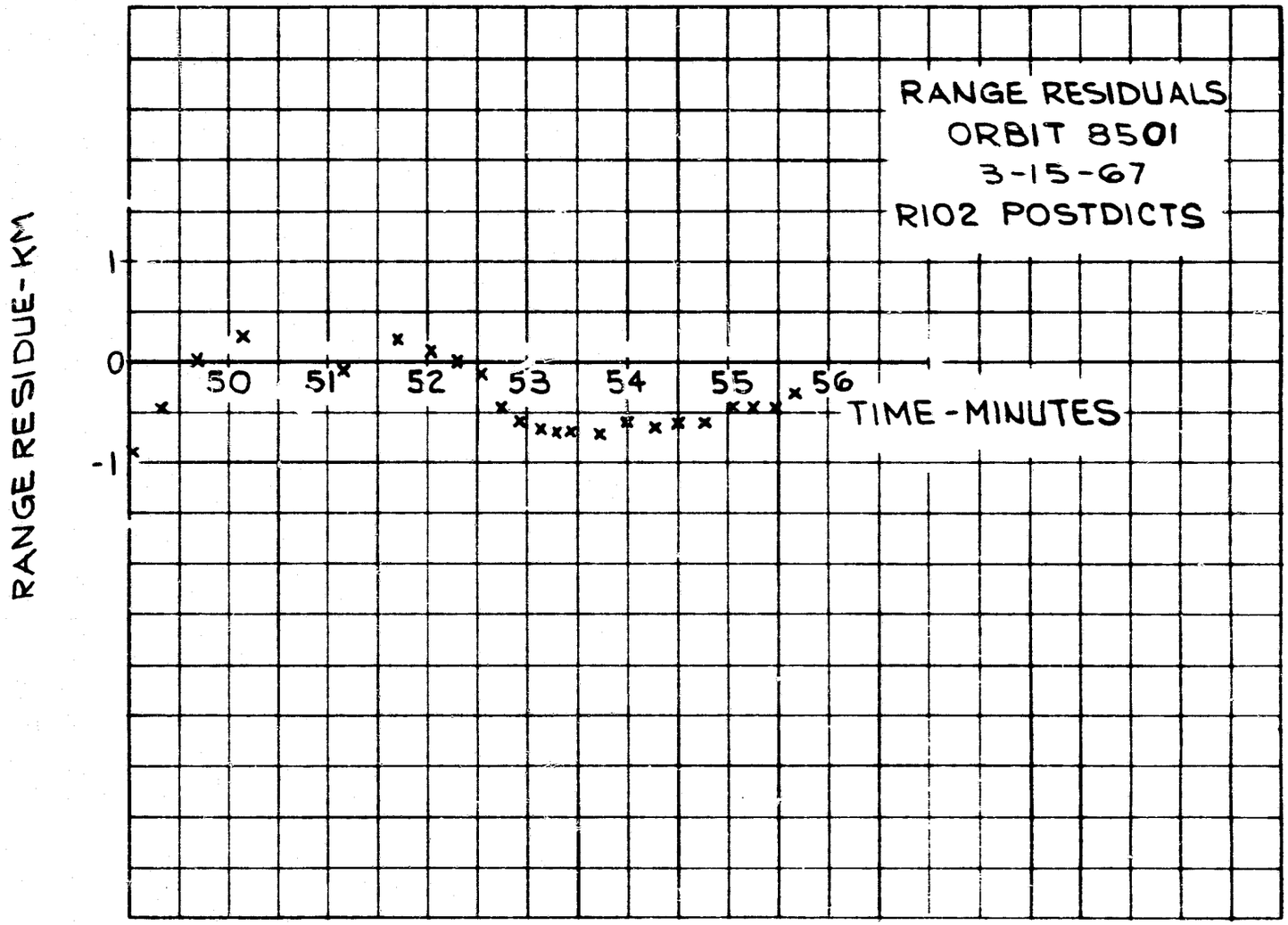

Figure 9.2-2. Range Residuals - Orbit 8501

10. CONCLUSIONS

The feasibility of acquisition and maintenance of synchronization in a TDMA system using a medium altitude satellite and a small ground station was successfully demonstrated. A terminal can completely acquire synchronization in less than one minute and maintain relative burst timing to an accuracy better than 0.1 microsecond.

A number of conclusions about specific areas of the system follow:

1. The doppler compensation system was found to be very successful and it is felt that it contributed significantly to achieving the excellent timing accuracy obtained.
2. The use of a low level ranging signal to avoid interference with occupied time intervals was another very successful technique. This is particularly appropriate with a hard limiting satellite transponder because the ranging signal uses full transponder output power when it falls on unoccupied time intervals. The suppression effect found when using a cw ranging signal indicates that a burst type ranging signal is more suitable.
3. The fact that a set of standard parameters were found best for normal operation shows that most of the switches used in the experimental equipment can be eliminated in an operational equipment. A number of threshold adjustments were provided, but it was found that they also could be fixed.
4. The use of phase modulation and coherent demodulation was appropriate. However, this puts more severe requirements on oscillator stability than necessary for fm systems. Specific recommendations about oscillator stability considerations are given in the next chapter. The difficulty with locking the carrier tracking loops to the correct spectral line has been discussed and is considered the main problem area encountered in the system.
5. The range measurements were not conclusive in determining the feasibility of simplifying slave acquisition by range prediction rather than ranging.
6. The crystal oscillator type frequency standards which were used were found to have excellent stability and are recommended for future systems. The 6.4 MHz voltage controlled crystal oscillators which were used have doubtful reliability; a number of problems with sporadic operation were experienced during initial system debugging. Provision should also be made for operating these units and their ovens continuously to improve stability.
7. The type of integrated circuit logic which was used gave excellent performance and reliability. There were no operational failures in any of the circuits. This logic is recommended for future systems.

8. There were no failures in the 70 MHz or other analog circuits. In addition, it was found that no adjustments in timing or gain were necessary during the test period.

9. Several power supply failures were experienced during the test period. It is felt that they were due to inadequate ventilation rather power circuit reliability.

11. RECOMMENDATIONS

Based on the experience gained with performing these tests, the following recommendations concerning an operational system and the associated synchronization equipment are made.

1. The doppler compensation used in this system is easily implemented and is recommended for any system in which the range varies with time. This would occur with either a moving satellite or with a stationary satellite and a moving terminal or both.
2. The idea of a low level ranging signal should be used in small terminals if it is not possible to predict range to within a fraction of a burst. A burst type ranging signal is recommended.
3. The standard parameters listed in Tables 6-7 and 7-2 are recommended as best for the particular format used in this program.
4. The use of phase modulation and coherent demodulation is recommended. However, a program to develop an automatic method of locking the carrier tracking loop to the correct spectral line is recommended. In addition, improved phase stability in the carrier loop voltage controlled oscillator and station local oscillator is necessary. Probably the best thing to try is to replace the LC tuned oscillator used in the carrier tracking loop by a voltage controlled crystal oscillator and then obtain the station's receive local oscillator signal by multiplying up from this voltage controlled crystal oscillator. This would put the local oscillator into the carrier tracking loop and reduce the tracking range required for the voltage controlled crystal oscillator.

APPENDIX I

OPERATIONS SUMMARY

Monthly summaries of the station operations between January 15 and June 1, 1967 follow.

January 1967

ORBIT NO.	DATE	REMARKS
8085	1-18-67	Satellite tracked, could not illuminate without interfering with tracking receiver.
8100	1-20-67	Satellite tracked and illuminated with 9 kw.
8144	1-26-67	Satellite tracked but not illuminated.
8173	1-30-67	Satellite tracked intermittently due to tracking receiver failure.
8181	1-31-67	Satellite not tracked due to intermittent tracking receiver operation.
		February 1967
8203	2-3-67	Could not lock TDMA due to strong interference.
8288	2-15-67	First successful lock of TDMA master terminal.
8303	2-17-67	Performed Experiment 1, Marginal tracking.
8339	2-21-67	Experiment 1.
8354	2-23-67	Experiment 1, experimented with klystron tuning.
8387	2-28-67	First successful lock of TDMA slave terminal, performed experiment 1.
		March 1967
8394	3-1-67	Pseudo noise timing error measured on scope, approx. 0.2 us.
8443	3-8-67	Maximum elevation 85°. Pseudo noise timing error measured on scope, same as prepass bias error. Motor in pseudo noise loop turned off for about 5 minutes, accumulated 0.2 us additional timing error over this period.
8458	3-10-67	Added fill bursts to see effect on pseudo noise loop. Loop consistently dropped out with 7 fill bursts and would not reacquire.
8487	3-13-67	Near zenith pass, 88.5° max. elevation. Used manual track near zenith. Initial TDMA lock slow due to doppler preset on transmit phase locked loop.

ORBIT NO.	DATE	REMARKS
8501	3-15-67	Initially tracked on antenna sidelobe. TDMA acquired but was noisy. Reacquired tracking on main lobe.
8516	3-17-67	TDMA acquisition slow due to transmit phase locked loop doppler preset.
8538	3-20-67	Transponder initially commanded into narrow-band mode. TDMA carrier acquired but suppressed when subcarrier transmitted. OK after transponder commanded to wideband mode.
8560	3-23-67	Two runs on experiment 1, slow acquisition both times due to transmit phase locked loop doppler preset.
8561	3-23-67	TDMA acquisition slow due to master carrier tracking loop doppler preset being too far off and locking on a spurious signal. Several runs of Experiment 1A.
8619	3-31-67	First use of modification to provide doppler preset for transmit loops. Three runs of Experiment 1A.
		April 1967
8641	4-3-67	Six runs of Experiment 1A.
8642	4-3-67	Eight runs of Experiment 1A.
8656	4-5-67	Experimented with fill bursts.
8657	4-5-67	Seven runs Exp. 2 and 3.
8671	4-7-67	Six runs Exp. 2 and 3, lost track temporarily at maximum elevation (85°).
8700	4-11-67	Five runs Exp. 2 and 3, experimented with carrier tracking PLL using 5000 Hz bandwidth.
8708	4-12-67	Ten runs Exp. 2 and 3.
8723	4-14-67	Nine runs Exp. 2 and 3.
8745	4-17-67	Seven runs Exp. 2 and 3.
8752	4-18-67	Six runs Exp. 2 and 3.
8759	4-19-67	Seven runs Exp. 2 and 3.
8760	4-19-67	Six runs Exp. 2 and 3.
8774	4-21-67	Three runs Exp. 2 and 3. Maximum elevation is 81°.
8775	4-21-67	Three runs Exp. 2 and 3.
8796	4-24-67	Pass cancelled, power supply failure in antenna compartment.
8797	4-24-67	Pass cancelled, power supply not repaired.

ORBIT NO.	DATE	REMARKS
8803	4-25-67	Eight runs Exp. 2 and 3.
8804	4-25-67	Six runs Exp. 2 and 3.
8818	4-25-67	Pass cancelled, Rosman antenna stuck in stow.
8819	4-27-67	Nine runs Exp. 2 and 3, temporarily lost track at 75° elevation.
8826	4-28-67	Seven runs Exp. 2 and 3, experimented with fill bursts.
		May 1967
8848	5-1-67	Seven runs Exp. 2 and 3, experimented with fill bursts.
8905	5-9-67	Exp. 4 Instrumentation checkout.
8906	5-9-67	Exp. 4 (Timing Error)
8920	5-11-67	First test with modified pseudo noise lock detector. Acquired with nine fill bursts. Exp. 4, lost track temporarily due to high (86.5°) elevation.
8921	5-11-67	Signal level calibration, recorded satellite AGC and return signal level with various transmit powers.
8951	5-15-67	Exp. 4, with zero and one fill burst. Lost track near end of pass due to unstable antenna servo caused by change in azimuth channel gain.
8958	5-16-67	Exp. 3 and 4 with zero to nine fill bursts.
8959	5-16-67	Exp. 3 and 4 with zero to nine fill bursts. Temporarily lost track due to high (87°) elevation.
8973	5-18-67	Exp. 2, 3 and 4 with zero to nine fill bursts.
8974	5-18-67	Exp. 2, 3 and 4 with zero to nine fill bursts.
9002	5-22-67	Exp. 2, 3 and 4 with zero to nine fill bursts.
9003	5-22-67	Exp. 2, 3 and 4 with zero to nine fill bursts.
9010	5-23-67	Exp. 2, 3 and 4 with zero to nine fill bursts and transmit powers to 0.5 and 1.0 kw.
9011	5-23-67	Exp. 2, 3 and 4 with zero to nine fill bursts.
9032	5-26-67	Transponder did not turn on until nearly the end of the pass. No experiments were performed.
9033	5-26-67	Exp. 2, 3 and 4 with zero to nine fill bursts.
9054	5-29-67	Exp. 2, 3 and 4 with zero and nine fill bursts.
9055	5-29-67	Exp. 2, 3 and 4 with zero and nine fill bursts.
9069	5-31-67	Exp. 2, 3 and 4 with zero and nine fill bursts.

ORBIT NO.	DATE	REMARKS
9070	5-31-67	Transponder did not come on until late in pass. Signal too weak to hold TDMA lock. This was due to poor look angle at end of pass.
		June 1967
9076	6-1-67	Exp. 2, 3 and 4 with zero and nine fill bursts. Transponder went off abruptly 1 minute before end of pass.
9077	6-1-67	Exp. 2, 3 and 4 with zero and nine fill bursts added from master and from slave.

APPENDIX - USE OF TDMA TO MEASURE SATELLITE RANGE

INTRODUCTION

This appendix discusses the use of a TDMA equipment to measure satellite range. This technique is of interest because:

1. It measures the accuracy of satellite predictions.
2. It can be used to eliminate the search mode of acquisition if predictions are good enough.
3. It can be used for navigation.
4. It provides a quantitative test of the TDMA theory and the various TDMA servomechanism loops.

The basic idea is most simply illustrated by Figure A1 for the case of a stationary satellite. There is no doppler in this case and the transmitting clock and the receiving clock have the same frequency. The phase relationship between the two clocks depends on the satellite range r and the wavelength λ corresponding to 2ω. If $r = \lambda (n + \theta)$ where n is an integer then the two clocks differ by θ revolutions.

This appendix treats the more complicated case which includes the effects of satellite motion, the master frequency servo loop, and various phase shifts in the system.

The conclusion of the analysis is that the more complicated case behaves essentially the same as the simple case. Thus a measurement of the relative phase between the transmitted clock and the received clock either at a master station or at a slave station which is transmitting in the TDMA mode is in effect a measurement of range at that instant to many decimal places. This result is not as obvious as it looks, since the master station servo uses the presently transmitted signal and a received signal whose doppler is related to the satellite velocity at some instant in the past.

The measurement of range from a fixed known location can be used to check the accuracy of predicted satellite orbits or conversely as a means of measuring satellite position and thus determining the orbit. Assuming that the satellite range from the station is known and absolute time is known, the appropriate phase between the transmitting and received clocks can be determined. Thus a slave station, once it has acquired the master received signal, can avoid almost all the search mode presently designed into the TDMA equipment. Alternately, if the satellite orbit is known but the station position is not as might very well be true for a TDMA station on an airplane, the TDMA equipment can be used as a radar by measuring the relative phase between the transmit and the receive clocks. Thus the TDMA is a navigation equipment. Lastly, an analysis of the relation between transmit and receive clocks on the master and slave stations in the present experiment is useful in evaluating the various TDMA servo loops.

A few words should be said about the ambiguities of this procedure. Because the basic period of the TDMA is about 125 microseconds, ranges which differ by an integer multiple of λ which is about 18.5 Km cannot be distinguished. For cases when the maximum range error is less than 9 Km, this is no problem. Otherwise, techniques which can resolve the range ambiguity will be needed.

This appendix A-II has three sections. The first section treats the idealized case of Figure A1. The second section analyses the effects of delays and phase shifts in the electronic equipment. The third section describes the measurements which need to be made in a practical case to measure satellite range.

SATELLITE RANGE RELATED TO CLOCK PHASE OFFSET

In this section the relation between the relative phase of the transmit and receive clocks and satellite range is calculated assuming an ideal master frequency loop as described in Section 3-2 and 3-4 of this report. (See equations 3.2-6 to 3.2-17)

The phase deviation of the signals at A, B, and C from the correct frequency are denoted by θ_A, θ_B, θ_C, respectively. Notice that if these angles grow linearly with time they will represent a frequency error.

signal at A = $S_A(t) = \sin(\omega t + \theta_A(t))$ (1a)

signal at B = $S_B(t) = \sin(\omega t + \theta_B(t))$ (1b)

signal at C = $S_C(t) = \sin(\omega t + \theta_C(t))$ (1c)

The distance from the satellite to the ground station at time t is denoted by r(t).

Range from satellite to ground at t = r(t) (2a)

c = velocity of light (2b)

We will assume that r(t) is parabolic. This will then have two non-zero derivatives of time

$$\frac{r(t)}{c} = r_0 + r_1 t + r_2 t^2 \qquad (3)$$

The peak values of r_0, r_1 and r_2 for Relay will be on the order of 10^{-1}, 10^{-5}, and 10^{-7}, respectively, so that equation 1 will be a good description of the satellite range for intervals of time as long as a minute, if the appropriate

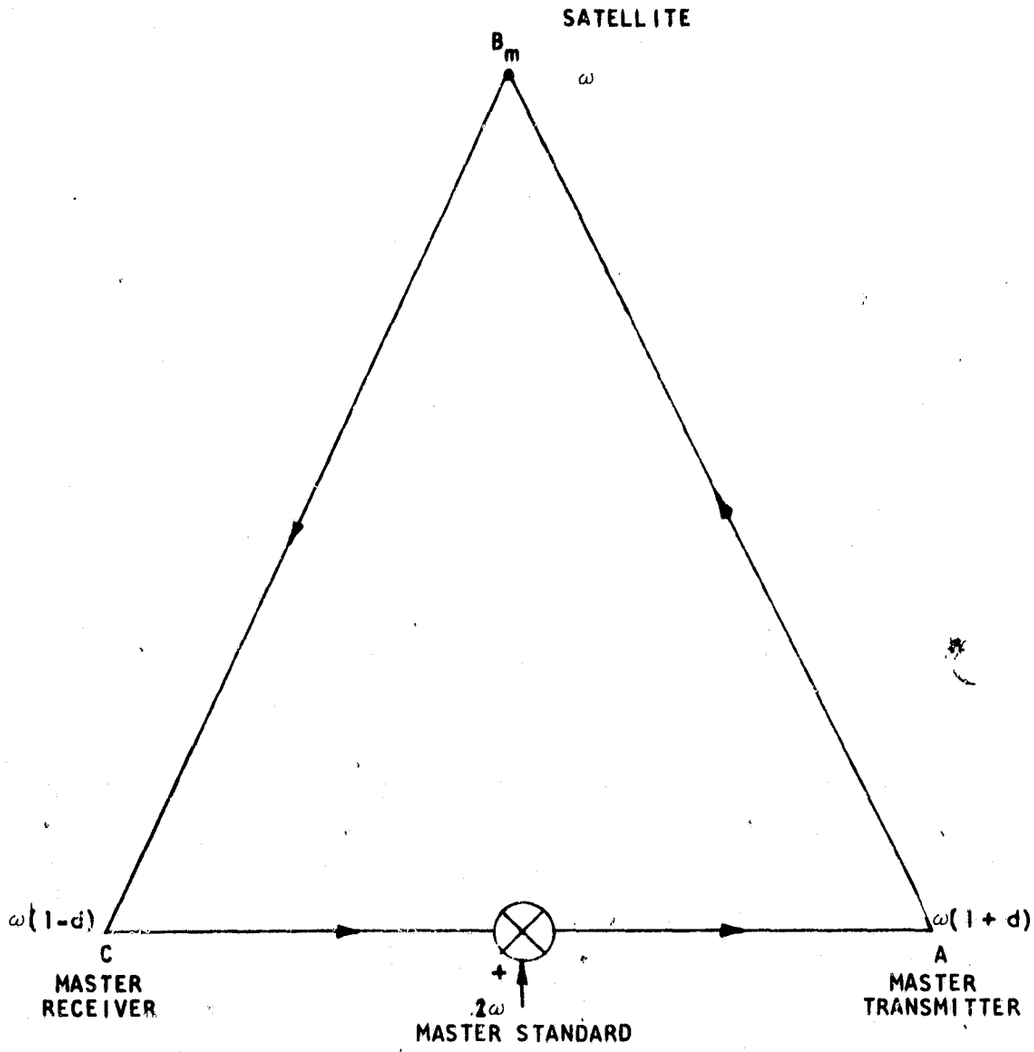

Figure A1. Nominal Master Frequency Loop

values of r_0, r_1, r_2, are chosen. For longer intervals, equation 1 will be clearly inappropriate as the velocities and ranges in equation 1 become infinite with increasing time while both the velocity and the range of Relay are bounded.

τ (t) = the propagation time from B to C of the signal now arriving at C = $\frac{r(t - \tau(t))}{c}$ 4)

The relation for θ_A alone is found by using the servomechanism relationship that the sum of the frequencies at C and A equal 2ω.

$$2wt = \omega t + \theta_C(t) + \omega t + \theta_A(t) \quad (5a)$$

$$\theta_A(t) = -\theta_C(t) \quad (5b)$$

$$\theta_A(t) + \theta_A\left[t - 2\tau(t)\right] = 2\omega\tau(t) \quad (6)$$

The quantity we are interested in is the offset between the transmit and receive clocks which is $\theta_A - \theta_C$. Using equation 5b.

$$\text{Offset between transmit and receive clocks} = \theta_A - \theta_C = 2\theta_A \quad (7)$$

The offset at time zero can be evaluated using equations 3.2-29a, 3.2-34a and 3.2-27 in Section 3.2 of this report. Only terms whose magnitude are greater than 10^{-11} are retained.

Offset between transmit and receive clocks at time O:

$$2\theta_A = 2\omega\theta_0 = 2\omega\tau_0\,(1 + \tau_1 + \tau_1^2)$$

$$= 2\omega r_0\,(1 - r_2\,r_0)$$

$$= 2\omega r\left(1 - \frac{r\ddot{r}}{2c^2}\right) \quad (8)$$

Equation 8 is a very interesting result as it says that the offset between the clocks is determined by the instantaneous range to about 8 decimal places, i.e., one meter out of 10,000 Km. Note, however, that the above ignores the effects of propagation through the troposphere and ionosphere which can introduce an error of many meters.

EFFECTS OF PHASE SHIFTS AND DELAYS

The previous section has considered an idealized case. Next, we consider the case when there are delays and phase shifts caused by the electronic equipment, waveguide runs, etc. As a matter of convenience in calculation all delays except for the free space delay will be replaced by phase shifts. Since all the frequencies in the system vary over a comparatively small range as a function of the doppler there is probably little difference between saying a given element causes a phase shift or a delay. In any case, the variation of phase shift with frequency should be examined experimentally. In addition, we will assume that the satellite delay is incorporated into the transmitter and receiver delay. This operation is correct to within a small fraction of a meter, i.e., $\frac{\dot{r}\dot{r} D_S}{2c^2}$ where D_S is the satellite delay as can be shown using the approach of Section 3.4 of this report.

The diagram of the equipment is shown in Figure A2. In this diagram

θ_A = transmit clock in equipment (9a)

θ_A^* = observed transmit clock (9b)

θ_C = receive clock in equipment (9c)

θ_C^* = observed receive clock (9d)

$\tilde{\theta}_A$ = actual transmitted signal(1)

$\tilde{\theta}_C$ = actual received signal(1)

The angles ϕ_1, and ϕ_2 are the phase shifts in the transmit and receive equipment including the satellite equipment delay. The angles ϕ_3 and ϕ_4 are the phase shifts between the equipment clocks and the observing test points. The master clock loop is driven by the angle ϕ_8 which is the output of a summer. Angles ϕ_5, ϕ_6, ϕ_7 are phase shifts between the summer and the various oscillators caused by the mixers and associated filters involved with the servo loop. In the following

(1)This assumes that there is no delay in the satellite. It could also be assumed that any satellite transponder delay is equally divided between ϕ_1 and ϕ_2.

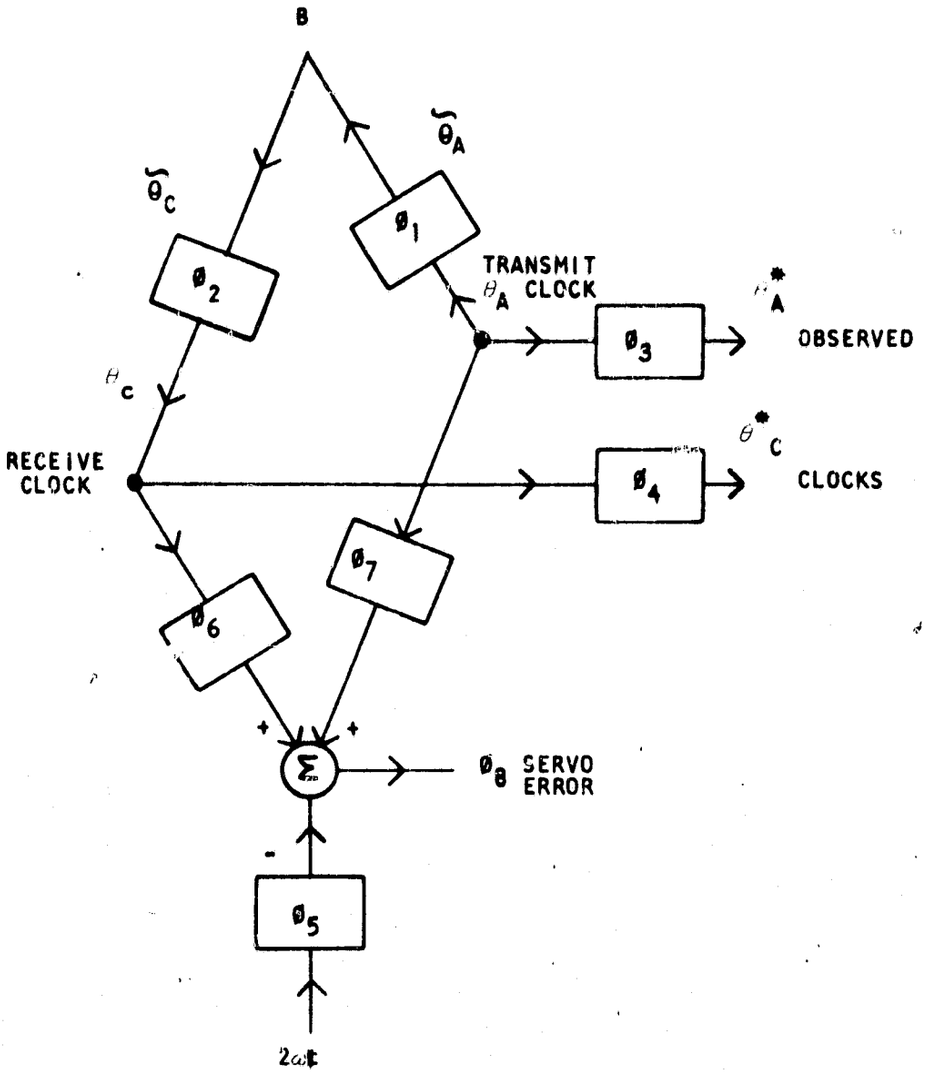

Figure A2. Master Frequency Loop with Phase Shifts

it is assumed that these angles vary at a rate slow compared to the master frequency loop response and thus a steady state servo analysis applies.

Using Figure A2

$$\omega t + \theta_A(t) + \phi_7 + \omega t + \theta_C(t) + \phi_6 - (2\omega t + \phi_5) = \phi_8 \tag{10}$$

$$\theta_A(t) + \theta_C(t) = \phi_8 + \phi_5 - \phi_6 - \phi_7 = \phi \tag{11}$$

Using equation 3.2-13b of this report

$$\tilde{\theta}_C(t) = \tilde{\theta}_A(t - 2\tau(t)) - 2\omega\tau(t) \tag{12}$$

$$\theta_C(t) = \tilde{\theta}_C(t) + \phi_2 \tag{13a}$$

$$\tilde{\theta}_A(t) = \theta_A(t) + \phi_1 \tag{13b}$$

Combining equations 11, 12, 13

$$\theta_A(t) + \theta_C(t) = \theta_A(t) + \theta_A(t - 2\tau(t)) + \phi_1 + \phi_2 - 2\omega\tau(t) = \phi \tag{14}$$

$$\theta_A(t) + \theta_A(t - 2\tau(t)) = 2\omega\tau(t) + \phi - \phi_1 - \phi_2 \tag{15}$$

Now calling $\theta_{A\tau}(t)$ and $\theta_{C\tau}(t)$ the corresponding phase for the idealized case with no equipment phase shift one recalls equations 5b, 6

$$\theta_{A\tau}(t) = \theta_{C\tau}(t) \tag{16a}$$

$$\theta_{A\tau}(t) + \theta_{A\tau}(t - 2\tau(t)) = \hat{2}\,\omega\tau(t) \tag{16b}$$

Next we review the variables of most interest and how they can be calculated.

$\tau(t)$ is a given function determined solely by the satellite orbit and station position (see equation 4). $\theta_{A\tau}(t)$ and $\theta_{C\tau}(t)$ are signal phases in a theoretical servo loop which has no equipment delays and no equipment phase shifts. $\theta_{A\tau}(t)$ is defined implicitly by equation 16b and the condition that the system response is smooth (i.e., no oscillation in $\theta_{A\tau}(t)$ with a period of the order of $2\tau(t)$). An approximation to $\theta_{A\tau}(t)$ which is accurate enough for any desired measurement can be derived using the techniques of section 3.2 and 3.4 of the final report phase 1. $\theta_{C\tau}(t)$ can be derived from $\theta_{A\tau}(t)$ and equation 16a.

Similarly, $\theta_A(t)$ and $\theta_C(t)$ are actual equipment clocks and $\theta_A^*(t)$ and $\theta_C^*(t)$ are the observed clocks. $\theta_A(t)$ is defined implicitly by means of equation 15 and

the condition that the system response is smooth. An approximation to $\theta_A(t)$ can be derived using the techniques of sections 3.2 and 3.4 of the final report phase I.

$\theta_C(t)$ can be derived from $\theta_A(t)$ and equation 11. θ_A^* and θ_C^* are offset from θ_A and θ_C by phase shifts ϕ_3 and ϕ_4, respectively, as shown in Figure A2.

Next the relation between equipment measurements and the measurements for an idealized servo are described. Assume that we have found $\theta_{A_T}(t)$ which satisfies equation 16b. Then $\theta_A(t)$ chosen as shown in equation 17 will satisfy equation 15 as can be seen by the substitution of equations 17 and 16b in 15.

$$\theta_A(t) = \theta_{A_T}(t) + \frac{\phi}{2} - \frac{(\phi_1 + \phi_2)}{2} \tag{17}$$

Now, using equations 11, 17, and 16a

Offset between transmit and receive clocks with equipment phase shift

$$= \theta_A(t) - \theta_C(t) = 2\theta_A(t) - \phi \tag{18}$$

$$= 2\theta_{A_T}(t) - (\phi_1 + \phi_2)$$

$$= \theta_{A_T}(t) - \theta_{C_T}(t) - (\phi_1 + \phi_2).$$

Next one can evaluate $\theta_A^*(t) - \theta_C^*(t)$

$$\text{Observed offset} = \theta_A^*(t) - \theta_C^*(t) = \theta_A(t) - \theta_C(t) + \phi_3 - \phi_4 \tag{19}$$

$$= \theta_{A_T}(t) - \theta_{C_T}(t) - (\phi_1 + \phi_2) + (\phi_3 - \phi_4)$$

$$= \begin{matrix}\text{Offset with} \\ \text{no equipment phase} \\ \text{shift}\end{matrix} - \begin{matrix}\text{equipment} \\ \text{delay}\end{matrix} + \begin{matrix}\text{differential} \\ \text{delay to test} \\ \text{points}\end{matrix} \tag{20}$$

PRACTICAL PROCEDURES FOR MEASURING RANGE

There are a number of comments which can be made about measuring satellite range using the TDMA clock offset.

1. One can measure satellite range either by measuring the clock offset at a given time or by measuring the time when the offset is zero. The latter measurement requires less accurate timing.
2. One can measure the electronic delay using the satellite simulator and the station equipment. The quantity measured is $-(\phi_1 + \phi_2) + \phi_3 - \phi_4$. The

relation between delay and frequency should be examined. If extra cabling is required to use the satellite simulator the delay of this cabling should be measured or estimated and subtracted from equipment delay. The equipment delay should be measured with the master frequency servo loop operative and inoperative. Both measurements should give the same result.

3. For the phase detector in the present experiment one should measure the time difference and the jitter between actual clock coincidence and that indicated by the phase detector.

4. This measurement depends heavily on the behavior of the master frequency servo loop. Thus the frequency response of this loop and waveform of the servo error during a pass and the relation between servo error and doppler shift should be measured.

Calculation of Wavelength

$$\lambda = \frac{c}{2\omega}$$

$$\text{TDMA frame rate} = \frac{8 \times 10^5/\text{sec}}{99}$$

$$\lambda = \frac{99 \times 2.997925 \times 10^5 \text{ Km/sec}}{2 \times 8 \times 10^5/\text{sec}}$$

$$\lambda = 18.54966 \text{ Km}$$